Novel bio-based materials from cellulose and chitin

Dissertation

zur Erlangung des Doktorgrades der Naturwissenschaften (Dr. rer. nat.)

der Fakultät für Chemie und Pharmazie

der Universität Regensburg

vorgelegt von

Auriane Freyburger

aus Mulhouse (Frankreich)

Regensburg 2018

Doctorate information

This doctoral thesis was accomplished at the Institute of Physical and Theoretical Chemistry at the University of Regensburg between December 2013 and December 2017 under the supervision of Prof. Dr. Werner Kunz. It was supported by the Bavarian State Ministry for Environmental Affairs and Consumer Protection as part of the project group ForCycle.

Dissertation submission:	01/11/2018
Dissertation defense:	04/13/2018
Ph. D. Supervisor:	Prof. Dr. Werner Kunz

Ph. D. Committee:

- 1st Reviewer	Prof. Dr. Werner Kunz
- 2nd Reviewer	Prof. Dr. Cordt Zollfrank
- 3rd Examiner	Apl. Prof. Dr. Rainer Müller
- Committee Chairman	Prof. Dr. Henri Brunner

Acknowledgement

Before starting, I wish to express my gratitude to all who helped me and contributed to this work.

First and foremost, I would like to thank Prof. Dr. Werner Kunz who gave me the opportunity to work in Germany on this interesting project. He supported me, guided me, and invested time to the realization of this project. He allowed me to acquire new skills and to go to many conferences to open my critical scientific curiosity.

I also wish to express my gratitude to Prof. Dr. Cordt Zollfrank and Yaqing Duan from the Center of Science in Straubing, who participated in part of this work. It was a pleasure to work with you and to share point of views.

I am very thankful to the Bavarian State Ministry for Environmental Affairs and Consumer Protection for its financial support and to all the members of the project ForCycle for their organization and the good working atmosphere during meetings.

Thanks to Prof. Dr. Richard Buchner and Prof. Dr Rainer Müller from the Institute of Physical and Theoretical Chemistry at the University of Regensburg for giving me access to their equipment and for their good advices and assistance. Additionally, I would like to thank the mechanical and electrical workshop from the University of Regensburg for building the fiber spinning, water and O_2 permeability experimental apparatuses and for all the reparations.

I am really thankful to Dr. Thomas Röder from Lenzing AG for giving me the opportunity to visit the company and to gain knowledges in cellulose fibers production. Also thanks to Walter Roggenstein from Kelheim Fibres, who performed some measurements on my fibers and to Dr. Robert Meier from PreSens, who lent me the device for the O_2 permeability experiments.

I deeply thank my colleagues: Roland Neueder, Sergej Friesen, Andreas Nazet, Katharina Häckl, Mathias Hofmann, Damian Brock, Evi Müller, Veronika Fischer, and Sebastian Krickl for their scientific help and kindness. Furthermore, thanks to all the members of

the institute for helping me to become integrated and to improve my German/Bavarian. Working conditions, discussions, lunchtimes, and organized events were good moments that I will never forget.

I shall not, of course, omit to thank all the students: Quirin Prasser, Sophia Sokolov, Jakob Asenbauer, Lukas Wirth, Michael Weinhart, Rainer Herzog, Stefanie Ritter, and Virginie Desriac who helped me in some laboratory experiments as part of their internship.

Finally, I would like to express my gratitude to Fabian Glaab, Lenz Franzke, Nicola Lang, Sergej Friesen, Mathias Hofmann, Alexander Wollinger, and Katharina Häckl who read and made critical corrections about this manuscript.

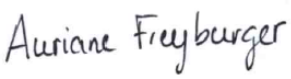

Abstract

Chitin and cellulose are the most abundant natural polymers. They have unique properties suitable for the design of new bio-sourced and biodegradable materials for various applications such as textile fibers, food packaging, and biomedical products. Unfortunately, these biopolymers suffer from a lack of solubility in regular solvents. But, due to their intractable bulk structure, the dissolution of such polymers is a crucial step for their processing. In this context, the solubility of non-modified cellulose and chitin in different solution media such as ionic liquids, deep eutectic solvents, and other conventional solvent systems was first studied in this work. It was found that the ionic liquid, 1-butyl-3-methylimidazolium acetate (BmimOAc), was the most efficient solvent for the dissolution of both polymers. Despite its good solubilizing capacity, BmimOAc is neither biodegradable nor bio-renewable. As the aim of this thesis was to provide an easy and environmentally friendly method to process cellulose and chitin, a second solvent was added in the dissolution process to reduce the necessary amount of BmimOAc. The biodegradable and bio-based co-solvent, γ-valerolactone (GVL), was an ideal candidate for this purpose. In order to assess its potential, the influence of GVL in the cellulose proceeding was also evaluated according to the industrial Lyocell process. *N*-methylmorpholine *N*-oxide monohydrate (NMMO) was used for this procedure. Besides increasing the sustainability of the studied systems, GVL was observed to enhance polymer dissolution and to facilitate manufacturing of the regenerated polymers. To understand these positive effects, physicochemical properties of binary mixtures (GVL/BmimOAc or NMMO) were characterized by viscosity, ionic conductivity, and thermal analysis measurements. The properties of the polymer solutions were also investigated by thermal and rheological studies. In a third step, materials such as cellulose fibers and new cellulose/chitin composite materials were successfully prepared from these solutions. All produced materials were characterized in detail by means of spectroscopical, morphological, and mechanical analysis methods. Wetting and permeability studies were additionally performed to demonstrate the advantages of a chitin coat on the properties of cellulose-based textiles. The results showed that the presence of chitin decreases the water wettability of the textiles on the coated site. Furthermore, the chitin layer acts as a promising water and oxygen barrier, which makes these novel materials potential candidates for various applications such as impermeable textiles for hygiene products.

Keywords: chitin, cellulose, dissolution, ionic liquid, deep eutectic solvent, γ-valerolactone, fiber, chitin coating, textile.

Zusammenfassung

Cellulose und Chitin sind Polymere, die in großen Mengen in der Natur vorkommen. Ihre einzigartigen Eigenschaften machen sie zu idealen Kandidaten für neue bioabbaubare Kompositmaterialien in vielfältigen Anwendungen wie Textilfasern, Verpackungen oder biomedizintechnische Produkte. Allerdings sind sie in vielen, häufig verwendeten organischen Lösungsmitteln praktisch unlöslich, jedoch müssen beide Biopolymere zu ihrer Verarbeitung unbedingt gelöst werden. In diesem Zusammenhang wurde zuerst die Löslichkeit der beiden natürlichen und nicht-modifizierten Polymere in verschiedenen Lösungsmitteln, wie zum Beispiel in ionischen Flüssigkeiten, tiefen Eutektika und anderen klassischen Lösemitteln, untersucht. Die ionische Flüssigkeit 1-Butyl-3-Methylimidazoliumacetat (BmimOAc) erwies sich als das effizienteste Lösungsmittel für beide Polymere. Um die Nicht-Bioabbaubarkeit und die nicht nachwachsenden Naturrohstoffe des Lösungsmittels weiter zu verringern und den Auflösungsprozess mit BmimOAc umweltfreundlicher zu gestalten, wurde als zweites das biogene und biologisch leicht abbaubare Lösungsmittel γ-Valerolacton (GVL) in signifikanten Mengen hinzugefügt. Um andere Einsatzmöglichkeiten von GVL zu bewerten, wurde dessen Einfluss auf die Lösungseigenschaften von Cellulose im Lyocell-Verfahren untersucht. *N*-Methylmorpholin *N*-Oxid-Monohydrate (NMMO) wurde deshalb als Lösungsmittel hergenommen. Neben der zunehmenden Nachhaltigkeit der getesteten Systeme zeigte die Zugabe von GVL weitere positive Einflüsse, insbesondere eine verbesserte Löslichkeit der Polymere und eine erleichterte Herstellung von Materialien aus wiedergewonnenen Polymeren. Um diese Effekte zu verstehen, wurden die physikalisch-chemischen Eigenschaften von binären Mischungen (GVL/BmimOAc oder NMMO) durch Viskositäts- und Leitfähigkeitsmessungen und thermische Analyse bestimmt. Außerdem wurden die rheologischen und thermischen Charakteristika von Polymerlösungen gemessen. Zuletzt wurden die Polymere aus diesen Lösungsmittelgemischen erfolgreich als Cellulosefasern und als Cellulose/Chitin-Kompositmaterialien gewonnen. Alle produzierten Materialien wurden mit Hilfe von spektroskopischen, morphologischen und mechanischen Methoden analysiert. Zusätzlich wurden Benetzungs- und Permeabilitätsstudien durchgeführt, um die Vorteile einer Chitin-Beschichtung gegenüber den Eigenschaften von Cellulosetextilien zu demonstrieren. Die Ergebnisse zeigten, dass Chitin die Hydrophobie der Textilien nur auf der beschichteten Seite erhöhte. Zudem zeigten die mit Chitin beschichteten

Cellulosefilme eine geringere Wasser- und Sauerstoffdurchlässigkeit. Dadurch stellen diese Polymere interessante Materialien für unterschiedliche potentielle Anwendungen dar, wie zum Beispiel impermeable Stoffe für Hygieneprodukte.

Stichwörter: Chitin, Cellulose, Lösung, ionische Flüssigkeit, tiefe Eutektika, γ-Valerolacton, Faser, Chitinbeschichtung, Textilien.

Abbreviations

A102	Ammoeng 102
AGU	Anhydroglucose unit
AIL	Aprotic ionic liquid
AmimBr	1-Allyl-3-methylimidazolium bromide
AmimCl	1-Allyl-3-methylimidazolium chloride
ATR	Attenuated total reflectance
$BmimBF_4$	1-Butyl-3-methylimidazolium tetrafluoroborate
BmimCl	1-Butyl-3-methylimidazolium chloride
BmimOAc	1-Butyl-3-methylimidazolium acetate
$BmimPF_6$	1-Butyl-3-methylimidazolium hexafluorophosphate
BU	Betaine/urea
BuAF	Butylammonium formate
C_4CarBr	Butylcarnitine bromide
CCU	Choline chloride/urea
CCT	Choline chloride/thiourea
ChC_4	Choline butanoate
ChLac	Choline lactate
ChOH	Choline hydroxide
Cuam	Cuprammonium hydroxide
DA	Degree of acetylation
DES	Deep eutectic solvent
DLS	Dynamic light scattering
DMAc	Dimethyl acetamide
DMF	Dimethylfuran
DMSO	Dimethyl sulfoxide
DP	Degree of polymerization
DSC	Differential scanning calorimetry
EAF	Ethylammonium formate
ECU	Ethylammonium chloride/urea
EL	Ethyl lactate
EmimCl	1-Ethyl-3-methylimidazolium chloride
EmimOAc	1-Ethyl-3-methylimidazolium acetate
FTIR	Fourier transform infrared spectroscopy
GBL	γ-Butyrolactone
GHB	γ-Hydroxybutyrate
GHL	γ-Hexalactone
GVL	γ-Valerolactone
HBA	Hydrogen bond acceptor
HBD	Hydrogen bond donor
HMF	Hydroxymethylfurfural
$HmimNTf_2$	1-Hexyl-3-methylimidazolium bis(trifluoromethylsulfonyl)imide
IL	Ionic liquid
IR	Infrared
MF	2-Methylfuran
MCC	Microcrystalline cellulose
$MimC_1$	Imidazolium formate

$MimC_2$	Imidazolium acetate
$MimC_3$	Imidazolium propionate
$MimC_4$	Imidazolium butanoate
$MimC_5$	Imidazolium pentanoate
$MimC_6$	Imidazolium hexanoate
$MimC_7$	Imidazolium heptanoate
$MimC_8$	Imidazolium octanoate
$MimC_9$	Imidazolium nonanoate
Mono.	Monohydrate
MTHF	Methyltetrahydrofuran
NMMO	*N*-Methylmorpholine *N*-oxide
NMR	Nuclear magnetic resonance
NS	Not soluble
$OmimBF_4$	1-Octyl-3-methylimidazolium tetrafluoroborate
$P_{14}DCA$	*N*-Butyl-*N*-methylpyrrolidinium dicyanamide
PC	Propylene carbonate
PIL	Protic ionic liquid
PTFE	Polytetrafluoroethylene
$PyrC_1$	Pyrrolidinium formate
$PyrC_2$	Pyrrolidinium acetate
$PyrC_3$	Pyrrolidinium propionate
$PyrHSO_4$	Pyrrolidinium hydrogen sulfate
RTIL	Room temperature ionic liquid
SEM	Scanning electron microscopy
T_c	Crystallization temperature
TBAF	Tetrabutylammonium fluoride
TBPOH	Tetrabutylphosphonium hydroxide
T_g	Glass transition temperature
TGA	Thermogravimetric analysis
T_m	Melting temperature
wt%	Weight percent

Symbols

ΔG_m	Gibbs energy of mixing (J)
ΔH_m	Enthalpy of mixing (J)
ΔS_m	Entropy of mixing (J/K)
T	Temperature (°C) or absolute temperature (K)
R	Ideal gas constant (J/ K/ mol)
N	Number of moles (mol)
Φ	Volume fraction
χ_{12}	Parameter of solvent-polymer interactions
K	Calibration constant
η	Dynamic viscosity (mPa.s)
t	Time (s)
ρ	Density (g/cm^3)
G'	Storage modulus (Pa)
G''	Loss modulus (Pa)
η^*	Complex viscosity (Pa.s)
ω	Angular velocity (rad/s)
κ	Electrical conductivity (S/cm)
R	Electrical resistance (S^{-1})
υ	Frequency (Hz)
K_{cell}	Cell constant (cm^{-1})
Λ	Molar conductivity (S.cm^2.mol^{-1})
ω_x	Weight fraction of x
M	Molar mass (g/mol)
A, B, T_0, α	Constants
x_x	Molar fraction of x
P	Permeability coefficient (m/s)
J	Flux (mol/m^2/s)
D	Diffusion coefficient (m^2/s)
C	Concentration (mol/m^3)
Δx	Distance (m)
V	Volume (m^3)
A	Permeation area (m^2)
n	Amount in moles (mol)
p	Partial pressure (hPa)
R	Gas constant (m^{3}Pa/K/mol)

Table of contents

Introduction **1**

Chapter 1 Fundamentals **5**

1.1 Cellulose and chitin: biopolymers and sustainable raw materials *6*
1.1.1 Biopolymers and sustainable applications 6
1.1.2 Cellulose and chitin structures and properties in the solid state 8
1.1.2.1 Cellulose 9
1.1.2.1.1 Sources and extraction 9
1.1.2.1.2 Molecular structure 10
1.1.2.1.3 Crystalline structure 11
1.1.2.1.4 Properties 11
1.1.2.2 Chitin 12
1.1.2.2.1 Sources and extraction 12
1.1.2.2.2 Molecular structure 14
1.1.2.2.3 Crystalline structure 15
1.1.2.2.4 Properties 15

1.2 Cellulose and chitin solubilization *16*
1.2.1 Theory on the solubility of polymers 16
1.2.2 Classical solvent systems 17
1.2.2.1 Cellulose 17
1.2.2.2 Chitin 22
1.2.3 Alternative solvents 23
1.2.3.1 Environmental aspects 23
1.2.3.2 Ionic liquids 24
1.2.3.2.1 General aspects and properties 24
1.2.3.2.2 Dissolution of cellulose and chitin in ILs 25
1.2.3.2.3 ILs as cellulose solvents 26
1.2.3.2.4 ILs as chitin solvents 28
1.2.3.2.5 Mechanism of dissolution 30
1.2.3.3 Deep eutectic solvents 33
1.2.3.3.1 General aspects and properties 33
1.2.3.3.2 Dissolution of cellulose and chitin 34

1.3 Cellulose and chitin materials *38*
1.3.1 Production process of materials and applications 38
1.3.2 Cellulose and chitin fibers 39
1.3.2.1 Regenerated cellulosic fibers at the industrial scale 40
1.3.2.1.1 Viscose process 40
1.3.2.1.2 Lyocell process 41
1.3.2.2 Regenerated cellulose/chitin fibers from IL solutions 43

Chapter 2 Dissolution of cellulose and chitin in various solvents **45**

2.1 Introduction *46*

2.2 Experimental section *47*

2.2.1 Chemicals 47
2.2.1.1 Chemicals used for the biopolymers 47
2.2.1.2 Chemicals used for the ionic liquids 47
2.2.1.3 Chemicals used for the deep eutectic solvents 48
2.2.1.4 Chemicals used for the other organic solvents 48
2.2.2 Experimental methods 49
2.2.2.1 Solvent synthesis and preparation 49
2.2.2.1.1 Preparation of ionic liquids 49
2.2.2.1.2 Preparation of deep eutectic solvents 52
2.2.2.2 Dissolution method 53
2.3 Results and discussion 54
2.3.1 Dissolution in ionic liquids 54
2.3.2 Dissolution in deep eutectic solvents 61
2.3.3 Dissolution in other organic solvents 65
2.4 Concluding remarks 69
Chapter 3 Effects of a co-solvent in dissolution processes 71
3.1 Introduction 72
3.2 Experimental section 74
3.2.1 Chemicals 74
3.2.2 Experimental methods 75
3.2.2.1 Tolerance test 75
3.2.2.2 Physicochemical properties of solvents and polymer solutions 75
3.2.2.2.1 Density and dynamic viscosity 75
3.2.2.2.2 Viscoelastic properties 76
3.2.2.2.3 Electrical conductivity 77
3.2.2.2.4 Dynamic Light Scattering measurements 77
3.2.2.2.5 Thermal analysis 78
3.3 Results and discussion 79
3.3.1 Co-solvent for cellulose and chitin solubilization in BmimOAc 79
3.3.1.1 Research of a suitable co-solvent 79
3.3.1.2 Tolerance and effect of GVL in the dissolution process 80
3.3.1.3 Impact of GVL on BmimOAc physicochemical properties 82
3.3.1.4 Influence of GVL on the rheological properties of polymer solutions 87
3.3.2 Co-solvent for cellulose solubilization in NMMO monohydrate 93
3.3.2.1 Suitable co-solvent and tolerance 93
3.3.2.2 Effect of GVL during the dissolution process 96
3.3.2.3 Impact of GVL on NMMO monohydrate physicochemical properties 97
3.3.2.4 Influence of GVL on the cellulose dope 99
3.4 Concluding remarks 106
Chapter 4 Production of new polymer materials 109
4.1 Introduction 110
4.2 Experimental section 112

4.2.1 Chemicals 112
4.2.2 Material production methods 112
4.2.2.1 Preparation of polymer solutions 112
4.2.2.2 Fiber spinning equipment and experiment 113
4.2.2.2.1 Cellulose fibers produced without an air gap 113
4.2.2.2.2 Cellulose fibers produced with an air gap 115
4.2.2.2.3 Cellulose/chitin fibers produced with an air gap 116
4.2.2.3 Chitin coating on cellulosic material procedure 118
4.2.2.4 Solvent recycling 119
4.2.3 Material characterization 119
4.2.3.1 Fiber characterization 119
4.2.3.1.1 Structural analysis 119
4.2.3.1.2 Mechanical tests 119
4.2.3.2 Coated material characterization 120
4.2.3.2.1 Composition 120
4.2.3.2.2 Morphology 120
4.2.3.2.3 Contact angle measurements 120
4.2.3.2.4 Water permeability equipment and experiment 121
4.2.3.2.5 Oxygen permeability equipment and experiment 122

4.3 Results and discussion 125
4.3.1 Fibers 125
4.3.1.1 Cellulose regenerated fibers from NMMO/GVL solutions 125
4.3.1.1.1 Lab-scale spinning 125
4.3.1.1.2 Industrial spinning performed by Lenzing AG 128
4.3.1.2 Cellulose/chitin fibers from IL 129
4.3.2 Coated cellulose materials with chitin 130
4.3.2.1 Filter paper coating 130
4.3.2.2 Textiles coating 131
4.3.2.2.1 Coating procedure 132
4.3.2.2.2 Structure of the coated textiles 133
4.3.2.2.3 Evaluation of new functional properties 137
4.3.2.2.4 Recycling of BmimOAc 143

4.4 Concluding remarks 145

Conclusions and summary 147

References 153

Appendices 163

List of Figures 168

List of Tables 173

List of Publications 175

Declaration 177

Introduction

Polymers are defined as compounds of many (from greek *polus*) parts (*meros*) or in other words large molecule with multiple repeating units. The existence of these molecules has revolutionized the scientific world since the 19th century. The initial studies of man-made polymers were performed thanks to the transformation of natural polymers, such as cellulose or rubber into "artificial polymers".[1] For instance, the first "artificial polymer" was nitrocellulose, which was prepared by Christian Schönbein in 1846 by means of cellulose esterification with a blend of sulfuric and nitric acids.[2] Since then, a lot of new and performant synthetic polymers have been developed and improve our daily lives as additives or material products. As shown in the overview in Figure I.1, polymers are found in a wide range of applications such as packaging, automobile and building components or electronics.[3]

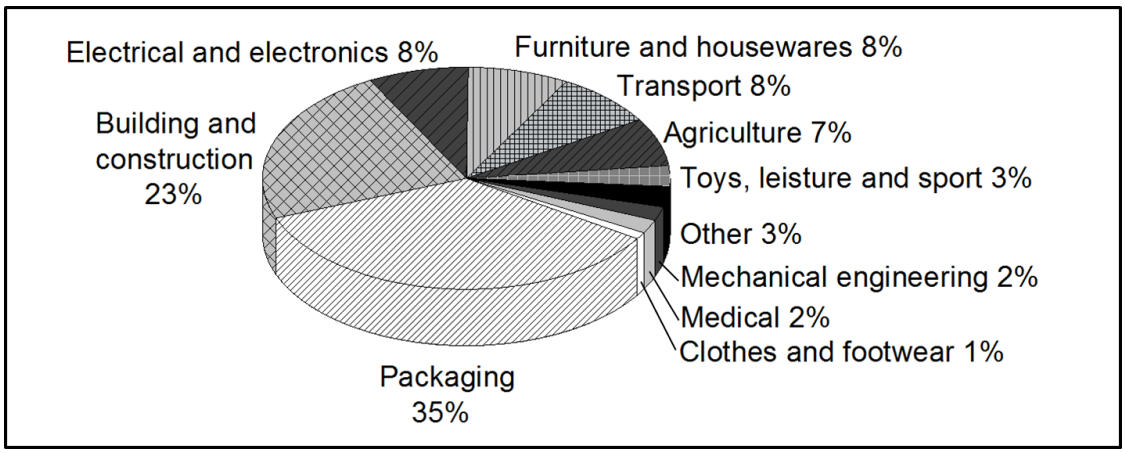

Figure I.1: *Overview of the uses of synthetic polymers in 2012.*

Unfortunately, the intensive use of synthetic polymers, such as nylon, polyvinyl chloride, polystyrene or polyethylene terephthalate, commonly known as plastics, has created a lot of non-biodegradable and hazardous waste, causing serious environmental problems.[4] Despite the widening consciousness for the necessity of recycling these materials, other solutions

have to be found to reduce the environmental impact of these harmful materials. In this context, the research and the development of biodegradable materials have gained more and more importance. As it can be seen in the bibliometric study from SciFinder® database in Figure I.2, the growing interest of the research on biodegradable materials started in the 2000s and led to an inflation of articles. Biodegradable materials can be defined as products capable of undergoing decomposition principally through enzymatic action of microorganisms into CO_2, water, methane, and other inorganic compounds in a limited duration of time.[5] The use and transformation of renewable resources such as biomass- or bio-based raw materials are the most promising aspects of the manufacturing of these biodegradable products. Typically, starch, vegetable crop derivatives, and wood are used for this purpose and cellulosic, starch-, and soy-based plastics have emerged.[5,6] These biodegradable products have already shown their potential to be used in a variety of industrial applications. Examples are packaging (bags, sacks, food packaging), domestic and hygiene goods (cups, cutlery, plates, diapers), agriculture (plant labels), and building materials (wall plasters).[5,7,8] In addition, other biodegradable polymers from other sources than land-based origins can be also used for the processing of such materials. For example marine feedstocks are a rich source of proteins, polysaccharides (e.g. chitin, agar, alginate, and carrageenan), and other polymeric compounds. These oceanic-derived compounds have potential uses in a wide variety of fields, such as in food, beverage, pharmaceutical, and cosmetic.[9]

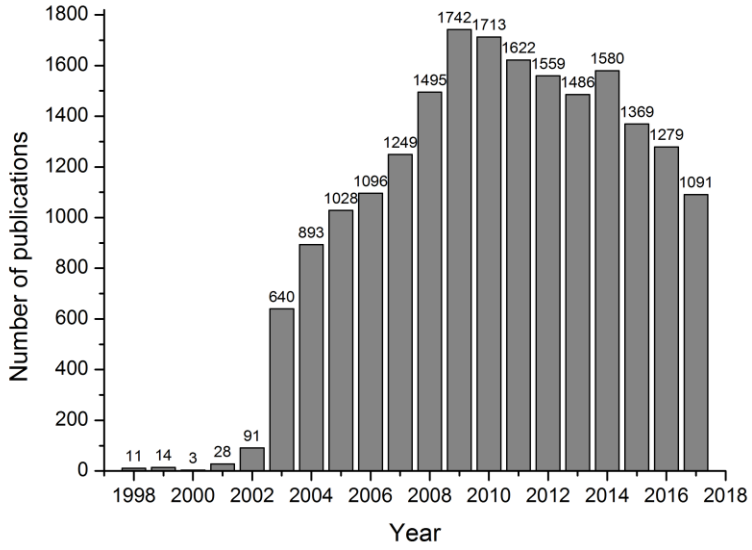

Figure I.2: *Bibliometric analysis from Scifinder® database about the number of publications (including scientific journals, patents, conferences) dealing with biodegradable materials.*

Materials can be simply composed of one biodegradable polymer or they can be designed through blend of two or more biopolymers. Novel bio-sourced products can thus be developed and adapted for specific requirements and for a more sustainable future.

This doctoral thesis deals with the preparation and the characterization of novel composite materials from cellulose and chitin. Cellulose and chitin are two abundant biopolymers, one from vegetal origin and the other mainly from marine source. Cellulose already plays a significant role in the production of daily materials such as textile fibers, paper or packaging.[10] However chitin still remains widely less utilized and a large part of its production (i.e. 60-70%) is used to produce its deacetylated derivative chitosan.[11] Cellulose and chitin are linear polysaccharides having a similar structure. Their tendency to decompose upon heating before reaching their melting point presents a major challenge. In order to process these biopolymers into materials, the main task is to dissolve them in appropriate solvents.

In this work, both polymers are equally investigated. First, the state of the art of their properties, implementations, and applications found in literature is presented. In the second part, proper solvents for cellulose and chitin dissolution are searched with the aim to provide an easy and eco-friendly method to process both biopolymers. In a further step, the effect of a sustainable co-solvent in the dissolution process of these two biopolymers is studied. All benefits of this addition are characterized to fully evaluate its potential in industrial manufacturing. Lastly, different novel materials comprising cellulose and chitin are prepared. For this purpose, cellulose and chitin blend materials as well as cellulosic textile coated with chitin are designed. Their new functional properties are characterized to assess their technological importance. Possible industrial implementations are studied in collaboration with Lenzing AG, leader in innovation for the manufacturing of cellulose fibers.

Chapter 1
Fundamentals

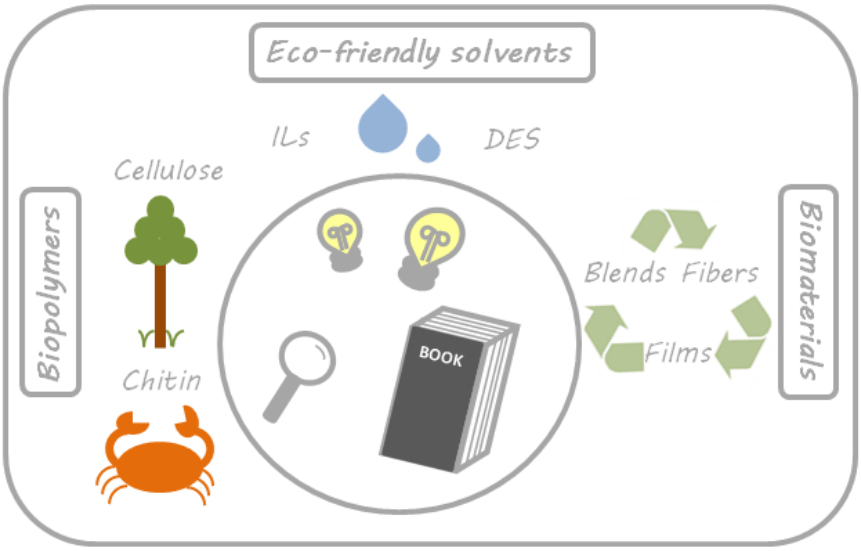

1.1 Cellulose and chitin: biopolymers and sustainable raw materials

1.1.1 Biopolymers and sustainable applications

The term biopolymer includes polymers derived from living organisms or synthetized from renewable resources. They can be categorized into three major families: (1) natural polymers such as proteins and polysaccharides, (2) synthetic polymers from bio-sourced monomers such as polyester (e.g. polylactic acid), and (3) polymers from microbial fermentation (e.g. polyhydroxyalkanoates).[12] Their study and utilization have attracted more and more the interest of researchers over the last 50 years as it is shown by the bibliometric study from SciFinder® database in Figure 1.1. The main reasons for this growing interest are the anticipation to the exhaustion of fossil energy resources and the awareness of the environment impacts of petrochemicals, which can accumulate in nature and are lethal threats for human beings.

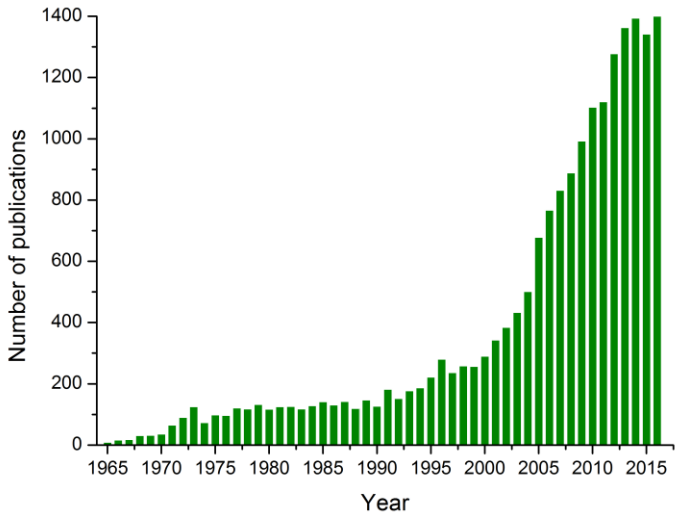

Figure 1.1: *Bibliometric analysis from Scifinder® database about the number of publications (including scientific journals, patents, and conferences) dealing with biopolymers.*

Natural polymers are available in high quantities on land and at sea. They are biodegradable and have diverse interesting properties and versatile utilities. These polymers can be used

alone or more generally combined with other polymers, as blend or reinforced fibers, to produce biodegradable materials with newly added values. Their different applications sectors are diversified and include medicine (e.g. drug delivery), packaging (e.g. composting bags), commodities (e.g. clothing and diapers), automotive (e.g. car components), building materials (e.g. wall plasters), and agriculture (e.g. pots).[5,7,13,14] Today, the best examples of manufacturing materials from renewable sources are starch-based bioplastics, produced by Novamont SpA under the name Mater-Bi®, and cellulosic fibers (TENCEL®, Lenzing Modal®, and Lenzing Viscose®) manufactured by Lenzing AG.[7,15]

Besides the development of biodegradable materials, natural polymers have also gained attention as a platform to produce fine chemicals and bioenergy as fuels, power, and heat. They are indeed considered as an abundant sustainable source of organic carbons and ideal alternatives to fossil resources. By using biorefinering technologies, which combine physical, chemical, thermochemical, and biotechnical methods, polymers from biomass can be separated, refined, and transformed into a large portfolio of bioderived intermediates and products.[16,17] For instance, the three major polymers contained in lignocellulosic biomass, i.e. cellulose, hemicellulose, and lignin, can be converted into more than 200 value-added compounds.[18] Figure 1.2 depicts an overview of the platform molecules produced from these polymers. Lignin, a three dimensional aromatic polymer, can generate mainly aromatic compounds such as substituted quinines, phenols (e.g. vanillin), and catechols. The two polysaccharides, cellulose and hemicellulose, are converted into sugar compounds (C_5 and C_6). Cellulose is hydrolyzed into glucose, whereas the depolymerization of hemicellulose results in the formation of the C_5 (xylose and arabinose) and C_6 (glucose, mannose, galactose, rhamnose) sugars. Via biological or chemical conversions, these sugars can be converted into a large number of valuable chemicals such as furfural, xylitol, sorbitol, and 5-hydroxymethylfurfural (HMF), and further transformed to various other fine chemicals (e.g. ethanol, levulinic acid).[18-20]

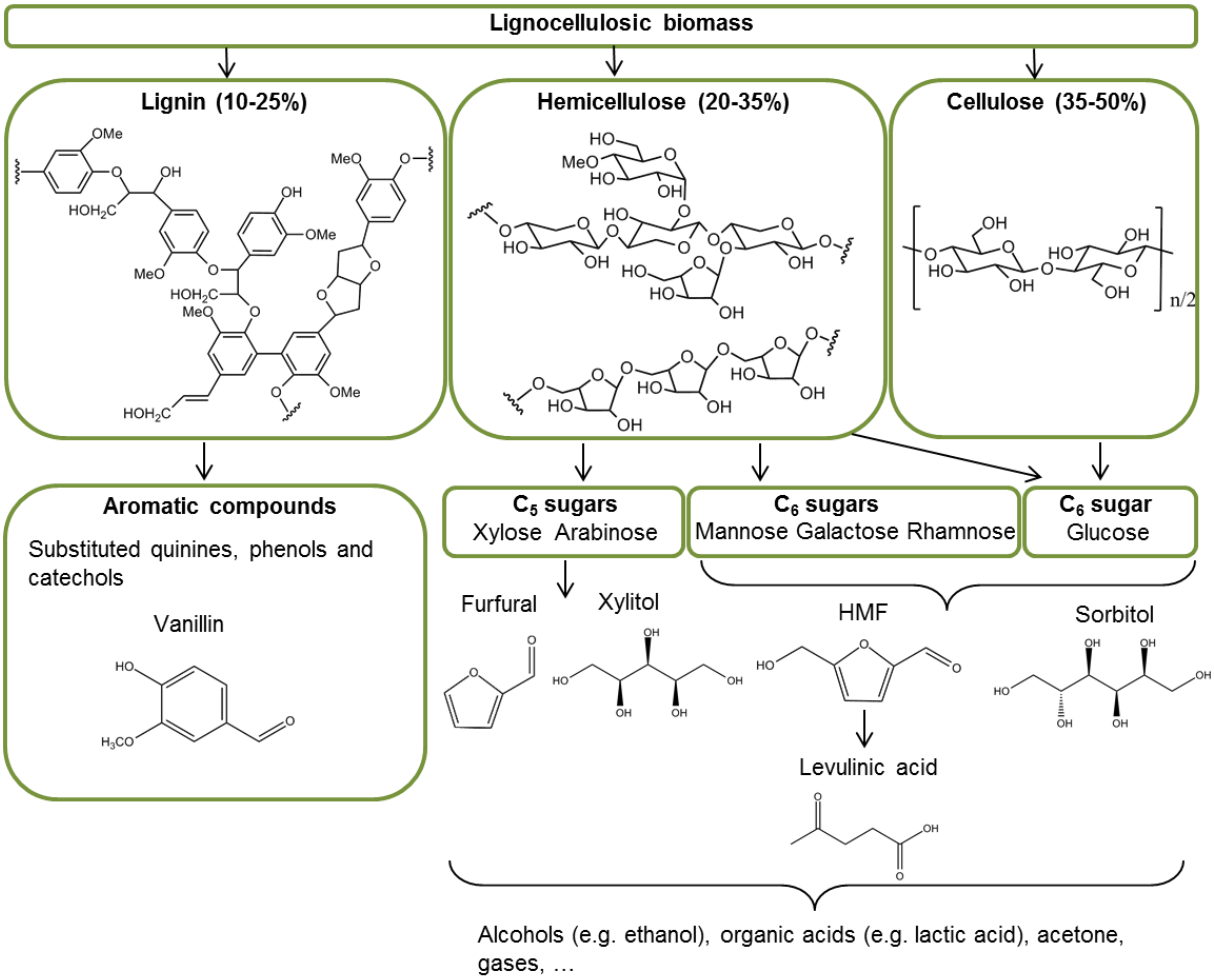

Figure 1.2: *Overview of the main platform molecules produced from lignocellulosic biomass.*[18-20]

1.1.2 Cellulose and chitin structures and properties in the solid state

Among the numerous natural polymers, cellulose and chitin are the most abundant biopolymers in nature. These polysaccharides have unique properties and characteristics which give them potential as alternative sources of materials to reduce the dependence on petrochemical feedstocks.

1.1.2.1 Cellulose

Since cellulose was discovered and isolated from green plants in 1838 by the French chemist Anselme Payen, the structure and the properties of this molecule have been intensively investigated.[10,21,22]

1.1.2.1.1 Sources and extraction

Cellulose is considered as the most abundant polymeric resource on earth with an annual production from biomass estimated to be about 10^{12} tons. This biopolymer is the principal skeletal component in all plants and can be found in smaller amounts in other living organisms such as bacteria, algae, and animals.[10,12,23] Table 1.1 illustrates the amount of cellulose present in some plants. Wood, cotton fibers, and cotton linters are the principal raw material sources for cellulose industrial processing. Typically cellulose is combined with lignin and hemicellulose in the cell wall of plants. Cellulose can be extracted from these plants thanks to different processes, for instance mechanical methods (e.g. cryocrushing or grinding), chemical treatments (e.g. acid hydrolysis or Kraft process), enzymatic treatments, and intensive ultrasonication.[24]

Table 1.1: *Percentage of cellulose present in some plants.*[24]

Source	Amount of cellulose (%)
Wood:	
Hardwood	43-47
Softwood	40-44
Non-wood:	
Cotton	95
Hemp	70
Jute	71
Corn cobs	45
Bagasse	40
Corn stalks	35
Coir	32-43
Wheat straw	30

1.1.2.1.2 Molecular structure

Cellulose is a linear polysaccharide composed of β-D-glucopyranose molecules linked through β-1,4-glycosidic bonds as shown in Figure 1.3. The repeat unit cellobiose contains two anhydroglucose rings. Each anhydroglucose unit (AGU) is 180° rotated axially from the previous unit and is in the energetically favorable $^4C_1$ conformation. This means that the hydroxyl groups, the hydroxymethyl groups, and the glycosidic bonds are equatorial. The two terminal units of the cellulose chain have different chemical properties. The glucose unit having the hydroxyl group at the C_1 carbon is referred to the reducing end because the anomeric carbon is free to convert to an aldehyde structure. In contrast, the anomeric carbon in the other terminal glucose with the hydroxyl group at the C_4 carbon is involved in a glycosidic bond. Therefore, it has no reducing properties.[10,23,25] The average number of AGU gives the chain length or degree of polymerization (DP) of the cellulose. The value of DP depends on the cellulose source material and extraction method. It can vary from 100 to 15 000.[10]

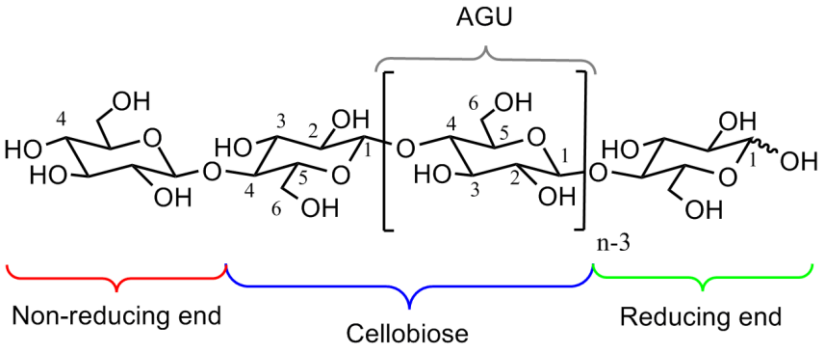

***Figure 1.3**: Molecular structure of cellulose. AGU stands for an anhydroglucose unit and n for the degree of polymerization.*

The hydroxyl groups placed at the positions C_2, C_3, and C_6 form with the oxygen atoms a large number of intra- and inter-molecular hydrogen bonds which are responsible for the stable polymer network (see Figure 1.4). The intrachain bonding gives the linear configuration of cellulose. The van der Waals forces and intermolecular hydrogen bonds cause the parallel aggregation of multiple cellulose chains forming elementary fibrils, which aggregate themselves into microfibrils.[26] These fibrils can contain cellulose chains regions,

which are highly ordered (crystalline structure) or disordered (amorphous structure). The ratio of amorphous cellulose to crystalline cellulose is defined by the degree of crystallinity and again depends on the cellulose source material and extraction method.[27]

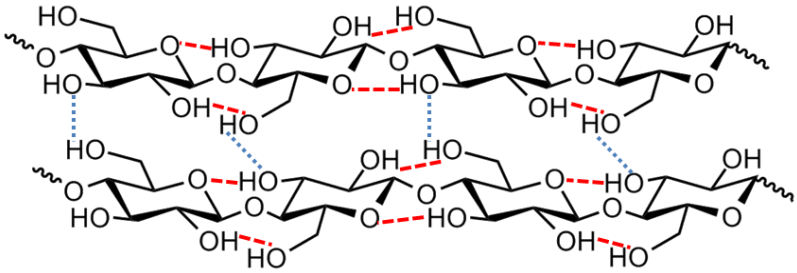

Figure 1.4: *Intermolecular (blue dotted line) and intramolecular hydrogen bonds (red dotted line) between two parallel cellulose chains.*[28]

1.1.2.1.3 Crystalline structure

There are different crystalline structures of cellulose: cellulose I, II, III_I, III_{II}, IV_I, and IV_{II}.[29] Cellulose I, or native cellulose, is the polymorph of cellulose found naturally in cellulose-based organisms. The cellulose chains in this structure are arranged in a parallel configuration. Cellulose II, or regenerated cellulose, is rarely present in nature but can be produced from cellulose I by solubilization and recrystallization (regeneration) or by aqueous sodium hydroxide treatment (mercerization). It is the most thermodynamically stable form and bears cellulose antiparallel chains.[30] Cellulose III_I and III_{II} are obtained from cellulose I and II treated with liquid ammonia or some amines, respectively. Subsequent heating up to 206 °C in glycerol produces the polymorph cellulose IV_I and IV_{II}.[31,32]

1.1.2.1.4 Properties

The hierarchical structure of cellulose described above governs its physical, chemical, and thermal properties. First, cellulose is a renewable, biodegradable, non-toxic, and non-edible polysaccharide. The extensive hydrogen bond network gives it high tensile and compressive strength. This network makes it also insoluble in water and in most organic solvents. This organization is also responsible for the non-thermoplastic properties of cellulose, which decomposes upon heating (above 240 °C) before reaching its melting point.[24,33] The hydroxyl groups of the molecule, especially in the amorphous regions, cause the hydrophilic and

hygroscopic character of the polymer as well as its large chemical modifying capacity.[10,24] Cellulose also possesses some other promising properties such as high sorption capacity, relative thermostabilization, and alterable optical appearance.[34]

1.1.2.2 Chitin

Chitin was first isolated from the fungal cell wall in 1811 by the French chemist Henri Braconnot and then in 1823 from the cuticle of an insect by Auguste Odier.[35,36] However, intensive research on this molecule and its applications began only later in the 1970's.[37]

1.1.2.2.1 Sources and extraction

After cellulose, chitin is the second most abundant natural polymer present on earth. This polymer is distributed in a wide variety of species such as arthropods, microorganisms, and invertebrate animals as it can be seen in Table 1.2. It is a major structural component in the cuticle of insects, in the backbone of squids, and in the exoskeleton of crustaceans and mollusks. In these organisms, chitin forms a complex network with proteins and minerals (mainly calcium carbonate). It contributes to their strength, reinforcement, and protection. Concerning the microorganisms, chitin is a characteristic component of the cell walls of fungi and certain green algae.[38,39]

Table 1.2: *Percentage of chitin present in some of its main sources.*

Source			Amount of chitin (%)
Arthropods	**Crustaceans:**		
		Crab	20-40 [39]
		Lobster	20-40 [39]
		Shrimp	20-40 [39]
		Krill	<10 [39]
	Insects:		
		Tobacco hornworm	2-34 [40]
		Cockroaches	30-42 [40]
		Coleoptera	11-41 [40]
		House fly	45 [40]
Microorganisms	**Algae:**		
		Coralline algae	<4.5 [41]
	Fungi:		
		Yeast	0.45 [39]
		Filamentous fungi	10-40 [39]
		Aquatic molds	58 [39]
Invertebrate animals	**Mollusks:**		
		Cuttlefish	6-40 [37]
		Octopus	6-40 [37]
		Squid	6-40 [37]
	Annelids:		
		Earthworm	0.2-38 [37]
		Leech	0.2-38 [37]

Despite the variety of sources, chitin has mainly been commercially produced up till now from crustacean shells (especially crabs and shrimps).[42] The easy accessibility of these materials as waste from the seafood processing industry and the high containing amount of chitin are the reasons of this only commercial exploitation.[37] The annual production of chitin from these resources is estimated to be about 75 000 tons.[39] The biopolymer is mainly used as raw material to produce chitosan. This deacetylated derivative finds application in cosmetic, biomedical, and food sector.[37] Chitin is extracted from shell wastes by a process, which removes the other compounds of shells (proteins, calcium carbonate, and pigments) step-by-step. After being washed and crushed, the shells are first treated with diluted hydrochloric acid to remove calcium carbonate and then deproteinized with a hot sodium hydroxide solution.[39] A decolorization step with oxidizing agents (e.g. potassium permanganate, sodium hypochlorite or hydrogen peroxide) can be additionally used to obtain a white powder.[37]

1.1.2.2.2 Molecular structure

Chitin is structurally similar to cellulose, but it is an amino-polysaccharide bearing acetamido groups at the C_2 positions, instead of hydroxyl groups for the cellulose molecule. Thus, the ideal structure of chitin is a linear polymer composed of *N*-acetyl-D-glucopyranose repeat units linked through β-1,4-glycosidic bonds as shown in Figure 1.5. However, in reality, 100% acetylated chitin cannot be obtained from the sources described above because of the alkaline treatment. Commercial chitin additionally contains *N*-glucosamine monomers (see Figure 1.5). The number of acetamido groups present in the molecule is defined by the degree of acetylation (DA), i.e. the ratio of *N*-acetyl-D-glucopyranose to *N*-glucosamine units. The term "chitin" is given to all copolymers composed of *N*-glucosamine and *N*-acetyl-D-glucosamine monomers with a DA bigger than 50% (generally 70-90%). Otherwise they are termed "chitosan". Thus, chitin is a heteropolymer while cellulose is a homopolymer.[43]

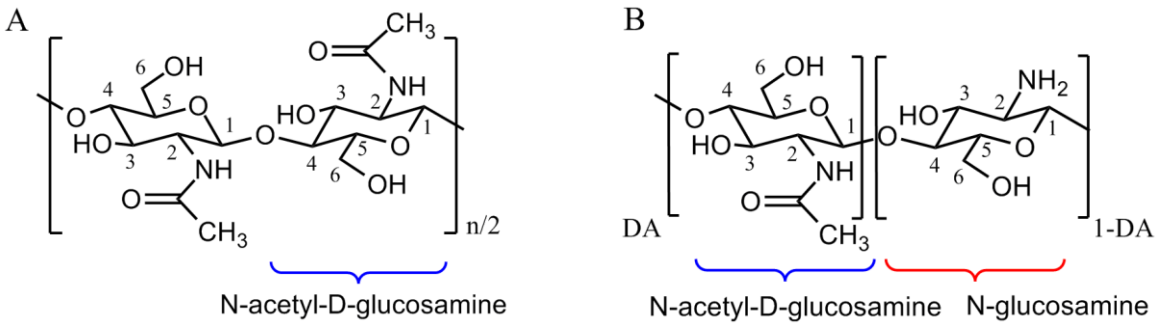

Figure 1.5: *(A) Idealized representation of the molecular structure of chitin and (B) real representation of commercial chitin. n stands for the degree of polymerization and DA for the degree of acetylation.*

The degree of polymerization of chitin extracted from crustaceans shells and squid pens is reported to be about 2000-4000.[44] Contrary to cellulose, which can have DPs lower than 500, chitin cannot be found with such low values.[45] This can be due to the fact that no depolymerization treatment has been found yet without affecting the DA of the chitin.[37]

As cellulose, the structural network of chitin is governed by a large number of inter- and intra-molecular hydrogen bonds making it stable and intractable. The additional acetamido group in the repeating unit increases the hydrogen bonding between adjacent chains (with C=O HN and –OH O=C associations) causing chitin network to be more complex than

cellulose.[45] These hydrogen bonds influence chitin to form crystalline microfibrils, which are usually embedded in a protein matrix in living organisms.[46]

1.1.2.2.3 Crystalline structure

Three polymorphic forms of chitin termed α-, β-, and γ-chitin are known. α-Chitin is the most abundant polymorph of chitin and occurs in the crustacean exoskeletons, in insect cuticles, and in fungal or yeast cell walls.[46] The chitin chains are organized in an antiparallel arrangement which is favorable for the formation of additional strong intermolecular hydrogen bonding. α-Chitin is the most stable form among the three crystalline variations.[47] β-Chitin is found in squid pens and in the endoskeleton of cuttlefish.[37,46] The molecule chains in this structure type are arranged in a parallel manner which forms weaker intermolecular hydrogen bonds.[48] γ-Chitin, less commonly found in nature, occurs in insect cocoons.[37] The structure of this polymorph is a mixture of α- and β-chitin, with two parallel strands alternate with one antiparallel.[49]

1.1.2.2.4 Properties

Chitin has similar properties as cellulose regarding its renewability, biodegradability, biocompatibility, and non-toxicity. Its structure renders it similarly insoluble in water or in the most organic solvents.[42] Chitin also degrades upon heating, at around 250 °C, before melting.[37] However, the presence of the amine groups (acetylated or deacetylated) confers its advantages over cellulose as strong antibacterial effect and other biological properties such as antitumor, analgesic or hemostatic.[50] It also enables chitin to have a less hydrophilic character, water retention capacity, and adsorption properties (with metal ions or hydrophobic organic compounds, for instance). The presence of functional groups (hydroxyl, acetamide, and amine) allows chitin to have a larger chemical modifying capacity than cellulose.[37,42,44]

1.2 Cellulose and chitin solubilization

As highlighted before, despite their abundance and interesting properties, cellulose and more particularly chitin potential remains under-exploited. They are limited by the fact that the biopolymers cannot be melted and degrade at elevated temperatures. To be processed, they can be chemically modified or dissolved. However, polymer dissolution without degradation or modification is essential to keep its native properties. Therefore, the research on suitable solvents for both biopolymers is a necessity. The state of the art of the effective solvents and especially direct ones (without chemical modification) will be discussed in this section as well as some theories about polymer solutions.

1.2.1 Theory on the solubility of polymers

A "good solvent" for a polymer is commonly defined as a substance that dissolves it well, while a "non-solvent" does not possess the power of dissolving this polymer. When a polymer is dissolved, solutions obtained are clear and uniform, whereas adding a non-solvent will cause the polymer precipitation.[51] The solution process of a polymer is more complex and slower than for non-polymeric materials. A multistep process occurs during polymer dissolution. Solvent molecules first diffuse into the polymer network and lead to the swelling of the polymer. If polymer-solvent interactions can overcome the polymer-polymer interactions, the polymer chains then disentangle and transfer into a true solution.[52]

From a thermodynamic point of view, the solubility of a substance (e.g. a polymer) is governed by the Gibbs free energy (Equation 1.1).

$$\Delta G_m = \Delta H_m - T\Delta S_m \quad (1.1)$$

where ΔG_m is the Gibbs energy of mixing, ΔH_m is the enthalpy of mixing, ΔS_m the entropy of mixing, and T the temperature.[52]

Solubility takes place when a negative value of the Gibbs energy of mixing occurs. That means that the enthalpy of mixing can be negative or balanced by the entropy term. For a

polymer, a high molecular weight induces a low entropic driving force. Therefore, the dissolution rate of a polymer decreases with increasing molecular weight.[53]

Specifically for macromolecules in solution, a mathematical model of the Gibbs energy was developed by Flory and Huggins. This model describes the free energy of mixing, ΔG_m, by:

$$\Delta G_m = RT[N_1 ln\Phi_1 + N_2 ln\Phi_2 + \chi_{12} N_1 \Phi_2] \quad (1.2)$$

where R is the gas constant, T the temperature, N_1 and N_2 the numbers of moles of solvent and polymer, Φ_1 and Φ_2 the volume fractions of solvent and polymer, and χ_{12} the parameter of solvent-polymer interactions. The values of χ allow distinguishing a good solvent from a bad one. A solvent with $0 \leq \chi \leq 0.3$ is called a good solvent, with $0.4 \leq \chi \leq 0.5$ it is a mediocre solvent, and with $\chi = 0.5$ the solvent is called ϴ solvent. The latter corresponds to the critical transition range from good to bad solvent conditions. Finally, a solvent with $\chi > 0.5$ is called a poor solvent or non-solvent. Unfortunately, the Flory Huggins model is not applicable to all polymer solutions. Very dilute polymer solutions are discontinuous in structure and have domains of polymer chain segments and regions of polymer-free solvent. This is not compatible with the Flory Huggins model. Anyway, this theory can give good thermodynamic features of solvent/polymer system.[51,54]

To completely understand the dissolution of polymers in solvents, kinetics has to be also considered. It plays an important role and controls the dissolution of a polymer. If a solvent is thermodynamically ideal, it can happen that the dissolution rate is too slow to form a homogeneous and bulk solution. Kinetics can be manipulated by different factors. Heat and mechanical energy generally enhance the diffusion of large molecules in a solvent, for example.[55]

1.2.2 Classical solvent systems

1.2.2.1 Cellulose

Cellulose solvents are known for a rather long time and can be classified into two categories: (1) derivatizing and (2) non-derivatizing solvent systems, depending on their interactions

with the cellulose molecules. Non-derivatizing solvents interact by physical intermolecular interactions which separate the polymer chains from each other, while derivatizing solvents dissolve cellulose by modifying it chemically and form derivatives.[56] For instance, carbon disulfide with sodium hydroxide (CS_2/NaOH) is utilized as a derivatizing solvent in the industrial viscose process and transforms cellulose into cellulose xanthate.[57] Concerning the most relevant non-derivatizing solvent systems, an overview of these solvents is given in Figure 1.6. Aqueous systems such as (1) inorganic-transition metal complexes (e.g. cuprammonium hydroxide (Cuam)), (2) mineral acids (e.g. H_3PO_4), (3) molten inorganic salt hydrates (e.g. LiX*H_2O and $ZnCl_2$*$4H_2O$), and (4) aqueous bases including ammonium hydroxides (e.g. tetraethylammonium hydroxide), phosphonium hydroxide (e.g. tetrabutylphosphonium hydroxide), pure alkali hydroxides (e.g. NaOH, efficient only for low DP cellulose), and alkali hydroxides with additives (e.g. NaOH with urea or thiourea) were found to be efficient media.[55,56] Also non-aqueous system has been found as direct solvents for cellulose. This category includes (1) single component solvents (e.g. *N*-ethylpyridinium chloride, *N*-methylmorpholine *N*-oxide), (2) mixtures of organic liquid with inorganic salts (e.g. *N*,*N*-dimethylacetamide/lithium chloride and dimethyl sulfoxide/tetrabutylammonium fluoride), (3) mixtures of organic liquid with amines and sulfur dioxide (e.g. dimethyl sulfoxide/diethylamine/sulfur dioxide), and (4) mixtures of ammonia or ammonium salts (e.g. NH_3/NaI (NH_4I)).[56]

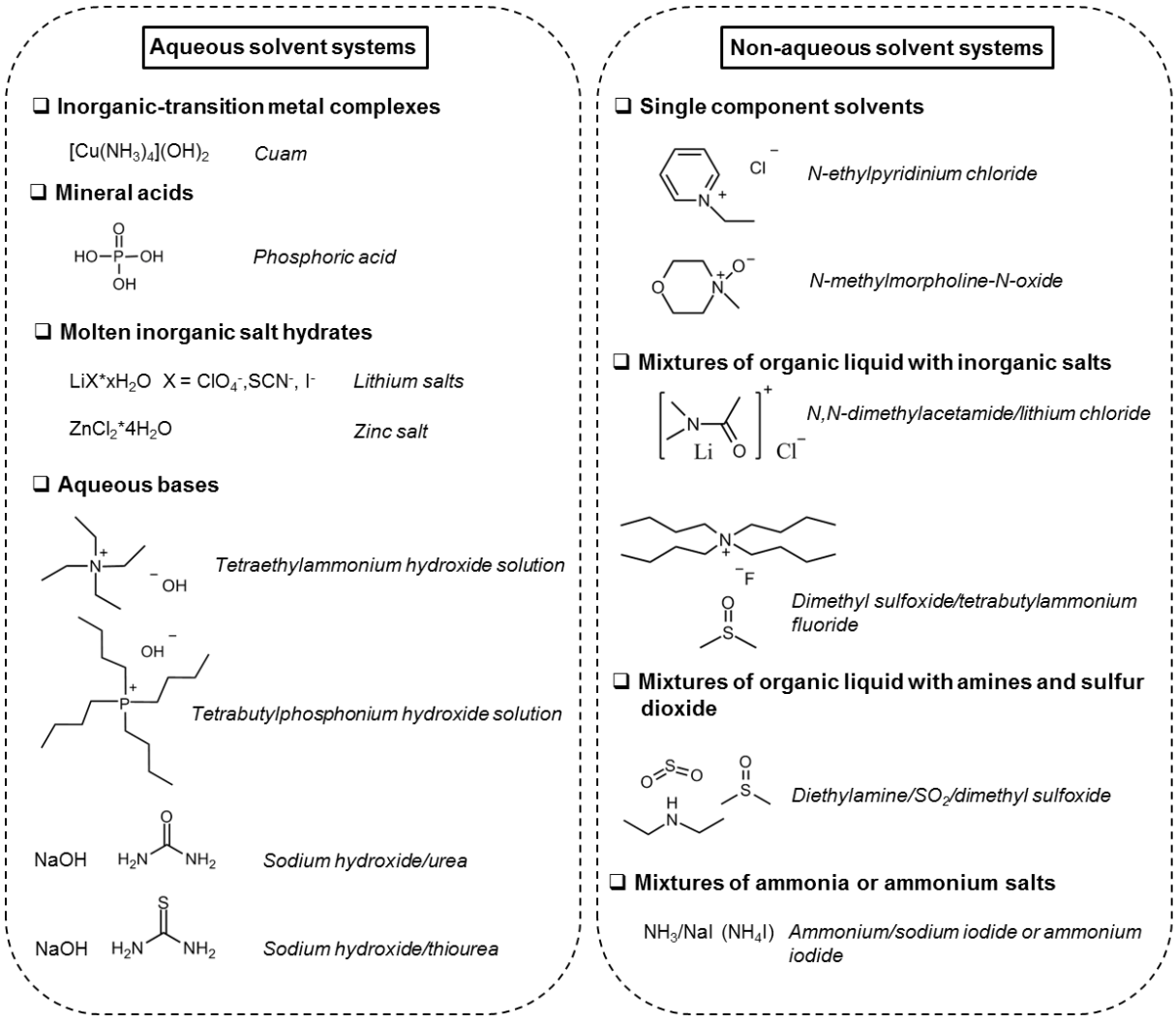

Figure 1.6: *Relevant examples of non-derivatizing cellulose solvents.*

Generally, the efficiency of the solvents is governed by their ability to interfere with and break the existing intermolecular hydrogen bonds of cellulose, according to many author's opinions.[53,56,58] It has to be mentioned that other parameters such as the mixing conditions (time, temperature, etc.), the viscosity of the solvent, the crystallinity and the DP of cellulose can also influence the dissolution success.[58]

The exact interactions between the solvent system and cellulose can differ according to the physical-chemical properties of the used solvents (aqueous or non-aqueous media, simple or multicomponent mixtures, organic or inorganic compounds, ...). A lot of reviews have

summarized these interactions more in detail.[53,55,56,58] However, for some solvent systems, the specific solvation mechanism is sometimes interpreted differently or is not completely understood. For instance, the most frequently used solvent mixture *N*,*N*-dimethylacetamide/ lithium chloride (DMAc/LiCl) has received different hypotheses concerning its interaction with cellulose. The mechanism proposed by McCormick *et al*. was that the lithium ions form macrocations with the carbonyl group of DMAc while the unencumbered small electronegative anion Cl^- plays the major role in breaking the intra- and inter-hydrogen bonds of the cellulose.[59] But some other authors (e.g. El-Kafrawy, Morgenstern *et al.*) questioned the role of the lithium cations in the solvation process. The cation could be associated not only with the carbonyl oxygen of DMAc but also with the hydroxyl oxygen of the cellulose.[60,61] Figure 1.7 illustrates these two proposed dissolution mechanisms.

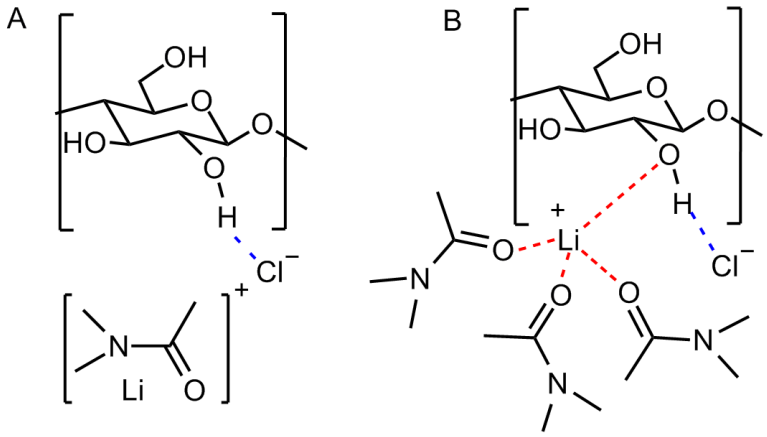

Figure 1.7: *Proposed interaction between LiCl/DMAc and cellulose acting as the dissolution mechanism by (A) McCormick et al. (B) Morgenstern et al.*

Some researchers have thought about a hypothetic systemization for the cellulose dissolution mechanism. After structural studies of three traditional non-derivatizing solvents, *N*-methylmorpholine *N*-oxide (NMMO), DMAc/LiCl, and dimethyl sulfoxide tetrabutyl-ammonium fluoride (DMSO/TBAF), Pinkert *et al.* proposed that all non-dervatizing solvents for cellulose can be hypothetically arranged with themselves in cyclic structures (see Figure 1.8). The involvement of the compounds in this arrangement is related to their dissolution ability because energetically favored geometries enable the solvents to give hydrogen bonds of high stability compared to those in cellulose.[58] For instance, the ring

formation is assisted more favorably by small ions and polar characteristics than larger cations such as NMMO and TBAF. Thus, the dissolution ability of small ions, such as lithium, is enhanced compared to compounds with steric hindrance.[58]

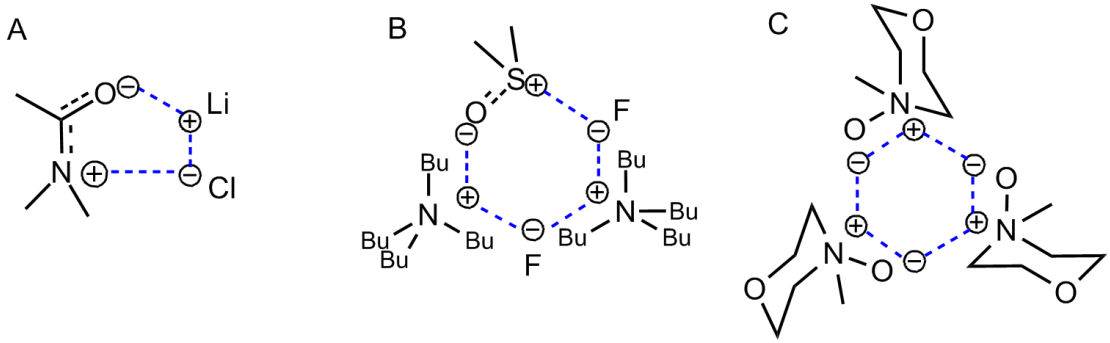

Figure 1.8: *Hypothetical ability of the three non-derivatizing solvents to arrange in a cyclic formation: (A) DMAc/LiCl (5-ring geometry), (B) DMSO/TBAF (6-ring geometry), (C) NMMO (6-ring geometry).*[58]

Contrary to the majority of opinions, Lindman *et al.* proposed another systematic pattern. They highlighted the amphiphilic character of cellulose. These authors suggested that the key to dissolve cellulose is the elimination of the hydrophobic interactions between cellulose molecules rather than hydrogen bonding interactions.[53,62,63] Thus, they implied that cellulose dissolution would be facilitated in amphiphilic solvents. For example, they illustrated this hypothesis with the efficiency of NMMO, which contains polar and non-polar parts, or with the enhancing solubility in NaOH solutions with the addition of specific additives, such as urea, or amphiphilic organic cation.[63,64]

This "new" vison of cellulose dissolution mechanism is a matter of debate between the cellulose scientists.[65] The amphiphilic character of cellulose is not contested. However, the (in)solubility explanations, the tardive realization, and some irrelevant observations in the Lindman hypothesis are still up to discussion.[65] In this way, the exact understanding of cellulose dissolution mechanism is still challenging scientists.

Another challenge for researchers is the development of alternative and more sustainable solvent systems for the dissolution of cellulose. Indeed, the classical solvents mentioned above suffer from a lack of compatibility with the environment. They lead to some concerns

regarding their toxicity, volatility, high cost, non-biodegradability, unrecoverability or even thermal instability.[58,66,67]

1.2.2.2 Chitin

For the dissolution of chitin, only a limited number of classical solvent systems are known in contrast to cellulose solubilization. The more complex hydrogen bonds network of chitin can be the factor for this restriction.[68] The most popular solvents are (1) halogenated solvents, such as di- and tri-chloroacetic acid, formic acid/dichloroacetic acid mixtures and hexafluoroisopropyl alcohol;[69] (2) salt solutions such as DMAc/LiCl, *N*-methyl-2-pyrrolidone/LiCl and $CaCl_2 \cdot 2\,H_2O$/saturated methanol;[70,71] and (3) alkali aqueous systems, e.g. urea or thiourea/NaOH solutions.[72,73] Figure 1.9 gives an overview of these relevant examples.

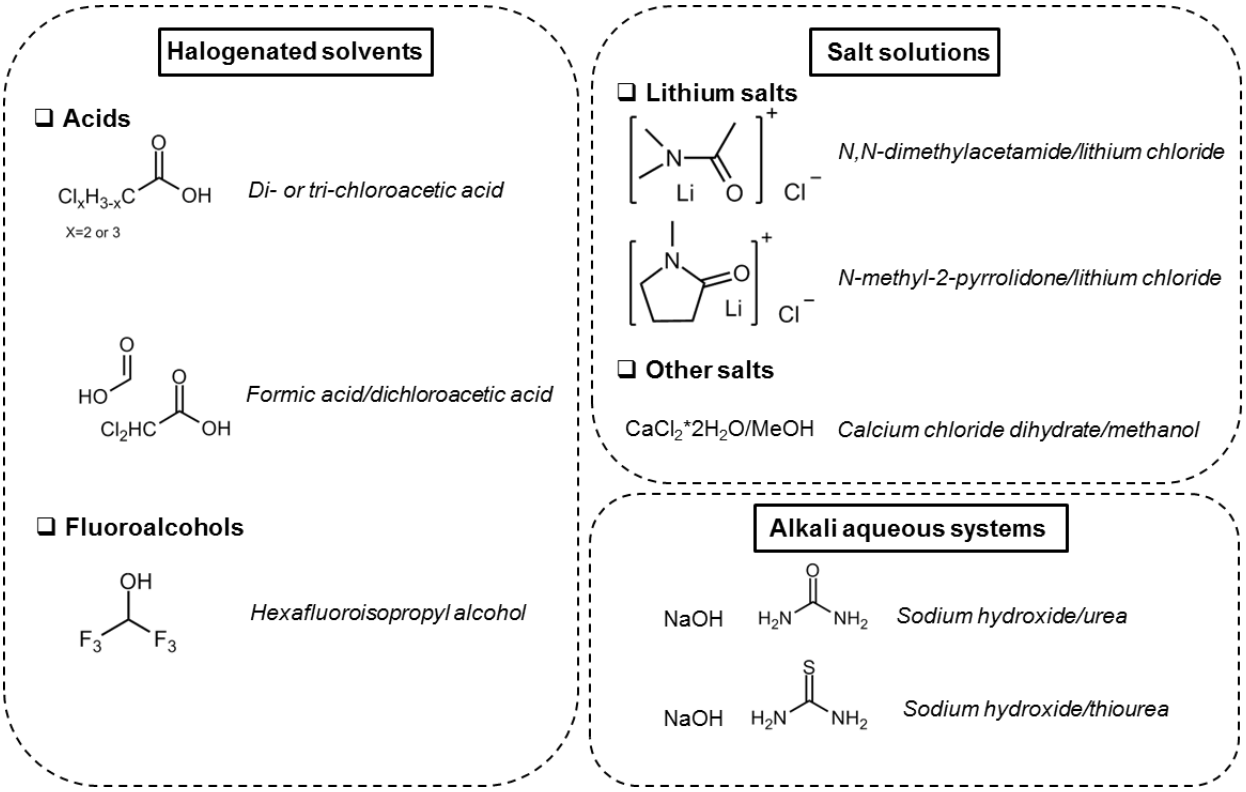

Figure 1.9: *Main classical solvents used for chitin dissolution.*

The mechanism of the dissolution of chitin in all these solvents has not been fully resolved. As for cellulose, the common opinion suggests that the solvent systems with hydrogen bond acceptors (e.g. Cl^-) or donors (NH_2 in urea or thiourea) break up the intra- and inter-molecular hydrogen bonds of chitin.[68,74] Again many of these solvents are toxic, corrosive, mutagenic, non-biodegradable, not easy to recycle or degrade chitin during the dissolution process.[68]

With regard to common solvents for cellulose and chitin, the capacity to dissolve both polymers is limited to *N*,*N*-dimethylacetamide/lithium chloride and alkaline (NaOH) urea or thiourea mixtures. Hence, the development of alternative solvents persists as a crucial interest for researchers.

1.2.3 Alternative solvents

1.2.3.1 Environmental aspects

The need of alternative and green solvents appeared with the concept of green chemistry two decades ago. Most solvents used in chemical processes are volatile, toxic and have an impact on the environment and human health. They have to be eliminated from the industrial process and replaced by chemical products and processes that are more environmentally friendly. For this, Paul Anastas and John Warner created in 1998 twelve principles as guidelines for sustainable chemistry and processes.[75] Jérôme *et al.* adapted these principles to solvents solely and proposed a list of criteria that a green solvent has to follow:

"**(1) Availability:** a green solvent needs to be available on a large scale, and the production capacity should not greatly fluctuate in order to ensure a constant availability of the solvent on the market.

(2) Price: green solvents have to be not only competitive in terms of price but also their price should not be volatile during time in order to ensure sustainability of the chemical process.

(3) Recyclability: in all chemical processes, a green solvent has to be fully recycled, of course using eco-efficient procedures.

(4) Grade: technical grade solvents are preferred in order to avoid energy-consuming purification processes required to obtain highly pure solvents.

(5) Synthesis: green solvents should be prepared through an energy-saving process and the synthetic reactions should have high atom-economy.

(6) Toxicity: green solvents have to exhibit negligible toxicity in order to reduce all risks when manipulated by humans or released in nature when used for personal and home care, paints, etc.

(7) Biodegradability: green solvents should be biodegradable and should not produce toxic metabolites.

(8) Performance: to be eligible, a green solvent should exhibit similar and even superior performances (viscosity, polarity, density, etc.) compared to currently employed solvents.

(9) Stability: for use in a chemical process, a green solvent has to be thermally and (electro)chemically stable.

(10) Flammability: for safety reasons during manipulation, a green solvent should not be flammable.

(11) Storage: a green solvent should be easy to store and should fulfill all legislations to be safely transported either by road, train, boat or plane.

(12) Renewability: the use of renewable raw materials for the production of green solvents should be favored with respect to the carbon footprint." [76]

In practice, it is quite difficult to find a solvent that meets all these criteria. Nevertheless, few solvents such as ionic liquids, deep eutectic solvents, water, and bio-based solvents fulfill some of these principles and are considered as more or less "green".[76,77]

1.2.3.2 Ionic liquids

1.2.3.2.1 General aspects and properties

Ionic liquids (ILs) are by definition salts consisting entirely or almost exclusively of ions and melt below 100 °C. When they are liquid at room temperature, they are called "room-

temperature ionic liquids (RTILs)".[78] They are formed from bulky, unsymmetrical ions with delocalized charge and are generally classified into two groups: (1) protic ILs (PILs) and (2) aprotic ILs (AILs).[79] AILs consist of non-protonated cations and anions, while PILs are formed by proton transfer from a Brønsted acid to a Brønsted base.[78] The first reported IL, ethylammonium nitrate, was discovered by Walden in 1914. However, massive investigations of novel ILs (especially RTILs) as a new class of solvent began only in the 1990's.[77] Due to their specific characteristics such as negligible vapor pressure, non-inflammability, high thermal and chemical stability, recyclability, and wide viscosity range, ILs have some advantages over classical volatile solvents. They are thus classified as "green solvent".[77] Moreover, a huge variety of anions and cations combinations (estimated to be around 10^{18}) allows the formation of ILs with specific properties, designated as task-specific ionic liquid.[80] Recently, several studies have shown that some ILs are toxic, poorly degradable or not degradable at all. They are also generally considered as very expensive solvents and thereby have questioned the determining "green solvents".[81,82]

1.2.3.2.2 Dissolution of cellulose and chitin in ILs

Over the last decades, ILs have been thoroughly investigated and widely exploited in various fields of science and technology. Among other things, they appeared to be the ideal alternative to the classical solvents for the dissolution of cellulose and chitin. In Figure 1.10, a bibliometric analysis from SciFinder® database combining "cellulose"/"chitin" "dissolution" in "ionic liquids" as keywords highlights the intensive interest of scientists for this purpose. It also illustrates the higher number of publications (including scientific journals, patents, and conferences) about cellulose over the last 15 years. In contrast, publications about chitin dissolution in ILs are less recurrent. For instance, in 2012, 313 publications can be found for cellulose whereas only 19 dealt with the dissolution of chitin in ILs. Chitin has more solubility problems than cellulose leading to less processability.

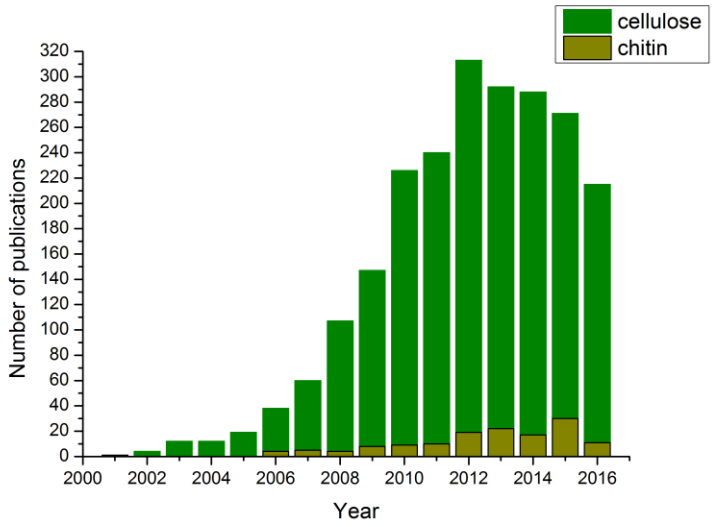

Figure 1.10: *Bibliometric analysis from Scifinder® database dealing with the dissolution of cellulose and of chitin in ILs.*

1.2.3.2.3 ILs as cellulose solvents

The first molten salt system employed for the dissolution of cellulose was reported in 1934 by Graenacher with a mixture of pyridinium salt and nitrogen-containing bases.[83] Later, in 2002, Swatloski *et al.* revealed several RTILs containing 1-alkyl-3-methylimidazolium cations and different anions (chloride, bromide, and thiocyanate) able to dissolve cellulose.[84] Since then, a huge variety of ILs has been investigated as cellulose solvents and detailed lists can be found in several reviews.[28,79,85] Briefly, the most famous ILs for cellulose include several class of cations, mainly imidazolium, pyridinium, ammonium, and phosphonium derivatives, shown in Figure 1.11. As anion, they are mainly composed of halide (e.g. chloride, bromide), carboxylate (e.g. formate, acetate), and thiocyanate, also shown in Figure 1.11. Table 1.3 gives examples for the combinations of these cations and anions forming ILs able to solubilize cellulose. These data are extracted from the review of Pinkert *et al.*[79] It should be mentioned that methylimidazolium-based RTILs with different alkyl substituents are the most predominant ILs as cellulose solvents in literature. For the anion, chloride and acetate seemed to be the most efficient ones.[79] It can additionally be observed that many factors such as the DP of cellulose and the dissolution conditions (temperature, thermal or microwave heating) significantly influence the cellulose solubility in ILs. This can

be well illustrated with the IL 1-butyl-3-methylimidazolium chloride (BmimCl, see Table 1.3). Under the same experiment conditions, 18 wt% cellulose with a DP of 286 were dissolved in BmimCl while only 13 wt% cellulose with a higher DP of 593 were solubilized. Moreover, the solubility of cellulose (with a DP of 1000) in BmimCl could be increased by 2.5 times through microwaving instead of regular thermal heating.[79] The presence of water and impurities in ILs and the high viscosity can also be an obstacle in the dissolution process of cellulose because of competitive hydrogen bonding and lower ion mobility.[58,84,86]

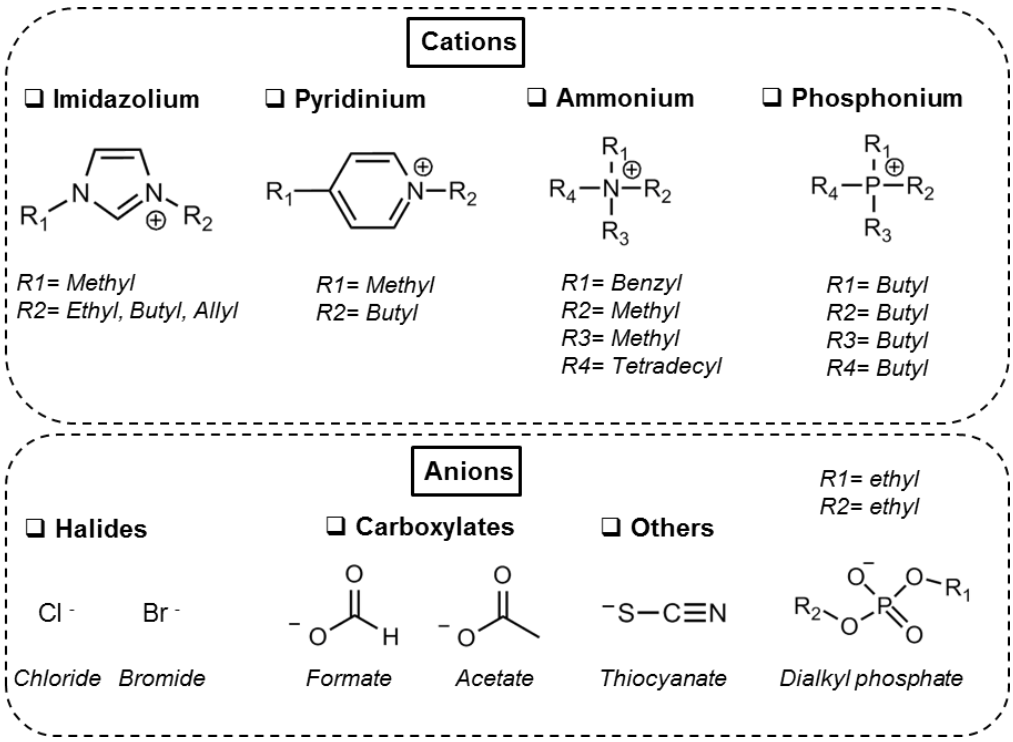

Figure 1.11: *Relevant cations and anions present in ILs having the capacity to dissolve cellulose.*

Table 1.3: *Examples of some ILs able to dissolve cellulose, their cellulose dissolving capacities according to the DP of cellulose and the solubility conditions.*

Ionic liquid	DP of cellulose	Conditions	Cellulose solubility (wt%)
1-Butyl-3-methylimidazolium chloride	286	83 °C, 12 h	18
	593	83 °C, 12 h	13
	1000	100 °C, n.a.[a]	10
	1000	70 °C, n.a.[a]	3
	1000	MW[b]	25
1-Butyl-3-methylimidazolium bromide	1000	MW[b]	5-7
	α-Cellulose	90 °C, 12 h	Insoluble
1-Butyl-3-methylimidazolium thiocyanate	1000	MW[b]	5-7
1-Butyl-3-methylimidazolium acetate	569	n.a.[a]	13.2
1-Ethyl-3-methylimidazolium acetate	225	110 °C, n.a.[a]	15
	569	n.a.[a]	13.5
1-Allyl-3-methylimidazolium formate	250	85 °C, n.a.[a]	21.5
3-Methyl-*N*-butylpyridinium chloride	286	105 °C, 12 h	39
	593	105 °C, 12 h	37
	1198	105 °C, 12 h	12
Benzyldimethyl(tetradecyl)ammonium chloride	286	62 °C, 12h	5
	593	62 °C, 12 h	2
	1198	62 °C, 12 h	1
Tetrabutylphosphonium formate	225	110 °C, n.a.[a]	6
1-Ethyl-3-methylimidazolium diethyl phosphate[87]	398	100 °C, 2 h	12-14

[a]n.a. = not specified by the authors [b]MW = microwave heating

From a guidance standpoint, Pinkert *et al.* compared the structural aspects of the dissolving and non-dissolving IL ions. They suggested a list of the characteristics for a good cellulose solvent. Cations favorable for the cellulose solubilization are (1) nitrogen-containing aromatic heterocycles with the ability to delocalize their positive charge within the aromatic π-system and (2) ring molecules with dipolar character (heteroatom) or very polar character for the non-rings. The anions require an ability to act as a hydrogen bond acceptor, preferably small in size, and their substituents should not be bulky or hydrophobic.[58]

1.2.3.2.4 ILs as chitin solvents

Due to strong structural similarities between cellulose and chitin, the ILs used for cellulose dissolution have been also investigated for chitin. However, only a few of them, mostly methylimidazolium based RTILs were efficient for chitin.[88] Table 1.4 gives an overview of the IL solvents for chitin found in several publications. The most promising ILs seem to be 1-

allyl-3-methylimidazolium bromide and 1-butyl-3-methylimidazolium acetate. Once more, the dissolution conditions and the properties of chitin (namely its crystallinity, molecular weight and DA) affected the dissolution of chitin in ILs, as shown in Table 1.4. Wang *et al.* studied for instance the influence of the molecular weight and the DA of the chitin on the dissolution.[89] They demonstrated that alkali treatments to deacetylate chitin render it more easily soluble in ILs compared to the native chitin. The deacetylation process has namely several impacts on chitin. First, the extensive hydrogen bond interactions are reduced by the decrease of the carbonyl groups. In addition, the molecular weight decreases and the amorphous domains in chitin increase. All these modifications facilitate the penetration of IL between the chitin chains.[89] Finally, it is quite important to know the exact information about the chitin used (source, DA, molecular weight, purity) for dissolution studies.

Table 1.4: *Examples of ILs able to dissolve chitin, their chitin dissolving capacities according to the information given by the authors about the chitin used.*

Ionic liquid	**Chitin information**	**Conditions**	**Chitin solubility (wt%)**
1-Butyl-3-methylimidazolium chloride	n.a.[a]	110 °C, 5 h	10 [90]
	α-Chitin (η=35 cp, DA=99%)[b,c]	110 °C	Partially soluble[45]
	β-Chitin (η=15 cp)[b]	110 °C	Partially soluble[45]
	β-Chitin (η=15 cp)[b]	110 °C	Partially soluble[45]
1-Butyl-3-methylimidazolium acetate	α-Chitin (η=35 cp, DA=99%)[b,c]	110 °C	6 [45]
	β-Chitin (η=15 cp)[b]	110 °C	6-7 [45]
	β-Chitin (η=278 cp) [b]	110 °C	3 [45]
1-Ethyl-3-methylimidazolium acetate	Pure and practical grade	MW[b]	3.8 [91]
1-Ethyl-3-methylimidazolium chloride	Pure grade	100 °C, 19 h	3.5 [91]
	Practical grade	100 °C, 19 h	1.5 [91]
1-Allyl-3-methylimidazolium bromide	α-Chitin (DA=94.6%)[c]	100 °C, 48 h	5-7 [92]
1-Allyl-3-methylimidazolium chloride	DA=91.6%[c], Mv=1.23x10^5 g/mol[d]	<45 °C	0.5 [89]
1-Allyl-3-methylimidazolium acetate	DA=91.6%[c], Mv=1.23x10^5 g/mol[d]	110 °C	5 [89]
1-Methyl-3-methylimidazolium dimethyl phosphate	DA=91.6%[c], Mv=1.23x10^5 g/mol[d]	<60 °C	1.5 [89]
1-Ethyl-3-methylimidazolium dimethyl phosphate	DA=91.6%[c], Mv=1.23x10^5 g/mol[d]	<60 °C	1.5 [89]

[a]n.a. = not specified by the authors [b]η = intrinsic viscosity [c]DA = degree of acetylation
[d]Mv = molecular weight [e]MW = microwave heating

1.2.3.2.5 Mechanism of dissolution

The dissolution mechanism of cellulose and chitin in ILs has been again proposed by the majority of the authors to be a question of cleavage of the hydrogen bonds interaction between the polymer chains.[58,84,88,89,93]

Cellulose

Authors first assumed that the anion of the IL bears the main responsibility to break the hydrogen bonding to dissemble cellulose chains with no specific role for the cation.[84,94] For example, Swatloski *et al.* investigated the solubilization power of 1-butyl-3-methylimidazolium ILs with different anions. They suggested that anions, which are small and strong hydrogen bond acceptors (such as chloride) were more efficient than ILs containing larger or non-coordinating anions such as tetrafluoroborate or hexafluorophosphate.[84] However, it was observed that certain combinations of ILs containing good hydrogen bond accepting anions can be ineffective with certain cations. For instance, ILs containing chloride and cations such as pyrrolidinium or piperidinium or longer-chain substituted (hexyl,octyl) methylimidazolium cations were found to be not or less powerful.[58,84] These observations and further studies (i.e. ILs screening with a variety of combinations, NMR studies, and molecular dynamics simulations) have motivated scientists to investigate the role of individual ionic species in the dissolution process.[28,66,95-99] Zhang *et al.* suggested with the study of 1-allyl-3-methylimidazolium chloride (AmimCl) that the ion pairs dissociate to free $Amim^+$ and Cl^- above the critical temperature. Cation and anion individually play a role in the disruption of the cellulose hydrogen bonding. Cl^- ions interact with the cellulose hydroxyl proton while free $Amim^+$ forms complex with the hydroxyl oxygen. This suggested mechanism scheme is represented in Figure 1.12.[66,97]

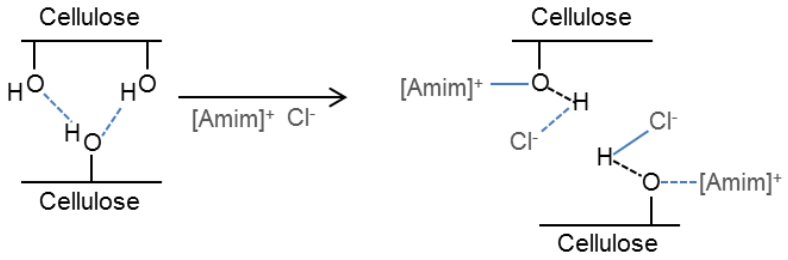

Figure 1.12: *Dissolution mechanism of cellulose in the IL 1-allyl-3-methylimidazolium chloride (AmimCl) proposed by Zhang et al.*

Generally, mostly all depth researches are in accordance with the predominant role of the anion in the dissolution pattern due to its interactions with the cellulose hydroxyls as suggested by Zhang *et al.*[95,98,100] However, the exact role of the cation is still unclear and different interpretations about the cations-cellulose interactions can be found in literature. A brief overview of these controversial explanations is presented below. Zhang *et al.* argued with NMR experiments on the cellobiose solvation with 1-ethyl-3-methylimidazolium acetate (EmimOAc) that both, anion and cation, associate with the hydroxyl groups. The anion forms hydrogen bonds with the hydrogen atoms of the hydroxyl groups. The cation, thanks to the most acidic proton, associates with the oxygen of the hydroxyls with less steric hindrance.[98] Conversely for the same IL, Youngs *et al.* demonstrated that the IL cation plays only a minor role via van der Waals interactions and does not participate in hydrogen bonding. These observations were performed with NMR and molecular dynamics study of glucose dissolved in EmimOAc and extrapolated to cellulose.[99] According to Lindman *et al.*, the cations of ILs have amphiphilic properties and interact through hydrophobic associations with cellulose.[53] Recently, with the study of 13 different cations combined with an acetate anion, Lu *et al.* suggested that cations affect the cellulose dissolution in two ways. First, acidic protons in cation form hydrogen bonds with cellulose hydroxyl oxygen and ether oxygen and are important for the dissolution. Secondly, strong cation-anion interactions or steric hindrance of large sized groups in cation negatively affect the dissolution. In addition, they supposed that van der Waals interactions between cations and cellulose are irrelevant for the dissolution mechanism.[95] A larger molecular dynamics study with anions, i.e. chloride, acetate, and dimethylphosphate, paired with alkylimidazolium-based cations was done by

Rabideau *et al.* to understand the individual role of IL ions in the cellulose solvation. They suggested that cations interact mainly at the cellulose surface with the anions bound at the polar domains of cellulose via electrostatic interactions. In addition, they showed that cations are also in contact with the non-polar domains of cellulose via van der Waals interactions and fill the gaps between the cellulose-bound anions sites.[96] Thus, the role of the cation is still the subject of an ongoing debate.

As for the cellulose classical solvents, Pinkert *et al.* have shown the possible arrangement of the most effective ILs into stable cyclic arrangements and thus postulated that all non-derivatizing solvents follow a similar pattern. For example, the hypothetical ability of 1,3-dialkylimidazolium chloride to form a 6-ring geometry and the involvement of the acidic imidazolium proton in this structure is illustrated in Figure 1.13.[58]

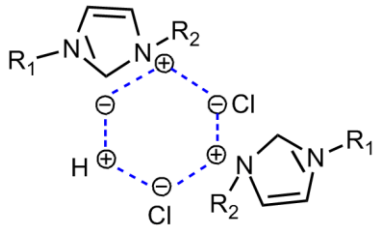

Figure 1.13: *Hypothetical ability of a 1-3-dialkylimidazolium chloride IL to arrange in a 6-ring geometry.*[58]

Chitin

The limited reports on chitin dissolution in ILs have not carefully investigated its exact solvation mechanism. It was generally assumed that the anions play the key role in the dissolution, analogous to cellulose dissolution. Anions with strong hydrogen bond acceptor ability were suggested to cleave the extensive hydrogen bond network of chitin.[45,88,89,91] To our knowledge, the role of cations in chitin dissolution has not been elucidated yet.

After all, ILs are new promising efficient solvents for the solubilization of cellulose and chitin. However, as outlined before, their disadvantages such as high costs and toxicity are obstacles to their industrial scale applications and processing. Thus, scientists tried to replace them with other greener solvents such as deep eutectic solvents.

1.2.3.3 Deep eutectic solvents

1.2.3.3.1 General aspects and properties

Deep eutectic solvents (DESs) are fluids obtained by heating two or more components capable of association with each other through hydrogen bond interactions. They form a eutectic mixture, i.e. a mixture with a lower melting point than that of the individual components. For instance, the most widely used DES, choline chloride + urea (in a molar ratio of 1:2), has a melting point of 12 °C, whereas choline chloride and urea melt at 302 °C and at 133 °C, respectively.[101] DESs are generally liquid at temperatures lower than 150 °C, mostly between room temperature and 70 °C.[101] Contrary to ionic liquids, which are entirely composed of ionic species, DESs comprise also non-ionic ones.[101] Indeed, most of the DESs are obtained by complexation of a quaternary ammonium halide salt with a metal salt (e.g. metal halides) or hydrogen bond donor like carboxylic acids, amides, amino acids, and alcohols.[102] Depending on the nature of the complexing agent, DESs are generally classified into four groups:[102,103]

Type I: organic halide salt + metal chloride (e.g. 1-ethyl-3-methylimidazolium chloride/ $AlCl_3$)

Type II: organic halide salt + hydrated metal chloride (e.g. choline chloride/$CoCl_2$*6H2O)

Type III: organic halide salt + hydrogen bond donor (e.g. choline chloride/urea)

Type IV: metal chloride + hydrogen bond donors (e.g. $ZnCl_2$/urea)

Concerning their physicochemical properties, DESs have similarities with ILs. DESs are also tunable solvents which can be customized, according to the components used. Specific DES with different properties can thus be obtained for a huge potential of different applications. As ILs, they are non-volatile, non-flammable, and exhibit a wide liquid range.[102] DESs mostly show also a very high viscosity as the common ILs. Besides having most of the ILs advantages, DESs also overcome some ILs limitations. First, their preparation is easier because it generally involves the simple mixing of components at moderate heating. Therefore, it avoids the purification, the multi steps, and the waste problems present in some IL syntheses. Secondly, most of the components used to obtain DESs are cheaper, non-

reactive with water, biocompatible, biodegradable, and non-toxic.[101] Thus, DESs can be considered as environmentally benign alternative solvents to ILs for many applications, in particular in the dissolution of polysaccharides.

1.2.3.3.2 Dissolution of cellulose and chitin

The definition of DES appeared only in 2003 with the work of Abbott *et al.* on choline chloride/urea mixtures. Their application can already be found in various fields such as electrochemistry, catalysis and organic synthesis, extraction processes, and material preparation.[101,104] However, the research field on the dissolution of cellulose and chitin in DESs is not as developed as for ILs. The bibliometric analysis from SciFinder® database combining "cellulose" or "chitin" "dissolution" in "deep eutectic solvents" drew up a list of 13 and 2 publications for cellulose and chitin, respectively. As it can be seen in Figure 1.14, the interest of scientist on these subjects started only recently, in 2012. The reason behind this may be the high viscosity of some DESs and/or their poor dissolution power towards these polysaccharides.[101]

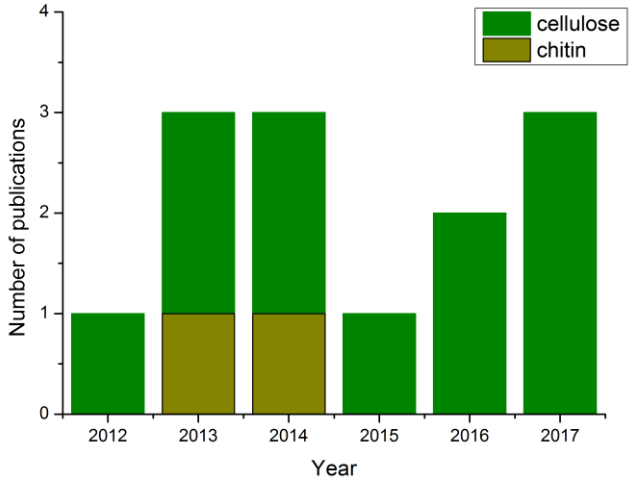

Figure 1.14: *Bibliometric analysis from Scifinder® database about the number of publications (including scientific journals, patents, and conferences) dealing with the dissolution of cellulose and chitin in DES.*

Table 1.5 gives an overview of the DESs efficient for the cellulose and/or chitin solubilization found in literature. These DESs are all from Type III and contain mostly choline chloride as organic salt. Choline chloride was principally investigated because it is cheap, non-toxic, biodegradable, and easily available on the market.[105] Moreover, chloride is well known for its efficiency to break the hydrogen bond network of cellulose and chitin (see Sections 1.2.2 and 1.2.3.2). Regarding Table 1.5, except the work of Sharma *et al.* put in brackets, only modest cellulose concentrations of less than 2.5 wt% were dissolved in choline chloride based DESs. To overcome this limitation, several studies proposed different strategies.[106,107] For instance, Hiltunen *et al.* enhanced the cellulose solvation from above 4 wt% in choline chloride/boric acid DES by adding water, betain solutions or aqueous mixtures of betaine and sodium hydroxide.[106] Ren *et al.*, for their part, showed that the exchange of choline cation with allyl triethyl ammonium can drastically enhance the cellulose solubility to 6.5 wt%, particularly because of the allyl substitution of the hydroxyl group, which decreases the viscosity of the DES.[107]

Table 1.5: *Examples of DESs able to dissolve cellulose and/or chitin, their dissolving capacities according to the information given by the authors on the polymer used and the solubility conditions. The data written in brackets are extracted from the work of Sharma et al.*

DES (molar ratio)	Information about the polysaccharide	Conditions	Solubility (wt%)
Choline chloride/urea (1:2)	Cotton linter pulp (DP=575.6)[a] activated by ultrasonication with saturated calcium chloride	(20<T<120 °C), 2h	1.43[108]
	Microcrystalline cellulose	110 °C, 12h	<0.2[105]
	[Microcrystalline cellulose (M_W=3.12x10^5 Da)][b]	[100 °C, 10h]	[8][109]
	[α-Chitin (DA=94.1%)][c]	[MW 80 °C, 2h][d]	[7][109]
Choline chloride/imidazole (3:7)	Cotton linter pulp (DP=575.6)[a] activated by ultrasonication with saturated calcium chloride	(20<T<120 °C), 1.5h	2.48[108]
Choline chloride/ammonium thiocyanate (1:1)	Cotton linter pulp (DP=575.6)[a] activated by ultrasonication with saturated calcium chloride	(20<T<120 °C), 3h	0.85[108]
Choline chloride/oxalic acid (1:1)	Cotton linter pulp (DP=575.6)[a]	110 °C, n.a.[e]	<1[107]
Choline chloride/thiourea (1:2)	[Microcrystalline cellulose (M_W=3.12x10^5 Da)][b]	[100 °C, 6h]	[10][109]
	[α-Chitin (DA=94.1%)][c]	[100 °C, 6h]	[9][109]
Choline chloride/glycerol (1:2)	[Microcrystalline cellulose (M_W=3.12x10^5 Da)][b]	[MW 80 °C, 2h][d]	[3.5][109]
Choline bromide/urea (1:2)	[Microcrystalline cellulose (M_W=3.12x10^5 Da)][b]	[MW 80 °C, 2h][d]	[6][109]
	[α-Chitin (DA=94.1%)][c]	[MW 80 °C, 2h][d]	[7][109]
Chlorocholine chloride/urea (1:2)	[Microcrystalline cellulose (M_W=3.12x10^5 Da)][b]	[100 °C, 10h]	[5][109]
	[α-Chitin (DA=94.1%)][c]	[100 °C, 10h]	[8][109]
Betaine hydrochloride/urea (1:4)	[Microcrystalline cellulose (M_W=3.12x10^5 Da)][b]	[100 °C, 10h]	[2.5][109]
	[α-Chitin (DA=94.1%)][c]	[100 °C, 10h]	[5][109]
Proline/malic acid (3:1)	Cellulose (purity of 90%)	100 °C, n.a.[e]	0.78[110]
Allyltriethyl-ammonium chloride/oxalic acid (1:1)	Cotton linter pulp (DP=575.6)[a]	110 °C, n.a.[e]	6.48[107]

[a]DP = degree of polymerization [b]Mw = molecular weight [c]DA = degree of acetylation
[e]n.a.= not specified by the authors
[d]MW = microwave heating

Surprisingly, the work of Sharma, Prassad *et al.* is the only study where relatively high amounts of microcrystalline cellulose (MCC) can be solubilized in choline-based DESs. Contradictory, several authors found that MCC or cellulose with higher DP are sparingly or not at all soluble in choline based DESs.[105,107,108] For example, the solubility of MCC was inferior as 0.2 wt% for Zhang *et al.* while it was 8 wt% for Sharma *et al.* in roughly the same conditions, as presented in Table 1.5. The presence of protic hydroxyl groups in choline cation were suggested to compete in cleaving the hydrogen bonds of cellulose. Therefore choline-based DESs are inefficient for the dissolution of high amounts of cellulose.[107]

For chitin, only the works of Sharma *et al.* deal with its dissolution capacity in DESs.[109,111] Choline chloride/thiourea was observed to be the most effective medium for the solubilization of α-chitin (see Table 1.5). Sharma *et al.* hypothesized that thiourea interacts with the acetoamido group of chitin as with the membrane of proteins.[109]

Finally, DESs were assumed to be suitable and alternative greener solvents to ILs for the cellulose and chitin dissolution. However, they seemed to be poorly efficient compared to ILs and the development of more powerful DESs has still to be investigated.

1.3 Cellulose and chitin materials

The development of efficient cellulose and chitin solvents had an important impact on cellulose and chitin processing. The polymers put into solutions have shown to have the potential to produce different cellulose and/or chitin materials such as fibers, films, nanomaterials, gels, and membranes.[26,92,112-115] All these materials cannot be described in detail but some relevant examples and applications will be presented in this part.

1.3.1 Production process of materials and applications

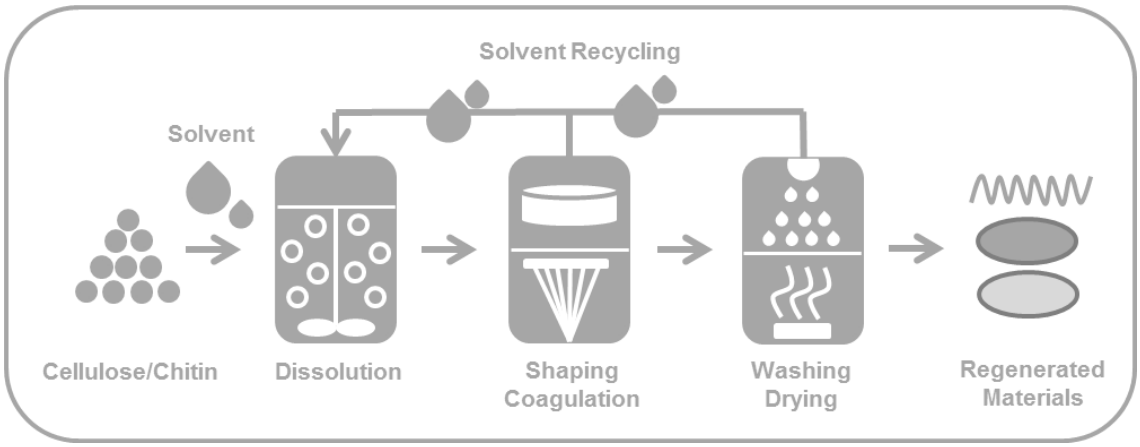

Figure 1.15: *Schematic of the production process for the materials composed of cellulose and chitin.*

Figure 1.15 illustrates the common process used to produce the materials listed above. After the dissolution of the biopolymer in a solvent, the regenerated polymer materials are generally produced by first shaping the polymer solution into the required form. For instance, films are obtained by casting the polymer solution onto glass plates, fibers by extrusion, and nano-composites under vigorous stirring or by top-down or bottom-down procedures.[28,116,117] Then, an anti-solvent (mainly water, ethanol or acetone) is added, leading the polymer to be regenerated and the solvent to be removed. The final material is washed with the anti-solvent and dried. The regenerated cellulose or chitin generally showed lower degree of crystallinity than the native polymers. For instance, it was reported that cellulose I changes to cellulose II

and amorphous cellulose or α-chitin to semi α-chitin.[28,45,88,118] At the end of the process, the initial solvent can be potentially recovered and reused.[28]

Table 1.6: *Applications of cellulose and chitin materials according to their form.*

Material form		**Applications**
Cellulose	Fibers	Reinforcement material for construction and automotive industry,[119] textile and paper industry[34]
Chitin	Fibers	Antibacterial fibers for textiles, tissue engineering and wound healing[50], wastewater treatment[42]
Cellulose	Films/membranes	Water treatment[120], paper and packaging industry[10]
Chitin	Films/membranes	Water treatment[120], coating materials, pharmaceutical and biomedical field (e.g. drug carrier, wound healing)[50]
Cellulose	Nanomaterials	Barrier film, transparent films for packaging, thermal and mechanical reinforcement material, biomedical implants, pharmaceuticals, drug delivery, conductive material[26]
Chitin	Nanomaterials	Gas barrier material[115], practical additive to synthetic polymers[116]
Cellulose	Gels	Porous materials[121], superabsorbent hydrogel for drug delivery[74]
Chitin	Gels	Superabsorbent hydrogel for drug delivery[74], porous matrixes for tissue engineering[50]

Cellulose and chitin exhibit diverse properties (detailed in Sections 1.1.2.1.4 and 1.1.2.2.4) that enable them to be applied to various sectors. Table 1.6 lists some examples of applications found in literature concerning materials based on cellulose or chitin in function of their forms. Chitin-based materials are especially found in biomedical science while cellulose-containing materials are used in a vaster array of fields such as textile, paper, biomedical materials, packaging, and water treatment. Cellulose and chitin composite materials are also produced to combine the unique properties of each polymer and used in the application sector mentioned above. For instance, the addition of chitin into cellulose–based materials has shown to significantly increase their mechanical strength and bactericidal properties.[122]

1.3.2 Cellulose and chitin fibers

Fibers are materials worldwide produced for consumer goods. In the course of "green" chemistry, the development of renewable and biocompatible fibers gains more and more

importance as alternatives to synthetic fibers. This section will describe the production of these materials from cellulose and/or chitin.

1.3.2.1 Regenerated cellulosic fibers at the industrial scale

Cellulosic fibers are predominant on the industrial market, especially in the textile industry.[123] Textiles are produced from two types of cellulosic fibers, natural (e.g. cotton) or man-made fibers. The latter are the most promising substitutes for cotton as they exhibit some further advantages as lower costs, higher availability, higher mechanical resistance, and higher wet strength. [124] Man-made cellulosic are produced by two types of techniques, the viscose and the Lyocell process, illustrated in Figure 1.16.[124]

1.3.2.1.1 Viscose process

The first manufactured technique is the viscose process which has been applied at industrial scale since the 1930s and is still mainly used to produce the viscose and Modal fibers. This technology consists first in purifying the cellulose pulp with caustic soda (NaOH) and in transforming cellulose with carbon disulfide (CS_2) into cellulose xanthate. The cellulose xanthate is then dissolved in NaOH giving a dope. This solution is filtrated, degassed, and treated before to be spun through a spinneret into a chemical bath containing sulfuric acid, zinc sulfate, and sodium sulfate. In this bath, cellulose is regenerated in a filament form (see Figure 1.16).[125] However, the viscose route contains a lot of complicated steps. They cause energy consumption, environmental pollution with the use of CS_2 and heavy metals, production of by-products, and releasing of toxic gaseous hydrogen sulfide.[57,125] The viscose fibers, or also called viscose rayon, are soft, highly absorbent, comfortable, and moderate dry strong. They exhibit a serrated cross section and a skin core structure with large voids in the core region and a densified skin layer.[126] For textile and nonwoven application, standard viscose fibers are characterized by a fineness ranging from 1 to 10 dtex, an elongation at break from 18 to 25%, and a tensile strength from 20 to 26 cN/tex and from 10 to 15 cN/tex in wet conditions. Fiber fineness, also called titer, specifies the relation of mass to length (dtex = mass (dg)/length (km)). Viscose rayons are mainly used for outerwear manufacturing such as dress, skirts or t-shirts or as reinforced material for tire cords.[127]

Modal fibers are produced by a modified viscose process, namely other precipitation baths and a pulp with a higher degree of polymerization are proceeded.[57] These modifications cause better mechanical properties than for viscose fibers, namely a higher tensile strength (up to 42 cN/tex), a higher wet tensile strength (19-30 cN/tex) and a lower elongation at break (8-18%). Modal fibers are generally used as a substitute for cotton and are found in high quality textiles such as bed and sports clothes, technical and home textiles, and toweling goods.[127]

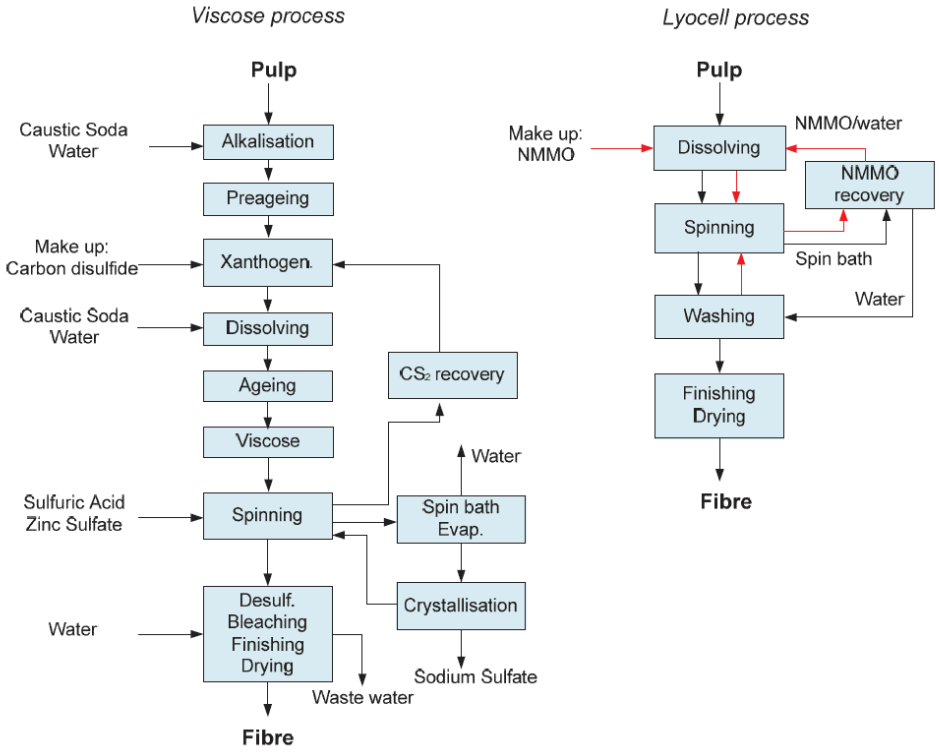

Figure 1.16: *Detailed diagram of the viscose and Lyocell process.*[128]

1.3.2.1.2 Lyocell process

Recently (in the 1990's), an environmentally friendlier and easier technique, the Lyocell process, was developed to replace the viscose method. A direct dissolution of the pulp is performed without pre-treatment or derivatization, thus no by-products are formed. The first commercial Lyocell fibers were produced by Courtaulds (Great Britain) and are currently

made by Lenzing AG (Austria) under the TENCEL® trade name on a huge industrial scale (100 ktons/year).

The Lyocell process, or also called NMMO process, uses *N*-methylmorpholine *N*-oxide (NMMO) in presence of water as solvent to dissolve cellulose pulp (detailed in Figure 1.16). The initial solution is generally composed of 10-15% cellulose, 50-60% NMMO, 20-30% water, and stabilizers. Aqueous NMMO solutions are preferred to facilitate the cellulose dissolution. The excess of water is extracted under mechanical stirring of the dope at reduced pressure and high temperature until complete dissolution of cellulose is obtained. Generally, appropriate slurries are obtained when the water amount is close to the percentage of water present as NMMO would be monohydrate. A typical dope is, for instance, composed at the industrial scale of 14% cellulose, 10% water, and 76% NMMO.[129] This spinning dope is then extruded according to a dry-jet wet spinning process, illustrated in Figure 1.17. This technique consists in spinning the solution at elevated temperature (90-120 °C) through an air gap into a water bath. There, the extrudate is impoverished of NMMO, which allows the regeneration of the cellulose in form of filament. The resulting fibers are washed and dried. At the end of the process, NMMO is recovered from the baths and reused for a new spinning route.[126,129,130] Theoretically, the Lyocell process overcomes the disadvantages of the toxic and multi-steps viscose technique. However, some drawbacks also remain in this process, such as the high energy consumption and the thermal instability of NMMO and cellulose.[129]

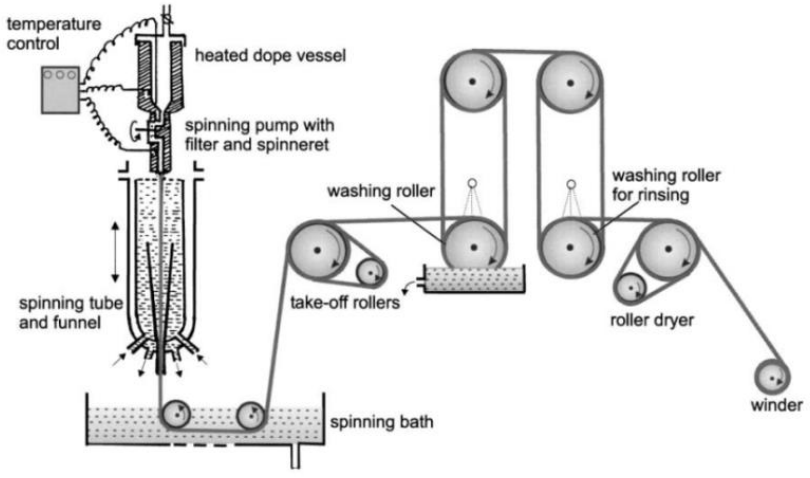

Figure 1.17: *Schema of the dry-jet wet fiber spinning process used in Lyocell process.*[126]

TENCEL® fibers exhibit a different morphology and better performant properties than the viscose fibers because of the different processing technique. In contrast to viscose, the forming fibers have smaller and circular cross section (10 µm diameter) and present fibrillar structure with microfibrils parallel to the fiber axis.[117] The air gap conditions have a big influence on this highly oriented structure. [126,131] Lyocell fibers properties differ from viscose by considerable higher dry and wet strength (38-47 cN/tex and 26-40 cN/tex, respectively) and by their tendency to fibrillate especially in the wet state. Their enormous application potential extends from clothing to technical sectors. Their particular characteristic properties, mentioned above, allow Lyocell fibers to be used particularly well in the nonwoven sector or for filters and special papers manufacturing.[127]

1.3.2.2 Regenerated cellulose/chitin fibers from IL solutions

As already mentioned, ILs have been thoroughly investigated as direct and powerful solvents for cellulose and chitin and are therefore used for material processing. Among other, one potential application of cellulose/chitin-dissolving IL solutions is the production of fibers. Research on the spinnability of these solutions and the characterization of the forming fibers has gained more and more importance. For cellulose-based fibers, the aim is to substitute the currently commercialized viscose and Lyocell process. Concerning chitin, its derivative chitosan was mainly used to produce fibers because of the limited solvent systems which can readily dissolve pure chitin.[68,91,112,124,132]

Fibers from IL solutions are produced according to the same dry-jet wet fiber spinning process as in the Lyocell process.[124] Highly oriented fibers with promising properties could be obtained with different ILs. Imidazolium-based ILs such as 1-butyl-3-methylimidazolium chloride (BmimCl), 1-butyl-3-methylimidazolium acetate (BmimOAc), 1-ethyl-3-methylimidazolium chloride (EmimCl), 1-ethyl-3-methylimidazolium acetate (EmimOAc), and non-imidazolium-based ILs such as 1,5-diazabicyclo[4.3.0]non-5-ene acetate were successfully used to produce cellulose fibers.[66,124,132,133] Chitin fibers were manufactured with EmimOAc und cellulose/chitin filament from ethylmethylimidazolium propionate.[112,134]

Regenerated cellulose fibers from IL (BmimCl, BmimOAc, EmimCl, EmimOAc) solutions were compared by Lenzing AG with the Lenzing Viscose®, Lenzing Modal®, and TENCEL® fibers. Fibers made from ILs showed similar properties to the TENCEL® fibers. However, no real improvement of the characteristic of the fibers could be observed.[135] The influence of the process parameters on the mechanical properties of fibers spun from IL solutions has to be investigated more to have one day maybe the possibility to overcome the TENCEL® fibers. In addition, up to now the spinning process from IL solutions has not been applied to industrial production yet. Intrinsic drawbacks of ILs such as high costs, difficulty to be synthesized at a large scale with a high purity, high water absorption, and negative health and environmental impacts cause problems.[136]

Chapter 2
Dissolution of cellulose and chitin in various solvents

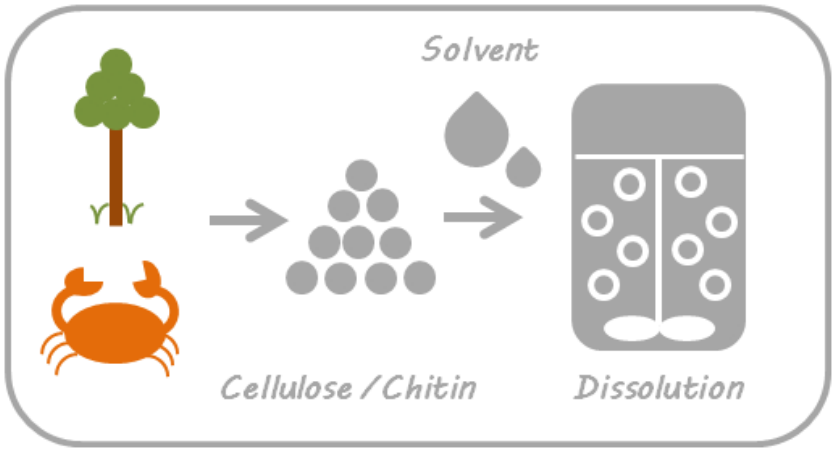

2.1 Introduction

As already mentioned in Chapter 1, cellulose and chitin cannot be melted and are difficult to process in solution because of their rigid bulk structures caused by extensive hydrogen bonding.[10,42] Thus, the dissolution of cellulose and chitin in proper solvents has been the most important challenge before processing these polymers into novel biodegradable materials. The development of these solvents has been already a longstanding field of research. The state of the art concerning the different kinds of solvents is detailed in Chapter 1. On the basis of the results yielded by this survey, the majority of the solvents revealed shortcomings such as environmental and health hazards. It is still necessary to search for more efficient and environmentally friendly solvents for cellulose and chitin.

For this purpose, the investigated solvents should meet certain criteria. First of all, they have to be effective solvents for both polymers to avoid the use of different compounds. A single solvent system for both polymers will facilitate processing and will avoid costs as well as intense energy consumption, especially for solvent recovery. Secondly, they should be non-derivatizing and direct solvents. This means that they should have the ability to dissolve polymers without chemically damaging them and without being altered themselves. Moreover, no multi-step pretreatment or activation of the polymers should be performed prior to use in order to keep intact the properties of each polymer. For sustainable development and environmental concerns, solvents have to be environmentally friendly. In other words, biocompatible, low toxic, biodegradable, bio-resourced, and thermally stable solvents are preferably required for this work. Finally, they should also be easily removable from polymers and recyclable at the end of the process.

Herein, a broad range of solvents was investigated to identify suitable solubilizing agents for cellulose as well as for chitin. Three types of solvents, namely ionic liquids (ILs), deep eutectic solvents (DESs), and other organic compounds were tested. Their dissolution capacity towards cellulose and chitin was examined by performing dissolution tests. These experiments were carried out using microcrystalline cellulose and α-chitin. The aim is to provide an easy and environmentally friendly method to process both cellulose and chitin.

2.2 Experimental section

The presence of water and other impurities can reduce the effectiveness of the solvents for dissolution experiments.[86,137] Therefore, some precautions were taken with the chemicals and during the preparation of solvents in order to use dried and highly pure compounds. The water content was determined with a Karl Fischer coulometer (899 Metrohm, Switzerland).

2.2.1 Chemicals

2.2.1.1 Chemicals used for the biopolymers

Microcrystalline cellulose (MCC) was purchased from Merck (Germany). α-Chitin from shrimp shells were obtained from Sigma Aldrich (Germany). Chitin extracted from mealworms (*Tenebrio molitor*) was donated by Ynsect (France) and was in the form of flocks. This chitin was first ground in a ball mill (Fritsch Pulverisette 6, Germany) to obtain a fine powder. The degree of polymerization (DP) of each polymer was measured by Yaqing Duan (from the Straubing Center of Science) using an Ubbelohde viscometer. These DP values were evaluated to be 124 for MCC, 1542 for chitin from mealworms, and 1691 for chitin from shrimp shells. The degree of acetylation of the chitin from shrimp shells is $92 \pm 4\%$ and was determined by Yaqing Duan by elemental analysis and infrared spectroscopy. All polymer powders were dried at 70 °C for 5 days and then stored in a glove box, prior to use.

2.2.1.2 Chemicals used for the ionic liquids

The ionic liquids whose structures are represented in Figure 2.1, Ammoeng 102 (purity ≥ 95%), 1-ethyl-3-methylimidazolium acetate (purity ≥ 95% and ≥ 98%), 1-butyl-3-methylimidazolium acetate (purity ≥ 98%), 1-hexyl-3-methylimidazolium bis(trifluoro-methylsulfonyl)imide (purity ≥ 99%), and *N*-butyl-*N*-methylpyrrolidinium dicyanamide (purity ≥ 98%) were purchased from IoLiTec (Germany). Prior to use, they were dried using a high vacuum setup (10^{-6}-10^{-7} mbar) consisting of a rotary vacuum pump and an oil

diffusion pump for 5 days. They were stored in sealed vials in a nitrogen-filled glove box. For the synthesis of 1-allyl-3-methylimidazolium bromide, allyl bromide (Reagent Plus®, 99%) and 1-methylimidazole (purity ≥ 99%) were obtained from Sigma Aldrich and Carl Roth (Germany), respectively. They were both distilled under reduced pressure, prior to use. Methanol (anhydrous, purity ≥ 99.8%) was purchased from Sigma Aldrich and potassium hydroxide (KOH) from Merck. All other ILs were synthesized at our chair.

2.2.1.3 Chemicals used for the deep eutectic solvents

The following chemicals used to produce the deep eutectic solvents were dried with a turbomolecular pump under vacuum (10^{-6} mbar) for 5 days. They were stored in a nitrogen-filled glove box to avoid water uptake. The water content of these chemicals was found to be lower than 500 ppm. Choline chloride (purity ≥ 98%) was obtained from Alfa Aesar (Germany). Urea (purity ≥ 99%), thiourea (purity ≥ 98%), and ethylammonium chloride (purity ≥ 98%) were purchased from Merck. Betaine (purity ≥ 99%) was obtained from Sigma Aldrich.

2.2.1.4 Chemicals used for the other organic solvents

All other chemicals were used without further purification. γ-Valerolactone (Reagent Plus®, purity ≥ 99%), γ-hexalactone (purity ≥ 98%), ethyl lactate (purity ≥ 98%), ethyl acetate (purity ≥ 99.5%), 4-methylmorpholine *N*-oxide monohydrate (NMMO mono., purity ≥ 95%), and tetrabutylphosphonium hydroxide solution (40% in H_2O) were purchased from Sigma Aldrich. γ-Butyrolactone (purity , ≥ 99%), lithium chloride (purity ≥ 99%), and propylene carbonate (purity ≥ 99%) were obtained from Merck. 2,5-Dimethylfuran (purity ≥ 98.7%), 2-methylfuran (purity ≥ 98.7%), and 2-methyltetrahydrofuran were donated by Pennakem (USA). Choline hydroxide (with 45 wt% H_2O) was donated by Taminco (Germany). Dimethyl sulfoxide (purity ≥ 99.98%) was purchased from Fisher Scientific (UK). The nominal water content of tetrabutylphosphonium hydroxide solution (60 wt%), choline

hydroxide (45 wt%), and NMMO mono. (13.3 wt%) were additionally confirmed by coulometric Karl Fischer titration.

2.2.2 Experimental methods

2.2.2.1 Solvent synthesis and preparation

All sample preparations were carried out gravimetrically with an estimated uncertainty lower than ± 0.001 g.

2.2.2.1.1 Preparation of ionic liquids

1-Allyl-3-methylimidazolium bromide was synthesized by reaction of 1-methylimidazole with allyl bromide according to the modified method of Schneider *et al.*[138] First, 1-methylimidazole and allyl bromide were distilled over KOH under reduced pressure to obtain highly pure products. The reaction was then carried out by adding slowly and dropwise allyl bromide into 1-methylimidazole dissolved in anhydrous methanol under an atmosphere of dry nitrogen at 25 °C for several days. The completion of 1-metylimidazole reaction was monitored with thin layer chromatography. Allyl bromide, supplied in slight excess, and methanol were removed afterwards under reduced pressure (10^{-3} mbar). The resulting IL, a clear viscous liquid was dried using the high vacuum setup to remove remaining traces of solvent. The purity of the synthesized IL was confirmed by ^{1}H- and ^{13}C-NMR (data are detailed in Appendix 2.1).

1-Butyl-3-methylimidazolium tetrafluoroborate and 1-butyl-3-methylimidazolium hexafluorophosphate were synthesized by Johannes Hunger. The ILs were prepared via anion metathesis. Equimolar amounts of 1-butyl-3-methylimidazolium chloride and $NaBF_4$/$NaPF_6$ dissolved in water were stirred in an ice bath to avoid hydrolysis of anions. The obtained ILs were extracted three times with dichloromethane to remove the aqueous phase. To eliminate the traces of NaCl, the organic phase was washed three times with small amount of water. The ILs were pre-dried over $MgSO_4$ and dichloromethane was evaporated under vacuum. Colorless liquids were obtained.[139]

1-Octyl-3-methylimidazolium tetrafluoroborate was synthesized by Alexander Stoppa. To prepare this IL, equimolar amounts of 1-octyl-3-methylimidazolium chloride dissolved in dichloromethane and aqueous solution of $NaBF_4$ were stirred in an ice bath to minimize the hydrolysis of BF_4^-. To remove the aqueous phase, the solution was extracted three times with dichloromethane. After combining all the organic fractions, NaCl was extracted by washing the organic phase three times with small amounts of water. After removal of the dichloromethane under vacuum, the procedure yielded a yellowish liquid.[140]

Ethylammonium formate and butylammonium formate were synthesized by Andreas Nazet following the approach of Burrel *et al.*[141] The reactions were started by the neutralization of the bases, *N*-ethylamine for ethylammonium formate and *N*-butylamine for butylammonium formate, with formic acid. Equimolar amounts of acid and base were simultaneously mixed dropwise into a reaction vessel to keep the mixture near stoichiometric neutrality and thus ensure low by-product formation. The reaction being very exothermic, the temperature was maintained at 0 °C with an ice cooled water bath. After 4 h, ethylammonium formate and butylammonium formate were obtained as colorless liquids. The protic ionic liquids were dried with the high vacuum setup for 5 days at 40 °C to remove water and unreacted reactants.[142]

Imidazolium carboxylate anions (from formate (C_1) to nonanoate (C_9)) were prepared by Andreas Nazet from imidazole and carboxylic acid (from formic acid to nonanoic acid) according to the same route described for ethylammonium formate. The obtained ILs were dried under reduced pressure (10^{-2} mbar) at 40 °C for a time span from 1 to 3 days.[142]

Pyrrolidinium hydrogen sulfate and **pyrrolidinium carboxylate anions (from formate (C_1) to propionate (C_3))** was synthesized by Andreas Nazet from pyrrolodine and sulfuric acid/carboxylic acid (formic, acetic, and propionic acid) according to the same route described for ethylammonium formate.[142]

Choline butanoate was synthesized by Theresa Höß by neutralizing a solution of choline hydroxide with butyric acid according to the modified procedure of Fuyaka *et al.*[143] A slight excess of butyric acid was slowly and dropwise added to a choline hydroxide solution in methanol in an ice bath. The solution was stirred at room temperature for 12 h and then

extracted with diethyl ether several times to remove unreacted acid. The ionic liquid was filtered through a fluted filter and dried under reduced pressure. Further drying was performed with the high vacuum setup at 40 °C and a white salt was obtained.[144]

Choline lactate was synthesized by Stefan Wolfrum according to the method of Vijayaraghavan *et al.*[145] Lactic acid was slowly added to methanolic choline hydroxide in an ice bath and stirred for about 20 h at room temperature. The mixture was extracted with diethyl ether to eliminate unreacted acid. The final product was filtered through a fluted filter, dried by rotary evaporation and then with the high vacuum setup. A brownish and viscous liquid was obtained.

Butylcarnitine bromide was synthesized by Katharina Häckl according to the modified route of Andrea Mülbauer.[146] Carnitine and 1-bromobutane were slowly mixed under nitrogen atmosphere in acetonitrile. The mixture was stirred under reflux over night at 80 °C. Evaporation of solvent was performed under reduced pressure with a rotary evaporator and then with the high vacuum setup.[147]

The purity of the synthetized ILs was controlled by ^{1}H- and ^{13}C-NMR measurements, recorded for the majority with a Bruker Avance 300 spectrometer (Billercia, USA) at 300 MHz. They were all stored in sealed vials in a nitrogen-filled glove box to avoid air contact. The residual water content of the ILs was determined by coulometric Karl Fischer titration. The values are listed in Table 2.1. All the investigated ILs contained very low water fraction (<1.2 wt%). Their dissolving behavior was thus assumed to be not influenced by the residual water.

Table 2.1: *Water content in mass fraction of the ILs used in the dissolution tests after drying.*

Ionic Liquid	Abbreviation	Water content (ppm)
1-Allyl-3-methylimidazolium bromide	AmimBr	300
1-Ethyl-3-methylimidazolium acetate (purity ≥ 95%)	EmimOAc 95%	2730
1-Ethyl-3-methylimidazolium acetate (purity ≥ 98%)	EmimOAc 98%	2080
1-Butyl-3-methylimidazolium acetate	BmimOAc	<2760
1-Butyl-3-methylimidazolium hexafluorophosphate	$BmimPF_6$	75
1-Butyl-3-methylimidazolium tetrafluoroborate	$BmimBF_4$	70
1-Hexyl-3-methylimidazolium bis(trifluoromethylsulfonyl)imide	$HmimNTf_2$	15
1-Octyl-3-methylimidazolium tetrafluoroborate	$OmimBF_4$	50
Imidazolium formate	$MimC_1$	1100
Imidazolium acetate	$MimC_2$	1250
Imidazolium propionate	$MimC_3$	580
Imidazolium butanoate	$MimC_4$	150
Imidazolium pentanoate	$MimC_5$	150
Imidazolium hexanoate	$MimC_6$	100
Imidazolium heptanoate	$MimC_7$	150
Imidazolium octanoate	$MimC_8$	200
Imidazolium nonanoate	$MimC_9$	160
Ethylammonium formate	EAF	1600
Butylammonium formate	BuAF	4300
Pyrrolidinium formate	$PyrC_1$	<12000
Pyrrolidinium acetate	$PyrC_2$	3780
Pyrrolidinium propionate	$PyrC_3$	950
Pyrrolidinium hydrogen sulfate	$PyrHSO_4$	50
Choline butanoate	ChC_4	230
Choline lactate	ChLac	500
Butylcarnitine bromide	C_4CarBr	200
N-Butyl-*N*-methylpyrrolidinium dicyanamide	$P_{14}DCA$	200
Ammoeng 102	A102	80

2.2.2.1.2 Preparation of deep eutectic solvents

DESs were prepared by mixing the desired components, a hydrogen bond donor and a hydrogen bond acceptor, in sealed glass vials in a nitrogen-filled glove box. The vials were then heated and stirred under nitrogen atmosphere in an oil bath until a colorless and homogeneous liquid was formed.

2.2.2.2 Dissolution method

Dissolution experiments were carried out by mixing desired amounts of polymer (cellulose or chitin) with a pure solvent (or a mixture) in sealed glass vials under nitrogen atmosphere. For the majority of the selected solvents, the samples were continuously stirred with a magnetic stirrer at elevated temperatures between 70 °C and 110 °C in an oil bath, until a homogeneous and clear solution was obtained. The dissolution process was first visually monitored and the total dissolution of the polymers was confirmed using a polarized optical microscope (Leitz Orthoplan, Germany).

Other procedures were also investigated for the dissolution of polymers in certain solvents. Ultrasonication in a water bath was performed by a heated ultrasonic bath (Bandelin Sonorex RK 510 H, Germany) under nitrogen atmosphere. Dissolution tests were also carried out with heating under microwave irradiation for 2 h at a power of 100 W using a SP Discover microwave synthesis system (CEM, Germany). Furthermore, mixing was achieved using a PT 3100 Polytron Ultra-Turrax (Kinematica, Germany).

The polymers were considered not soluble when the addition of 1 wt% of cellulose or chitin to the solvent yielded turbid mixtures after 24 h heating and stirring. The maximal amount of polymers was increased up to 10-15 wt%. Above this value, solutions were too viscous and the stirring was too weak to induce an efficient mass transport.

2.3 Results and discussion

The goal of this study was to investigate direct solvents for cellulose and chitin processing. In this context, 49 candidates were screened as solvents for cellulose as well as for chitin. Ideally, the solvent should follow the maximum possible number of criteria outlined in the introduction.

Microcrystalline cellulose was selected as the main cellulose substrate as its low degree of polymerization (i.e. 124) ensures a relatively fast dissolution and solutions of moderate viscosity. Regarding chitin substrate, α-chitin from shrimp shells was chosen since it was the only chitin powder commercially available on the German market.

2.3.1 Dissolution in ionic liquids

Herein, dissolution of cellulose and chitin in ILs with different cations and anions is studied. An overview of all ILs, their chemical structures and their abbreviations are given in Figure 2.1. These solvents were classified on the basis of their structure. From this selection, 1-alkyl-3-methylimidazolium-, ammonium- and pyrrolodinium-based ILs as well as protic and bio-sourced ILs were thus investigated.

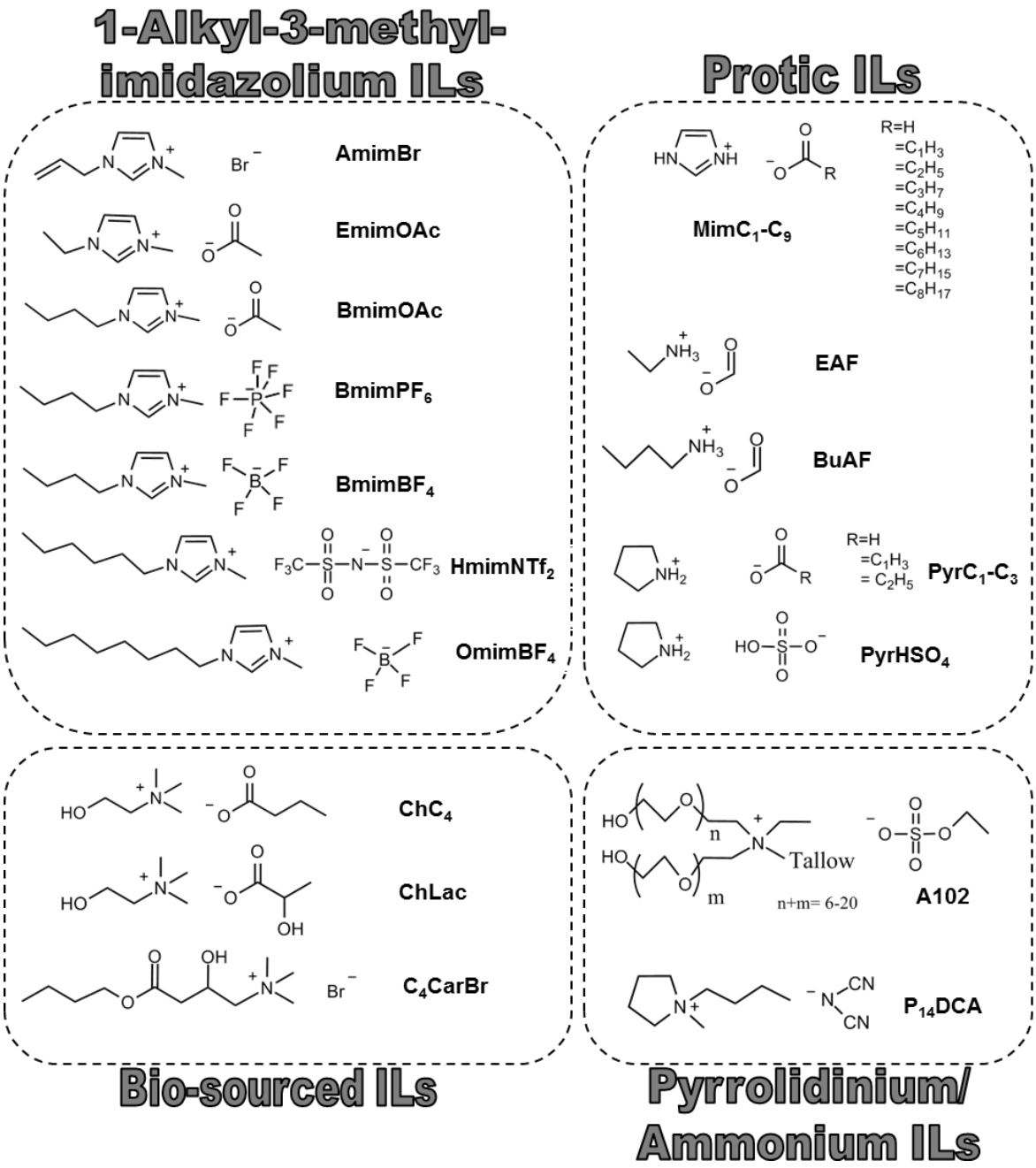

Figure 2.1: *Overview of the ionic liquids used in the dissolution tests: 1-allyl-3-methylimidazolium bromide (**AmimBr**), 1-ethyl-3-methylimidazolium acetate (**EmimOAc**), 1-butyl-3-methylimidazolium acetate (**BmimOAc**), 1-butyl-3-methylimidazolium hexafluorophosphate (**$BmimPF_6$**), 1-butyl-3-methylimidazolium tetrafluoroborate (**$BmimBF_4$**), 1-hexyl-3-methylimidazolium bis(trifluoromethyl sulfonyl)imide (**HmimNTf2**), 1-octyl-3-methylimidazolium tetrafluoroborate (**$OmimBF_4$**), choline butanoate (**ChC_4**), choline lactate (**ChLac**), butylcarnitine bromide (**C_4CarBr**), imidazolium formate up to nonanoate (**$MimC_1$-C_9**), ethylammonium formate (**EAF**), butylammonium formate (**BuAF**), pyrrolidinium formate up to propionate (**$PyrC_1$-C_3**), pyrrolidinium hydrogen sulfate (**$PyrHSO_4$**), tetraalkyl ammonium sulfate Ammoeng 102 (**A102**), and N-methyl-N-butyl-pyrrolidinium dicyanoamide (**$P_{14}DCA$**). Tallow is a C_{18} acyl group.*

Table 2.2: *Dissolution experiments of microcrystalline cellulose (MCC) and α-chitin in different ionic liquids (ILs).*

IL	Dissolution conditions	Solubility (wt%)[b]	
		MCC	α-chitin
AmimBr	Stirring[a] and heating at 100 °C	NS	5
EmimOAc (purity ≥ 95%)	Stirring[a] and heating at 90 °C	>15	<1
	Ultra-Turrax and heating at 90 °C	-	<1
	Microwave irradiation and heating at 55 °C	-	NS
	Ultrasonication and heating at 80 °C	-	<1
EmimOAc (purity ≥ 98%)	Stirring[a] and heating at 90 °C	-	<1
BmimOAc	**Stirring[a] and heating at 110 °C**	**>10**	**3**
$BmimPF_6$	Stirring[a] and heating at 90 °C	NS	NS
$BmimBF_4$	Stirring[a] and heating at 110 °C	NS	NS
$HmimNTf_2$	Stirring[a] and heating at 100 °C	NS	NS
$OmimBF_4$	Stirring[a] and heating at 100 °C	NS	NS
$MimC_1$	Stirring[a] and heating at 90 °C	NS	NS
$MimC_2$	Stirring[a] and heating at 90 °C	NS	NS
$MimC_3$	Stirring[a] and heating at 90 °C	NS	NS
$MimC_4$	Stirring[a] and heating at 90 °C	NS	NS
$MimC_5$	Stirring[a] and heating at 90 °C	NS	NS
$MimC_6$	Stirring[a] and heating at 90 °C	NS	NS
$MimC_7$	Stirring[a] and heating at 90 °C	NS	NS
$MimC_8$	Stirring[a] and heating at 90 °C	NS	NS
$MimC_9$	Stirring[a] and heating at 90 °C	NS	NS
EAF	Stirring[a] and heating at 100 °C	NS	NS
BuAF	Stirring[a] and heating at 100 °C	NS	NS
$PyrC_1$	Stirring[a] and heating at 70 °C	NS	NS
$PyrC_2$	Stirring[a] and heating at 70 °C	NS	NS
$PyrC_3$	Stirring[a] and heating at 70 °C	NS	NS
$PyrHSO_4$	Stirring[a] and heating at 90 °C	NS	NS
ChC_4	Stirring[a] and heating at 90 °C	NS	NS
ChLac	Stirring[a] and heating at 90 °C	NS	NS
C_4CarBr	Stirring[a] and heating at 90 °C	NS	NS
$P_{14}DCA$	Stirring[a] and heating at 100 °C	NS	NS
A102	Stirring[a] and heating at 90 °C	NS	NS

[a]Magnetic stirring [b]NS = Not Soluble

Table 2.2 shows the conditions employed for the dissolution experiments as well as the results concerning the ability of the ILs to dissolve microcrystalline cellulose and α-chitin. A common solvent for both biopolymers is of most importance to this study. In this context, it was observed that only one IL among the 17 tested could dissolve both cellulose and chitin, namely 1-butyl-3-methylimidazolium acetate (BmimOAc). More than 10 wt% cellulose and

3 wt% chitin could be dissolved in BmimOAc. Photographs of the resulting solutions are shown in Figure 2.2. For weight percentages above the given values, the high viscosity of the solutions inhibited a fast and complete dissolution. Similar results have been reported in literature.[45,79,93] Authors suggested that the solvation involved the disruption of the complex hydrogen bond network of cellulose or chitin and was principally caused by the acetate anion. This strong hydrogen bonding acceptor and coordinating anion is supposed to interact strongly with the protons of the amino and hydroxyl groups for chitin and with the protons of hydroxyl group for cellulose.[45,100] In addition, it is assumed that the cation may be also involved in the dissolution process for cellulose. However, the exact role is still subject to different interpretations as already mentioned in Chapter 1.[53,96,98]

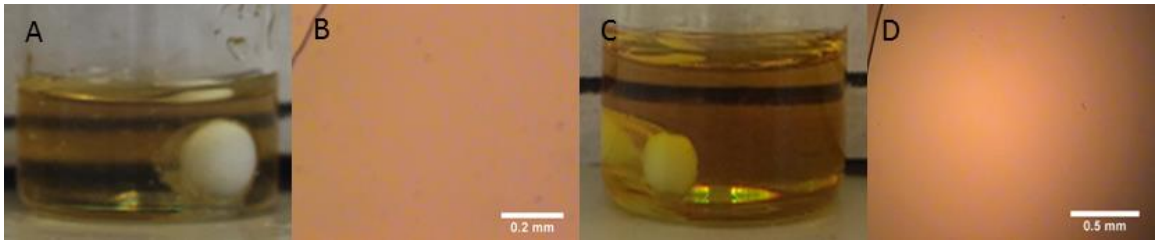

Figure 2.2: *(A) Mixture containing 3 wt% of α-chitin dissolved in BmimOAc, (B) its image obtained by polarized light microscope, (C) mixture containing 10 wt% of microcrystalline cellulose dissolved in BmimOAc, and (D) its image obtained by polarized light microscope. The white object in solution is a magnetic stirrer.*

The results from Table 2.2 suggest that 1-allyl-3-methylimidazolium bromide (AmimBr) shows high solubility of chitin (up to 5 wt%), while cellulose was found to be immiscible in this solvent. This result is in agreement with reported chitin dissolution studies.[92,113] Due to the allyl group, this IL has a relatively low viscosity compared to other ILs substituted by saturated alkyl.[97] Moreover, AmimBr was reported to be used for the synthesis of polyamide and polyimide, polymers having the –NC=O groups in common with chitin.[92] The dissolution ability of AmimBr has been considered to be caused by some specific interactions formed by AmimBr with the chitin chains.[113] For cellulose, 1-allyl-3-methylimidazolium-based ILs such as 1-allyl-3-methylimidazolium chloride or 1-allyl-3-methylimidazolium formate and bromide-based ILs such as 1-butyl-3-methylimidazolium bromide and 1-allyl-2,3-dimethyl-imidazolium bromide were found to dissolve this polysaccharide.[28,97] However, the

combination of 1-allyl-3-methylimidazolium and bromide has not been reported as cellulose solvent.

It can be observed from Table 2.2 that the contrary occurs for 1-ethyl-3-methylimidazolium acetate (EmimOAc). More than 15 wt% cellulose could be dissolved in EmimOAc, while chitin solubility was found to be very poor and negligible in this IL. When 1 wt% chitin was mixed and stirred in EmimOAc (with a purity ≥ 95%) at 90 °C for 24 h, a turbid and slightly more viscous solution than the pure IL was obtained. The presence of undissolved chitin particles was still noticeable (see Figure 2.3 A). A part of chitin seemed to be dissolved due to the increase of the viscosity of the solution. Nevertheless, no complete dissolution of chitin was achieved. Previous studies on dissolving chitin in ILs have shown that EmimOAc is yet a good solvent for this biopolymer.[88,91,148] Changing the dissolution method into Ultra-Turrax mixing, microwave irradiation, and heating assisted by ultrasonication did not lead to an enhanced solubility of chitin in EmimOAc (see Figure 2.3). It should be noted that microwave heating produced degradation of the IL as a brownish solution was obtained (Figure 2.3 C). ILs are good microwave absorbers and heating occurs more rapidly leading to faster degradation.[28] In addition, impurities in ILs are known to influence the dissolution capacity of these solvents and could be an explanation of EmimOAc inefficiency.[96,137] Hence, EmimOAc with a higher purity (≥ 98%) was also investigated. However, again only partial solubilization of chitin was obtained, which is in disagreement with previous studies.[91,148]

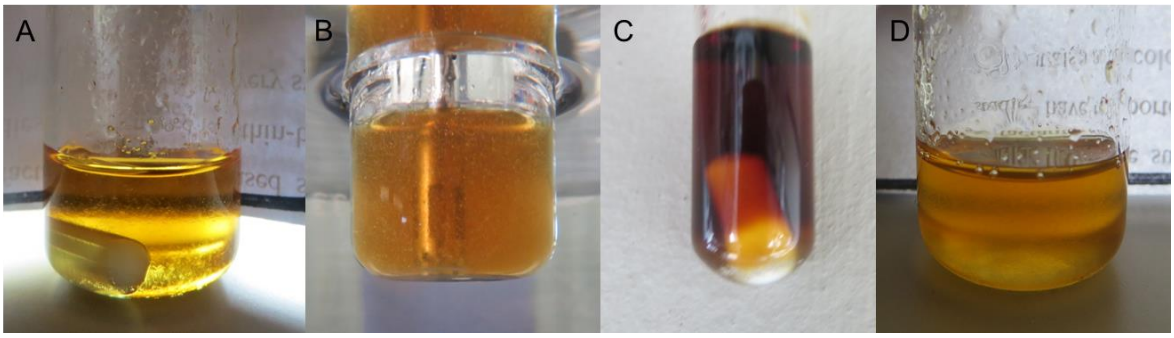

Figure 2.3: *Chitin in EmimOAc after different dissolution methods: (A) magnetic stirring and heating at 90 °C, (B) Ultra-Turrax and heating at 90 °C, (C) microwave irradiation and heating at 55 °C, and (D) ultrasonication and heating at 80 °C. Objects in solutions are magnetic stirrers in (A)/(C) and Ultra-Turrax disperser in (B).*

No cellulose as well as no chitin solubility was found in the other studied ILs. In the case of 1-butyl-3-methylimidazolium hexafluorophosphate ($BmimPF_6$), 1-butyl-3-methyl-imidazolium tetrafluoroborate ($BmimBF_4$), and 1-octyl-3-methylimidazolium tetrafluoro-borate ($OmimBF_4$), the insolubility can be explained by the presence of large non-coordinating anions. Apparently, BF_4^- and PF_6^- are not able to deconstruct the hydrogen bonding network of the polymers.[84] As already mentioned in Chapter 1, the dissolution effectiveness of ILs is determined by an appropriate combination of cation and anion. However, the role of the anion is predominant.[149] For 1-hexyl-3-methylimidazolium bis(trifluoromethylsulfonyl)imide ($HmimNTf_2$), the presence of the long alkyl chain on the imidazolium ring, the large size of the anion, and its weakly basic character are opposite characteristics of a good cellulose solvent according to Pinkert *et al*.[58] In addition, ILs with NTf_2^- counterions are known for their inability to dissolve cellulose.[58]

Protic ILs (PILs) were selected on the basis of their advantages over common aprotic ILs. By definition, PILs are formed by proton transfer from a Brønsted acid to a Brønsted base.[150] Thus, they are typically easy to produce from low-priced chemicals. Furthermore, no by-products are generated during their preparation.[151] The transfer of a proton induces hydrogen bond donor and hydrogen bond acceptor sites on the ions. [151] This implies that PILs are capable of hydrogen bonding and this subset of ILs was expected to be able to dissolve cellulose and chitin. However, no solving ability was confirmed for the tested PILs (see Table 2.2). This may be interpreted by the presence of the strong acidic hydrogen on the high electronegativity nitrogen present in the cation. It can be supposed that NH^+ prefer to interact with O^- of the anion rather than with the oxygen of the polymers. This further prevents anion-polymer interactions and leads to insolubility. Moreover, it was observed that in the case of ethylammonium and butylammonium formate decomposition under heating of formate into formamide and water occurred and can explain the inefficiency of these PILs.[152]

Carnitine and choline are bio-sourced quaternary ammonium compounds present in food, animals, plants, and micro-organisms.[153,154] They are ideal candidates for the design of biocompatible and biodegradable ILs as well as for the replacement of the toxic and non-biodegradable imidazolium-based ILs.[146,147,155] For this reason, the ability of three bio-sourced ILs: choline butanoate, choline lactate, and butylcarnitine bromide to dissolve

cellulose and chitin was investigated. All were found to be inefficient for this task (see Table 2.2). This is due to the hydroxyl group on the cationic part of the ILs, as it has been already reported for ILs with cationic hydroxyl groups.[95,156] Hydroxyl protons may form hydrogen bonds with the anion, leading to weaken the hydrogen bonding capacity of the latter for the polymers dissolution process.[95]

Ammoeng 102 (A102) is a tetraalkyl ammonium-based IL containing sulfate as anion as well as ethylene oxide groups and a long chain acyl group (C_{18}) on the cation. Its reasonable price (60 €/kg) and its lower toxicity render this IL an interesting alternative to much more expensive and toxic imidazolium-based ILs.[82] As expected, A102 was able to dissolve neither cellulose nor chitin. The hydroxyl end groups, the oxygens of the ethylene oxide units, and the long alkyl chain are different factors that cause strong interactions with the anion (anionic competition) or steric hindrance.[95] Nevertheless, Ammoeng-based ILs are reported in literature as cellulose solvent. Zhao *et al.* have shown that Ammoeng 110 chloride, Ammoeng 110 formate, and Ammoeng 110 acetate could dissolve microcrystalline cellulose.[157] The difference in the structure of Ammoneg 102 and 110 is represented in Figure 2.4. But under close scrutiny, the given solubility of cellulose was only of 0.5 wt%, which is negligible for this project.[157] The trial with an IL with a nonaromatic cyclic cation, *N*-butyl-*N*-methylpyrrolidinium, and a dicyanamide anion (IL short as P_{14}DCA) failed. ILs, which have a pyrrolidinium cation, have been already described as non-dissolving solvents for cellulose.[58]

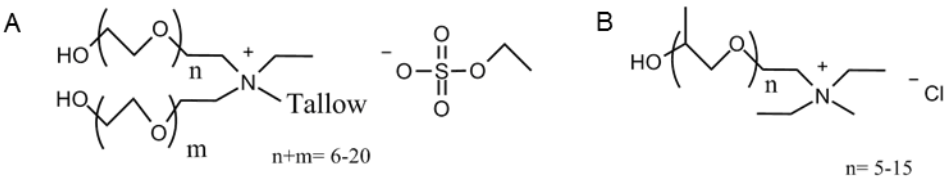

Figure 2.4: *Structure of (A) Ammoeng 102 and (B) Ammoeng 110 chloride.*

In brief, despite their structural similarity, cellulose and chitin showed different solubility in the studied ILs. Solely BmimOAc proved capability for dissolving both biopolymers to sufficient content (>2 wt%) to produce blend materials.

2.3.2 Dissolution in deep eutectic solvents

The objective of this part is to study whether deep eutectic solvents (DESs) are able to dissolve microcrystalline cellulose and α-chitin. Figure 2.5 illustrates the prepared DESs with corresponding chemical structures and abbreviations. Choline chloride/urea (molar ratio 1:2), choline chloride/thiourea (1:2), ethylammonium chloride/urea (1:2), and betaine/urea (1:2) were screened for biopolymer solubility. The selection of these DESs was made on the basis of their advantages over traditional ILs such as their easy preparation (mixing of two coumpounds at moderate heating) from low cost and environmentally-friendlier substances. For instance, the most famous DES composed of choline chloride and urea is completely bio-sourced and costs 0.52-0.62 €/kg.[101,158] The conditions and the results of the dissolution tests using freshly prepared DESs are summarized in Table 2.3.

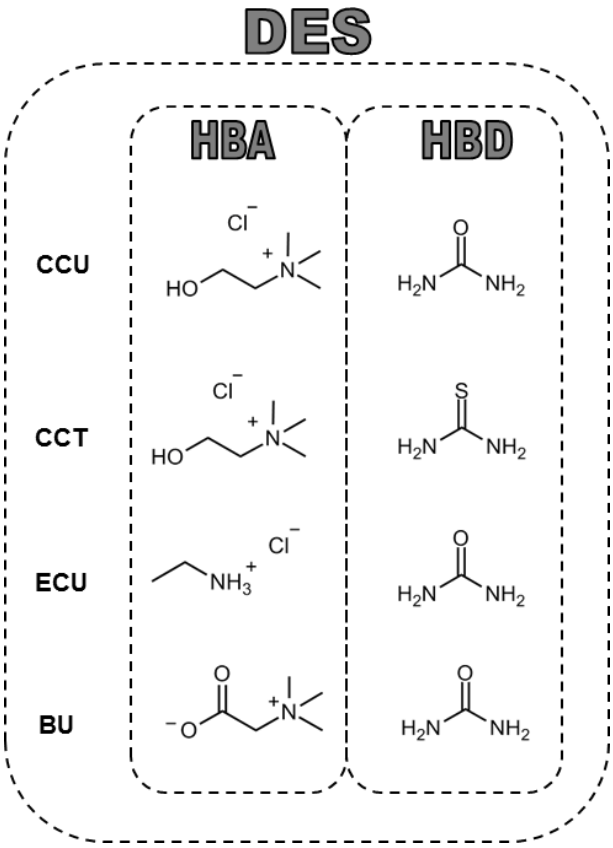

Figure 2.5: *Overview of the hydrogen bond acceptors (**HBA**) and the hydrogen bond donors (**HBD**) for the formation of deep eutectic solvents used in the dissolution tests. **CCU** corresponds to the DES choline chloride/urea, **CCT** to choline chloride/thiourea, **ECU** to ethylammonium chloride/urea, and **BU** to betaine/urea.*

Table 2.3: *Dissolution experiments of microcrystalline cellulose (MCC) and α-chitin in various deep eutectic solvents (DESs).*

DES (HBA:HBD)[a]	Dissolution conditions	Solubility (wt%)[c]	
		MCC	α-chitin
CCU (1:2)	Stirring[b] and heating at 80 °C	NS	NS
	Ultrasonication and heating at 80 °C	NS	NS
CCT (1:2)	Stirring[b] and heating at 80 °C	NS	NS
	Ultrasonication and heating at 80 °C	NS	NS
ECU (1:2)	Stirring[b] and heating at 100 °C	NS	NS
BU (1:2)	Stirring[b] and heating at 100 °C	NS	NS

[a]Molar ratio HBA = Hydrogen Bond Acceptor HBD = Hydrogen Bond Donor [b]Magnetic stirring [c]NS = Not Soluble

The dissolution tests were first performed by conventional heating and with mechanical stirring using a magnetic stirrer. Both microcrystalline cellulose and α-chitin were found to be insoluble in all prepared DESs. Turbid solutions were obtained and many undissolved particles could be seen under the microscope. For instance, Figure 2.6 shows the micrographs of 1 wt% MCC and 1 wt% of chitin in choline chloride/urea (1:2) after dissolution test.

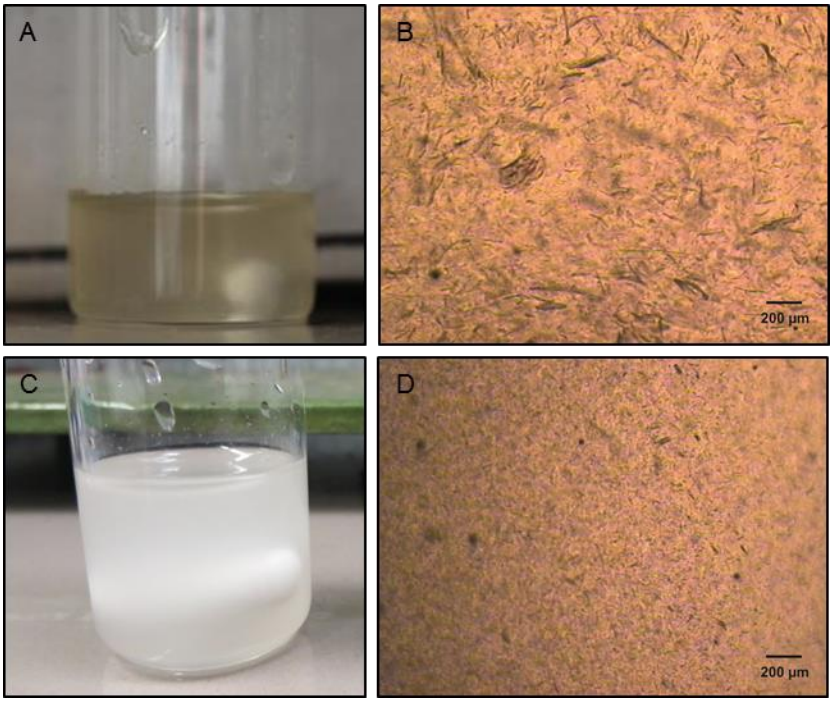

Figure 2.6: *Appearance of the mixtures containing (A) 1 wt% of chitin, (C) 1 wt% of MCC, in choline chloride/urea (1:2) after dissolution test by mechanical stirring at 80 °C. (B) is the corresponding micrograph to the chitin solution and (D) to the MCC solution obtained by polarized light microscope. The white object in solutions is a magnetic stirrer.*

Secondly, dissolution trials with the two DESs choline chloride/urea (1:2) and choline chloride/thiourea (1:2) were performed applying ultrasonication at 80 °C. Ultrasonication is known to facilitate and accelerate dissolution of sample. Nonetheless, the results were unchanged, no solubility was observable. As it can be seen from Figure 2.7, 1 wt% chitin and 1 wt% MCC mixed with CCT by ultrasonication gave turbid solutions. The undissolved polymers can be visually observed at the bottom of the vials.

The insoluble behavior of chitin and cellulose in DESs could result from the strong interactions between the DES compounds caused by hydrogen bonds as well as from the high viscosity of DESs.[159,160]

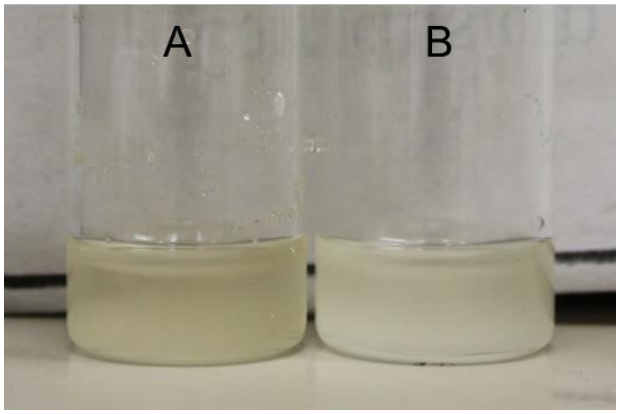

Figure 2.7: *Appearance of the solutions containing (A) 1 wt% of chitin, (B) 1 wt% of MCC, in choline chloride/thiourea (1:2) after dissolution test by ultrasonication at 80 °C.*

All these collected results on the choline chloride-based DESs disagree with the published works from Prasad *et al.*[109,111] Indeed, they have reported that choline chloride/urea (1:2) and choline chloride/thiourea (1:2) could dissolve microcrystalline cellulose and α-chitin in larger quantity than 5 wt%.[109] After correspondence with the authors, we noticed that they did not mention a pre-treatment step performed on the used chitin in their works. They purified chitin (from crab shells from TCI Fine chemicals, Japan) according to the following method. Chitin was first treated with 2 M HCl (1:10 w/v) for 48 h at room temperature and then washed with water. The obtained powder was mixed with 1 M NaOH for 72 h at 80 °C, washed with water and dried prior to use. This omission opened the doors to several questionings. For instance, (1) does the degree of acetylation of chitin (DA = 94.1%)

mentioned in the papers correspond to the unpurified chitin? If yes, (2) is the DA of chitin affected by the purification step? (3) How can the process of chitin purification influence the dissolution? To solve these questions, the same pre-treatment procedure was performed on our chitin. The degree of acetylation of the non-purified and purified chitin determined by elemental analysis and infrared spectroscopy was 92 ± 4% and 93 ± 2%, respectively. Thus, the chitin was not degraded into chitosan and the purification process had no drastic incidence on the DA value. According to Percot *et al.*, the DA of chitin extracted from shrimp shells under approximately the same conditions, just a milder acidic treatment (0.25 M HCl for 15 min), remains also stable.[161] Dissolution tests were then investigated with purified chitin and with the two choline chloride-based DESs under the same dissolution technique (heating at 100 °C) described by Prasad et *al.*[109] Turbid solutions were again obtained after 22 h and undissolved particles were easily observed under the microscope. As it can be seen in Figure 2.8, the size of the undissolved particles, though, was smaller for the purified than for the unpurified chitin solution in CCU (1:2). Accordingly, the purification of the chitin did not lead to its complete dissolution in choline chloride-based DESs and the results of Prasad *et al.* remained unreproducible. Concerning the conflicting results about cellulose solubility in DESs, a study is in concordance with our results and has also shown that microcrystalline cellulose was insoluble in CCU (1:2).[105]

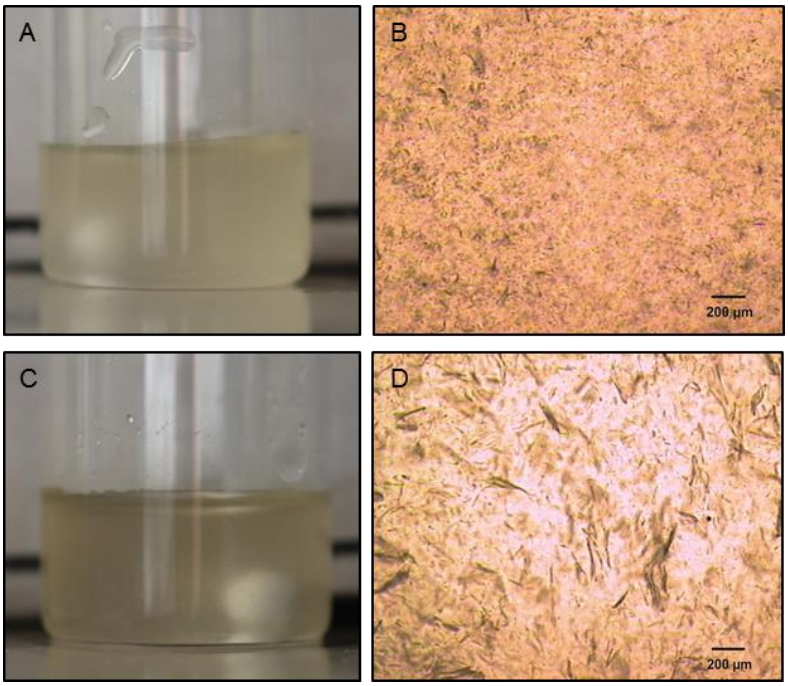

Figure 2.8: *Appearance of the mixtures containing (A) 1 wt% of purified chitin, (C) 1 wt% of unpurified chitin, in choline chloride/urea (1:2) after dissolution test by mechanical stirring at 100 °C. (B) is the related micrograph to the purified chitin solution and (D) to the unpurified solution obtained by polarized light microscope. The white object in solutions is a magnetic stirrer.*

2.3.3 Dissolution in other organic solvents

Other solvent systems, which do not belong to the IL or DES classes, were additionally investigated as cellulose and α-chitin solubilizing agents. Figure 2.9 illustrates an overview of the tested solvents with corresponding chemical structures and abbreviations. Table 2.4 lists the results of the solubility of MCC and α-chitin in these solvents. It can be seen that both cellulose and chitin were dissolved neither in the bio-sourced solvents such as 2-methyltetrahydrofuran (MTHF), 2-methylfuran (MF), 2,5-dimethylfuran (DMF), γ-valero-lactone (GVL), choline hydroxide (ChOH), ethyl lactate (EL), and ethyl acetate (EA), nor in the conventional non-ionic solvents such as γ-butyrolactone (GBL), γ-hexalactone (GHL), propylene carbonate (PC), and dimethyl sulfoxide (DMSO). Except the ionic solvents, the others have no hydrogen bond-breaking properties and were studied to check whether they

can be used as co-solvent in the following Chapter. Requirements of a good co-solvent are to be a non-solvent for the biopolymers and to be chemically inert with the true solvent.[162]

Choline hydroxide is a strong base, which tends to decompose slowly upon storage and when heated. This and the high amount of water (45 wt% H_2O) resulted in insolubility of the polymers. *N*-methylmorpholine *N*-oxide monohydrate and tetrabutylphosphonium hydroxide (with 60 and 40 wt% H_2O) are well-known for their ability to dissolve cellulose.[126,163] They were mainly studied to verify if they can similarly dissolve chitin. However, the complex network of chitin has proven to be insoluble in these solvents.

Inspired by the dissolution ability of solvent systems containing lithium chloride in the polar aprotic solvent *N*,*N*-dimethylacetamide or thiourea in NaOH aqueous solution, this specific additives were mixed with the greener and aprotic solvent GVL.[59,68,72,164] Thus, mixtures composed of 1 wt% LiCl (maximal amount soluble in GVL), of 8 wt%, and of 15 wt% thiourea in GVL were screened as cellulose and chitin solvents. However, none of the studied solutions was able to dissolve cellulose or chitin. It can be presumed that the small amount of LiCl present in the solution was a limiting factor and did not create sufficient interactions of Cl^- and Li^+ with the polymer molecules leading to the dissolution.[60] For the thiourea mixtures, the absence of aqueous NaOH solution and the high temperature employed could explain the insolubility. It was suggested that NaOH, thiourea, water cluster, and cellulose form a new hydrogen bond network at low temperature leading to the disruption of the intramolecular hydrogen bonds of cellulose.[164]

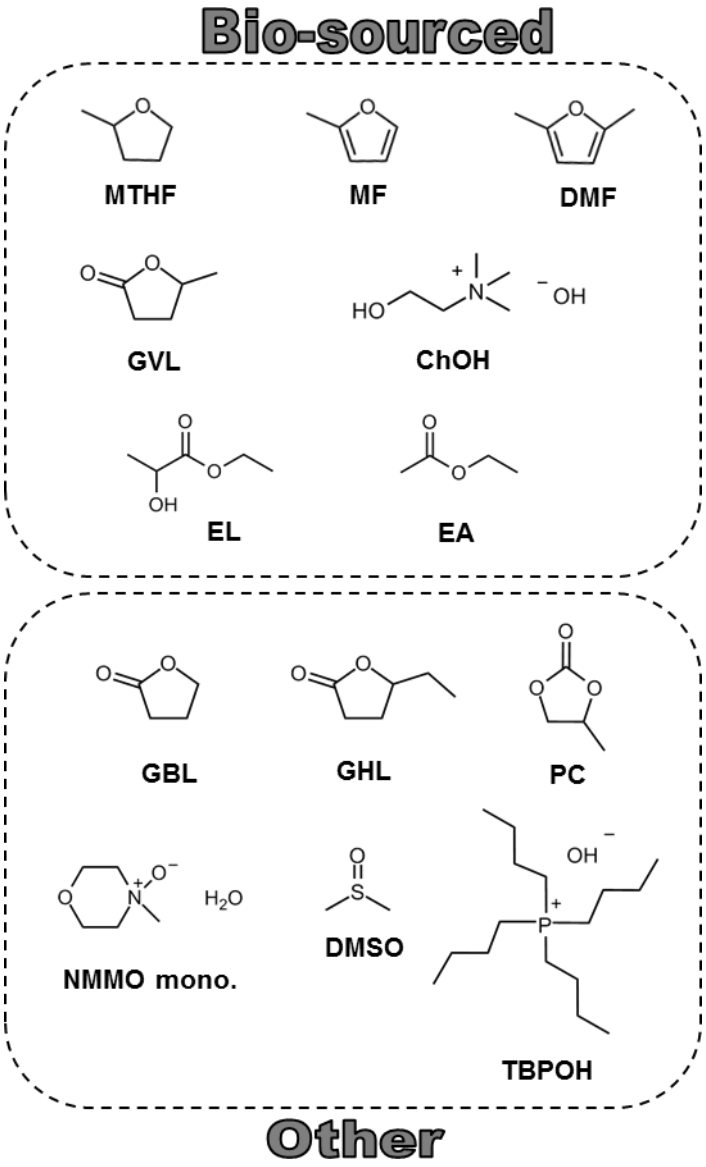

Figure 2.9: *Overview of the organic solvents used in the dissolution experiments: 2-methyltetrahydrofuran (**MTHF**), 2-methylfuran (**MF**), 2,5-dimethylfuran (**DMF**), γ-valerolactone (**GVL**), choline hydroxide (**ChOH**), ethyl lactate (**EL**), ethyl acetate (**EA**), γ-butyrolactone (**GBL**), γ-hexalactone (**GHL**), propylene carbonate (**PC**), N-methylmorpholine N-oxide monohydrate (**NMMO mono.**), dimethyl sulfoxide (**DMSO**), and tetrabutylphosphonium hydroxide (**TBPOH**).*

Table 2.4: *Dissolution experiments of microcrystalline cellulose and α-chitin in organic solvents, which do not belong to the category DES or IL.*

Solvent	**Dissolution conditions**	**Solubility (wt%)**[b]	
		MCC	**α-chitin**
GVL	Stirring[a] and heating at 100 °C	NS	NS
1 wt% LiCl in GVL	Stirring[a] and heating at 40 °C	NS	NS
8 wt% thiourea in GVL	Stirring[a] and heating at 100 °C	NS	NS
15 wt% thiourea in GVL	Stirring[a] and heating at 100 °C	NS	NS
MTHF	Stirring[a] and heating at 75 °C	NS	NS
MF	Stirring[a] and heating at 55 °C	NS	NS
DMF	Stirring[a] and heating at 75 °C	NS	NS
EL	Stirring[a] and heating at 100 °C	NS	NS
EA	Stirring[a] and heating at 70 °C	NS	NS
GBL	Stirring[a] and heating at 100 °C	NS	NS
GHL	Stirring[a] and heating at 100 °C	NS	NS
PC	Stirring[a] and heating at 90 °C	NS	NS
NMMO mono. (~13.3 wt% H_2O)	Stirring[a] and heating at 90 °C	>10	NS
DMSO	Stirring[a] and heating at 90 °C	NS	NS
ChOH in 45 wt% H_2O	Stirring[a] at 0 °C	NS	NS
	Stirring[a] and heating at 60 °C	NS	NS
TBPOH in 60 wt% H_2O	Stirring[a] and heating at 25 °C	5	NS
TBPOH in 40 wt% H_2O	Stirring[a] and heating at 25 °C	>10	NS

[a]Magnetic stirring [b]NS = Not Soluble

Due to the challenge to process chitin, another type of this polymer originating from an alternative source other than shrimp was studied. For this purpose, chitin extracted from mealworms and holding a lower DP (i.e. 1542 instead of 1691 for chitin from shrimp shells) was selected. Dissolving trials with the ILs AmimBr, EmimOAc 98%, and BmimOAc, with the DES CCU (1:2), and with the solvent NMMO mono. were performed. No dissolving enhancements were observed. Chitin from mealworms was insoluble in EmimOAc 98%, CCU, NMMO mono. as for chitin extracted from shrimps. In addition, AmimBr showed a weaker ability to dissolve this chitin while solely BmimOAc was effective.

2.4 Concluding remarks

The main intention of this work was to screen different solvents as dissolving media for microcrystalline cellulose and α-chitin. Ionic liquids, deep eutectic solvents and other organic solvents were therefore investigated. Most of these solvents showed poor chitin solubility and few of them were able to dissolve cellulose.

Cellulose was soluble in five solvents, which can be ordered in function of their effectiveness as **1-ethyl-3-methylimidazolium acetate > 1-butyl-3-methylimidazolium acetate ≈ *N*-methylmorpholine *N*-oxide monohydrate > tetrabutylphosphonium hydroxide (with 40 wt% H_2O) > tetrabutylphosphonium hydroxide (with 60 wt% H_2O)**. The complete dissolution of chitin was only successful with two ionic liquids, ranged in the following order: **1-allyl-3-methylimidazolium bromide > 1-butyl-3-methylimidazolium acetate**. The only common solvent for processing both biopolymers is thus the ionic liquid 1-butyl-3-methylimidazolium acetate. Based on these results, it can be concluded that chitin solubility is more difficult than cellulose and the disruption of chitin complex network, without degradation into chitosan, remains a real challenge.

Despite an effort to find bio-sourced and alternative solvents, none were identified as good solvents for cellulose and chitin dissolution. The efficient solvents mentioned above are neither novel nor highly eco-friendly. The imidazolium-based ionic liquids suffer from non-biodegradability, toxicity, and high cost while *N*-methylmorpholine *N*-oxide monohydrate and tetrabutylphosphonium hydroxide can cause degradation of cellulose at high temperatures.[67,155] Alternative solutions will be developed in the following Chapter in order to minimize some of these disadvantages.

Chapter 3
Effects of a co-solvent in dissolution processes

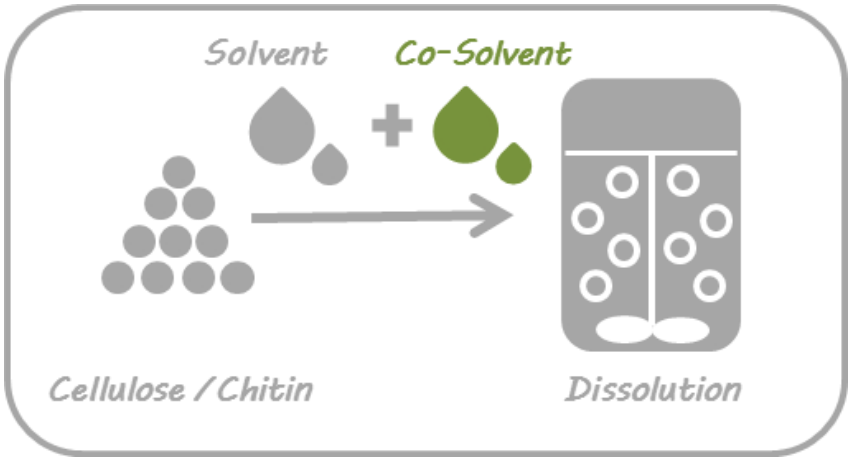

The study concerning the effect of γ-valerolactone on the cellulose dissolution with N-methylmorpholine N-oxide monohydrate presented in this section is submitted to an inventor's notification and a patent application (see list of Publications).

3.1 Introduction

N-methylmorpholine-*N*-oxide (NMMO) and imidazolium-based ionic liquids (ILs) were introduced as greener solvents and alternatives to replace the classical and hazardous solvents for dissolving cellulose.[97,126] ILs have also shown solvating powers towards chitin.[88] Unfortunately, there are still several disadvantages in the use of these solvents despite their perceived environmentally friendlier nature. Slow dissolution rate, complex processing procedures, toxicity, elevated costs, and high energy consumed are part of these limiting factors.[28,81,126] The high viscosity of these solvents is also particularly inconvenient for the dissolution process. For instance, it has been reported that ILs are much more viscous than conventional organic solvents by a factor ranged from 10 to 10 000.[165] Adding a polymer into these viscous liquids was found to increase the viscosity of the solutions even more.[166] Consequently, the mass transfer and the polymer-solvent interactions are weaker, making the solubilization of high amounts of polymer and practical use more challenging. To overcome this problem, high temperatures and long operating times are generally employed, leading sometimes to polymer and solvent degradation.[67,167] Incorporating a less viscous co-solvent into the dissolution process of polymers has been identified as a more effective strategy to enhance polymer dissolution.[168-170] Several co-solvents have been already investigated for the improvement of cellulose dissolution in ILs or NMMO, while no studies about chitin solubilization in presence of a co-solvent were found in literature.[162,168,169,171-173]

Some aprotic solvents, such as dimethyl sulfoxide (DMSO), *N*-methylimidazole, *N*,*N*-dimethylformamide, *N*,*N*-dimethylacetamide, 1,3-dimethyl-2-imidazolidinone, γ-valero-lactone (GVL), and *N*-methyl-2-pyrrolidinone have been proved to be appropriate co-solvents for cellulose dissolution in ILs.[170-172,174-176] Concerning NMMO, *N*-methyl-2-pyrrolidinone, DMSO, and *N*,*N*-dimethylformamide have been reported as efficient aprotic diluents.[162,173] Unfortunately, the majority of them suffer from health and safety issues and from lack of sustainability.[176] Protic solvents such as water, methanol, formamide, and acetamide have been also studied as co-solvent. However, it has been shown that this kind of solvents formed hydrogen bonds with ILs anions, which can compete with the IL-cellulose interactions. Thereby solely small amount of protic co-solvents are tolerated.[170,172,177]

Among all the aprotic co-solvent mentioned above, the effect of DMSO on cellulose dissolution in ILs has been extensively investigated. It was shown that the addition of DMSO "help" cellulose dissolution by decreasing the viscosity of ILs as well of the polymer solution. Thus, the presence of DMSO enables to facilitate the mass transfer, to accelerate dissolution kinetics, and to reduce the dissolution temperature.[169,178] DMSO mitigates also the high costs of ILs.[170] From a molecular point of view, different interpretations for the role of DMSO can be found in scientific literature. For example, with regard to the IL 1-butyl-3-methylimidazolium acetate (BmimOAc), Andanson *et al.* proposed from molecular simulation that DMSO significantly affect neither the hydrogen bond network of BmimOAc nor the IL-glucose interactions.[169] In contrast, Zhao *et al.* postulated that DMSO enhanced the hydrogen bonds interactions between the anion and the hydroxyl protons of cellulose by partially breaking down the ionic association, i.e. between $Bmim^+$ and OAc^-. Thus, dissociated anions are produced and are "more free" to interact with the cellulose.[177]

Although these co-solvents have significantly expanded the range of solvents for cellulose, chitin is again left behind as well as the green credentials. Therefore, the goal of this part was, as a first step, to find a greenest possible co-solvent for the dissolution of both microcrystalline cellulose and α-chitin using BmimOAc as solvent. The latter was the most competitive IL for both polymers according to our findings in Chapter 2. The second step was to enhance the Lyocell process through an eco-friendly co-solvent. In both cases, the maximal concentrations of co-solvent tolerated in the different mixtures were studied by polarized-light optical microscopy. The benefits of the co-solvent on the dissolution were characterized in details with the help of kinetics, viscosity and conductivity measurements. The properties of the resulting polymer solutions were also investigated with thermal and rheological studies to assess the influence of the co-solvent in material processing.

3.2 Experimental section

3.2.1 Chemicals

Microcrystalline cellulose (MCC) and α-chitin used as raw materials are already described in Section 2.2.1.1. Bleached Eucalyptus Kraft pulp was provided by Lenzing AG (Austria) with a degree of polymerization of 950. All polymer powders were dried at 70 °C for at least 5 days prior to use and stored in a glove box.

Solvents mixed with different co-solvents were the IL 1-butyl-3-methylimidazolium acetate (BmimOAc) and the hydrated compound 4-methylmorpholine *N*-oxide monohydrate (NMMO mono.), whose origin and purity are mentioned in Section 2.2.1. Prior to use, BmimOAc was dried using a high vacuum setup at 10^{-6} mbar for 5 days. Water content was controlled with coulometric Karl Fischer titration (899 Coulometer, Metrohm, Switzerland).

2,5-Dimethylfuran, 2-methylfuran, 2-methyltetrahydrofuran, γ-valerolactone, γ-hexalactone, γ-butyrolactone, propylene carbonate, and dimethyl sulfoxide were the co-solvents investigated in this study. Origin and purity of these solvents are described in Section 2.2.1. The co-solvents mixed with NMMO mono. were previously dried with 3 Å molecular sieves for several days to avoid additional water uptake. The water content of these co-solvents is summarized in Table 3.1 and was determined by coulometric Karl Fischer titration.

Table 3.1: *Water content in mass fraction of the co-solvents used in the tolerance tests with NMMO mono. after drying with 3 Å molecular sieves.*

Co-solvents	Water content (ppm)
γ-Valerolactone	40
γ-Hexalactone	130
γ-Butyrolactone	120
Propylene carbonate	95
Dimethyl sulfoxide	150

3.2.2 Experimental methods

3.2.2.1 Tolerance test

The tolerance of a co-solvent in the dissolution process of polymers was performed with the following method. First, a fixed amount of polymer was mixed with a selected ratio of solvent and co-solvent in sealed glass vials in the glove box. The mixture was then heated in an oil bath to a desired temperature and continuously stirred. If a homogenous solution was obtained and no undissolved particles were observed under the polarized optical microscope, a new mixture was prepared with the same amount of polymer but with a lower mass ratio of solvent/co-solvent. The stability of the mixture was also observed at room temperature, especially in the case of NMMO mono. Conversely, if the polymer was not dissolved after 12 h, a new mixture would be prepared with a higher ratio solvent/co-solvent. The aim of this study was to find the maximal amount of co-solvent tolerated to dissolve a certain amount of polymer.

3.2.2.2 Physicochemical properties of solvents and polymer solutions

For the determination of the physicochemical properties, binary mixtures of solvent/co-solvent were prepared gravimetrically using an Entris® Sartorius (Germany) balance with an accuracy of ± 0.1 mg without buoyancy correction. The polymer solutions were produced by dissolving cellulose and chitin in a co-solvent/solvent mixture as explained before.

3.2.2.2.1 Density and dynamic viscosity

Density of solutions was measured with a vibrating tube densimeter DMA 5000M from Anton Paar (Austria) equipped with a precision thermostat. Measurements were performed between 25 °C to 90 °C (in increments of 5 °C). A linear extrapolation was used to calculate the density values higher than 90 °C. The accuracy of the instrument is estimated to be ± 5 10^{-6} g.cm^{-3} and ± 0.01 °C. Density values were used to calculate the dynamic viscosity and the molar conductivity (see Equation 3.1 and Equation 3.4).

Dynamic viscosity measurements of the solutions were performed with a rolling ball viscometer (Anton Paar AMVn, Austria) at temperatures from 25 °C to 110 °C. The principle is the determination of the rolling time of a steel ball in a glass capillary filled with the solution at a given slope angle (30° or 70°). The dynamic viscosity, η, is connected to the rolling time by Equation 3.1.

$$\eta = K \times (\rho_{\text{ball}} - \rho_{\text{solution}}) \times t \tag{3.1}$$

where K is a calibration constant, ρ_{ball} and ρ_{solution} the densities of the ball and the solution respectively, and t the measured rolling time of the ball in the capillary. Capillaries of 1.6 and 1.8 mm diameter were used to perform the measurements and calibrated using a suitable standard oil (from Cannon Instrument Company, USA) to obtain K. For each solution, 5 measurements were repeated. The relative uncertainty of the dynamic viscosity results is lower than 2%.

3.2.2.2.2 Viscoelastic properties

Dynamic viscoelastic behavior of polymer solutions was examined by oscillatory tests using a Bohlin CVO 120 rheometer (Malvern, Germany) at different temperatures ranging from 25 °C to 100 °C. All samples were measured with a 20 mm parallel plate under nitrogen atmosphere to prevent absorption of moisture. The gap between the two plates was set to 300 µm for cellulose dope prepared from NMMO mono. and to 600 µm for IL-based formulations. Each polymer solution was equilibrated at the different experimental temperatures for 600 s before measurement. First, the linear viscoelastic range of stress was determined with amplitude sweep tests at a constant angular velocity (ω = 1 rad/s). Secondly, dynamic frequency sweep tests were performed from 0.1 to 100 rad/s at a constant stress within the linear viscoelastic regime. A chosen stress of 5 and 10 Pa were applied for IL- and NMMO mono.-based solutions, respectively. The dynamic viscoelastic functions such as the storage modulus (G') describing the elastic properties and the loss modulus (G'') characterizing the viscous properties of the sample were measured as a function of angular velocity (ω). These moduli are connected to the complex viscosity ($|\eta^*|$) by Equation 3.2. Each sample was measured three times from low to high and back to low velocities.

$$|\eta^*| = \left(\left(\frac{G''}{\omega}\right)^2 + \left(\frac{G'}{\omega}\right)^2\right)^{1/2} \quad (3.2)$$

3.2.2.2.3 Electrical conductivity

Frequency dependent measurements of the resistance using two platinum electrodes in a capillary cell were performed to determine the electrical conductivity of the solutions. For this purpose, the custom-designed equipment used consists of a cell connected to a switchboard, a LCR bridge HM 8118, a thermometer and a home built precision thermostat (± 0.005 °C). The cell was filled with the solution under nitrogen atmosphere and sealed to avoid contact with air. The cell constant (K_{cell}) of the capillary cell was determined with KCl solutions and was 12.551 ± 0.004 cm^{-1}.[179] Measurements were carried out at temperatures from 25 °C to 100 °C, which were recorded with a calibrated PT-100 thermometer connected to a ASL F250. The electrical resistance (R) of the sample was measured in the frequency (υ) range from 0.2 to 10 kHz to avoid polarization effects at the surface of the electrodes. The resistance at the infinite frequency was obtained by extrapolation of the resistance values to infinite frequency, $R_\infty = \lim_{\upsilon\to\infty} R(\upsilon)$ and was then used to calculate the electrical conductivity (κ) according to Equation 3.3.

$$\kappa = \frac{K_{\text{cell}}}{R_\infty} \quad (3.3)$$

The overall uncertainty of the electrical conductivity was estimated to be lower than 0.75%.

The molar conductivity was then calculated from the measured electrical conductivity (κ) with the help of the molar mass (M) of the IL, the density of the solution (ρ_{solution}), and the weight fraction of GVL (ω_{GVL}) by using the following equation:

$$\Lambda = \frac{\kappa \times M}{(1 - \omega_{GVL}) \times \rho_{\text{solution}}} \quad (3.4)$$

3.2.2.2.4 Dynamic Light Scattering measurements

Binary mixture nano-structures were studied using dynamic light scattering (DLS). The measurements were carried out using a goniometer system CGS-II from ALV (Germany)

equipped with an ALV-7004/FAST Multiple Tau digital correlator and a vertical-polarised 22-mW HeNe laser (wavelength λ = 632.8 nm). Correlation functions were recorded at a scattering angle of 90° for 300 s at 25 °C for the GVL/BmimOAc mixtures and at 40 °C for mixtures containing NMMO mono. In order to remove all dust particles, samples were first filtered through a 0.2 or 0.45 µm polytetrafluoroethylene membrane filter depending on the viscosity of the sample and transferred in a cylindrical light scattering cell. The cells were then thermostated in a toluene bath for 10 min before measuring.

3.2.2.2.5 Thermal analysis

Thermal properties of solvent mixtures and polymer solutions were determined by differential scanning calorimetry (DSC) using a Perkin Elmer DSC 8000 (UK) under nitrogen atmosphere. The calorimeters were calibrated with a standard sample of indium. Measurements were performed in sealed stainless steel crucibles (50 µL Perkin-Elmer pan type B014, Germany). Pans were prepared gravimetrically with roughly 15 mg of solution using a precision balance (Mettler Toledo, AX26 Comparator, Germany) with an accuracy of ± 1 µg without buoyancy correction.

The melting temperature of NMMO mono./GVL mixtures was obtained with a heating scan rate of 20 °C/min and a cooling rate of 5 °C/min at temperatures in the range from -60 to 85 °C. All samples were equilibrated for 30 min at the lowest temperature before being heated up and for 3 min at the highest temperature before being cooled down to guarantee fully melted or crystallized samples. The same procedure was repeated for each sample three times. The melting points were taken from the average onset of the peaks. Thus, the melting value corresponds to the beginning of the disappearance of crystalline phase.

In the case of cellulose solutions, the same procedure was employed. Solely, the scan rates were modified and set at 5 and 2 °C/min for the heating and cooling rate, respectively. Three cycles were collected for each sample at temperatures between -50 and 90 °C. Different transition temperatures were observed and defined as T_C (onset of an exothermic peak) for the crystallization temperature, T_m (onset of an endothermic peak) for the melting temperature, and T_g (midpoint of a small and endothermic stepwise heat flow change) for the glass transition temperature.

3.3 Results and discussion

3.3.1 Co-solvent for cellulose and chitin solubilization in BmimOAc

3.3.1.1 Research of a suitable co-solvent

The search of a co-solvent for cellulose and chitin solubilization in BmimOAc was done with different bio-sourced aprotic solvents: GVL, 2,5-dimethylfuran, 2-methylfuran, and 2-methyltetrahydrofuran. For the dissolution test, 20 wt% of each bio-sourced solvent were mixed either with 1 wt% of chitin or 5 wt% of MCC in BmimOAc. These solutions were stirred and heated to 55 °C, 75 °C, 75 °C, and 110 °C for 2-methylfuran, dimethylfuran, 2-methyltetrahydrofuran, and GVL, respectively. These temperatures were selected to stay below the boiling point of each co-solvent. All of these investigated co-solvents were proven to be non-solvent for cellulose and for chitin in the previous chapter. Protic solvents were not selected here, because they can form hydrogen bonds with the IL and thus hinder polymer dissolution, as already mentioned before.[170]

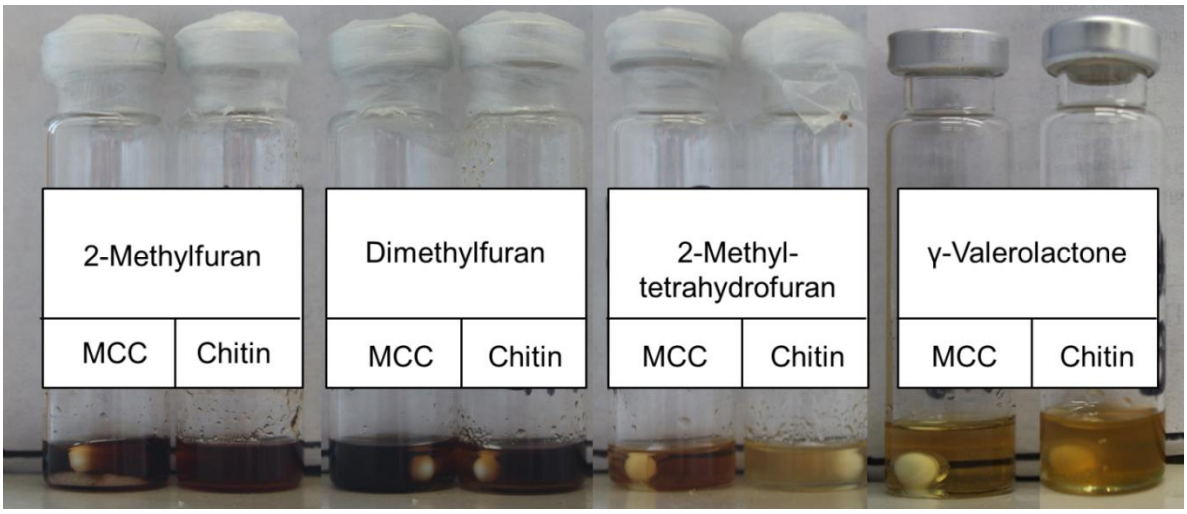

Figure 3.1: *Appearance of the mixtures containing either microcrystalline cellulose (MCC) or chitin, BmimOAc, and 20 wt% of co-solvent (2-methylfuran, 2,5-dimethylfuran, 2-methyltetrahydrofuran, or GVL) after the dissolution test. The white rods in the solutions are magnetic stirrers.*

Figure 3.1 shows the appearance of the mixtures obtained after the dissolution test. It was not possible to dissolve cellulose and chitin using 2,5-dimethylfuran and 2-methylfuran as co-solvents. The solutions became brown during the dissolution process due to a reaction occurring between the co-solvents and BmimOAc. With 2-methyltetrahydrofuran, chitin was not solubilized while cellulose was slowly dissolved after 12 hours. Its boiling point of 78-80 °C inhibited the increase of the dissolution temperature and can be a major drawback in polymer dissolution.[180] In contrast, both polymers could be successfully dissolved in GVL/BmimOAc mixtures in less than 4 hours. Translucent gels were obtained and they can be seen in Figure 3.1. In addition, GVL is an excellent sustainable liquid. It has low toxicity, a high boiling point of 207-208 °C, and is biodegradable. It does not decompose in presence of water or oxygen and does not form an azeotrope with water, rendering it easily removable by distillation.[181] Consequently, GVL was selected as suitable co-solvent for cellulose and chitin solubilization in BmimOAc.

3.3.1.2 Tolerance and effect of GVL in the dissolution process

To balance the toxicity and non-biodegradability of BmimOAc, the maximal amount of GVL tolerated during the dissolution of different chitin or cellulose amounts was studied at 110 °C (Figure 3.2). GVL amounts from 80 to 55 wt% were tolerated for the dissolution of 1-10 wt% MCC in BmimOAc. Maximal GVL contents of 25 and 20 wt% could be added to dissolve 1 and 2 wt% chitin, respectively. Interestingly, a higher amount of GVL could be added to the mixtures with cellulose than to those with chitin. Possible reasons include the high difference of degree of polymerization between MCC (i.e. 124) and chitin (i.e. 1691) and different interactions of GVL with cellulose molecules than with chitin. The addition of GVL drastically increased the sustainability of the mixtures and offered lower costs and a reduced toxicity. For instance at the laboratory scale, pure BmimOAc (with a purity > 98%) can be purchased for 795 €/kg versus 294 €/kg for GVL (with a purity > 99%). Of course, on a production scale, the prices are orders of magnitude lower (e.g. around 15 €/kg for GVL).

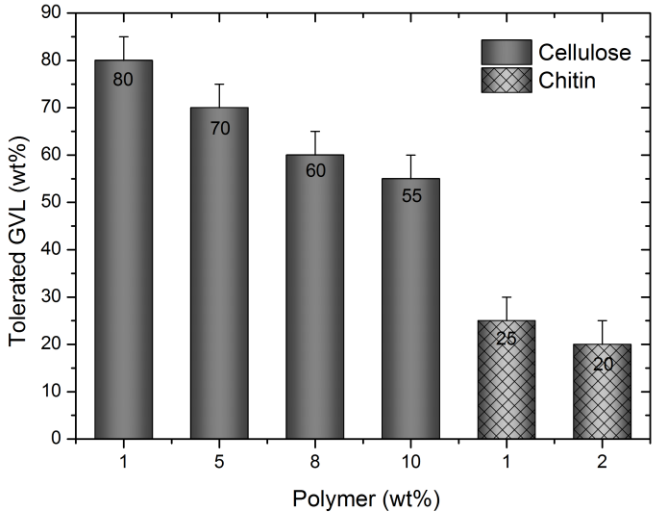

Figure 3.2: *GVL-tolerance in mixtures to dissolve 1-10 wt% of MCC in BmimOAc and 1-2 wt% chitin in BmimOAc at 110 °C. The proportion of BmimOAc in each solution can be calculated according to the following equation: 100 - wt%(MCC or chitin) - wt%(GVL).*

The effect of the sustainable co-solvent GVL on the dissolution duration was investigated with MCC/GVL-containing mixtures selected according to the tolerance results and is represented in Table 3.2. Without the assistance of GVL, 1 wt% cellulose dissolved in 1 hour while with GVL (i.e. 80 wt%), its dissolution time was four times lower. The effect of GVL was also observed for cellulose concentration of 5 wt%, 8 wt%, and 10 wt%. Solubilization durations lower than 1 hour, i.e. 20 and 45 min, were observed for 5 and 8 wt% MCC, respectively. It was possible to dissolve 10 wt% cellulose in 75 min. It has to be mentioned that these durations are shorter compared to reported values in literature.[79] Thus, the addition of GVL helped not only to increase the sustainability but it also accelerated the dissolution process.

Table 3.2: *Effect of GVL on the dissolution duration of MCC in BmimOAc at 110 °C.*

MCC (wt%)	GVL (wt%)	BmimOAc (wt%)	Dissolution time (min)
1	0	99	60
1	80	19	15
5	70	65	20
8	60	32	45
10	55	35	75

3.3.1.3 Impact of GVL on BmimOAc physicochemical properties

In order to better understand the improvements caused by GVL, the properties of binary mixtures composed of BmimOAc and GVL were studied. As BmimOAc is fully miscible with GVL, the viscosity and the conductivity of different mixture compositions ranging from 0 to 100 wt% GVL were measured. These two parameters are very important to characterize the transport properties of these new systems. Viscosity values are related to mass transport phenomena. Studies of molar conductivity coupled with the inverse of the viscosity give information about ion association and are usually illustrated by a Walden plot.[182,183] Measured data of temperature-dependent density, dynamic viscosity, and electrical conductivity are given in Appendix 3.1. Figure 3.3 shows the dynamic viscosity-temperature profile of the pure BmimOAc, the pure GVL, and binary mixtures between 25 °C and 110 °C. For all solutions, the viscosity decreased with increasing temperature by following the Vogel-Fulcher-Tammann equation. This empirical equation is commonly used for ILs to describe the temperature dependent evolution of their dynamic properties. Therein, the dynamic viscosity η (or other dynamic properties) is mathematically expressed by Equation 3.5.[184]

$$\eta = A \times \exp\frac{B}{T - T_0} \tag{3.5}$$

where A, B, and T_0 are adjustable parameters and T is the absolute temperature.

The addition of the low viscous co-solvent to the IL decreased its viscosity significantly (see Figure 3.3). For instance, the addition of 20.3 wt% GVL resulted in a viscosity decrease of 48% at 110 °C. Such a reduction leads to a facilitation of mass transport in these binary

mixtures and an enhancement of the contact between polymer molecules and BmimOAc. It is thus easy to understand the decrease of the time needed for polymer dissolution in BmimOAc/GVL mixtures. Generally, high temperatures (>100 °C) are used to dissolve polymers because of the lower viscosity of ILs at these conditions. With the addition of GVL, lower dissolution temperatures might be used. This should be beneficial on a large scale in terms of energy consumption and possible polymer or IL degradation.

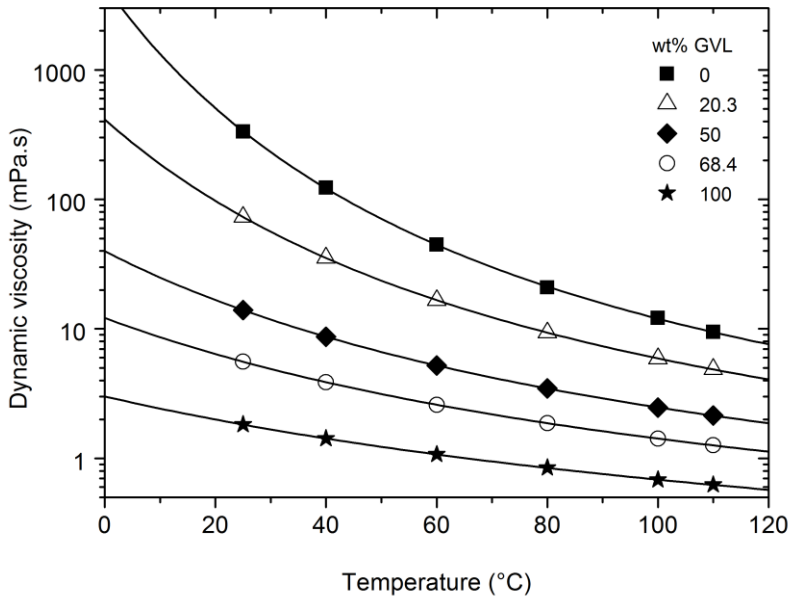

Figure 3.3: *Dynamic viscosity of pure GVL, mixtures composed of BmimOAc and GVL, and pure BmimOAc as a function of temperature. Lines correspond to the best fits using the Vogel-Fulcher-Tammann equation.*

The influence of GVL concentration on the viscosity of BmimOAc/GVL mixtures at a selected temperature, here 25 °C, is shown in Figure 3.4. It can be seen that the viscosity of the solution decreased exponentially with the increase of GVL. According to previous studies, the impact of an organic solvent on the viscosity of an IL can be described by a general equation having the form of Equation 3.6.[137,178]

$$\ln\left(\frac{\eta}{\eta_{IL}}\right) = -\frac{x_{co-solvent}}{\alpha} \quad (3.6)$$

where η and η_{IL} are the viscosities of the mixture and the pure IL, $x_{co-solvent}$ is the mole fraction of the co-solvent in the mixtures, and α is a fitting constant, which depends on the studied system.

As shown in the inset of Figure 3.4, experimental data of the viscosity for different GVL/BmimOAc mixtures at 25 °C follow well Equation 3.6 with a coefficient of determination $r^2 > 0.99$ and a value for α of 0.198. The same procedure was performed for the viscosity data at the other measured temperatures and the results of α and r^2 are represented in Table 3.3. It can be noted that α increased linearly with temperature (T) in the measured temperature range. The relationship between these two parameters can be expressed by Equation 3.7 ($r^2 > 0.99$).

$$\alpha = 0.0024 \times T(°C) + 0.1409 \quad (3.7)$$

Consequently, according to Equation 3.6 and 3.7, the viscosity of all BmimOAc/GVL mixtures at temperatures from 25 °C to 110 °C can be predicted by the concentration of GVL and the viscosity of pure BmimOAc at the desired temperature.

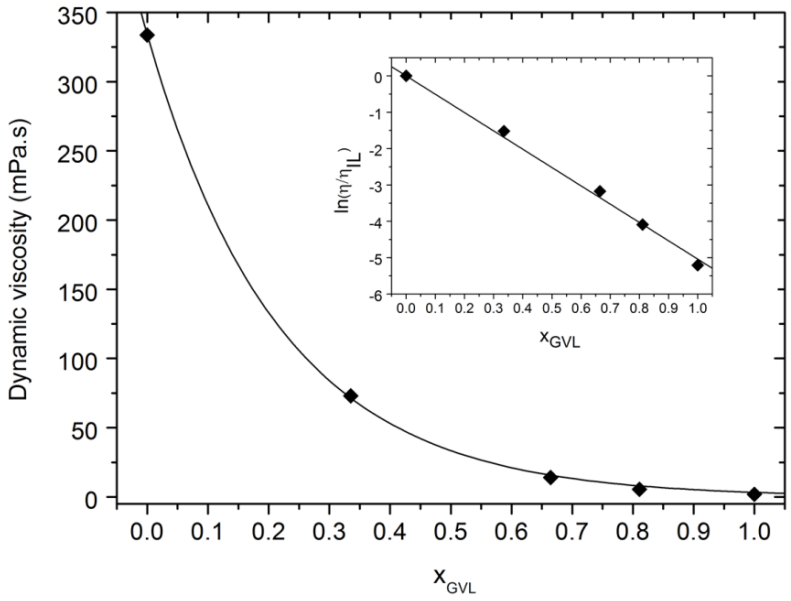

Figure 3.4: *Effect of GVL on the viscosity of BmimOAc/GVL mixtures at 25 °C. The line corresponds to the best fit using an exponential equation. The inset represents the linear change of $\ln(\eta/\eta_{IL})$ as a function of GVL mole fraction using Equation 3.6.*

Table 3.3: *Values of the constant α from Equation 3.6 as a function of temperature.*

Temperature (°C)	***α***	***r²***
25	0.198	>0.99
40	0.234	0.99
60	0.284	0.99
80	0.334	0.98
100	0.374	0.98
110	0.398	0.98

Figure 3.5 illustrates the Walden plot for the pure BmimOAc and mixtures composed of BmimOAc and GVL. According to the Walden rule, the molar conductivity is inversely proportional to the viscosity for diluted electrolyte solutions.[185] This rule has been used to provide a qualitative approach of the ionicity for ILs. In this graph, the relationship between the molar conductivity and the fluidity (i.e. the inverse of the viscosity) of the IL-based solutions is compared to the line of a so-called "ideal" electrolyte solution. Generally, an 1

molar aqueous KCl solution is used for this purpose.[183] In Figure 3.5, it can be observed that the addition of GVL did not disturb the linear behavior of the points displayed for each solution. The slope of the lines ranged from 0.95 to 1.09. That means that the addition of GVL to the IL did not severely change the structure of BmimOAc in terms of ion interactions. For a same molar conductivity value, the fluidity is shifted to the right on the x-axis of Figure 3.5 by increasing GVL concentration. In other words, the ionicity of the mixture decreased with the dilution of BmimOAc with GVL.

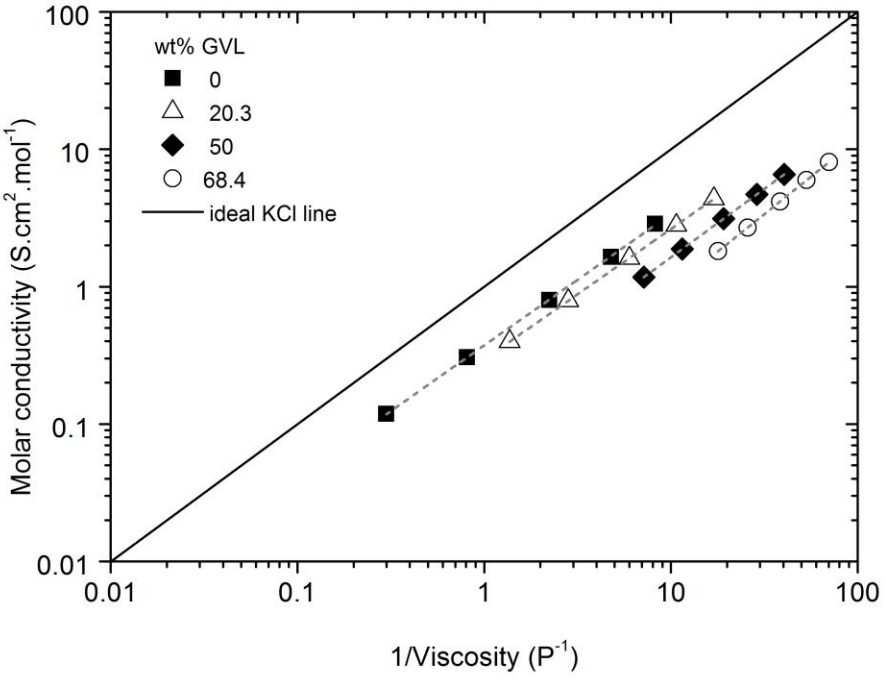

Figure 3.5: *Walden plot of pure BmimOAc and mixtures composed of BmimOAc/GVL. The solid line corresponds to the "ideal" behavior of an 1 M aqueous KCl solution and the dashed line to the best linear fits.*[183]

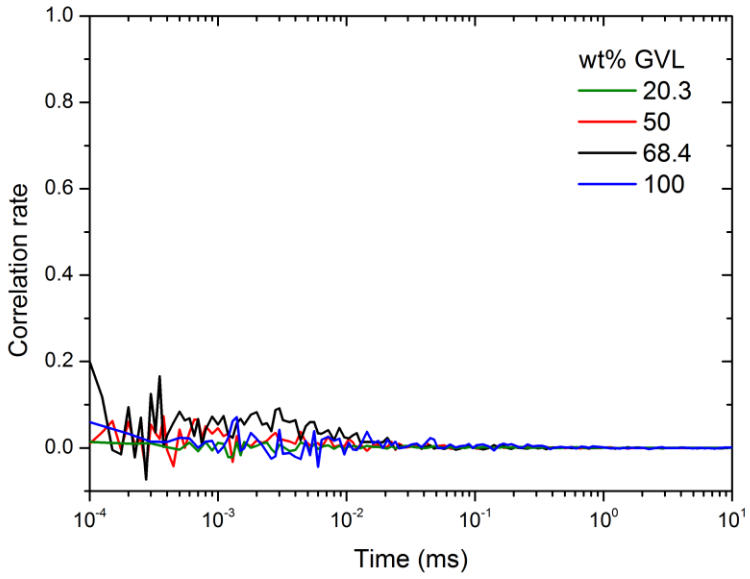

Figure 3.6: *Autocorrelation functions obtained by DLS for BmimOAc/GVL mixtures at 25 °C.*

The presence of nano-structures in GVL/BmimOAc mixtures was checked by means of DLS measurements at 25 °C. As visible from Figure 3.6, no well-defined autocorrelation functions were found in the solutions. This indicates that no nano-structures are formed between GVL and BmimOAc and that GVL plays the role of a simple co-solvent.

3.3.1.4 Influence of GVL on the rheological properties of polymer solutions

Rheology plays an important role in polymer material processing because it explains how a system will respond to a mechanical stimulus regarding elastic deformations and viscous flow.[186] Therefore it is essential to observe the influence of the co-solvent GVL on the rheological properties of cellulose and chitin dissolved in BmimOAc/GVL mixed solutions.

Concerning the cellulose solutions, four solutions were prepared on the basis of a constant cellulose concentration, i.e. 5 wt% MCC. Different amounts of GVL, within a range from 0 to 65 wt%, were used as co-solvent in addition to BmimOAc. Dynamic rheological

measurements were performed yielding the storage modulus (G'), the loss modulus (G''), and the complex viscosity ($|\eta^*|$) for the studied solutions as a function of angular frequency (ω). Figure 3.7 shows the changes of the dynamic moduli, G' and G'', versus ω for the cellulose mixtures at 25 °C. These two parameters give information on polymer interactions and on the time for mechanical relaxation processes in the samples. For the solution without GVL, G'' was always higher than G' (with $G' \sim \omega^2$ and $G'' \sim \omega$ for $\omega \rightarrow 0$) and no crossover is present within the studied angular frequency range (see Figure 3.7 A). The solution thus exhibited the behavior of a viscoelastic liquid. By increasing the GVL concentration, it can be first noticed that the dynamic moduli values tend to become smaller (Figure 3.7). This means that the viscoelastic behavior of the solution is sensitive to GVL content. Secondly, crossover points were noticeable within the measured angular frequency range. The solutions with GVL exhibited a gel-like behavior ($G' > G''$) at high ω. The crossover frequency occurred at lower values with increasing GVL concentration. This indicates that a longer relaxation time of the cellulose chain was needed with the increase of GVL content. Cellulose molecules seemed to be less flexible and less mobile in presence of GVL. Cellulose chains segments might be closer to each other or interlinked with GVL. The change of the complex viscosity, $|\eta^*|$, as a function of ω for the cellulose solutions at 25 °C is shown in Figure 3.8. It can be observed that $|\eta^*|$ values decreased with increasing GVL content. In addition, the samples exhibited a constant plateau (called Newtonian plateau) at low ω values, while a slight shear-thinning behavior was detected at higher ω. This latter trend was more pronounced for the cellulose solution without GVL. To clearly observe the influence of GVL, $|\eta^*|$ data at an angular velocity of 1.18 rad/s as a function of temperature for two solutions are represented in Figure 3.9. The effect of only 20 wt% GVL on the decrease of $|\eta^*|$ was significant, notably at low temperatures. Above 80 °C, the complex viscosity results with and without GVL are similar.

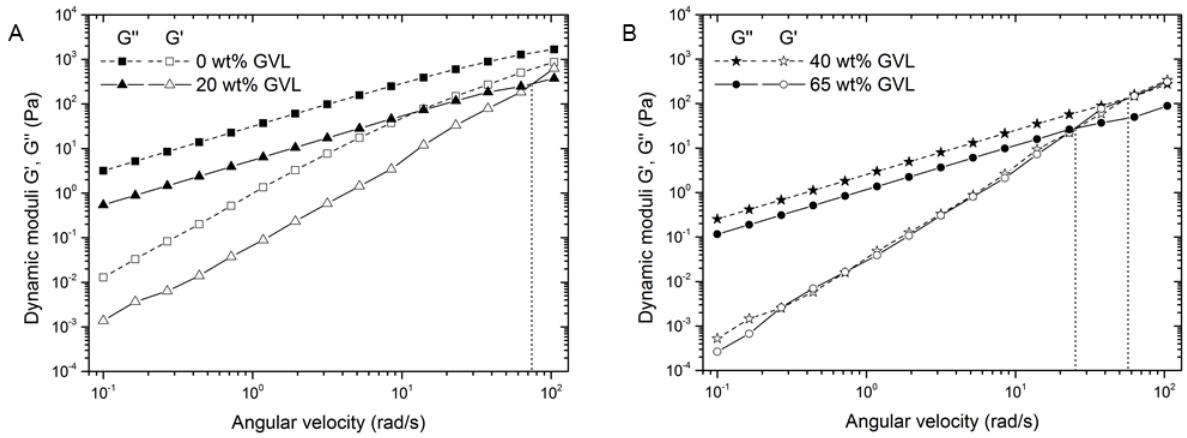

Figure 3.7: *Loss modulus (G'', solid symbol) and storage modulus (G', open symbol) as a function of angular frequency for the solutions composed of 5 wt% MCC dissolved in BmimOAc with different amount of GVL: (A) 0 and 20 wt%, (B) 40 and 65 wt% at 25 °C.*

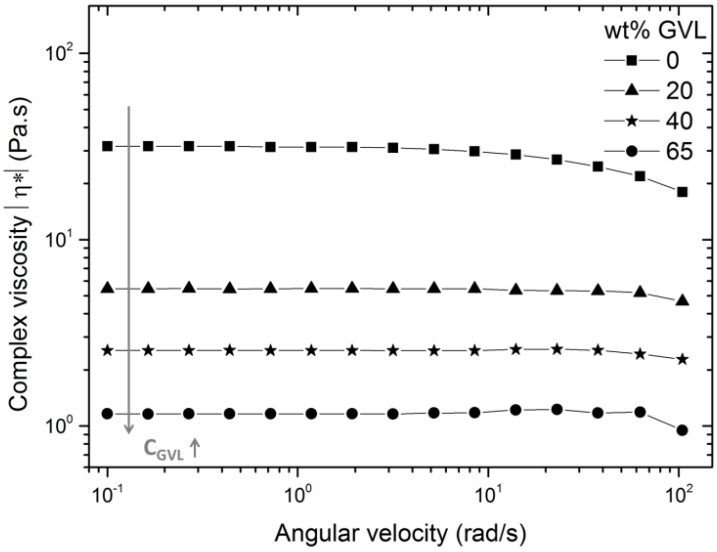

Figure 3.8: *Complex viscosity as a function of angular velocity for the solutions composed of 5 wt% MCC dissolved in BmimOAc with different amounts of GVL at 25 °C.*

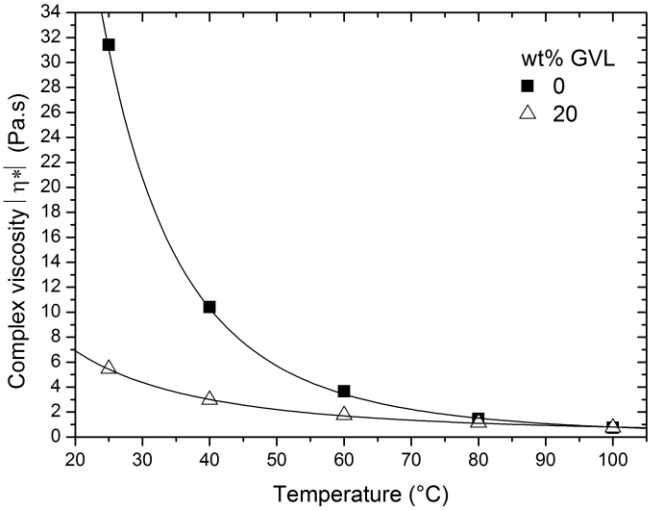

Figure 3.9: *Effect of GVL on the complex viscosity for cellulose solutions composed of 5 wt% MCC dissolved in BmimOAc and in BmimOAC/GVL (75/20 wt%). The viscosity values were measured at an angular velocity of 1.18 rad/s at different temperatures. The lines correspond to the best exponential fits.*

Dynamic rheological behaviors of chitin in BmimOAc/GVL mixtures were investigated with solutions having the same chitin concentration (i.e. 1 wt%). Two solutions were therefore prepared: (1) 1 wt% chitin dissolved in BmimOAc and (2) 1 wt% chitin dissolved in 20 wt% GVL and 79 wt% BmimOAc. The change of dynamic moduli, *G'* and *G''*, for these two chitin dopes as a function of angular velocity at 25 °C is shown in Figure 3.10. At low angular frequencies, *G''* values were higher than *G'* ones for both solutions. This indicates that the viscous response dominated, i.e. polymer chains had enough time to disentangle due to higher flexibility. After the crossover, *G' > G''* and elastic response dominated, i.e. the polymer chains did not have enough time to relax, the network of entanglement was more rigid. This is a typical behavior of a polymer gel.[187] With the addition of 20 wt% GVL, the dynamic moduli decreased and the crossover point shifted to a higher ω (from 0.5 to 1.7 rad/s). This shift is the opposite of what was observed with cellulose solutions and suggests an acceleration of the chitin chain relaxation. In this case, GVL allowed the chitin chains to be more flexible and mobile. This difference can be explained by either the difference in chain length between MCC and α-chitin or by a different interaction in the

polymer solvation mechanism caused by GVL. To fully understand the role of GVL in the dissolution mechanism, further investigation is needed. Figure 3.11 presents the flow curves (dependence of $|\eta^*|$ on ω) for the chitin solutions at 25 °C. On the one hand, the viscosity decreased with the increase of ω, indicating a shear-thinning behavior for both chitin solutions. On the other hand, $|\eta^*|$ values became smaller by the addition of GVL. To illustrate the impact of GVL, $|\eta^*|$ values at an angular velocity of 1.18 rad/s for both solutions are plotted as a function of temperature in Figure 3.12. The addition of GVL tended to significantly decrease $|\eta^*|$ values. This effect was more pronounced for measurements at temperatures lower than 80 °C. For instance, the viscosity at 100 °C for the chitin solution prepared only in BmimOAc was similar to the one at 60 °C for the solution with 20 wt% GVL.

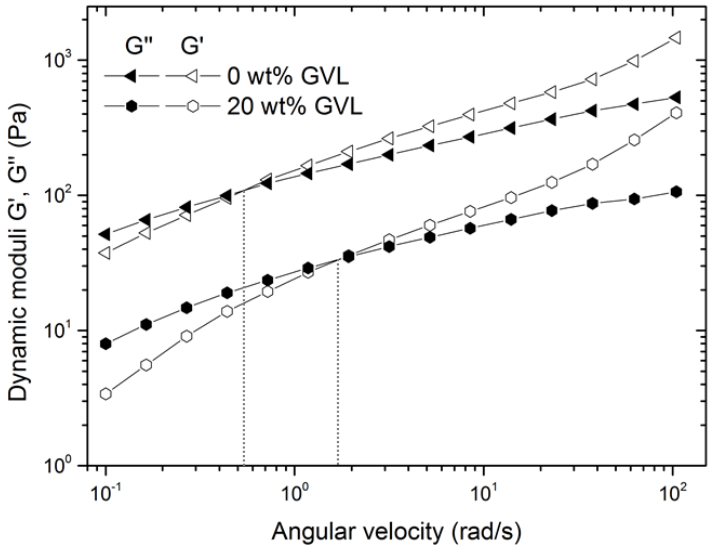

Figure 3.10: *Loss modulus (G‘‘, solid symbol) and storage modulus (G‘, open symbol) as a function of angular frequency for the solutions composed of 1 wt% chitin dissolved in only BmimOAc and of 1 wt% chitin dissolved in BmimOAc and in presence of 20 wt% GVL at 25 °C.*

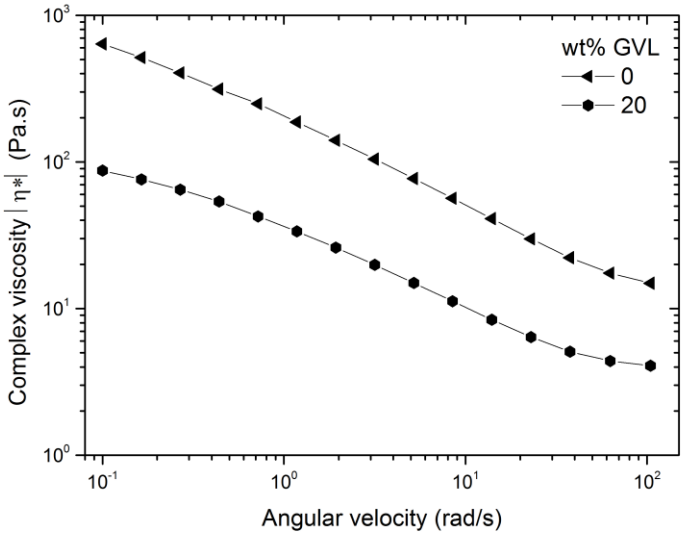

Figure 3.11: *Complex viscosity as a function of angular velocity for the solutions composed of 1 wt% chitin dissolved in BmimOAc with 0 and 20 wt% GVL at 25 °C.*

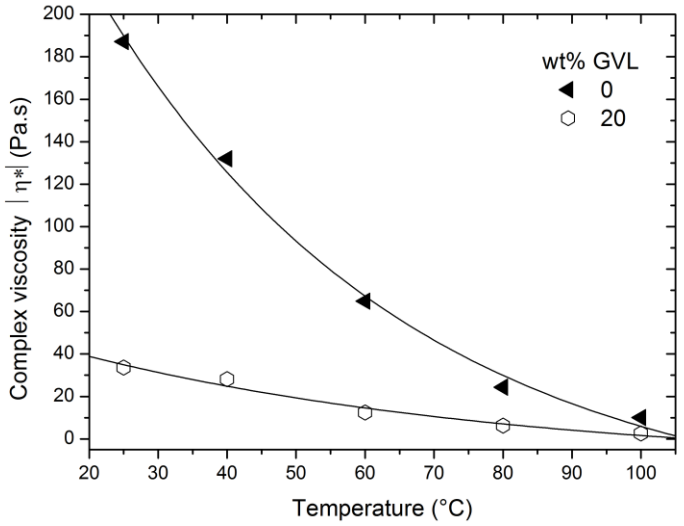

Figure 3.12: *Effect of GVL on the complex viscosity for chitin solutions: 1 wt% chitin dissolved in BmimOAc and in BmimOAC/GVL (79/20 wt%). The viscosity values were measured at an angular velocity of 1.18 rad/s at different temperatures. The lines correspond to the best exponential fits.*

3.3.2 Co-solvent for cellulose solubilization in NMMO monohydrate

3.3.2.1 Suitable co-solvent and tolerance

For the search of a suitable co-solvent for cellulose dissolution in NMMO mono., some aprotic organic solvents with a dipole moment >3.5 Debye (D) were investigated. A high degree of polarity has been proposed to be a significant criteria for a suitable co-solvent according to Franks *et al.*[162] The three different lactones, γ-valerolactone (GVL), γ-butyrolactone (GBL), and γ-hexalactone (GHL), the carbonate ester having structural similarities to these lactones, propylene carbonate (PC), and the most used co-solvent, dimethyl sulfoxide (DMSO), were studied. All these solvents were demonstrated to be non-solvent for cellulose in the previous chapter. The gas-phase dipole moment of each solvent was estimated by quantum mechanical, semi empirical calculations with MOPAC (PM6) and is given in Table 3.4. The maximal tolerance of each diluent in the dissolution of MCC in presence of NMMO mono. was determined at 80 °C. Results are represented as a bar graph in Figure 3.13. Among the lactones, GBL could be added in higher amounts without disturbing the dissolution process. On the contrary, GHL showed to be the least tolerated. By translating these results into mole fraction, the lactone tolerance varied according to a similar tendency, i.e. GBL > GVL > GHL. GVL and GHL are the 4-methyl and 4-ethyl analog of GBL, respectively. Accordingly, it seems that an increased hydrophobicity is connected to a lower tolerance of the respective lactone in the cellulose dissolution.

Concerning the solvents, which do not belong to the lactone class, their addition and tolerance were also investigated during cellulose solubilization. When PC was used as co-solvent, the dissolution process was inhibited due to a chemical reaction, possibly between NMMO mono. and PC. Therefore, this organic liquid was not compatible with the amine oxide. As for DMSO, similar amounts as reported for GHL could be added to give a clear and stable polymer solution at 80 °C as well as at room temperature (see Figure 3.13). Again, the mass fractions were transformed into mole fractions and the order of accepted co-solvent appeared to be GBL > GVL > DMSO > GHL. It can be seen from Table 3.4 that the dipole moment of a co-solvent, i.e. its degree of polarity, had no obvious influence on this classification.

Table 3.4: *Dipole moment of diluents estimated in the gas phase with MOPAC (PM6).*

Solvent	Dipole moment (D)
DMSO	4.71
GBL	5.10
GVL	5.20
GHL	5.28
PC	5.73

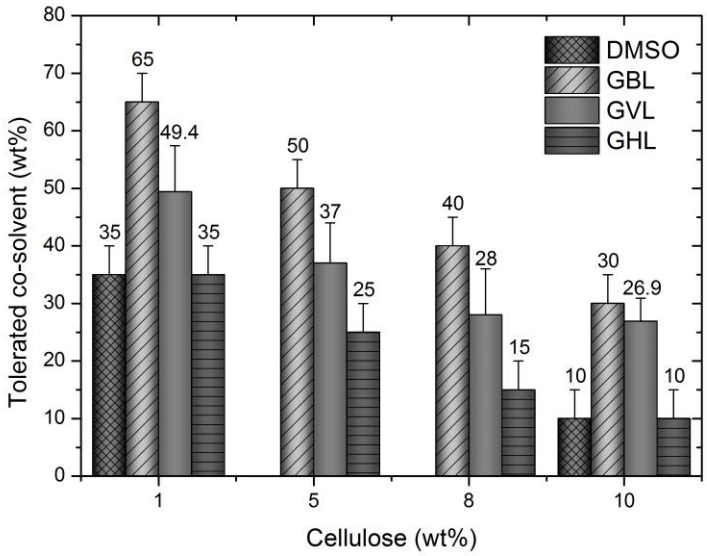

Figure 3.13: *Tolerance of co-solvents in mixtures to dissolve MCC at concentrations ranging from 1 to 10 wt% in NMMO mono. at 80 °C. The proportion of NMMO mono. in each solution can be calculated according to the following equation: 100 - wt%(MCC) - wt%(co-solvent).*

Although GBL is the most tolerated co-solvent, its ability to be metabolized to the drug γ-hydroxybutyrate (GHB) in the body is a major drawback in process operations.[188] Consequently, GVL was selected as relevant co-solvent for cellulose dissolution in NMMO mono. As already mentioned, this molecule can be produced from biomass and meet almost all the criteria of a green solvent.[189] As GVL does not form an azeotrope with water, it can be readily separated from water by distillation.[190] The recovery of solvent after regeneration of cellulose in a process such as the Lyocell process is an important step for a sustainable procedure. Several publications have shown that NMMO with a water composition up to 17 wt% was efficient to complete dissolution of cellulose.[126,129] Generally, aqueous NMMO

(with 20-30 wt% H_2O) is used as solvent system in the Lyocell process to enhance mixing. Cellulose dissolution is performed by eliminating water from the mixture.[126] Interestingly, with GVL, an amount higher than 17 wt% could be added to NMMO mono. to dissolve different cellulose concentrations. GVL might allow removing the step of water evaporation during cellulose dissolution in the Lyocell process.

The maximal tolerance of GVL in the dissolution of another type of cellulose in presence of NMMO mono. was investigated at 80 °C. For this purpose, pulp cellulose with a higher DP than microcrystalline cellulose (950 instead of 124) was taken. Remarkably, NMMO mono. was still able to dissolve cellulose pulp (1, 2 and 3 wt%) in presence of GVL content ranging from 40 to 50 wt% (see Figure 3.14). For cellulose concentrations higher than 3 wt%, the solutions were too viscous to be stirred by a simple magnetic stirrer. Lacking of a sealed precision mixer, no higher cellulose concentration could be studied and compared to MCC.

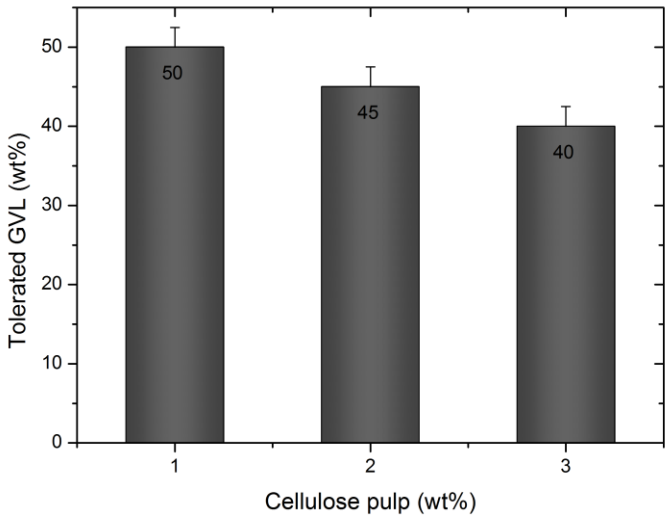

Figure 3.14: *Tolerance of GVL in mixtures to dissolve cellulose pulp in concentration ranging from 1 to 3 wt% in NMMO mono. at 80 °C. The proportion of NMMO mono. in each solution can be calculated according to the following equation: 100 - wt%(cellulose pulp) - wt%(co-solvent).*

3.3.2.2 Effect of GVL during the dissolution process

Beside the increase of sustainability of the process, the addition of GVL has three main observed benefits during the dissolution of cellulose:

1. The dissolution duration of cellulose in mixtures containing GVL was significantly decreased compared to solely in NMMO mono. (see Table 3.5). Without the assistance of GVL, solubilization times higher by a factor of 1.3, 2, and 4 were recorded for MCC concentration of 5, 8, and 10 wt%, respectively. As for GVL/BmimOAc solutions, GVL decreases the viscosity of NMMO mono. and facilitates the mass transport.
2. As seen in Figure 3.15, the solutions composed of cellulose dissolved in exclusively NMMO mono. became brown after dissolution. This could be a sign of cellulose and/or NMMO degradation. Optimally, NMMO is a direct and non-derivatizing solvent of cellulose. Nevertheless, it has been shown that stabilizers such as propyl gallate are needed in the Lyocell process to avoid side reactions.[67,129] Here, GVL seemed to prevent these undesired effects.
3. Crystallization was not observed at room temperature for the mixtures of 5 wt% MCC in NMMO mono./GVL, while the opposite happened for the solutions free of GVL (sample C and D in Figure 3.15). This effect should allow spinning solutions with GVL at lower temperature than without.

Table 3.5: *Effect of GVL on the dissolution duration of MCC in NMMO mono. at 80 °C.*

MCC (wt%)	GVL (wt%)	NMMO mono. (wt%)	Dissolution time (h)
5	37	58	0.75
5	0	95	1
8	28	64	1
8	0	92	2
10	26.9	63.1	1
10	0	90	4

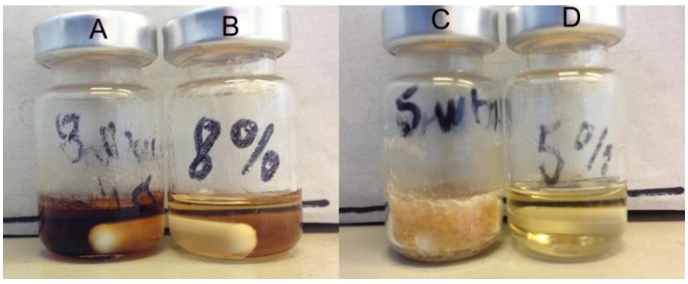

Figure 3.15: *Pictures of samples after dissolution at 80 °C. (A) 8 wt% MCC dissolved in NMMO mono. (B) 8 wt% MCC dissolved in NMMO mono./GVL (64/28 wt%). (C) 5 wt% MCC dissolved in NMMO mono. (D) 5 wt% MCC dissolved in NMMO mono./GVL (58/37 wt%). The white rod in the solutions is a magnetic stirrer.*

3.3.2.3 Impact of GVL on NMMO monohydrate physicochemical properties

In order to highlight the advantages provided by GVL in the Lyocell process, physicochemical properties of NMMO mono./GVL mixtures were investigated.

NMMO exists in different hydrate forms with melting points inversely proportional to the water content. Indeed, anhydrous NMMO melts at 184 °C, NMMO monohydrate (i.e. 13.3 wt% H_2O) between 72 and 78 °C depending on the measurement conditions, and the NMMO mixture composed of five H_2O molecules per two NMMO units (i.e. 28 wt% H_2O) at 39 °C.[191,192] To dissolve cellulose in NMMO, its liquid form is essential. Therefore, the melting behavior of NMMO mono./GVL mixtures was studied by differential scanning calorimetry (DSC) measurements. An example of DSC heating curves obtained for the binary mixtures composed of 10, 50, and 70 wt% GVL is shown Figure 3.16. Only three solutions were plotted for clear visual representation. The curves display a single melting endothermic peak, which is shifted to lower temperature with increase of GVL content. The full change of the melting points as a function of GVL concentration is given in Figure 3.17. Typically, the melting temperatures were reduced by increasing GVL amount and no eutectic was formed between the two compounds. These results indicate that the heating temperature during the dissolution of cellulose in NMMO mono./GVL mixtures can be readily reduced compared to solely in NMMO mono. For instance, for 1 wt% MCC, which was dissolved in a NMMO mono./GVL solution with a weight ratio of 1:1, the heating temperature should be

suitable between 50 and 60 °C, instead of 80 °C in pure NMMO mono. As a consequence, thermal degradations can be prevented and energy consumption can be reduced.

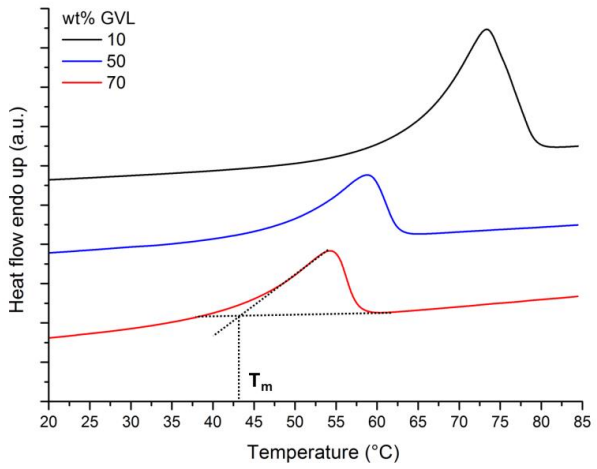

Figure 3.16: *DSC heating curves of NMMO mono./GVL mixtures recorded at a scan speed of 20 °C/min, showing the effect of GVL concentration. The second heating cycle is represented as well as the method to obtain the melting temperature, T_m, defined as the onset of the endothermic peak.*

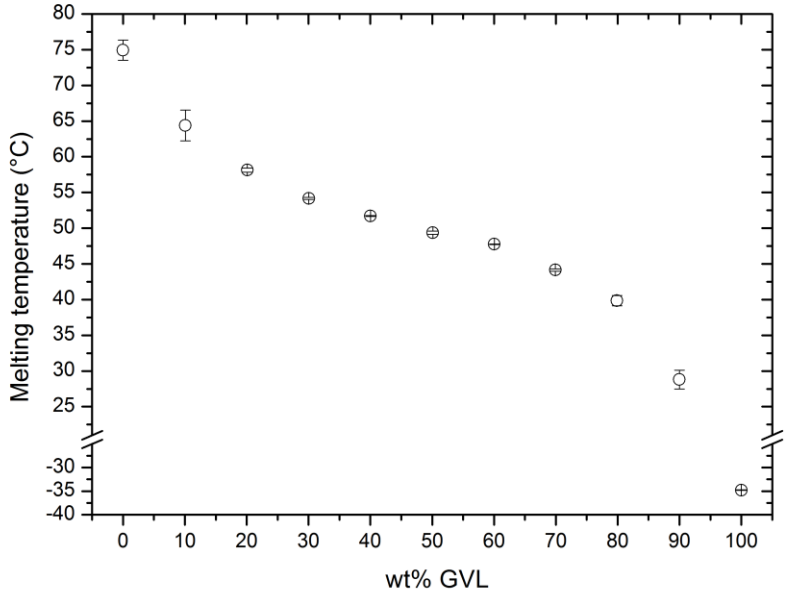

Figure 3.17: *Evolution of the melting temperature of NMMO mono./GVL mixtures as a function of GVL concentration.*

NMMO mono./GVL mixtures were studied using DLS measurements at 40 °C. As observed in Figure 3.18, different behaviors can be noted when increasing the GVL content. For mixtures composed of 30-50 wt% GVL and of 70 wt% GVL, bimodal and monomodal functions with a small intensity were obtained, respectively. In the case of solutions with a GVL content equal or higher than 90 wt%, these distributions disappeared. Accordingly, no significant nano-structures were found in the NMMO mono./GVL formulations. The alternating modalities of the correlation functions observed can be assigned to non-dissolved aggregates of NMMO.

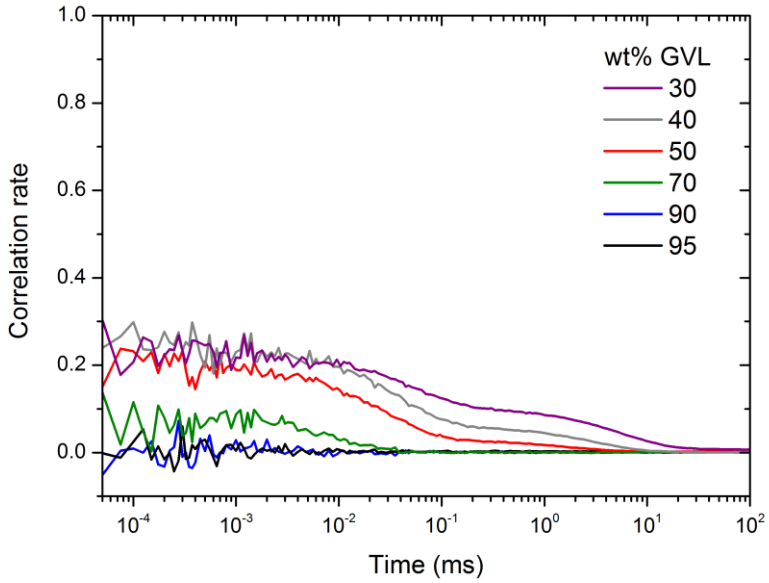

Figure 3.18: *Autocorrelation functions obtained by DLS for mixtures composed of NMMO mono. and GVL at 40 °C.*

3.3.2.4 Influence of GVL on the cellulose dope

Generally in the Lyocell process, highly viscous cellulose dopes with zero shear viscosities in the range of 5000–30000 Pa.s are extruded through a spinneret.[193] This proceeding operation requires elevated temperatures and pressures leading to high energy consumption. The influence of the addition of GVL on the dope properties is relevant to assess the benefits of this environmentally friendly co-solvent.

The flow behavior of cellulose dope containing GVL was characterized by oscillatory measurements. Cellulose solutions, wherein 3 wt% of cellulose pulp was dissolved in a mixture of NMMO mono. and GVL, were therefore studied. The dependence of the dynamic moduli G' and G'' on the angular velocity ω for GVL contents of 30 and 40 wt% at 25 °C is illustrated in Figure 3.19. When GVL concentration rose by 10 wt%, G' and G'' values decreased approximately by a factor of 2. For both solutions, $G' < G''$ during a broad range of angular frequencies indicating that solutions behaved as viscous fluids. As G' increased more sharply than G'' with the increase of ω, a crossover point ($G' = G''$) appeared at high angular frequency. With the increase of GVL content, the cross over point shifted to a higher value, i.e. 85 instead of 49 rad/s. This suggests an acceleration of the cellulose chain relaxation when cellulose dopes contain a larger proportion of GVL. It can be attributed to a distance and a difference in the mobility of cellulose chains due to GVL. Figure 3.20 shows the change of the complex viscosity as a function of ω for the cellulose dopes at 25 °C. The viscosity values of the cellulose solution prepared with 40 wt% GVL were reduced by a factor of two, compared to the solution with 30 wt% GVL. For instance, at ω = 1.27 rad/s, viscosity values of 22.12 and 12.47 Pa.s were recorded for cellulose dopes composed of 30 and 40 wt% GVL, respectively. Both dopes exhibited a Newtonian plateau at low ω values as well as a shear thinning behavior at higher angular frequencies. Finally, the reduction of the dope viscosity by addition of GVL may facilitate the spinnability and the processing of the solutions into cellulose materials.

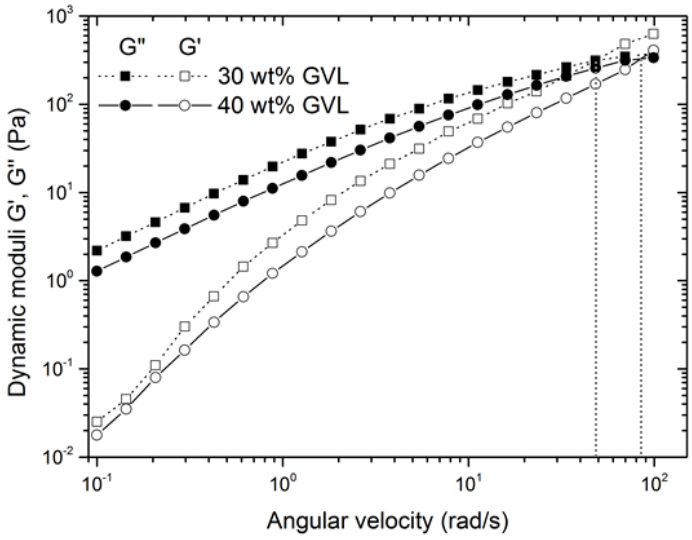

Figure 3.19: *Loss modulus (G‘‘, solid symbol) and storage modulus (G‘, open symbol) as a function of angular frequency for the cellulose dopes composed of 3 wt% cellulose pulp dissolved in NMMO mono./GVL at 25 °C.*

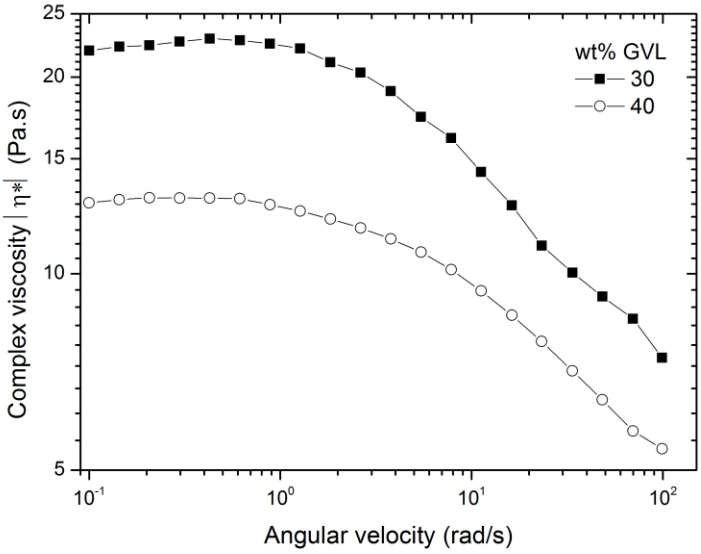

Figure 3.20: *Complex viscosity as a function of angular velocity for the cellulose dopes composed of 3 wt% cellulose pulp dissolved in NMMO mono./GVL at 25 °C.*

Considering the crystallization of cellulose dope made under cooling, the influence of GVL on the thermal behavior of the NMMO mono./MCC system was determined from DSC measurements. This precipitation has an important impact on the preparation of cellulose materials such as films and fibers and on the structure of the regenerated cellulose products. Contrary to other polymer solutions, crystallization of cellulose/NMMO/water is induced by the crystallization of the solvent and not due to the polymer.[194] For each cellulose concentration, a solution with the maximal tolerated amount of GVL and a formulation without this co-solvent were investigated. The thermal properties of these solutions and the pure NMMO mono. measured under the same conditions are given in Table 3.6. Four different thermal behaviors can be identified according to the composition of the mixture. For each kind, a corresponding thermogram is represented in Figure 3.21. The first behavior (group I) is characterized by one melting point upon heating and one crystallization peak upon cooling (see Figure 3.21 A). Like pure NMMO mono., cellulose mixtures containing up to 5 wt% MCC with GVL, as well as without, belong to this group. In this case, for compositions free of GVL, it can be noticed that increasing the cellulose content from 0 to 5 wt% leads to a slight decrease of the crystallization and melting temperatures. For instance, a solution with a concentration of 5 wt% MCC precipitated at about 21 °C, instead of 30 °C for solely NMMO mono. and melted at 70 °C instead of 75 °C. This phenomenon was already found in several studies and can emanate from the interactions between NMMO and cellulose created during dissolution.[191,195] Nevertheless, the majority of the solutions crystallized around room temperature. Adding GVL at a content comparable to that of cellulose (5 wt%), lowered the temperatures down to -11 °C and 43 °C for the crystallization and the melting transition, respectively. Clearly, the thermal transitions were strongly depressed in the presence of GVL. It seems that GVL retarded the diffusion of the crystallizing species and accelerated the melting process. This can be explained by the saturation of the N-O groups, which interact with the hydrogen bonding network of cellulose, and by the lower NMMO concentration present in these mixtures.

The second behavior (group II) exhibits diverse thermal transitions, i.e. one glass transition, one crystallization, and two melting peaks, solely upon heating (see Figure 3.21 B). Only the studied system, which contained 8 wt% MCC in NMMO mono., followed this pattern. The

exothermic peak occurring upon heating between the glass transition and the melting points is called “cold crystallization”. Above the glass transition, where the rigid and glassy state is transformed into soft rubbery state, cellulose chains are more mobile. The heat provides them more energy to move. Polymer chains tend towards a more stable state, the crystallization, and by even further heating, crystals melt.[196] The double melting peaks could be induced by imperfect crystallites, which melt and reorganize to form more perfect crystalline structures melting then at higher temperature.[191]

The third group shows a cold crystallization and a melting transition exclusively upon heating (see Figure 3.21 C). Such a behavior was exhibited by cellulose dopes containing a proportion of GVL and a cellulose concentration above 5 wt%. A glass transition was not observed in the measured temperature range.

The last behavior (group IV) gives a DSC thermogram with a single and low glass transition upon heating (see Figure 3.21 D) and was found for the 10 wt% cellulose solution with NMMO mono. Upon closer inspection of Figure 3.21 D, two small peaks are present on the heating curve and can be attributed to undissolved residues. Thus, 10 wt% MCC in NMMO mono. remained a fluid in the temperature range from -50 to 90 °C. Possible reasons of this phenomenon include the high viscosity of the solution and, as already mentioned, the involvement of the solvent in the cellulose solubilization.[195,197] As a consequence, operating temperature range of cellulose dope can be influenced by the polymer concentration and by the presence of GVL. GVL allows cellulose solutions to melt at temperatures below 50 °C and to crystallize at low temperatures far from room temperature. These results have a significant importance for the engineering and operating cellulose material manufactured from NMMO/GVL mixtures.

Table 3.6: *Variation of the thermal properties obtained by DSC for cellulose dopes composed of MCC, NMMO mono. and GVL. T_c stands for crystallization temperature, T_m for melting temperature, and T_g for glass transition temperature.*

Mixture composition			**Thermal properties**			
MCC (wt%)	**GVL (wt%)**	**NMMO mono. (wt%)**	**T_c (°C)**	**T_m (°C)**	**T_g (°C)**	**DSC behavior[a]**
-	-	100	30 ± 3	75 ± 1	-	I
1	-	99	19 ± 1	72.09 ± 0.02	-	I
1	49	50	-9.2 ± 0.4	49.4 ± 0.5	-	I
5	-	95	21± 2	70 ± 2	-	I
5	37	58	-11 ± 2	43 ± 3	-	I
8	-	92	12 ± 1	56.1 ± 0.6 61.1 ± 0.6	-48.5 ± 0.6	II
8	28	64	-25 ± 2	48.59 ± 2	-	III
10	-	90	-	-	-45.74 ± 0.04	IV
10	29	61	7 ± 2	41± 2	-	III

[a] Group I: one melting transition upon heating and one crystallization peak upon cooling
Group II: glass transition, crystallization point and two melting peaks on the heating curve
Group III: crystallization and melting transition upon heating
Group IV: solely glass transition upon heating

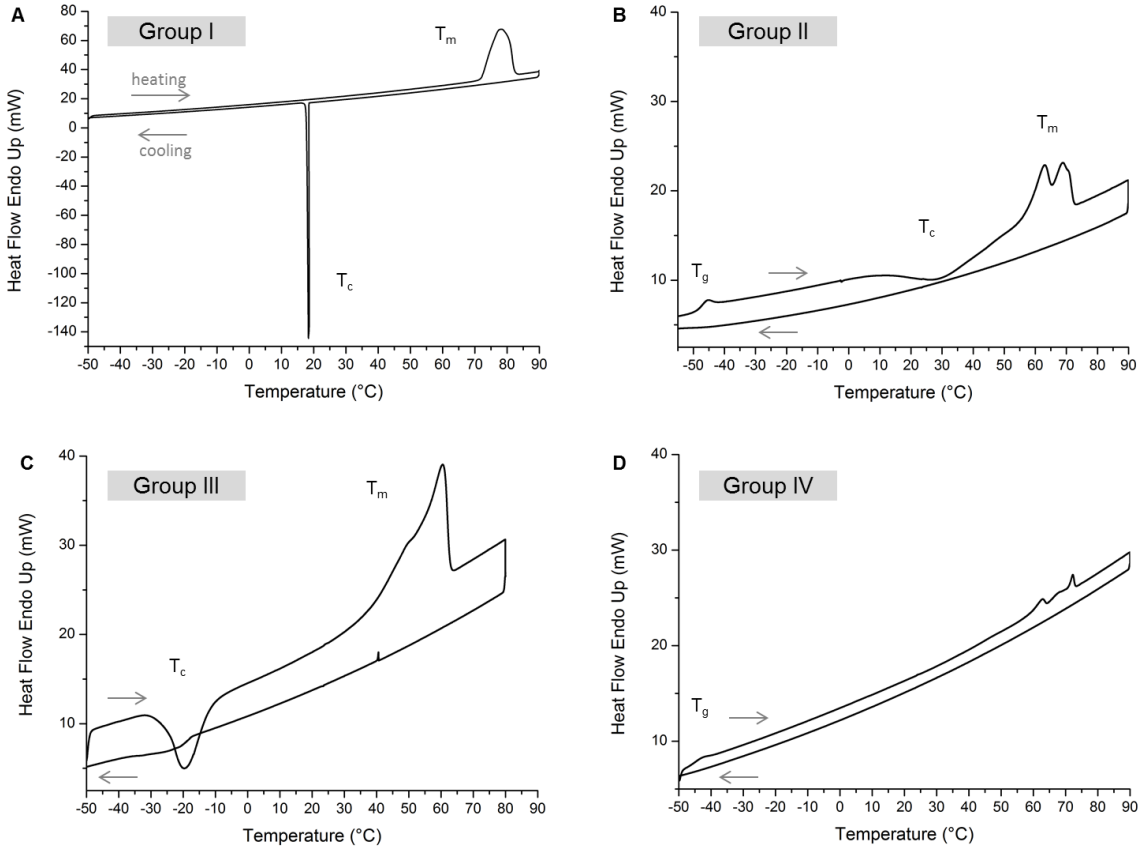

Figure 3.21: *DSC thermograms of the second heating and cooling cycle measured at a heating scan rate of 5 °C/min and a cooling scan rate of 2 °C/min for various cellulose dopes: (A) 1 wt% MCC dissolved in NMMO mono. depicting the DSC behavior of the Group I, (B) 8 wt% MCC dissolved in NMMO mono. (Group II), (C) 8 wt% MCC dissolved in NMMO mono./GVL (64/28 wt%, Group III), and (D) 10 wt% MCC dissolved in NMMO mono. (Group IV).*

3.4 Concluding remarks

A range of bio-sourced co-solvents were investigated for the dissolution of cellulose and chitin using the ionic liquid BmimOAc as solvent. It was revealed that γ-valerolactone was the only good candidate for this purpose. The addition of high concentrations of this sustainable and relatively economical solvent, particularly observed for cellulose, could mitigate the drawbacks caused by the IL, such as toxicity, non-biodegradability, and high cost.

The presence of GVL had a positive influence on the dissolution process. The time required for dissolution was reduced by a considerable factor and can be explained by an exponentially decrease in the viscosity of the medium. No significant change in ion interactions in the IL and no formation of nano-structures were observed experimentally by viscosity/ionic conductivity measurements and DLS studies, respectively.

In addition, GVL can facilitate further processing by decreasing the viscosity of polymer solutions. Dynamic oscillatory measurements have shown that the co-solvent caused differences in the mobility of the polymer chain and consequently in the rheological behavior of cellulose and chitin solutions. GVL allowed the chitin chains to be more mobile, while the contrary was observed for microcrystalline cellulose.

For the dissolution of cellulose in NMMO mono., different co-solvents (selected from aprotic solvents with a dipole moment greater than 3.5) were investigated, and their tolerance was found to follow the series: GBL > GVL > DMSO > GHL. Although GBL proved to be the most acceptable co-solvent, its conversion into the intoxicant γ-hydroxybutyric acid (GHB) when ingested in the human body can be an issue in a sustainable process. The bio-sourced solvent, GVL, was thus considered as ideal co-solvent for the dissolution of cellulose with NMMO mono. The influence of this green solvent on the Lyocell process was studied.

The addition of GVL offered significant improvements in the dissolution process by decreasing some dissolution parameters such as the duration and the temperature and by

increasing the stability of the solutions. The thermal properties of NMMO mono./GVL and cellulose/NMMO mono./GVL mixtures obtained by DSC suggested that GVL decreased the melting points of NMMO mono. and allowed cellulose solutions to melt and to crystallize at lower temperatures. Thus, novel cellulose dopes were prepared, paving the way for a more sustainable and low-temperature Lyocell process.

Chapter 4
Production of new polymer materials

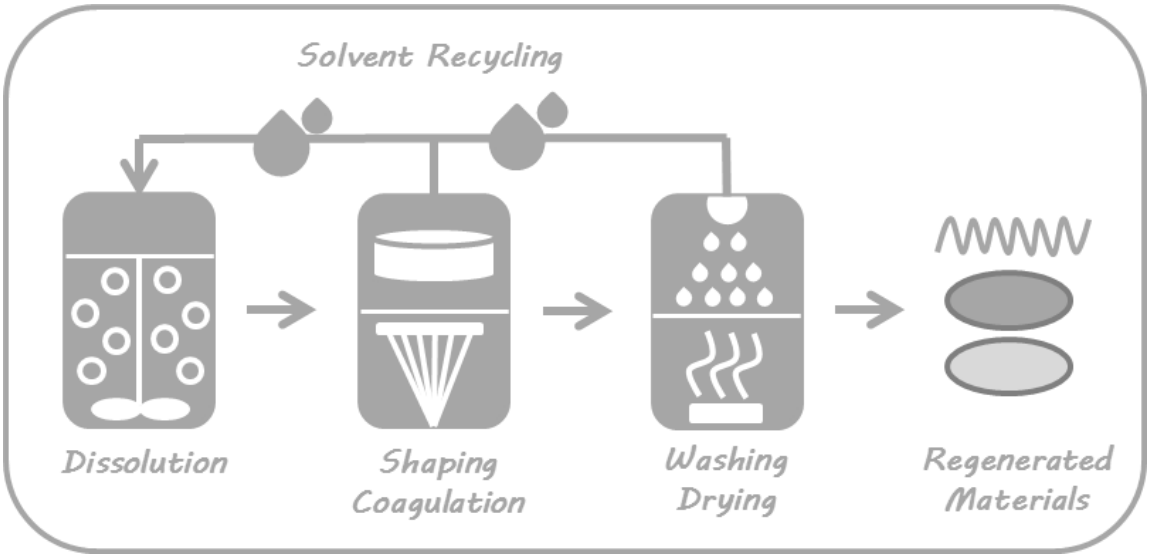

Parts of the work concerning the coated textiles presented in this section is submitted to the Lenziger Berichte in a publication entitled "Chitin coated cellulosic textiles as natural barrier materials" (see list of Publications).

4.1 Introduction

The extensive use of refined petroleum products has created first a depletion of petroleum reservoirs and an increasing global pollution of the environment. Thus, the development of renewable, recyclable, and biodegradable materials is essential to slowly substitute these harmful products, which are still currently dominating the markets.[5] A complete replacement by 100% biobased materials is not an economical and realistic solution. However, the research and the development of various possible applications for these sustainable elements are a major long-term study. Cellulose and chitin are the two most abundant biopolymers and have unique properties suitable for designing biodegradable materials. Their utilization under different structural forms such as fibers, films, membranes, nanomaterials, and gels have already found attractiveness in a wide range of applications including biomedical engineering, filtration processes, packaging, textile and hygienic products.[10,34,42,50] Cellulose-based materials are present in our daily life in a variety of objects like papers, paperboards, cellophane, filter papers, and textiles. On the contrary, chitin has not achieved the same commercial value and a large majority of its production (60-70%) is used to produce its deacetylated derivative chitosan.[11]

This part promotes the preparation of new materials from cellulose and/or chitin. These novel materials were characterized to assess their added values and possible applications. For this purpose, cellulosic fibers, cellulose/chitin composite fibers, gels and films as well as chitin coated cellulosic materials were manufactured.

On the one hand, the production of cellulosic fibers from *N*-methylmorpholine *N*-oxide monohydrate (NMMO mono.)/γ-valerolatone (GVL) mixtures was performed according to the industrial Lyocell process. The aim was to study the effect of the biomass-derived co-solvent GVL on the spinning route and on the fibers properties.

On the other hand, the production of cellulose/chitin materials was investigated using the ionic liquid 1-butyl-3-methylimidazolium acetate (BmimOAc) and GVL. The first approach was based on the formation and regeneration of chitin/cellulose blends to produce composite fibers, gels and films. In this work, manufacturing of fibers was performed using a dry-jet

wet spinning technique. The gels and the films were produced by Yaqing Duan, PhD student at the Straubing Center of Science (Germany) and are therefore not discussed in this part. For more details, please see the publication.[198] The second strategy focused on the realization of chitin-based coatings on cellulosic materials in the form of filter papers and textiles to give them new functional properties.

All produced materials were characterized in detail by thermal, morphological and mechanical analysis methods. Wetting and permeability studies were additionally performed on chitin coated materials to assess their technological importance and possible applications.

4.2 Experimental section

4.2.1 Chemicals

Microcrystalline cellulose (MCC) and α-chitin used as raw materials are already described in Section 2.2.1. All polymer powders were dried at 70 °C for at least 5 days prior to use and stored in a nitrogen-filled glove box.

Solvents used to prepare polymer dopes are the ionic liquid (IL) 1-butyl-3-methylimidazolium acetate (BmimOAc), the hydrated organic compound 4-methylmorpholine *N*-oxide monohydrate (NMMO mono.), and the co-solvent γ-valerolactone (GVL). Origin and purity of these solvents are described in Section 2.2.1. Prior to use, the IL was dried using a high vacuum setup at 10^{-6} mbar for 5 days. Water content was controlled using a coulometric Karl Fischer titration (899 Coulometer, Metrohm, Switzerland) after drying. BmimOAc and NMMO mono. were stored in sealed vials in a nitrogen-filled glove box to avoid moisture contamination. All other chemicals were used without further purification.

For the coating procedure, filter papers with a pore size of 4-7 µm were purchased from Schleicher & Schuell (Germany). Textiles were obtained from Lenzing AG (Austria) and produced from four different cellulosic fibers, namely TENCEL®, cotton, Lenzing Viscose®, and Lenzing Modal®. They were previously washed and desized in Lenzing AG. Textiles and filter papers were dried at 70 °C in an oven for 5 days to remove any moisture prior to use. The inorganic dye ruthenium red (purity > 85%, Fluka, Germany) was used to differentiate chitin from cellulose for light microscopic analyses of the coated filter papers.

4.2.2 Material production methods

4.2.2.1 Preparation of polymer solutions

A typical experimental procedure for preparation of cellulose and chitin materials started with the dissolution of the polymers in the appropriate solvent system. For this purpose, two solvent mixtures were used (1) NMMO mono./GVL for the production of cellulose fibers and

(2) BmimOAc/GVL for the cellulose/chitin composite fibers and the chitin coated materials routes.

For the production of cellulose fibers, a certain amount of cellulose, NMMO mono., and GVL were put into a sealed glass vial in the glove box. The sample was then mechanically stirred at 80 °C in an oil bath under nitrogen atmosphere until a homogenous solution was obtained (after approximately 2 h stirring). Complete dissolution of the resulting mixture was confirmed by a polarized optical microscope (Leitz Orthoplan, Germany) prior to further handling.

All chitin/cellulose-containing solutions were prepared in the glove box by mixing all components (cellulose, chitin, BmimOAc, and GVL) in desired amounts. In a sealed glass vial, the mixture was heated up to 100 °C under mechanical stirring and under nitrogen atmosphere. Again, complete dissolution was verified by means of microscopic analysis. If reluctant chitin fibers were still observed after 6 h of dissolution, the solution was centrifuged at 60 °C at 4500 rpm for 20 min with a Sigma 3-18KS centrifuge (Germany). The upper transparent solution was collected to avoid possible obstruction of the spinneret during the spinning process. Chitin solution for coating experiments was obtained with the same procedure except for the temperature process which was set to 110 °C.

Dopes were stored at room temperature in their sealed glass vials in absence of atmospheric water in case of no immediate use.

4.2.2.2 Fiber spinning equipment and experiment

Different self-developed lab-scale spinning devices were built to produce cellulose fibers from NMMO mono./GVL solution and cellulose/chitin composite fibers from BmimOAc/GVL mixtures.

4.2.2.2.1 Cellulose fibers produced without an air gap

First, a lab-scale spinning apparatus was developed with the equipment used in the master thesis of Alexander Wollinger.[199] The setup scheme is depicted in Figure 4.1 and consists of

a pressure system (items 1, 2, 3, 4 and 6), a syringe with a monofilament spinneret (5 and 7), a spinning bath (8), and a take-off roller (9 and 10).

The spinning principle of this setup can be described as follows. The polymer solution is discharged from the dope vessel (5) through a monofilament spinneret (7) under nitrogen pressure produced by a nitrogen pipe (1). A manometer (2) is used to check the actual pressure in the setup. Two valves (3 and 4) are connected between the dope vessel and the nitrogen pipe (1). The dope valve (4) allows regulation of the nitrogen flow and the second valve (ventilation valve (3)) is used to ventilate the apparatus at the end of the process. Control of both valves is possible either manually or automatically with an electronically controlled system (6). The temperature of the spinning dope is regulated using a sand bath (11). After passing through the spinneret, the solution is extruded into a precipitation bath (8) where the extrudate is impoverished of solvent. This allows the regeneration of the polymer in shape of a filament. Spun fibers are rolled onto a take-off roller (9) at linear speed, which is controlled by an electronic system (10).

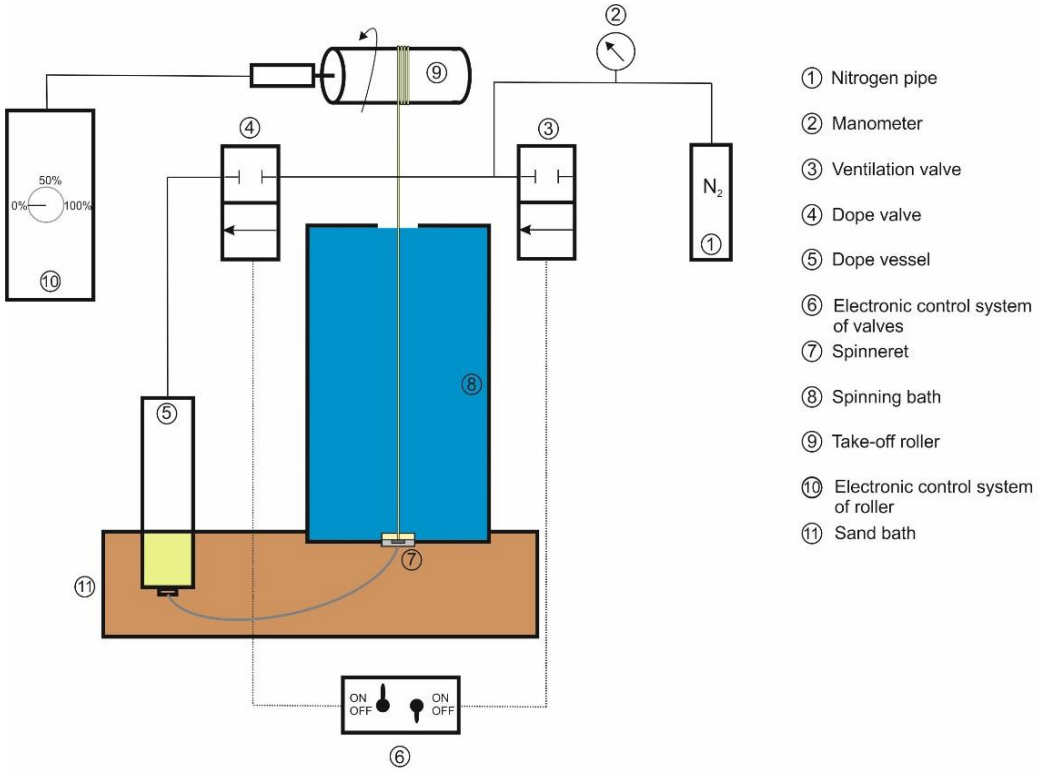

Figure 4.1: *Schematic of the first self-developed fiber spinning apparatus.*

For the manufacturing of the first fibers, the prepared dope was carefully introduced into the storage vessel without introducing any air bubbles, after being preheated at the desired spinning temperature. The spinning temperature was set between 25 and 80 °C and was controlled by a sand bath. Fibers were spun with a 200 µm- or 80 µm-monofilament spinneret. Dimensions of these two spinnerets are represented in Figure 4.2. Prior to each experiment, the cleanliness of the spinneret orifice was controlled with a microscope (Nikon Eclipse E400, Japan). The extrusion speed was restricted by the nitrogen pipe, which induced a pressure of 2.6 bars. The coagulation bath contained 1 L of deionized water at room temperature. Finally, the produced fibers were washed at least three times using a large quantity of sprayed deionized water, then immersed into water before they were dried at ambient air for several days.

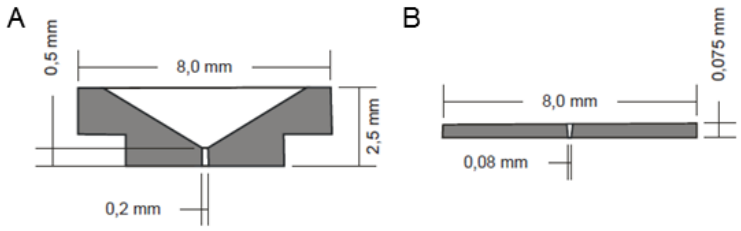

Figure 4.2: *Schematic of the (A) 200 µm-/(B) 80 µm-monofilament spinneret.*[199]

4.2.2.2.2 Cellulose fibers produced with an air gap

A second spinning apparatus was built similar to the dry-jet wet spinning technique used in the Lyocell process (detailed in Section 1.3.2.1.2). A scheme of this setup is depicted in Figure 4.3 and several parts from the first apparatus were reused, such as the pressure system (1, 2, 3, 4 and 12), the syringe with the monofilament spinneret (5 and 6), and the take-off roller (10) controlled by an electronic system (11). The system was modified by introducing an air gap after the spinneret (7) and a new spinning bath (9). The latter includes two godets (8) at a distance of 12 cm apart and with an immersion depth of 2.5 cm to provide a guide for the resulting filament until reaching the take-off roller (10).

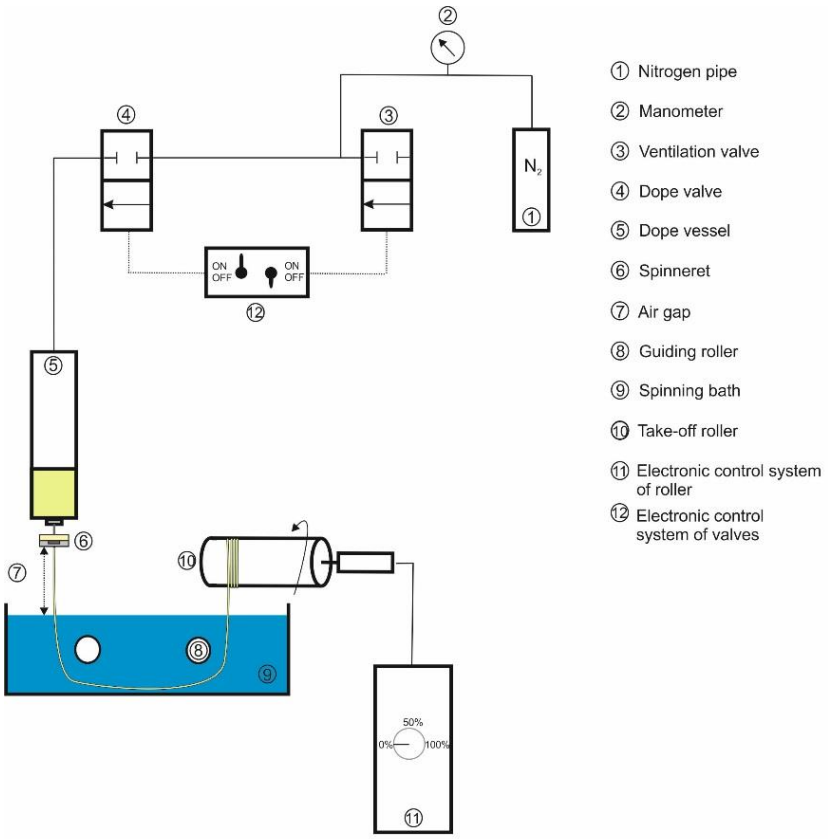

Figure 4.3: *Schematic of the second self-developed fiber spinning apparatus.*

The spinning procedure was the same as previously described. However, the spinning temperature could not be controlled and was 25 °C. An air gap of 2 cm was induced between the water surface and the spinneret. The air gap conditions (humidity and temperature) could not be controlled or modified at this level. The circulating ambient air in the laboratory was the environment surrounding the air gap during the spinning process.

4.2.2.2.3 Cellulose/chitin fibers produced with an air gap

A third spinning setup was developed for the production of cellulose and chitin composite fibers from BmimOAc by improving the second apparatus. This setup is schematized in Figure 4.4. An electric blanket (13) controlled by a transformer and a nitrogen bottle (1) was added to regulate the spinning temperature and the nitrogen flow.

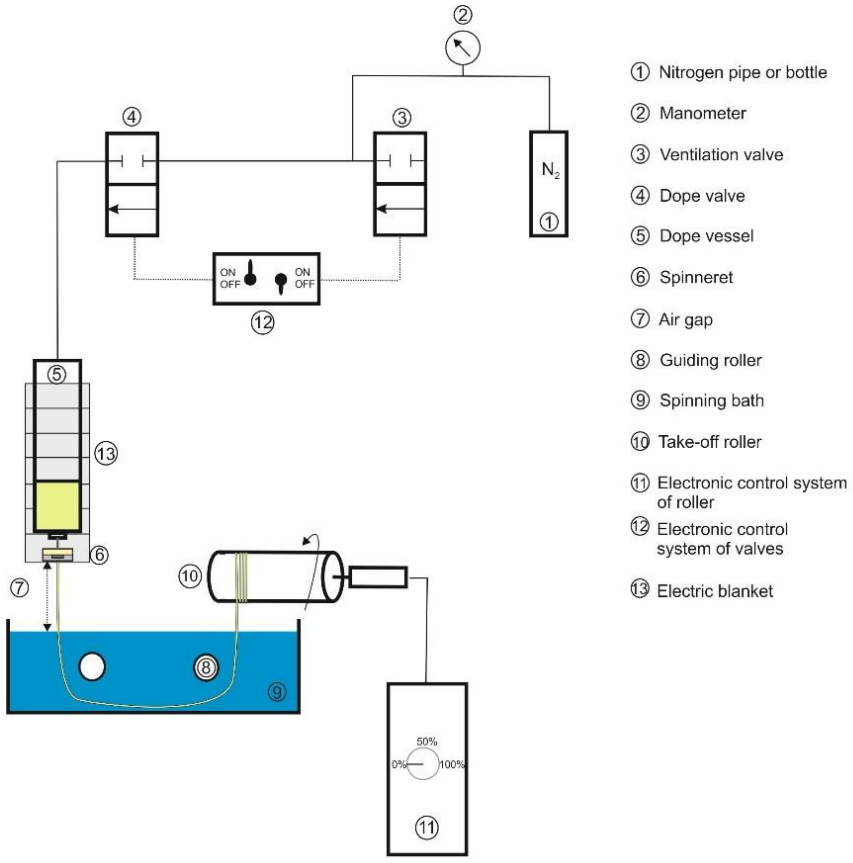

Figure 4.4: *Schematic of the third self-developed fiber spinning apparatus.*

The spinning temperature (between 25 and 70 °C) was controlled by an electric blanket. Fibers were spun with a 200 µm- or 80 µm-monofilament spinneret. The extrusion speed was restricted by the nitrogen bottle, which induced pressure from 2.6 to 4 bars. An air gap of 0.5 cm was set between the water surface and the spinneret. The coagulation bath contained 1 L of deionized water at 15 °C. The produced fibers were washed on the take-off roller at least three times using a large quantity of sprayed deionized water, then immersed into water to remove the solvent residues and dried at ambient conditions for several days.

4.2.2.3 Chitin coating on cellulosic material procedure

A procedure was developed for the chitin coating of cellulosic materials, i.e. cellulosic filter papers and textiles. The aim of this process was to create a thin and attached chitin layer on these materials. For this purpose, the ionic liquid BmimOAc was used as main chitin solvent to slightly dissolve the cellulosic materials at the surface and to allow the chitin to be imbedded within.

Chitin solutions were prepared by dissolving α-chitin (2 wt%) in BmimOAc (88 wt%) and GVL (10 wt%) under nitrogen atmosphere at 110 °C. For the filter paper coating, 0.7 wt% of ruthenium red was additionally added to the chitin solution to differentiate chitin from cellulose. After total dissolution of chitin, a small amount of GVL was added to dilute the highly viscous gel and to facilitate the coating process. The final solution was composed of 1.6 wt% chitin, 30 wt% GVL, and 68.4 wt% BmimOAc and was heated at 100 °C. One side of the cellulose materials was put in contact with this heated solution and moved on the solution surface by a pair of tweezers (see Figure 4.5). This mechanical stimulus provided a homogenization of the chitin layer on the surface. After a selected time (from 1 to 5 min), the chitin covered materials were removed from the chitin solution and left at room temperature for 2 hours to allow a slow gelation of the chitin. Each material was subsequently soaked in ethanol for 2 days and then in deionized water for 2 days to remove BmimOAc and GVL and to induce coagulation of the chitin layer. Finally, coated materials were dried between 2 glass plates at room temperature for several days.

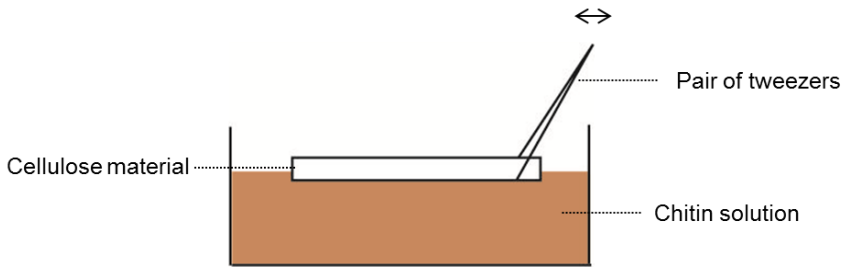

Figure 4.5: *Schematic of the chitin coating method on cellulose material.*

4.2.2.4 Solvent recycling

A method was developed to recover BmimOAc subsequent to the production of the coated materials. After chitin regeneration, the ethanol-based precipitation solutions were first filtrated with a 0.2 µm polytetrafluorethylene (PTFE) membrane filter to remove possible polymer residues. In a second step, ethanol was evaporated from these solutions for two hours under reduced pressure (100 mbar) and at 40 °C using a rotary evaporator. Under these conditions, GVL could not be evaporated. That is why the solutions were further dried at 40 °C at 10^{-6} mbar using the high vacuum setup for 5 days. The purity of the recycled BmimOAc was analyzed by ^{1}H- and ^{13}C-NMR measurements in dimethyl sulfoxide-d6 recorded with a Bruker Avance 300 spectrometer (Billercia, USA) at 300 MHz.

4.2.3 Material characterization

4.2.3.1 Fiber characterization

The quality of the produced fibers was evaluated by means of structural and mechanical characterization.

4.2.3.1.1 Structural analysis

Surface structure of the fibers was visualized and examined with a microscope (Nikon Eclipse E400, Japan) connected to a digital single-lens reflex camera (Canon EOS 650D, Japan). To obtain sharp pictures, several images of the same sample focused at different spots were taken and superimposed with the program "Zerene Stacker".

Fiber cross sections were investigated by the Analytical Laboratory of Kelheim Fibres. For this purpose, fibers were cut with a Microtome after being embedded in a matrix of wax and their cross sections were observed under a microscope.

4.2.3.1.2 Mechanical tests

Fiber properties were also measured by the Analytical Laboratory of Kelheim Fibres in terms of fineness (dtex), elongation at break (%) and tensile strength (cN/tex). These characteristics were obtained with a Fafegraph HR tensile tester (Textechno Herbert Stein GmbH & Co.

KG, Germany) for six fibers per sample. Tensile tests were performed with a clamping length of 20 mm, a pretention of 0.64 cN/tex, and a speed of 20 mm/min.

4.2.3.2 Coated material characterization

The effect of the regenerated chitin layer on the structure and the properties of the textiles were characterized by infrared spectroscopy, scanning electron microscopy, water contact angle measurements, and water/gas permeability studies.

4.2.3.2.1 Composition

To characterize the composition of the prepared materials, infrared spectra were recorded in the range from 400 to 4000 cm^{-1}. Measurements were performed with a Fourier transform infrared spectroscopy (FTIR) instrument with an attenuated total reflectance (ATR) sampler by pressing the samples against a Smart Diamond ATR sensor (Nicolet 380, Thermo Scientific, Germany).

4.2.3.2.2 Morphology

Morphologies of the produced materials were observed by scanning electron microscopy (SEM). Dried samples were placed on carbon tape and coated with Au/Pd. SEM images were obtained with a digital scanning electron microscope (DSM 940 A, Zeiss, Germany) in secondary imaging mode at an acceleration voltage of 10 kV.

4.2.3.2.3 Contact angle measurements

Wetting properties were characterized by water contact angle measurements, performed by establishing the tangent of a water drop on the material surface (see Figure 4.6). Contact angle values were recorded using a goniometer type P1 (Erna Inc., Japan) equipped with a microscope and a back light. Measurements were performed at room temperature on both sides of the coated films, i.e. on the chitin layer and the textile layer. A 2 µL drop of deionized and sterile filtrated water was formed by an automated micrometer pipette (Hamilton Company, USA) and placed on the sample surface. The angle of the tangent formed at the water drop base was recorded as well as the liquid drop absorption time on each material. Overall, five drops were placed on various locations for each sample.

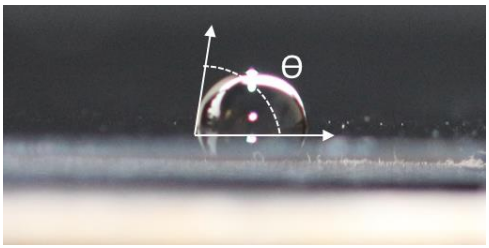

Figure 4.6: *Contact angle (Θ) of a water drop on a silicon wafer surface (Θ < 90°).*

4.2.3.2.4 Water permeability equipment and experiment

The ability of water to pass the materials was investigated by permeability tests. An experimental setup, illustrated in Figure 4.7, was therefore designed to allow the film to be in contact with water and another liquid through a defined area. This self-developed apparatus consists of two Plexiglas cells with a volume of 9 mL having a small hole of 3 mm in diameter at a height of 1.2 cm and a press system. The holes are surrounded by seal rings (in green and black in Figure 4.7) to have a liquid tight system.

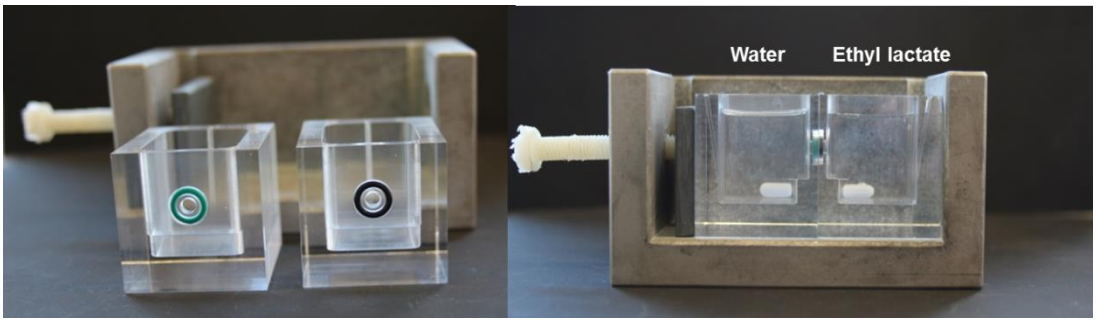

Figure 4.7: *Experimental setup for the water permeability test.*

Ethyl lactate was used as the second solvent because it is fully miscible with water and a green solvent (biodegradable, low toxic, non-carcinogenic, non-teratogenic and low volatile).[200] Once the setup was fixed by the press apparatus with the film in-between, the cells were filled at the same time, one with 8 mL of deionized water and the other with 8 mL of ethyl lactate. Both solutions were stirred at 200 rpm at constant temperature of 20 ± 1 °C for 7 h. Samples of 150 µL were collected with an Eppendorf pipette from each cell at the same time and at defined time intervals. The water concentration of these samples was

measured by volumetric Karl Fischer titration (870 KF Titrino plus, Metrohm, Switzerland) four times and the averaged value was recorded over time. For the coated materials, the chitin layer was in contact with the water cell.

The ability of water to pass the materials was characterized by a water permeability coefficient, P_{H_2O}, defined by Fick's first law as:[186]

$$J_{H_2O} = -D \times \frac{\Delta c_{H_2O}}{\Delta x} = -P_{H_2O} \times \Delta c_{H_2O} \quad (4.1)$$

where J_{H_2O} represents the flow of water per unit area, D the diffusion coefficient, Δc_{H_2O} the difference in water concentration between the ethyl lactate and the water filled cell, and Δx the distance between the two cells. The flux J_{H_2O} can also be expressed by Equation 4.2.

$$J_{H_2O} = \frac{1}{A} \times \frac{dc_{H_2O \text{ in EL cell}}}{dt} \times V \quad (4.2)$$

with A the permeation area, $c_{H2O \text{ in EL cell}}$ the water concentration in the ethyl lactate cell, V the volume related to the water concentration, and t the time. Combining Equations 4.1 and 4.2, the permeability coefficient P_{H_2O} can be calculated according to the following expression:

$$\left|P_{H_2O}\right| = \frac{dc_{H_2O \text{ in EL cell}}}{dt} \times \frac{V}{\left|\Delta C_{H_2O}\right|} \times \frac{1}{A} \quad (4.3)$$

Water permeability coefficients were calculated considering only the averaged values between 120 and 420 min. Before 120 min, the difference in water concentration between the two cells could not be precisely determined due to the uncertainty of the water concentration measurements in the pure water cell carried out by volumetric Karl Fischer titration.

4.2.3.2.5 Oxygen permeability equipment and experiment

Oxygen permeability was determined with an optical measurement under dry conditions. Illustrated in Figure 4.8, the measurement setup consists of a self-developed measurement cell, a chemical optical sensor spot (type PSt6 from PreSens, Germany), a stick-on adapter

(SAO from PreSens), a polymer optical fiber (POF-2SMA from PreSens), and a fiber optic oxygen transmitter (Fibox 4 trace from PreSens) connected to a computer. Oxygen concentration was measured with a non-invasive and non-oxygen consuming method thanks to the sensor type PSt6, which is composed of an oxygen sensitive dye embedded in a silicon matrix. This sensor spot, which can detect oxygen partial pressures in a trace range from 0 to 52 hPa, is read out via the polymer optical fiber connected to the transmitter Fibox 4 trace.

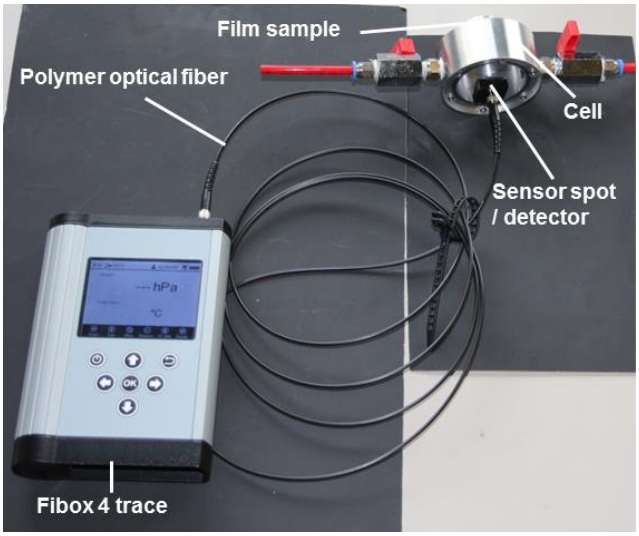

Figure 4.8: *Measurement setup for O_2 permeability experiment*

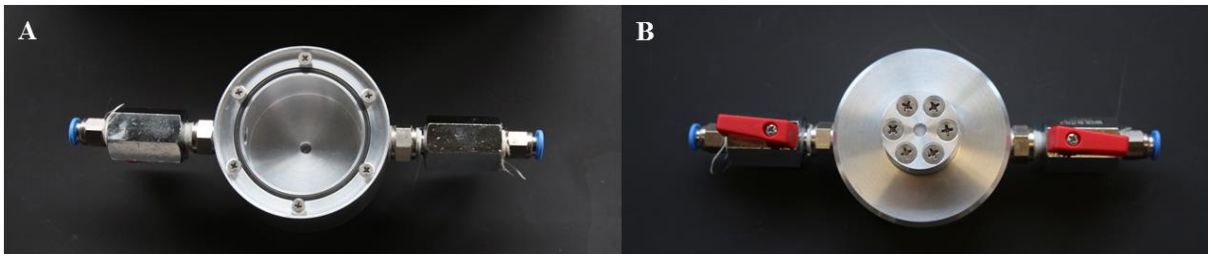

Figure 4.9: *Measurement cell for the O_2 permeability measurement. (A) View of the Plexiglas measurement window where the sensor spot will be stuck. (B) View of the counterplate containing the film sample.*

The designed cell, depicted in Figure 4.9, is composed of a chamber with two gas connectors, a measurement window in Plexiglas, and a counterplate with a central hole. The film sample can be fixed with seal rings on the top of the chamber having a volume of 49.38 cm^3 and is in contact with the ambient air through a hole of 0.5 cm diameter.

The sensor spot was first fixed inside the chamber on the Plexiglas with silicon glue (from RS Components, UK) and was facing a stick-on adapter, which holds the polymer optical fiber in place. The PSt6 sensor was already calibrated by PreSens prior to use. A series of 3 measurements for each sample was performed at a constant temperature of 20 °C. After flushing the chamber three times with nitrogen (zero value), the increase of the oxygen partial pressure over time was recorded. For the coated materials, the chitin layer was in contact with the ambient air of the laboratory room. The time range was selected from 0 to 13 min, which is the period of time where accurate oxygen partial pressures (from 0 to 52 hPa) could be measured by the sensor spot.

The oxygen barrier property of the films was characterized by the oxygen permeability coefficient, P_{O_2}, calculated using an adaptation of the ideal gas law (Equation 4.4) and of the Fick's first law (Equation 4.5).[186]

$$p_{O_2} \times V = n_{O_2} \times R \times T \quad (4.4)$$

$$J_{O_2} = -P_{O_2} \times \Delta c_{O_2} = \frac{1}{A} \times \frac{dn_{O_2}}{dt} \quad (4.5)$$

In Equation 4.4, p_{O_2} is the partial pressure of oxygen, V the volume of the chamber, n_{O_2} the amount in moles of oxygen, R the gas constant, and T the absolute temperature. In Equation 4.5, J_{O_2} represents the flow of oxygen per unit area, Δc_{O_2} the difference in oxygen concentration from the chamber to the outside, and A the permeation area. By combining the two equations, the oxygen permeability coefficient P_{O_2} is given by Equation 4.6.

$$\left|P_{O_2}\right| = \frac{V}{A \times \left|\Delta P_{O_2}\right|} \times \frac{dp_{O_2}}{dt} \quad (4.6)$$

The oxygen permeability coefficients were calculated considering only the average of the calculated values between 1 and 13 min.

4.3 Results and discussion

4.3.1 Fibers

4.3.1.1 Cellulose regenerated fibers from NMMO/GVL solutions

4.3.1.1.1 Lab-scale spinning

Preliminary tests were performed to produce cellulose fibers with the first self-developed spinning equipment described in Section 4.2.2.2.1. This apparatus imposed unchangeable parameters such as a pressure of 2.6 bars, an air gap length of 0 cm, a spinneret of 200 or 80 µm in diameter, and a minimal velocity of the take-off roller of 3.5 m/min. A solution of 5 wt% cellulose, 58 wt% NMMO mono. and 37 wt% GVL was spun into a water bath under different spinning conditions to evaluate the efficiency of the equipment. Table 4.1 shows the varied spinning parameters, their effect on the spinnability of the dope and on the surface structure of the fibers observed under light microscopy. The dope could be spun neither at 60 and 50 °C using an 80 µm spinneret due to a too high extrusion velocity, nor at 25 °C with a 200 µm spinneret because of a too low extrusion velocity. However, appropriate fibers were obtained between 25 and 40 °C with an 80 µm spinneret. The produced fibers exhibited a regular and smooth structure independently of the spinning temperature as shown in Figure 4.10.

Table 4.1: *Spinning conditions and their effects on the spinnability of cellulose dope and on the fiber structure.*

Spinning temperature (°C)	Spinneret (µm)	Take-off roller velocity (m/min)	Spinnability	Fiber surface structure
60	80	-	Extrusion velocity too high	-
50	80	-	Extrusion velocity too high	-
40	80	8.2	Acceptable	Regular structure
30	80	3.5	Acceptable	Regular structure
25	80	3.5	Acceptable	Regular structure
25	200	3.5	Only fragmentary spinning possible (repeated breakage of the filament) Extrusion velocity too low	Irregular structure

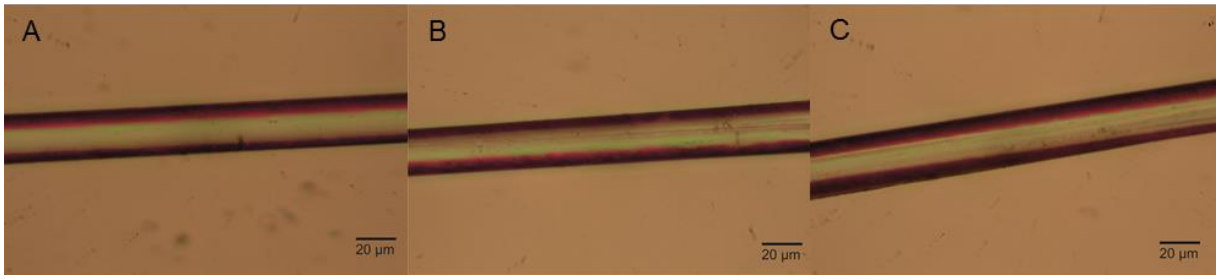

Figure 4.10: *Surface structure of cellulose fibers spun with an 80 µm spinneret from a solution of 5 wt% cellulose, 58 wt% NMMO mono., and 37 wt% GVL at different temperatures: (A) 25 °C (B) 30 °C (C) 40 °C.*

The properties of the regular fibers and the appearance of their cross section were analyzed by Kelheim fibers and are summarized in Table 4.2 and Figure 4.11. The cross sections of the fibers spun at 25 °C and 40 °C were irregular while fibers spun at 30 °C exhibited circular cross sections similar to TENCEL® fibers. The properties of the fibers spun at 40 °C could not be examined because some fibers were stuck together. The overall properties of the other fibers were far from being sufficient compared to commercial fiber characteristics. In addition, large variations of the measured values were obtained (see Table 4.2). These results could be expected as the fibers were produced with a self-developed lab-scale spinning equipment and without an air gap. The latter is an important parameter which affects the formation of the fibers. In the dry-jet wet spinning technique, the dope filament is stretched in the air gap with a positive draw ratio, which induces the orientation of the polymer chains. A high molecular orientation promotes crystallization and allows the formation of oriented and parallel microfibrils after precipitation of the cellulose in the coagulation bath that causes high tenacity fibers.[193,201]

Table 4.2: *Properties of cellulose fibers spun with an 80 µm spinneret and from a solution of 5 wt% cellulose, 58 wt% NMMO mono., and 37 wt% GVL and properties of commercial TENCEL® fibers.*

Fiber properties	Fiber spun at 25 °C	Fiber spun at 30 °C	Fiber spun at 40 °C	Commercial TENCEL® [117]
Fiber diameter (µm)	Irregular	22 ± 4	Irregular stuck fibers	10
Fineness (dtex)	11.6 ± 3.7	9.8 ± 2.7	-	1.3
Elongation at break (%)	6 ± 2	8 ± 3	-	13
Tensile strength (cN/tex)	4.3 ± 1.1	6.9 ± 2.4	-	40.2

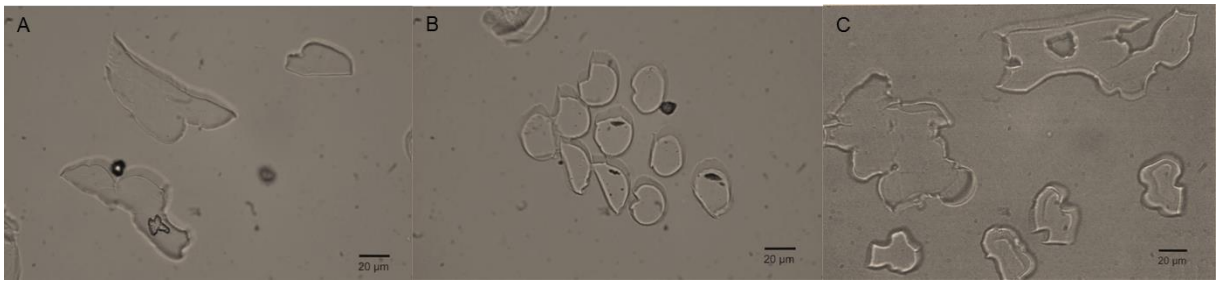

Figure 4.11: *Cross section view of generated cellulose fibers from a solution of 5 wt% cellulose, 58 wt% NMMO mono., and 37 wt% GVL and with an 80 µm spinneret at (A) 25 °C, (B) 30 °C, and (C) 40 °C.*

A second spinning apparatus was built allowing the cellulose dope to be discharged through an air gap into a water bath (see Section 4.2.2.2.2). Imposed parameters by this equipment were a N_2 gas pressure of 2.6 bars, a spinneret of 200 or 80 µm, a minimal velocity of the take-off roller of 3.5 m/min, and a spinning temperature of 25 °C. An air gap of 2 cm was selected and different dope compositions were spun under these conditions (see Table 4.3). As noticed in Table 4.3, no homogeneous fibers could be produced. The incipient filaments were not strong enough to be collected by the take-off roller without breaking. The control of the extrusion velocity was notoriously difficult because of the constant N_2 gas pressure and the constant temperature imposed by the apparatus.

Accordingly, the processability of cellulose solutions prepared from NMMO mono. and GVL and the possible advantageous effects of GVL could not be evaluated with the lab-scale spinning devices. To solve this problem, the pressure system has to be changed. A more

effective system, for instance a heated cylinder with a piston, would allow variations in the extrusion pressure and temperature. This equipment would additionally enable to spin higher cellulose concentration as well as cellulose with a higher degree of polymerization (DP).

Table 4.3: *Spinning conditions and their effects on the spinnability of cellulose dopes and on the fiber structure.*

Dope composition	Spinneret (µm)	Take-off roller velocity (m/min)	Spinnability	Fiber surface structure
5 wt% MCC 37 wt% GVL 58 wt% NMMO mono.	80/200	3.5	Only fragmentary spinning possible (repeated breakage of the filament) Extrusion velocity too low	Irregular structure
3 wt% MCC 40 wt% GVL 54 wt% NMMO mono.	80/200	3.5	Only fragmentary spinning possible (repeated breakage of the filament) Extrusion velocity too low	Irregular structure
1 wt% MCC 49.4 wt% GVL 49.6 wt% NMMO mono.	80	-	Not enough cellulose to form a filament Extrusion velocity too high	-

4.3.1.1.2 Industrial spinning performed by Lenzing AG

To evaluate some effects of GVL in the production of cellulose fibers, Lenzing AG performed an experiment by adding this bio-sourced solvent in their spinning procedure as follows. A solution composed of 25.7 wt% GVL, 9.6 wt% cellulose pulp (with a DP ranged from 800 to 900), 50.47 wt% NMMO, 14.23 wt% H_2O, and two unspecified stabilizers was kneaded in a mixer. Water was extracted at reduced pressure and at high temperature until complete dissolution of cellulose was obtained. The resulting solution contained 14.6 wt% GVL, 11.3 wt% cellulose, 66.5 wt% NMMO, and 7.5 wt% H_2O. A part of GVL was evaporated with water, which was not intended. The spinning dope was spun with a dry-jet wet spinning apparatus. Monofilaments were extruded at 75 °C through a 100 µm spinneret and over a 3 cm air gap into a water bath and were wound onto a godet at a velocity of 34 m/min.

Fibers properties of these filaments and commercial TENCEL® are presented in Table 4.4. Dry mechanical properties (i.e. tensile strength and elongation) were slightly lower than for normal TENCEL® fibers while wet tenacity value was below TENCEL® standards. Accordingly, no massive improvement of fiber mechanical properties was observed with this first test. However, no deterioration in the stability of the spinning mass occurred with the addition of GVL and the spinning temperature could be reduced to 75 °C instead of 120 °C. Further work is needed to promote other possible advantages of GVL in the dry-jet wet spinning process.

Table 4.4: *Fiber properties of regenerated cellulose fibers spun from NMMO/GVL by Lenzing AG and commercial TENCEL® fibers.*

Fiber properties	Fiber spun with GVL	Commercial TENCEL® [117]
Fineness (titre, dtex)	1.3 ± 0.3	1.3
Dry tensile strength (cN/tex)	32.9	40.2
Dry elongation at break (%)	9.2	13
Wet tensile strength (cN/tex)	lower	37.5

4.3.1.2 Cellulose/chitin fibers from IL

Ionic liquid solutions of cellulose and chitin were spun with the third self-developed dry-jet wet spinning equipment (details in Section 4.2.2.2.3). Spinnability studies were performed with a solution composed of 0.5 wt% chitin, 1 wt% cellulose, 20 wt% GVL, and 78.5 wt% BmimOAc spun first through a 200 µm spinneret over an air gap of 0.5 cm. Spinning trials were conducted at different spinning temperature, namely 25, 30, 50, and 70 °C and at different N_2-pressures ranging from 2.6 to 4 bars. For all tests, the incipient filaments were not strong enough to be continuously collected by the take-off roller without breaking. However, at 70 °C and with a pressure of 4 bars, relatively few interruptions in the spinning process were observed and some fibers could be wound. Microscopy analyses of these fibers showed regular as well as irregular structural segments along the fiber length, which were probably caused by the disruption in the spinning procedure (Figure 4.12). Due to lacking continuity of fiber generation, no further characterizations of the fibers were possible.

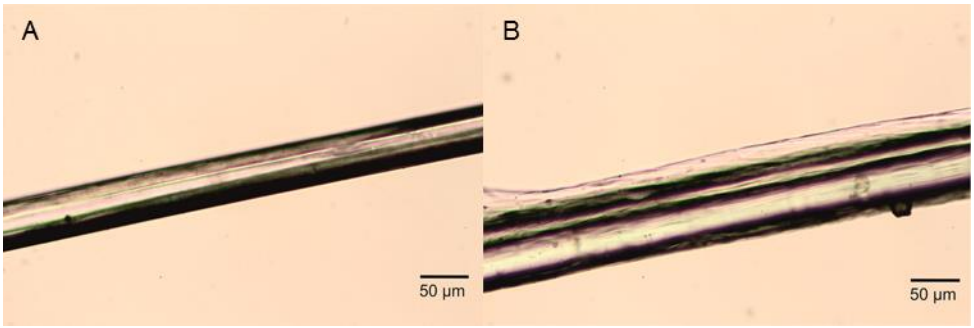

Figure 4.12: *Surface structure of cellulose/chitin fibers spun from a solution of 0.5 wt% chitin, 1 wt% cellulose, 20 wt% GVL, and 78.5 wt% BmimOAc at 70 °C with a 200 µm spinneret. (A) Regular and (B) irregular fiber segments.*

Additional experiments to clarify the impact of different cellulose/chitin mass ratios on the fibers properties could not be studied because of the poor performance of the spinning apparatus. Again, a more professional spinning system would be suitable to investigate this study.

4.3.2 Coated cellulose materials with chitin

Filter papers as well as textiles made from different cellulosic fibers were used as source for the cellulose-based materials because they are composed of uniform and interlaced cellulose fibers.

4.3.2.1 Filter paper coating

The coating procedure described in Section 4.2.2.3 was first studied on filter papers. Various durations of 1, 3, and 5 minutes were investigated to impregnate one side of the filter papers at 100 °C with the brown chitin solution. The brown color is caused by the ruthenium red dye. Figure 4.13 shows views of both sides for the resulting coated materials and accurate SEM pictures for the coated filter paper exposed to chitin solution for 3 minutes. All coated filter papers presented a thin smooth brownish film on the chitin side. On the untreated sides, degradation of the surface could be noticed by the presence of large holes induced by filter paper dissolution. The longer the filter was in contact with the chitin solution, the more pronounced were the holes on the filter paper side. Moreover, these interspaces allowed

chitin to penetrate up to the outer surface of the filter paper as visible in the SEM picture from Figure 4.13 B2'. This deleterious effect runs counter to the intended aim, which was the design of a thin and attached chitin layer without degradation of the starting materials.

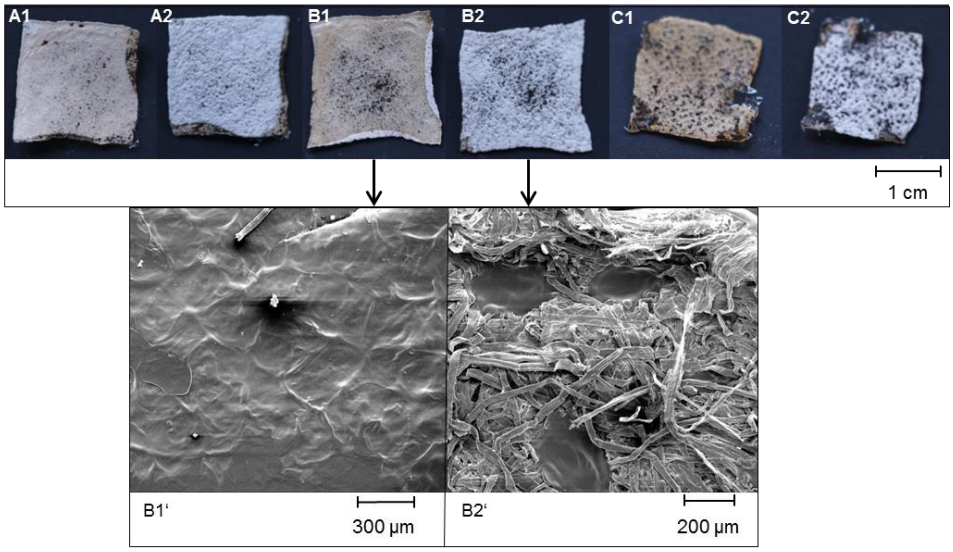

Figure 4.13: *(A, B, C) Pictures and (B') SEM images of chitin coated cellulose filters exposed for (A) 1 min, (B) 3 min, and (C) 5 min on the chitin solution during the coating process. (1) represents the chitin side and (2) the untreated filter paper side of each coated materials.*

Accordingly, filter papers were found to be a non-appropriate substrate for this coating method. The issue here is the rapid dissolution of the filter paper in the ionic liquid. In addition, the use of the dye was obsolete and hided the visualization of possible chitin degradation.

4.3.2.2 Textiles coating

Four textiles made from four different cellulosic fibers (TENCEL®, cotton, Lenzing Viscose®, and Lenzing Modal®) were utilized as cellulose substrate (hereinafter referred to as "Tencel", "cotton", "Viscose", and "Modal").

4.3.2.2.1 Coating procedure

First of all, the dissolution behavior of the textiles in BmimOAc was observed in order to optimize the coating procedure and to avoid textile degradation. 1 wt% of each textile as well as 1 wt% of filter paper was dissolved in BmimOAc at 100 °C. The time required to complete dissolution are reported in Figure 4.14. The textiles were more slowly dissolved than filter paper. Indeed, dissolution durations of 320 min for cotton, 180 min for Tencel, 131 min for Viscose, 121 min for Modal, and 20 min for the filter paper were recorded. Among the textile samples, cotton presented the highest dissolution time. This suggests that the IL had more difficulties to penetrate the cotton crystalline lattice and to break its hydrogen bonding network. The reason lies probably in the structural difference between the cellulose fibers and their degree of crystallinity. Native cotton fibers are known to be highly crystalline and oriented (cellulose I) while regenerated cellulose fibers are less crystalline and are composed of cellulose II and amorphous cellulose.[118,202] This structural difference will be well observed further by FTIR analysis.

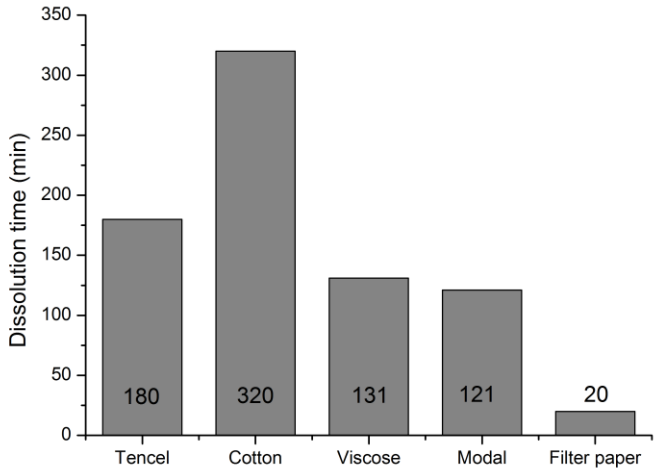

Figure 4.14: *Dissolution time of 1 wt% of the textiles (Tencel, cotton, Viscose, and Modal) and 1 wt% of filter paper in BmimOAc at 100 °C.*

Finally, according to these observations, a coating duration of 5 min was selected to avoid dissolution of the cellulosic substrates.

4.3.2.2.2 Structure of the coated textiles

The appearance of the untreated textiles and the coated materials is shown in Figure 4.15. Textiles from Lenzing consist of an ordered structural assembly of cellulosic fibers (TENCEL®, cotton, Lenzing Viscose®, and Lenzing Modal®) exhibiting a white color. The studied textiles were produced by interlacing warp fibers (longitudinal) and weft fibers (transversal) so that each warp fiber passes alternately under and over each weft fiber. This structural hierarchy can be well observed in the SEM image from Figure 4.16 A. After 5 min of impregnation of the textiles on a single side in the chitin solution (1.6 wt% chitin, 30 wt% GVL, and 68.4 wt% BmimOAc) at 100 °C, a chitin layer was formed on one side of the textiles by promoting its precipitation in ethanol. The coated textiles exhibited a thin transparent shiny film on the chitin side, while the untreated side was not visually modified during the coating (Figure 4.15).

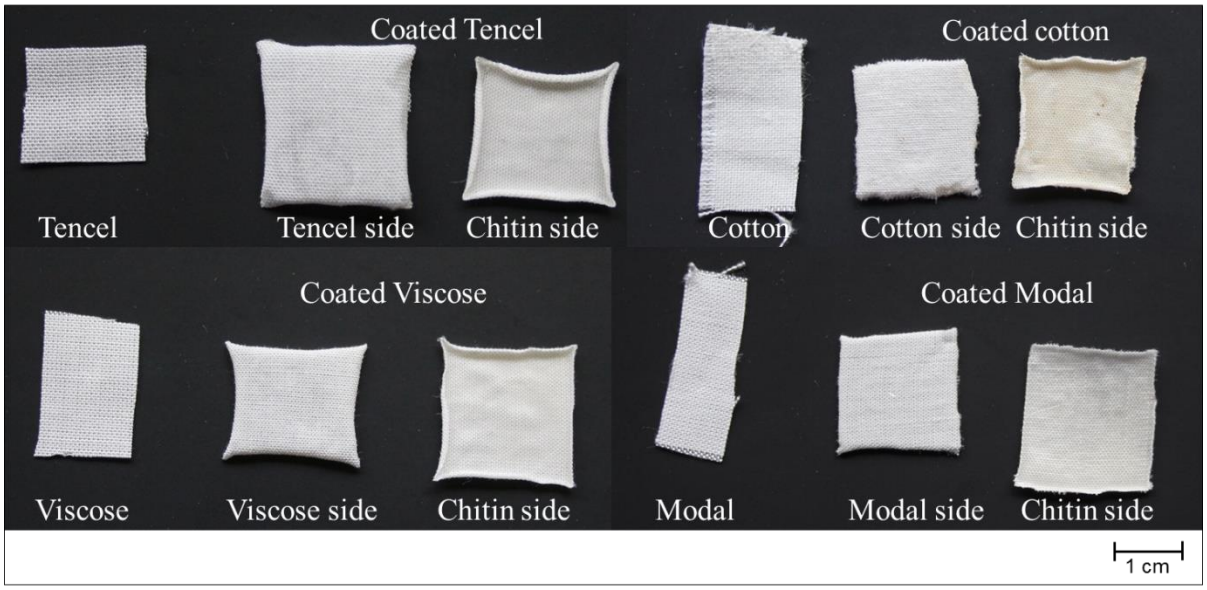

Figure 4.15: *Appearance of the untreated and chitin coated textiles.*

The morphology of the prepared materials was observed with SEM. Figure 4.16 shows an example of the obtained SEM images for the coated Viscose material performed on the surface of both sides, i.e. chitin and textile layer. The cross sections of all the coated textiles were also observed. On the one hand, it was observed that the Viscose network consisting of

interlaced fibers was not damaged by the coating procedure (Figure 4.16 A). The chitin side, on the other hand, bore a homogeneous and smooth surface without crevices or flaws (Figure 4.16 B). The chitin layer covered the pores of the textile without penetrating inside (Figure 4.16 C). These observations were the same for all the three other coated materials. The cross section of the coated materials displayed two distinct layers, i.e. the interlaced fibers representative of the textile side and a thin homogeneous chitin coat. The thickness of the chitin coat on all materials was estimated to be 10 ± 2 µm as inferred from the cross section SEM images (Figure 4.16 C-F).

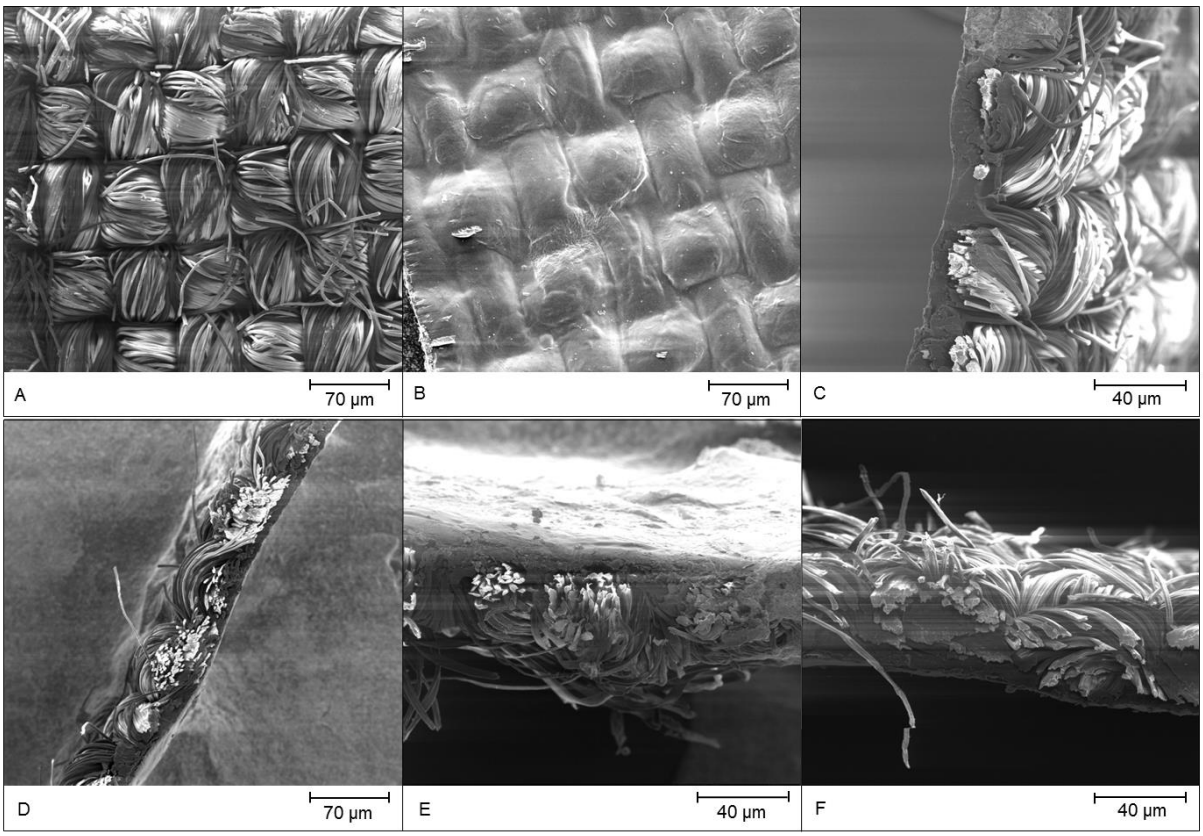

Figure 4.16: *SEM images of the coated textiles obtained from (A) the untreated side of the coated Viscose, (B) the chitin side of the coated Viscose, (C) the cross section of the coated Viscose, (D) the cross section of the coated Tencel, (E) the cross section of a coated cotton, and (F) the cross section of the coated Modal.*

To confirm the presence of chitin on the coated side and to exclude the possibility of textile degradation, all materials were characterized by FTIR in ATR mode. Figure 4.17 shows the

FTIR-ATR spectra of the chitin side for the four coated textiles. The IR curves were shifted by a constant value along the y-axis for visual clarity. First, no differences appeared comparing all spectra. Secondly, the typical bands of chitin were detected for all the materials.[203,204] Spectra show OH and NH stretching bands at 3430 and 3261 cm^{-1} and CH_3 asymmetric stretching band at 3090 cm^{-1}. The large band around 2875 cm^{-1} represents CH, CH_2, and CH_3 symmetric stretching. The doublet band at 1654 and 1625 cm^{-1} corresponds to the amide I band (C=O is engaged with two types of hydrogen bond groups, with N-H groups of the adjacent chain, and with the OH-groups of the same chain) and the peak at 1550 cm^{-1} to amide II band (CN stretching vibrations and in-plane NH bending).[203] The band at 1427 cm^{-1} is attributed to CH deformation, the one at 1373 cm^{-1} to C-CH_3 amide stretching, and the one at 1307 cm^{-1} to the amide III band (in plane mode of CONH group) and to CH_2 wagging. COC and CO stretching bands are represented by intense peaks at 1154-1010 cm^{-1}. The peak at 896 cm^{-1} confirms the presence of β-linkage in the molecule.[204] This indicated that chitin was successfully coated on the textiles and no obvious degradation or deacetylation occurred during the preparation.

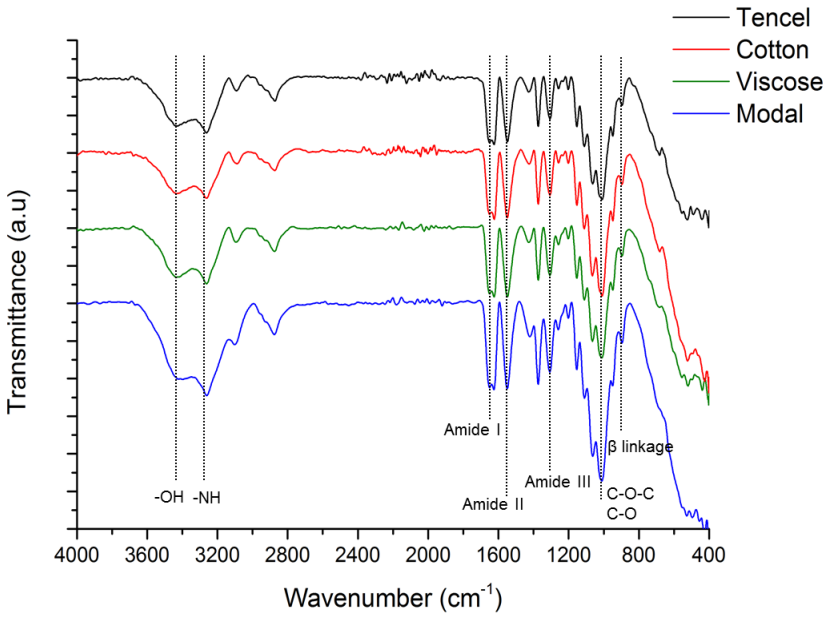

Figure 4.17: *FTIR-ATR spectra of the chitin coated side for the prepared textiles.*

Each starting material and its corresponding side on the coated textiles are compared by FTIR-ATR curves in Figure 4.18. Again, IR curves for the coated textiles were shifted as before for better display. The spectrum of each textile side was similar to the spectrum of the corresponding non-coated material. The cellulosic fibers were not chemically degraded during the coating process. In addition, the absence of the chitin characteristic bands confirmed the presence of chitin solely on the coated side of the prepared material as similarly observed under SEM.

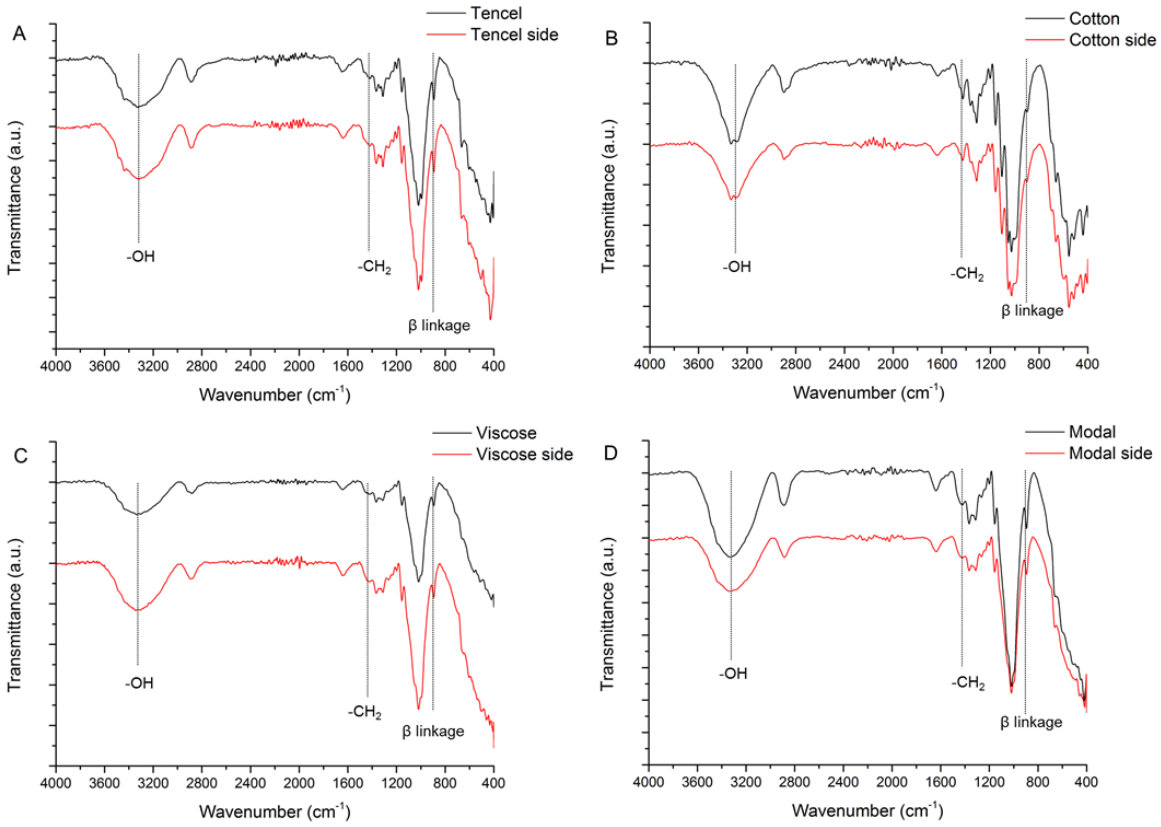

Figure 4.18: *Comparative FTIR-ATR spectra of each reference textile, (A) Tencel, (B) cotton, (C) Viscose, and (D) Modal with its corresponding untreated side on the coated materials.*

By carefully observing Figure 4.18, some differences can be observed between cotton and the other textile's absorption bands. Table 4.5 accurately reports the main absorption bands and their assignments for each textile.[118] The major infrared spectral difference between cotton and the other textiles is a sharper OH stretching band at around 3330 cm^{-1}. This means

that the hydrogen bonding network of cotton is different from the man-made fibers. The CH_2 bending band, known as the crystallinity band, is sharper for cotton and occurs at 1427 cm^{-1}, which is distinctive for cellulose I.[118] For the other textiles, this band is very weak and shifted to 1420 cm^{-1} which indicates that they are composed of cellulose II and amorphous cellulose.[205] Moreover, the weak intensity of the peak at 894 cm^{-1} for the cotton spectra indicates that crystalline cellulose II structures are not present for cotton.[118,205] For the other absorption bands no differences are observed.

Table 4.5: *Main absorption bands and their assignment for the different cellulosic textiles.*

Assignment	Wavenumber (cm^{-1})			
	Tencel	**Cotton**	**Modal**	**Viscose**
OH stretching intramolecular hydrogen bonds	3332	3332 (sharp)	3324	3337
CH stretching and CH_2 asymmetric stretching	2889	2897	2890	2883
OH of water absorbed from cellulose	1641	1633	1639	1641
CH_2 symmetric bending	1420	1427 (sharp)	1421	1421
CH bending	1366	1356	1366	1366
OH bending	1312	1314	1319	1308
COC stretching	1157	1158	1156	1156
CO stretching	1019	1027	1018	1017
Asymmetric C_1 (β-glucosidic linkage) out-of-plane stretching	893 (sharp)	893	894 (sharp)	894 (sharp)

To sum up these results, cotton is composed of cellulose I whereas the other textiles (Tencel, Viscose, and Modal) consist of cellulose II and amorphous cellulose.

4.3.2.2.3 Evaluation of new functional properties

In order to evaluate the specific properties of these new materials, a comparison of the untreated and the coated textiles was performed regarding their wetting and water/oxygen permeation performance.

Contact angle measurements

In a first step, it was studied whether the chitin coat can act as a water barrier, since this biopolymer is a major structural component in the exoskeleton of marine crustaceans and

contributes to their protection.[39] For this purpose, wetting properties of the films were characterized using water contact angle measurements. Typically, contact angles lower than 90° correspond to favorable wetting of the surface (quite hydrophilic), whereas low wettability materials (quite hydrophobic) induce contact angles higher than 90°.[206] The relation between the water contact angles and the type of textile (coated and non-coated) is illustrated in Figure 4.19 A. Due to the high hydrophilic behavior of cellulosic fibers and the porous structure of the textiles, no water contact angle could be measured for the non-coated materials as the water drop was immediately absorbed. Only cotton induced a contact angle of 85 ± 5° for a few seconds (10 s), probably due to its highly ordered structure (cellulose I). For the coated materials, the water contact angle tended to be identical on almost all chitin sides and was approximately 90° (90 ± 4° for the coated Tencel, 91 ± 3° for the coated cotton, and 90 ± 4° for the coated Viscose). Only the coated Modal textile exhibited a slightly smaller value of 84 ± 3°. These results proved that the chitin layers exhibit a poor degree of wetting towards water. After a long contact period on the surface of the chitin layer, decreasing water contact angles were detected and the absorption times were recorded (Figure 4.19 B). A complete absorption of a 2 µL drop on all chitin layers was reached after *circa* 20 min (24 ± 3 min for the coated Tencel, 22 ± 6 min for the coated cotton, 21 ± 1 min for the coated Viscose, and 19 ± 4 min for the coated Modal). Accordingly, the formed chitin layer is not fully impermeable to water but significantly retards its infiltration.

Since the untreated side of the coated textiles immediately absorbed the water drop, their wettability properties were not altered during the process (Figure 4.19 B). Consequently, the chitin coating affected only the wetting properties on one side of the processed materials, by making the textiles more hydrophobic. The water penetration into the cellulosic textiles was slowed down, probably due to the plugging of the holes and the increased wetting angles.

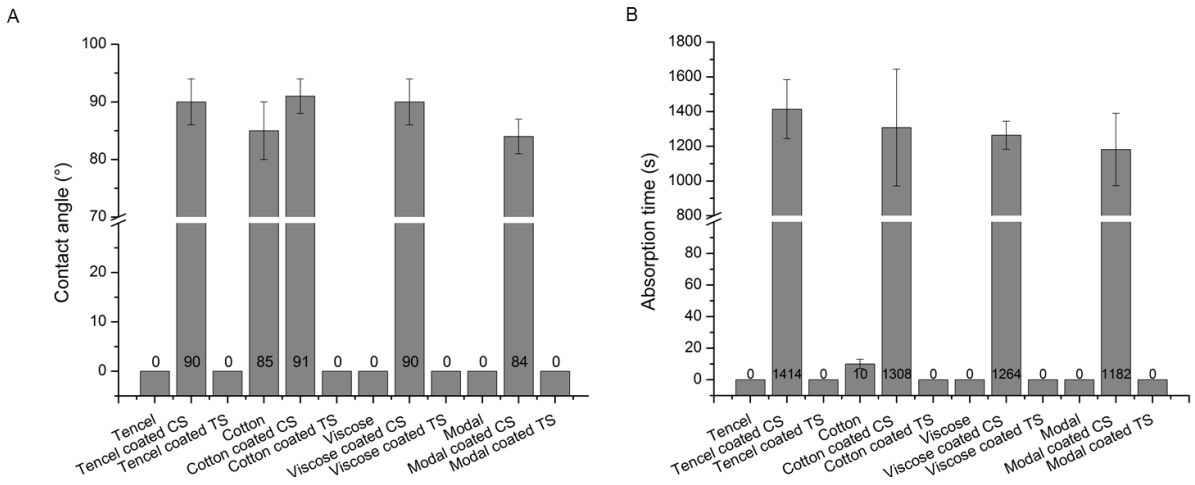

Figure 4.19: *(A) Contact angle and (B) absorption time of a 2 µL water drop on the surface of the textile materials non-coated and coated with chitin (CS stands for Chitin Side and TS for Textile Side).*

<u>Water permeability</u>

To study the influence of chitin on the water diffusion through the materials, water permeability tests for all of the coated and untreated materials were performed under identical conditions. Each film was placed between two cells, whereby one was filled with water and the other one with ethyl lactate (more details in Section 4.2.2.3). Figure 4.20 shows the comparative evolution of the water concentration in the ethyl lactate cell between the coated and uncoated textiles. The increase of the water concentration was drastically reduced when the material was coated with chitin. After 420 min, the water concentrations reached values of 0.044, 0.042, 0.032, and 0.080 g/mL for the uncoated Tencel, cotton, Viscose, and Modal, respectively, while water concentrations of 0.014, 0.014, 0.013, and 0.014 g/mL were recorded for the coated Tencel, cotton, Viscose, and Modal, respectively. The non-coated Modal material was the most water permeable among the untreated textiles.

From these experiments, water permeability coefficients were calculated according to Equation 4.3 and are reported in Table 4.6. As expected, the permeability coefficients for all non-coated textiles were higher than the ones for the coated ones, namely by a factor of 3.3, 3.2, 3.4, and 4.1 for Tencel, cotton, Viscose, and Modal, respectively. The water transport

was faster and easier through the unmodified textiles because of their porous and hydrophilic nature. As shown in Table 4.6, water permeability values for the coated textiles ranged from 4.83 to 6.76x10^{-8} m/s. This indicates that the water barrier properties of the chitin coats were independent of the nature of the textile. The chitin layer thus slowed down the water permeation.

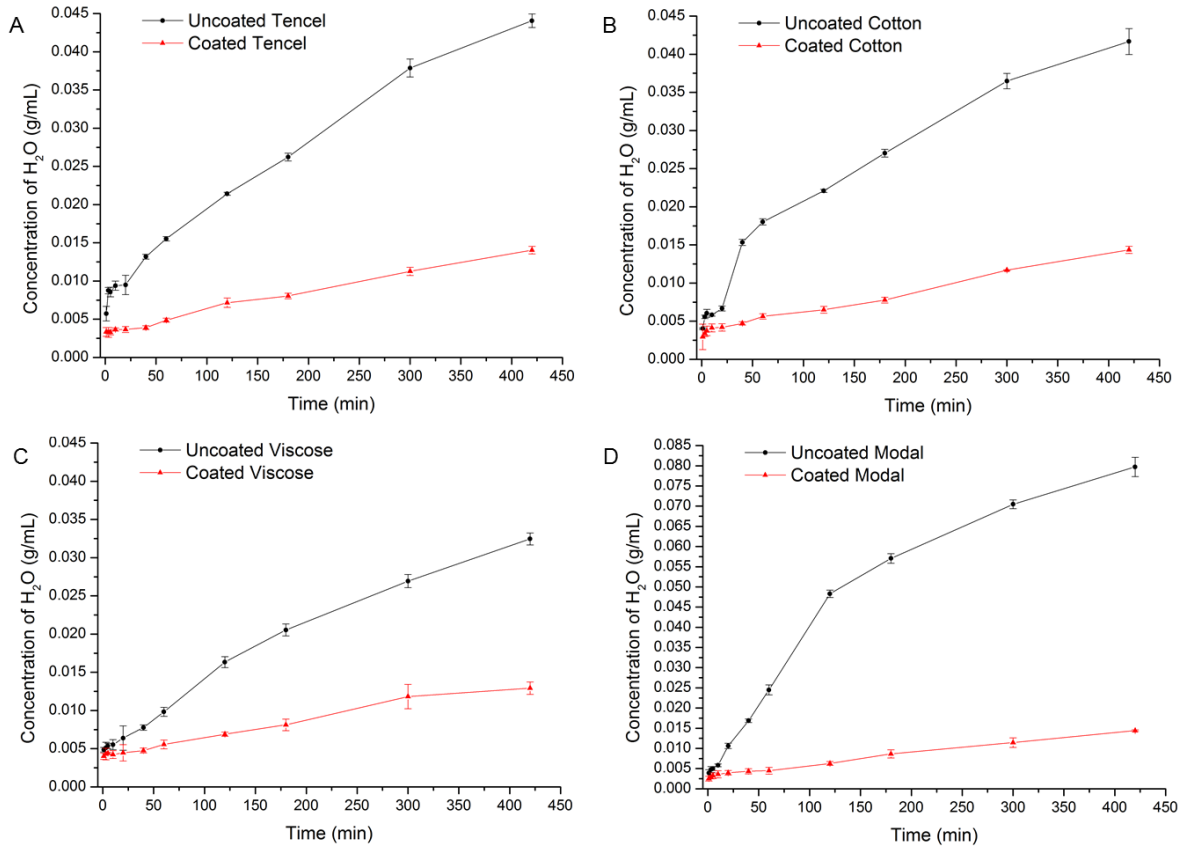

Figure 4.20: *Comparative evolution of the water concentration in the ethyl lactate cell over time between each uncoated and coated textile. (A) Tencel, (B) cotton, (C) Viscose, and (D) Modal.*

Table 4.6: *Water permeability coefficient, P_{H_2O}, with corresponding standard deviations.*

Material	P_{H_2O} **(x10^{-7} m/s)**
Tencel	2.0 ± 0.5
Tencel coated with chitin	0.6 ± 0.2
Cotton	1.6 ± 0.4
Cotton coated with chitin	0.5 ± 0.2
Viscose	1.7 ± 0.7
Viscose coated with chitin	0.5 ± 0.2
Modal	2.9 ± 0.8
Modal coated with chitin	0.7 ± 0.2

Gas permeability

In order to explore other barrier effects of the chitin layer, gas (i.e. O_2) permeability tests were carried out under dry conditions (more details in Section 4.2.3.2.5). Figure 4.21 shows the evolution of the oxygen partial pressure, p_{O_2}, in the measurement cell for all materials as a function of time. Oxygen permeability coefficients were calculated according to Equation 4.6 considering the quasi linear increase of the oxygen partial pressure and are reported in Table 4.7. For non-coated textiles, p_{O_2} identically increased from 0 to 51 hPa in 13 minutes. This generated high permeability coefficients for these materials in the range from 9.0 to 9.4 x10^{-7} m/s (Table 4.7). Furthermore, it should be noticed that this p_{O_2} raise followed the same trend as in the case when no membrane was fixed on the top of the permeation chamber. Independently of their nature, all textiles are highly permeable to oxygen due to the presence of open pores. In contrast, the oxygen diffusion through the coated materials was much slower as shown in Figure 4.21. After 13 minutes, p_{O_2}values of 3.1, 3.0, 2.8, and 2.7 hPa were recorded for the coated Tencel, cotton, Viscose, and Modal, respectively. As a result, coated textiles show significant lower permeability coefficients, which ranged from 0.42 to 0.46 x10^{-7} m/s. Comparing these values to those obtained for the non-coated textiles, it can be concluded that oxygen permeated through untreated Tencel, cotton, Viscose, and Modal textiles 19.8-22.8 times faster than through its corresponding coated materials.

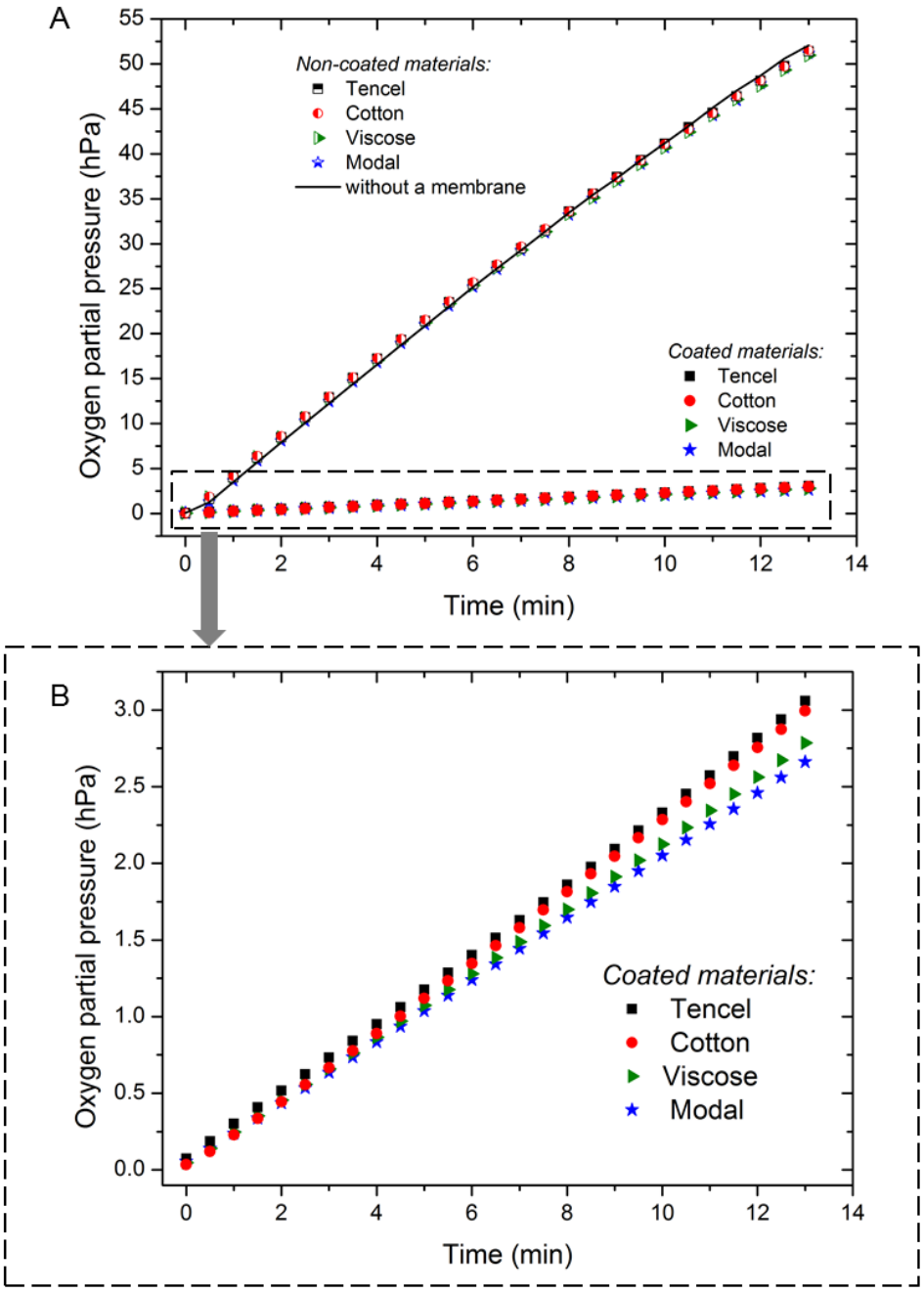

Figure 4.21: *Oxygen partial pressure over time measured in the O_2 permeation chamber for (A) all the non-coated and coated textiles and (B) specific for the coated materials with chitin.*

Table 4.7: *Oxygen permeability coefficients, P_{O_2}, with corresponding standard deviations.*

Material	$\boldsymbol{P_{O_2}}$ **(x10^{-4} m/s)**
Without membrane	9.4 ± 0.4
Tencel	9.1 ± 0.3
Tencel with chitin	0.46 ± 0.02
Cotton	9.1 ± 0.4
Cotton with chitin	0.46 ± 0.02
Viscose	9.0 ± 0.3
Viscose with chitin	0.42 ± 0.01
Modal	9.1 ± 0.3
Modal with chitin	0.40 ± 0.01

To prove that these new functional properties were caused by chitin and not just by the plugging of the textiles pores, the same coating procedure was performed with cellulose instead of chitin. To achieve this, a Tencel textile was coated with microcrystalline cellulose under the same conditions as previously described. It was not possible to reproduce a comparably thin 10 ± 2 µm cellulose layer as for chitin. Therefore, a precise quantitative comparison was not possible, especially for the permeability tests. However, it can be mentioned that cellulose coating induced a lower water contact angle of 54° instead of 90° for the chitin coating. The water drop was also two times faster absorbed by the cellulose layer than by the chitin coat. Concerning the gas/water permeability properties of the cellulose coated Tencel, it seems that the cellulose coat was more permeable to water but slightly less to oxygen than chitin. Further work has to be done to confirm these observations.

Probably further optimization, as for instance the increase of the thickness of the chitin coat, could improve the barrier properties of these new materials, making them potential candidates for various applications as impermeable textiles for hygiene products.

4.3.2.2.4 Recycling of BmimOAc

At the end of the coating process, the recycling of the ionic liquid was attempted for sustainability and profitability interests. Once chitin regenerated, the ethanol-based precipitation solutions were collected and submitted to a drying procedure detailed in

Section 4.2.2.4. Ethanol was successfully removed under reduced pressure using a rotary evaporator. However, GVL was still present in the residue due to its remarkable low vapor pressure (0.65 kPa at 25 °C and 3.5 kPa at 80 °C according to scientific literature).[181] A second step was carried out to remove GVL by using a high vacuum setup (10^{-6} mbar). Analysis of the obtained extract by ^{1}H- and ^{13}C-NMR revealed that BmimOAc remained unaltered and no trace of ethanol or GVL was detected (see Appendix 4.1). The recovered IL was reused to dissolve successfully 2 wt% of chitin in presence of 10 wt% GVL as performed for the coating procedure. BmimOAc was then recovered a second time and reused for a third time without appreciable decrease of its efficiency.

4.4 Concluding remarks

In this part, the main objectives were the production and characterization of novel polymer materials based on chitin and/or cellulose and the functionalization of cellulose-containing materials with chitin.

Cellulose fibers were produced according to the Lyocell process using *N*-methylmorpholine *N*-oxide (NMMO) hydrate. With the help of Lenzing AG, the impact of the addition of γ-valerolactone (GVL) on the spinning procedure was studied. It was revealed that this bio-sourced co-solvent could reduce the spinning temperature without deterioration in the stability of the spinning mass. However, no other improvements such as better mechanical properties of the fibers were observed so far. Further experiments have to be performed to fully characterize the advantages of GVL in this industrial process.

Cellulose and chitin composite fibers and films were produced using the ionic liquid 1-butyl-3-methylimidazolium acetate (BmimOAc) combined with GVL. Irregular composite fibers were spun with a self-developed dry-jet wet spinning apparatus. Accordingly, the fiber properties could not be fully characterized. Cellulose/chitin regenerated films were successfully prepared by Yaqing Duan by varying the mass ratio of chitin to cellulose. The properties of the resulting films were evaluated in detail by means of various analysis methods. It was demonstrated that chitin was not converted into chitosan by the dissolution process.

Chitin coated cellulosic textiles were prepared by regenerating chitin from a mixture of BmimOAc/GVL on one side of different textiles. A uniform, transparent, and non-modified chitin film of approx. 10 µm was successfully coated without damaging the textile network. The chitin coat influenced the properties of the resulting materials by making them more hydrophobic solely on the coated site. The penetration of water and oxygen into the coated materials were also slowed down leading to presume that chitin acted as a promising natural water and oxygen barrier. Finally, a procedure to recover the ionic liquid during the process was proposed for sustainable concerns. This step allows a multiple cycle use of the IL without any detectable loss of performance.

Conclusions and summary

The principal aim of this thesis was to prepare novel materials from cellulose and chitin using environmentally friendly techniques. In order to achieve this, different challenges were taken up. Figure C.1 gives an overview of the different tasks performed during this work. The first confrontation was the solubilization of cellulose and chitin (Chapter 2). The second part dealt with the influence of a green co-solvent in dissolution processes (Chapter 3). From the prepared polymer solutions, materials were formed, washed and dried. At the end, the recycling of the main solvent was investigated to be reused in the dissolution process (Chapter 4).

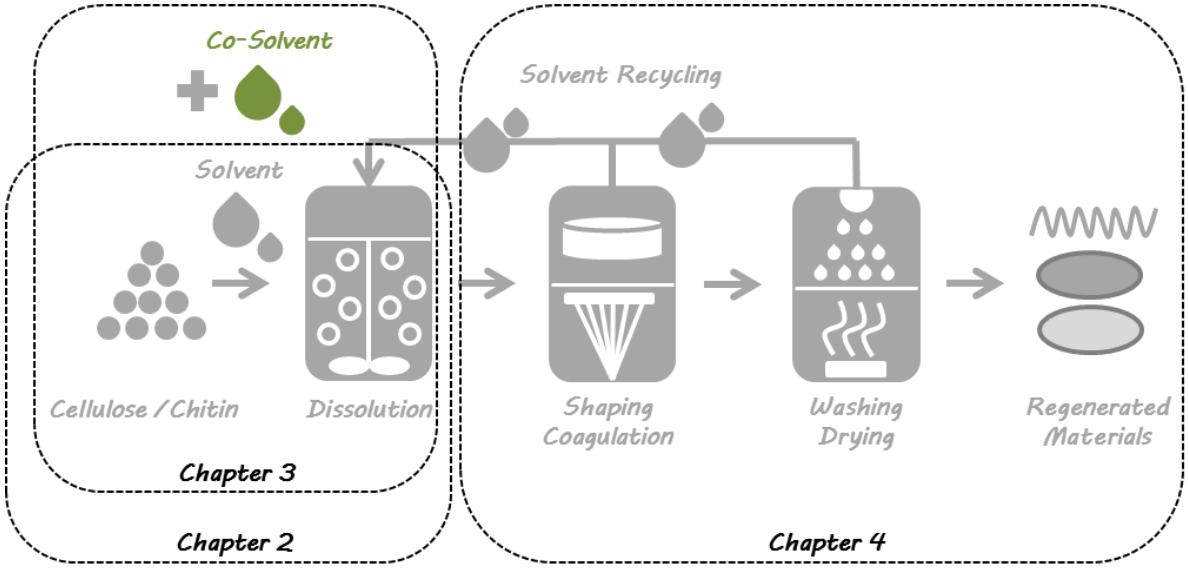

Figure C.1: *Overview of the chapters in this work.*

First of all, the solubilization of cellulose and chitin were investigated in different solvents. Deep eutectic solvents, ionic liquids (ILs) with various anion and cation combinations, and other more conventional solvent systems were evaluated towards their capacity to dissolve cellulose and chitin. The efficient solvents are shown in the Figure C.2. It was found that solely one IL, 1-butyl-3-methylimidazolium acetate (BmimOAc), could dissolve both

polymers in sufficient amounts to produce materials. Additionally, it was observed that chitin was poorly soluble in almost all the 49 solvents tested. It was found that despite similar structure, cellulose and chitin were not soluble in the same solvents. The high degree of polymerization of chitin and the additional intra- and inter-molecular interactions caused by the acetamido group present in chitin repeating unit may be the reasons of such a contrast.

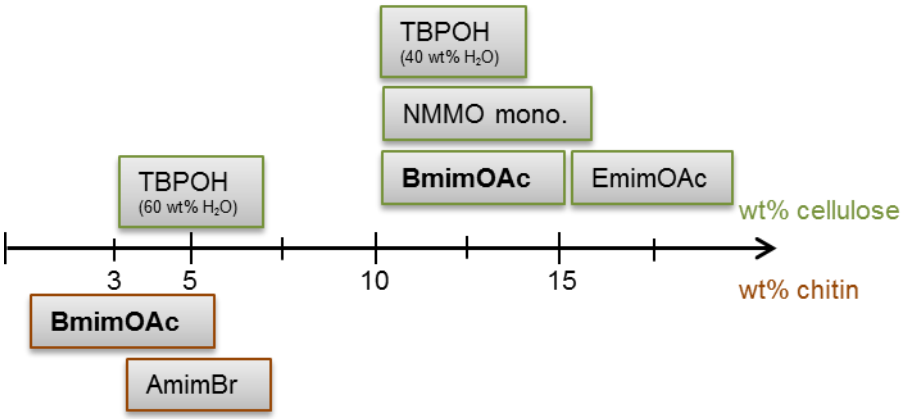

Figure C.2: *Overview of the solvents efficient for cellulose and chitin dissolution: 1-butyl-3-methyl-imidazolium acetate (BmimOAc), 1-allyl-3-methylimidazolium bromide (AmimBr), tetrabutyl-phosphonium hydroxide (TBPOH), N-methylmorpholine-N-oxide monohydrate (NMMO mono.), 1-ethyl-3-methyl-imidazolium acetate (EmimOAc).*

In order to reduce the lack of sustainability of the efficient imidazolium-based ionic liquid, a greener and bio-based co-solvent was added in the dissolution process. γ-Valerolactone (GVL), a sustainable chemical derived from levulinic acid, was found to be the most suitable candidate for this purpose. High concentrations of GVL, particularly for cellulose solubilization, were successfully added to BmimOAc in the dissolution process without precipitation of the polymers. This addition allowed a much faster dissolution, which can be explained by a significant decrease in the viscosity of the ionic liquid as well as of the resulting mixtures. No major disruptions on the ion interactions of BmimOAc and no formation of nano-structures were observed by Walden plot and dynamic light scattering techniques, respectively. In addition, rheological measurement of chitin and cellulose solutions after dissolution in BmimOAc and GVL revealed that GVL had a different influence on the rheological properties of these mixtures. While GVL allowed the chitin

chains to be more mobile, the contrary was observed for cellulose. Again the different chain length of the polymers can explain this dissimilarity.

Besides this study, the influence of GVL on the industrial Lyocell process was also investigated. For this task, the solvent *N*-methylmorpholine-*N*-oxide monohydrate (NMMO mono.) was used. Showing no solubility of chitin, NMMO mono./GVL solvent system was only investigated regarding cellulose dissolution. Improvements such as reduced dissolution duration, lower processing temperature, and more stable polymer solutions were obtained by introducing a significant amount of GVL (from 27 to 65 wt%). Possible reasons for these enhancements can be explained by the modified thermal and rheological properties caused by the addition of GVL. Thermal studies performed by differential scanning calorimetry showed that increasing GVL content in NMMO mono./GVL binary mixtures decreased their melting temperatures, enabling thus cellulose dissolution at lower temperatures. In addition, GVL allowed the ternary systems containing additionally cellulose to melt and to crystallize at reduced temperatures. This leads to a possible reduction of processing temperature in the manufacturing of fibers or any other materials. Lastly, GVL lowered the complex viscosity of ternary mixtures, facilitating thus the practical implementation of the cellulose dope. Combining higher performance and eco-friendly properties, this co-solvent may be of great interest for industrial applications.

Lastly, the production and characterization of novel materials were investigated (see Figure C.3). First, cellulosic textiles coated with a 10 µm chitin layer were successfully prepared by regenerating chitin from a BmimOAc/GVL mixture on one side of textiles. After removal of the solvent system and drying, the composite materials exhibited the unique properties of chitin on the coated side without sign of cellulose degradation. The influence of the chitin coat on the textiles properties was characterized by wetting and gas/water permeability comparative studies of the conventional and coated textiles. It was demonstrated that chitin layer rendered the materials more hydrophobic solely on the coated site. In addition, the penetration of water and oxygen into the coated materials were slowed down. This leads to presume that chitin can act as a promising natural water and oxygen barrier. Thus, these new

functional materials are potential candidates for various applications such as impermeable textiles for hygiene products. At the end of the process, a procedure to recover the ionic liquid was proposed for sustainable concerns. BmimOAc was reused and recycled at least two times without loss of performance.

Secondly, cellulose/chitin blend fibers were produced using BmimOAc/GVL as solvent system. For this purpose, a self-developed apparatus according to the dry jet-wet spinning process was employed. However, the lack of performance of this setup did not allow a successful production and complete characterization of these fibers. Further studies have to be performed to improve the apparatus.

Initially, the major intension of this project was focused on materials based on both, chitin and cellulose. Due to the lack of solubility of chitin in approximately all tested solvent, materials containing solely cellulose were produced as well. To further study the potential of GVL as co-solvent in the Lyocell process, cellulosic fibers were produced with the help of Lenzing AG. Preliminary experiments showed that the addition of the co-solvent could reduce the spinning temperature without deteriorating the stability of the spinning dope. No other enhancements, such as better mechanical properties of the fibers, were observed so far. However, the fact that this sustainable solvent can be added in an industrial process is quite remarkable.

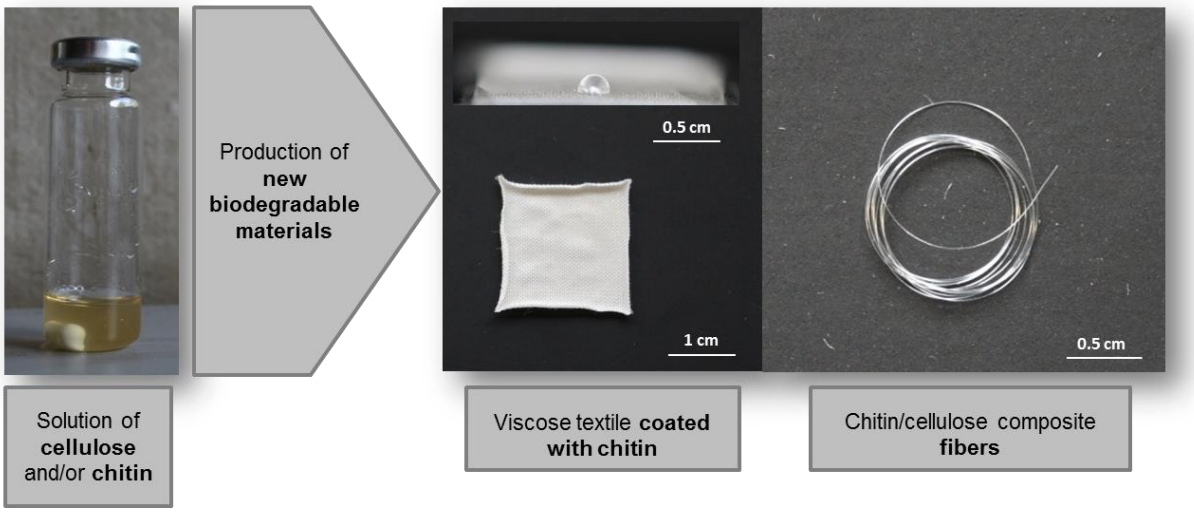

Figure C.3: *Overview of the produced biodegradable materials.*

To sum up, novel biodegradable materials from chitin and/or cellulose were produced in this thesis, which could provide promising high valuable products. To respect the greenness of cellulose and chitin, environmentally friendly chemicals were used, whenever applicable. If it was not possible to replace the harmful components by green ones, they were reduced to the possible minimum and their recycling was investigated. Two techniques were performed to produce the biodegradable materials, i.e. the coated textiles and the fibers. For the latter, lower temperatures compared to industrial process were used due the addition of a sustainable co-solvent, decreasing thus the energy consumption.

This thesis opens several doors and opportunities to go further in the development of greener process for designing biodegradable materials. In future, it would be essential to work on the solubility of chitin. Its high degree of polymerization may be one of the major problems and an approach to decrease the chitin chain lengths could facilitate its dissolution. However, this method should not lead to a reduced degree of acetylation with a risk of producing chitosan. The implementation of GVL in the Lyocell process can be also further investigated. It could be expected that GVL might facilitate the industrial process.

References

(1) Michel, J.-M.: History of industrial polymers. *Actual. Chim.* **2006**, *300*, 7-15.
(2) Schönbein, C.: Notiz über eine Veränderung der Pflanzenfaser und einiger andern organischen Substanzen. *Bericht über die Verhandlungen der Naturforschenden Gesellschaft in Basel* **1846**, *7*, 26-27.
(3) Saini, M. S.: Polymer and platic waste and recycling, *Video of a presentation online*. **2012**.
(4) Moore, C. J.: Synthetic polymers in the marine environment: A rapidly increasing, long-term threat. *Environ. Res.* **2008**, *108*, 131-139.
(5) Mohanty, A. K.; Misra, M.; Drzal, L. T.: Sustainable Bio-Composites from Renewable Resources: Opportunities and Challenges in the Green Materials World. *Journal of Polymers and the Environment* **2002**, *10*, 19-26.
(6) Vieira, M. G. A.; da Silva, M. A.; dos Santos, L. O.; Beppu, M. M.: Natural-based plasticizers and biopolymer films: A review. *European Polymer Journal* **2011**, *47*, 254-263.
(7) Bastioli, C.: Global status of the production of biobased packaging materials. *Starch/Staerke* **2001**, *53*, 351-355.
(8) Plank, J.: Applications of biopolymers and other biotechnological products in building materials. *Appl. Microbiol. Biotechnol.* **2004**, *66*, 1-9.
(9) Congress, U. S.: Chapter 2 - Technical overview of biopolymer field. In *Biopolymers: Making Materials Nature's Way- Background Paper*, **1993**; pp 39-43.
(10) Klemm, D.; Heublein, B.; Fink, H.-P.; Bohn, A.: Cellulose: Fascinating biopolymer and sustainable raw material. *Angew. Chem., Int. Ed.* **2005**, *44*, 3358-3393.
(11) Kurita, K.: Chitin and Chitosan: Functional Biopolymers from Marine Crustaceans. *Mar. Biotechnol.* **2006**, *8*, 203-226.
(12) Yu, L.: Chapter 1: Polymeric materials from renewable resources In *Biodegradable Polymer Blends and Composites from Renewable Resources*; Wiley, **2008**; pp 1-14.
(13) Vroman, I.; Tighzert, L.: Biodegradable Polymers. *Materials* **2009**, *2*, 307.
(14) Mohammed, L.; Ansari, M. N. M.; Pua, G.; Jawaid, M.; Islam, M. S.: A Review on Natural Fiber Reinforced Polymer Composite and Its Applications. *International Journal of Polymer Science* **2015**, *2015*, 15.
(15) Eichinger, D.: A vision of the world of cellulosic fibers in 2020. *Lenzinger Ber.* **2012**, *90*, 1-7.
(16) Koutinas, A. A.; Du, C.; Wang, R. H.; Webb, C.: Production of chemicals from biomass. In *Introduction to chemicals from biomass*; Clark, J., Deswarte, F., Eds.; Wiley, **2008**; Vol. 4; pp 77-102.
(17) de Jong, E.; Higson, A.; Walsh, P.; Wellisch, M.: Bio-based chemicals value added products from biorefineries. *IEA Bioenergy, Task42 Biorefinery* **2012**.
(18) Isikgor, F. H.; Becer, C. R.: Lignocellulosic biomass: a sustainable platform for production of bio-based chemicals and polymers. *arXiv.org, e-Print Arch., Condens. Matter* **2016**, 1-61.
(19) Luterbacher, J.; Alonso, D. M.; Dumesic, J.: Targeted chemical upgrading of lignocellulosic biomass to platform molecules. *Green Chemistry* **2014**, *16*, 4816-4838.
(20) Kobayashi, H.; Ohta, H.; Fukuoka, A.: Conversion of lignocellulose into renewable chemicals by heterogeneous catalysis. *Catal. Sci. Technol.* **2012**, *2*, 869-883.
(21) Payen, A.: Mémoire sur la composition du tissu propre des plantes et du ligneux. *Comptes rendus* **1838**, *7*, 1052-1056.

(22) Habibi, Y.; Lucia, L. A.; Rojas, O. J.: Cellulose Nanocrystals: Chemistry, Self-Assembly, and Applications. *Chem. Rev. (Washington, DC, U. S.)* **2010**, *110*, 3479-3500.
(23) Varshney, V.; Naithani, S.: Chemical functionalization of cellulose derived from nonconventional sources. In *Cellulose Fibers: Bio-and Nano-Polymer Composites*; Springer, **2011**; pp 43-60.
(24) Abdul Khalil, H. P. S.; Bhat, A. H.; Ireana Yusra, A. F.: Green composites from sustainable cellulose nanofibrils: A review. *Carbohydrate Polymers* **2012**, *87*, 963-979.
(25) Poletto, M.; Pistor, V.; Zattera, A. J.: Chapter 2: Structural Characteristics and Thermal Properties of Native Cellulose. In *Cellulose - Fundamental Aspects*; Ven, T. v. d., Godbout, L., Eds., **2013**.
(26) Moon, R. J.; Martini, A.; Nairn, J.; Simonsen, J.; Youngblood, J.: Cellulose nanomaterials review: structure, properties and nanocomposites. *Chemical Society Reviews* **2011**, *40*, 3941-3994.
(27) Fink, H. P.; Hofmann, D.; Philipp, B.: Some aspects of lateral chain order in cellulosics from X-ray scattering. *Cellulose (London)* **1995**, *2*, 51-70.
(28) Wang, H.; Gurau, G.; Rogers, R. D.: Ionic liquid processing of cellulose. *Chem. Soc. Rev.* **2012**, *41*, 1519-1537.
(29) Marchessault, R. H.; Sarko, A.: X-ray structure of polysaccharides. *Advan. Carbohyd. Chem. Biochem.* **1967**, *22*, 421-82.
(30) O'Sullivan, A. C.: Cellulose: the structure slowly unravels. *Cellulose (London)* **1997**, *4*, 173-207.
(31) Mann, J.; Marrinan, H. J.: Conversion of cellulose I to cellulose III by ethylamine. *Chem. Ind. (London, U. K.)* **1953**, 1092-3.
(32) Gardiner, E. S.; Sarko, A.: Packing analysis of carbohydrates and polysaccharides. 16. The crystal structures of celluloses IVI and IVII. *Can. J. Chem.* **1985**, *63*, 173-80.
(33) Baker, R. R.: Thermal decomposition of cellulose. *Journal of thermal analysis* **1975**, *8*, 163-173.
(34) Qiu, X.; Hu, S.: "Smart" Materials Based on Cellulose: A Review of the Preparations, Properties, and Applications. *Materials* **2013**, *6*, 738.
(35) Braconnot, H.: Sur la nature des champignons. *Ann Chim Phys* **1811**, *79*, 265-304.
(36) Odier, A.: *Mémoire sur la composition chimique des parties cornées des insectes*, **1823**.
(37) Crini, G.; Guibal, É.; Morcellet, M.; Torri, G.; Badot, P.-M.: Chitine et chitosane. Préparation, propriétés et principales applications. In *Chitine et chitosane, du biopolymère à l'application*; Presses universitaires de Franche-Comté, **2009**; pp 19-53.
(38) Rinaudo, M.: Chitin and chitosan: Properties and applications. *Progress in Polymer Science* **2006**, *31*, 603-632.
(39) Khor, E.: Chapter 5: the sources and production of chitin. In *Chitin: fulfilling a biomaterials promise*; Elsevier, **2014**; pp 63-72.
(40) Kramer, K. J.; Hopkins, T. L.; Schaefer, J.: Applications of solids NMR to the analysis of insect sclerotized structures. *Insect Biochemistry and Molecular Biology* **1995**, *25*, 1067-1080.
(41) Rahman, M. A.; Halfar, J.: First evidence of chitin in calcified coralline algae: new insights into the calcification process of Clathromorphum compactum. *Scientific Reports* **2014**, *4*, 6162.
(42) Ravi Kumar, M. N. V.: A review of chitin and chitosan applications. *Reactive and Functional Polymers* **2000**, *46*, 1-27.
(43) Khor, E.: Chapter 1: the relevance of chitin. In *Chitin: fulfilling a biomaterials promise*; Elsevier, **2014**; pp 1-8.
(44) Kurita, K.: Controlled functionalization of the polysaccharide chitin. *Prog. Polym. Sci.* **2001**, *26*, 1921-1971.
(45) Wu, Y.; Sasaki, T.; Irie, S.; Sakurai, K.: A novel biomass-ionic liquid platform for the utilization of native chitin. *Polymer* **2008**, *49*, 2321-2327.

(46) Muzzarelli, R. A. A.: Chitin Nanostructures in Living Organisms. In *Chitin: Formation and Diagenesis*; Gupta, N. S., Ed.; Springer Netherlands, **2011**; pp 1-34.
(47) Minke, R.; Blackwell, J.: The structure of α-chitin. *J. Mol. Biol.* **1978**, *120*, 167-81.
(48) Gardner, K. H.; Blackwell, J.: Refinement of the structure of β-chitin. *Biopolymers* **1975**, *14*, 1581-95.
(49) Rudall, K. M.: The Chitin/Protein Complexes of Insect Cuticles. *Advances in Insect Physiology* **1963**, *1*, 257-313.
(50) Islam, S.; Bhuiyan, M. A. R.; Islam, M. N.: Chitin and Chitosan: Structure, Properties and Applications in Biomedical Engineering. *J. Polym. Environ.* **2016**, Ahead of Print.
(51) Teraoka, I.: 2. Thermodynamics of dilute polymer solutions. In *Polymer Solutions: An Introduction to Physical Properties*; John Wiley & Sons Ltd, **2002**; pp 69-108.
(52) Billmeyer, F. W.: 2. Polymer solutions. In *Textbook of polymer science*; Wiley-Interscience, **1971**; pp 23-26.
(53) Medronho, B.; Lindman, B.: Competing forces during cellulose dissolution: From solvents to mechanisms. *Current Opinion in Colloid & Interface Science* **2014**, *19*, 32-40.
(54) Billmeyer, F. W.: 2. Polymer solutions. In *Textbook of polymer science*; Wiley-Interscience, **1971**; pp 32-39.
(55) Olsson, C.; Westman, G.: Chapter 6: Direct dissolution of cellulose: background, means and applications. In *Cellulose - Fundamental Aspects* van de Ven, T., Godbout, L., Eds., **2013**.
(56) Heinze, T.; Koschella, A.: Solvents applied in the field of cellulose chemistry - a mini review. *Polim.: Cienc. Tecnol.* **2005**, *15*, 84-89.
(57) Shen, L.; Patel, M. K.: Life cycle assessment of man-made cellulose fibers. *Lenzinger Ber.* **2010**, *88*, 1-59.
(58) Pinkert, A.; Marsh, K. N.; Pang, S.: Reflections on the Solubility of Cellulose. *Ind. Eng. Chem. Res.* **2010**, *49*, 11121-11130.
(59) Dawsey, T. R.; McCormick, C. L.: The lithium chloride/dimethylacetamide solvent for cellulose: a literature review *Journal of Macromolecular Science, Part C* **1990**, *30*, 405-440.
(60) Morgenstern, B.; Kammer, H. W.; Berger, W.; Skrabal, P.: 7Li-NMR study on cellulose/LiCl/N.N-dimethylacetamide solutions. *Acta Polymerica* **1992**, *43*, 356-357.
(61) El-Kafrawy, A.: Investigation of the cellulose/LiCl/dimethylacetamide and cellulose/LiCl/N-methyl-2-pyrrolidinone solutions by 13C NMR spectroscopy. *Journal of Applied Polymer Science* **1982**, *27*, 2435-2443.
(62) Lindman, B.; Karlstroem, G.; Stigsson, L.: On the mechanism of dissolution of cellulose. *J. Mol. Liq.* **2010**, *156*, 76-81.
(63) Medronho, B.; Romano, A.; Miguel, M. G.; Stigsson, L.; Lindman, B.: Rationalizing cellulose (in)solubility: reviewing basic physicochemical aspects and role of hydrophobic interactions. *Cellulose (Dordrecht, Neth.)* **2012**, *19*, 581-587.
(64) Alves, L.; Medronho, B.; Antunes, F. E.; Topgaard, D.; Lindman, B.: Dissolution state of cellulose in aqueous systems. 1. Alkaline solvents. *Cellulose* **2016**, *23*, 247-258.
(65) Glasser, W. G.; Atalla, R. H.; Blackwell, J.; Malcolm Brown, R., Jr.; Burchard, W.; French, A. D.; Klemm, D. O.; Nishiyama, Y.: About the structure of cellulose: debating the Lindman hypothesis. *Cellulose (Dordrecht, Neth.)* **2012**, *19*, 589-598.
(66) Cao, Y.; Wu, J.; Zhang, J.; Li, H.; Zhang, Y.; He, J.: Room temperature ionic liquids (RTILs): A new and versatile platform for cellulose processing and derivatization. *Chem. Eng. J. (Amsterdam, Neth.)* **2009**, *147*, 13-21.
(67) Rosenau, T.; Potthast, A.; Adorjan, I.; Hofinger, A.; Sixta, H.; Firgo, H.; Kosma, P.: Cellulose solutions in N-methylmorpholine-N-oxide (NMMO) -- degradation processes and stabilizers. *Cellulose (Dordrecht, Neth.)* **2002**, *9*, 283-291.
(68) Pillai, C. K. S.; Paul, W.; Sharma, C. P.: Chitin and chitosan polymers: Chemistry, solubility and fiber formation. *Progress in Polymer Science* **2009**, *34*, 641-678.

(69) Austin, P. R.: Solvents for and purification of chitin, patent US3892731 A. **1975**.
(70) Austin, P. R.: Chitin solution, patent DE2707164A1. **1977**.
(71) Tokura, S.; Nishizawa, K.; Kodera, F.: Process for production of high-purity chitin slurry, patent WO2010061454A1. **2010**.
(72) Serov, I. V.; Bochek, A. M.; Novoselov, N. P.; Zabivalova, N. M.; Lavrent'ev, V. K.; Vlasova, E. N.; Volchek, B. Z.: Chitin in Aqueous Alkaline Solutions with Urea and Thiourea Additives and the Structures of Films Obtained from Them. *Fibre Chem.* **2015**, *47*, 247-250.
(73) Hu, X.; Du, Y.; Tang, Y.; Wang, Q.; Feng, T.; Yang, J.; Kennedy, J. F.: Solubility and property of chitin in NaOH/urea aqueous solution. *Carbohydrate Polymers* **2007**, *70*, 451-458.
(74) Shen, X.; Shamshina, J. L.; Berton, P.; Gurau, G.; Rogers, R. D.: Hydrogels based on cellulose and chitin: fabrication, properties, and applications. *Green Chem.* **2016**, *18*, 53-75.
(75) Anastas, P.; Warner, J.: *Green Chemistry: Theory and Practice*; Oxford Univ Press, **1998**.
(76) Gu, Y.; Jerome, F.: Bio-based solvents: an emerging generation of fluids for the design of eco-efficient processes in catalysis and organic chemistry. *Chem. Soc. Rev.* **2013**, *42*, 9550-9570.
(77) Farran, A.; Cai, C.; Sandoval, M.; Xu, Y.; Liu, J.; Hernaiz, M. J.; Linhardt, R. J.: Green Solvents in Carbohydrate Chemistry: From Raw Materials to Fine Chemicals. *Chem. Rev. (Washington, DC, U. S.)* **2015**, *115*, 6811-6853.
(78) Freemantle, M.: Chapter 1: Introduction. In *An introduction to ionic liquids*; Royal Society of chemistry, **2010**; pp 1-10.
(79) Pinkert, A.; Marsh, K. N.; Pang, S.; Staiger, M. P.: Ionic liquids and their interaction with cellulose. *Chem. Rev. (Washington, DC, U. S.)* **2009**, *109*, 6712-6728.
(80) Branco, L. C.; Carrera, G.; Aires-de-Soua, J.; Martin, I. L.; Frade, R.; Afonso, C.: Physico-chemical properties of task-specific ionic liquids. In *Ionic liquids: theory, properties, new approaches*; Kokorin, A. I. i., Ed., **2011**; pp 61-94.
(81) Frade, R. F. M.; Afonso, C. A. M.: Impact of ionic liquids in environment and humans: an overview. *Hum. Exp. Toxicol.* **2010**, *29*, 1038-1054.
(82) Zhao, D.; Liao, Y.; Zhang, Z.: Toxicity of ionic liquids. *Clean: Soil, Air, Water* **2007**, *35*, 42-48.
(83) Graenacher, C.: Cellulose solutions, patent US1943176. **1934**.
(84) Swatloski, R. P.; Spear, S. K.; Holbrey, J. D.; Rogers, R. D.: Dissolution of cellose with ionic liquids. *Journal of the American Chemical Society* **2002**, *124*, 4974-4975.
(85) Meng, Z.; Zheng, X.; Tang, K.; Liu, J.; Qin, S.: Dissolution of natural polymers in ionic liquids: A review. *e-Polymers* **2012**, *56*, 33-38.
(86) Mazza, M.; Catana, D.-A.; Vaca-Garcia, C.; Cecutti, C.: Influence of water on the dissolution of cellulose in selected ionic liquids. *Cellulose* **2009**, *16*, 207-215.
(87) Vitz, J.; Erdmenger, T.; Haensch, C.; Schubert, U. S.: Extended dissolution studies of cellulose in imidazolium based ionic liquids. *Green Chem.* **2009**, *11*, 417-424.
(88) Jaworska, M. M.; Kozlecki, T.; Gorak, A.: Review of the application of ionic liquids as solvents for chitin. *J. Polym. Eng.* **2012**, *32*, 67-69.
(89) Wang, W.-T.; Zhu, J.; Wang, X.-L.; Huang, Y.; Wang, Y.-Z.: Dissolution Behavior of Chitin in Ionic Liquids. *J. Macromol. Sci., Part B: Phys.* **2010**, *49*, 528-541.
(90) Xie, H.; Zhang, S.; Li, S.: Chitin and chitosan dissolved in ionic liquids as reversible sorbents of CO2. *Green Chem.* **2006**, *8*, 630-633.
(91) Qin, Y.; Lu, X.; Sun, N.; Rogers, R. D.: Dissolution or extraction of crustacean shells using ionic liquids to obtain high molecular weight purified chitin and direct production of chitin films and fibers. *Green Chem.* **2010**, *12*, 968-971.
(92) Prasad, K.; Murakami, M.-a.; Kaneko, Y.; Takada, A.; Nakamura, Y.; Kadokawa, J.-i.: Weak gel of chitin with ionic liquid, 1-allyl-3-methylimidazolium bromide. *Int. J. Biol. Macromol.* **2009**, *45*, 221-225.

(93) Bochek, A. M.; Murav'ev, A. A.; Novoselov, N. P.; Zaborski, M.; Zabivalova, N. M.; Petrova, V. A.; Vlasova, E. N.; Volchek, B. Z.; Lavrent'ev, V. K.: Specific features of cellulose and chitin dissolution in ionic liquids of varied structure and the structural organization of regenerated polysaccharides. *Russ. J. Appl. Chem.* **2012**, *85*, 1718-1725.
(94) Remsing, R. C.; Swatloski, R. P.; Rogers, R. D.; Moyna, G.: Mechanism of cellulose dissolution in the ionic liquid 1-n-butyl-3-methylimidazolium chloride: a 13C and 35/37Cl NMR relaxation study on model systems. *Chem. Commun. (Cambridge, U. K.)* **2006**, 1271-1273.
(95) Lu, B.; Xu, A.; Wang, J.: Cation does matter: how cationic structure affects the dissolution of cellulose in ionic liquids. *Green Chem.* **2014**, *16*, 1326-1335.
(96) Rabideau, B. D.; Agarwal, A.; Ismail, A. E.: The Role of the Cation in the Solvation of Cellulose by Imidazolium-Based Ionic Liquids. *J. Phys. Chem. B* **2014**, *118*, 1621-1629.
(97) Zhang, H.; Wu, J.; Zhang, J.; He, J.: 1-Allyl-3-methylimidazolium chloride room temperature ionic liquid: A new and powerful nonderivatizing solvent for cellulose. *Macromolecules* **2005**, *38*, 8272-8277.
(98) Zhang, J.; Zhang, H.; Wu, J.; Zhang, J.; He, J.; Xiang, J.: NMR spectroscopic studies of cellobiose solvation in EmimAc aimed to understand the dissolution mechanism of cellulose in ionic liquids. *Phys. Chem. Chem. Phys.* **2010**, *12*, 1941-1947.
(99) Youngs, T. G. A.; Holbrey, J. D.; Mullan, C. L.; Norman, S. E.; Lagunas, M. C.; D'Agostino, C.; Mantle, M. D.; Gladden, L. F.; Bowron, D. T.; Hardacre, C.: Neutron diffraction, NMR and molecular dynamics study of glucose dissolved in the ionic liquid 1-ethyl-3-methylimidazolium acetate. *Chem. Sci.* **2011**, *2*, 1594-1605.
(100) Xu, A.; Wang, J.; Wang, H.: Effects of anionic structure and lithium salts addition on the dissolution of cellulose in 1-butyl-3-methylimidazolium-based ionic liquid solvent systems. *Green Chem.* **2010**, *12*, 268-275.
(101) Zhang, Q.; De Oliveira Vigier, K.; Royer, S.; Jerome, F.: Deep eutectic solvents: Syntheses, properties and applications. *Chem. Soc. Rev.* **2012**, *41*, 7108-7146.
(102) Smith, E. L.; Abbott, A. P.; Ryder, K. S.: Deep Eutectic Solvents (DESs) and Their Applications. *Chem. Rev. (Washington, DC, U. S.)* **2014**, *114*, 11060-11082.
(103) Abbott, A. P.; Barron, J. C.; Ryder, K. S.; Wilson, D.: Eutectic-based ionic liquids with metal-containing anions and cations. *Chem. - Eur. J.* **2007**, *13*, 6495-6501.
(104) Abbott, A. P.; Capper, G.; Davies, D. L.; Rasheed, R. K.; Tambyrajah, V.: Novel solvent properties of choline chloride/urea mixtures. *Chem. Commun. (Cambridge, U. K.)* **2003**, 70-71.
(105) Zhang, Q.; Benoit, M.; Vigier, K. D. O.; Barrault, J.; Jerome, F.: Green and inexpensive choline-derived solvents for cellulose decrystallization. *Chem. - Eur. J.* **2012**, *18*, 1043-1046, S1043/1-S1043/4.
(106) Hiltunen, J.; Vuoti, S.; Kuutti, L.: Deep eutectic solvents and their use, patent WO2015128550A1. **2015**.
(107) Ren, H.; Chen, C.; Guo, S.; Zhao, D.; Wang, Q.: Synthesis of a novel allyl-functionalized deep eutectic solvent to promote dissolution of cellulose. *BioResources* **2016**, *11*, 8457-8469.
(108) Ren, H.; chen, C.; Wang, Q.; Zhao, D.; Guo, S.: The properties of choline chloride-based deep eutectic solvents and their performance in the dissolution of cellulose. *BioResources* **2016**, *11*, 5435-5451.
(109) Sharma, M.; Mukesh, C.; Mondal, D.; Prasad, K.: Dissolution of α-chitin in deep eutectic solvents. *RSC Adv.* **2013**, *3*, 18149-18155.
(110) Francisco, M.; van den Bruinhorst, A.; Kroon, M. C.: New natural and renewable low transition temperature mixtures (LTTMs): screening as solvents for lignocellulosic biomass processing. *Green Chem.* **2012**, *14*, 2153-2157.
(111) Mukesh, C.; Mondal, D.; Sharma, M.; Prasad, K.: Choline chloride-thiourea, a deep eutectic solvent for the production of chitin nanofibers. *Carbohydr. Polym.* **2014**, *103*, 466-471.

(112) Mundsinger, K.; Mueller, A.; Beyer, R.; Hermanutz, F.; Buchmeiser, M. R.: Multifilament cellulose/chitin blend yarn spun from ionic liquids. *Carbohydr. Polym.* **2015**, *131*, 34-40.
(113) Kadokawa, J.-i.; Hirohama, K.; Mine, S.; Kato, T.; Yamamoto, K.: Facile Preparation of Chitin/Cellulose Composite Films Using Ionic Liquids. *J. Polym. Environ.* **2012**, *20*, 37-42.
(114) Zhang, L.; Guo, J.; Du, Y.: Morphology and properties of cellulose/chitin blends. Membranes from NaOH/thiourea aqueous solution. *J. Appl. Polym. Sci.* **2002**, *86*, 2025-2032.
(115) Wu, J.; Zhang, K.; Girouard, N.; Meredith, J. C.: Facile Route to Produce Chitin Nanofibers as Precursors for Flexible and Transparent Gas Barrier Materials. *Biomacromolecules* **2014**, *15*, 4614-4620.
(116) Kadokawa, J.-i.: Ionic liquid as useful media for dissolution, derivatization, and nanomaterial processing of chitin. *Green Sustainable Chem.* **2013**, *3*, 19-25, 7 pp.
(117) Roeder, T.; Moosbauer, J.; Kliba, G.; Schlader, S.; Zuckerstaetter, G.; Sixta, H.: Comparative characterization of man-made regenerated cellulose fibres. *Lenzinger Ber.* **2009**, *87*, 98-105.
(118) Carrillo, F.; Colom, X.; Sunol, J. J.; Saurina, J.: Structural FTIR analysis and thermal characterisation of lyocell and viscose-type fibres. *Eur. Polym. J.* **2004**, *40*, 2229-2234.
(119) John, M. J.; Thomas, S.: Biofibres and biocomposites. *Carbohydrate Polymers* **2008**, *71*, 343-364.
(120) Ma, H.; Hsiao, B. S.; Chu, B.: Thin-film nanofibrous composite membranes containing cellulose or chitin barrier layers fabricated by ionic liquids. *Polymer* **2011**, *52*, 2594-2599.
(121) Prasad, K.; Mine, S.; Kaneko, Y.; Kadokawa, J.-i.: Preparation of cellulose-based ionic porous material compatibilized with polymeric ionic liquid. *Polym. Bull. (Heidelberg, Ger.)* **2010**, *64*, 341-349.
(122) Yu, L.: Ch6. Blends and composites based on cellulose and natural polymers. In *Biodegradable Polymer Blends and Composites from Renewable Resources*; Wiley, **2008**; pp 135-139.
(123) Schurz, J.: From the fiber cellulose to the cellulose fiber - a further chance for the wood cluster. *Wochenbl. Papierfabr.* **2002**, *130*, 346-348.
(124) Michud, A.; Hummel, M.; Sixta, H.: Influence of process parameters on the structure formation of man-made cellulosic fibers from ionic liquid solution. *J. Appl. Polym. Sci.* **2016**, *133*, n/a.
(125) Wilkes, A. G.: 3. The viscose process. In *Regenerated Cellulose Fibres*; Woodhead Publishing Limited, **2001**; pp 37-61.
(126) Fink, H. P.; Weigel, P.; Purz, H. J.; Ganster, J.: Structure formation of regenerated cellulose materials from NMMO-solutions. *Prog. Polym. Sci.* **2001**, *26*, 1473-1524.
(127) Mieck, K.-P. B., E.; Ortlepp, G.; Albrecht, W.; Fuchs, H.; Guobiao, J.; and Gulich, B.: 1. Faserstoffe. In *Vliesstoffe - Rohstoffe, Herstellung, Anwendung, Eigenschaften, Prüfung*; Wiley-VCH, **2012**; pp 28.
(128) Abu-Rous, M. S., K.C.: Technical fibre formation: processes, fibre structure, fibre properties. *EPNOE summer school, Lenzing, Austria* **2006**.
(129) Rosenau, T.; Potthast, A.; Sixta, H.; Kosma, P.: The chemistry of side reactions and byproduct formation in the system NMMO/cellulose (Lyocell process). *Prog. Polym. Sci.* **2001**, *26*, 1763-1837.
(130) Gannon, J. M.; Graveson, I.; Mortimer, S. A.: Process for the manufacture of lyocell fibre, patent US5725821A. **1998**.
(131) Mortimer, S. A.; Peguy, A. A.: The influence of air-gap conditions on the structure formation of Lyocell fibers. *J. Appl. Polym. Sci.* **1996**, *60*, 1747-1756.
(132) Vinogradova, Y. S.; Chen, J. Y.: Micron- and nano-cellulose fiber regenerated from ionic liquids. *J. Text. Inst.* **2016**, *107*, 472-476.

(133) Sun, N.; Swatloski, R. P.; Maxim, M. L.; Rahman, M.; Harland, A. G.; Haque, A.; Spear, S. K.; Daly, D. T.; Rogers, R. D.: Magnetite-embedded cellulose fibers prepared from ionic liquid. *J. Mater. Chem.* **2008**, *18*, 283-290.
(134) Barber, P. S.; Kelley, S. P.; Griggs, C. S.; Wallace, S.; Rogers, R. D.: Surface modification of ionic liquid-spun chitin fibers for the extraction of uranium from seawater: seeking the strength of chitin and the chemical functionality of chitosan. *Green Chem.* **2014**, *16*, 1828-1836.
(135) Roeder, T.; Moosbauer, J.; Kraft, G.; Woess, K.; Schlader, S.: Man-made cellulose fibers: a comparison based on morphology and mechanical properties. *Lenzinger Ber.* **2013**, *91*, 07-12.
(136) Kunz, W.; Haeckl, K.: The hype with ionic liquids as solvents. *Chem. Phys. Lett.* **2016**, *661*, 6-12.
(137) Seddon, K. R.; Stark, A.; Torres, M.-J.: Influence of chloride, water, and organic solvents on the physical properties of ionic liquids. *Pure Appl. Chem.* **2000**, *72*, 2275-2287.
(138) Schneider, S.; Drake, G.; Hall, L.; Hawkins, T.; Rosander, M.: Alkene- and alkyne-substituted methylimidazolium bromides: structural effects and physical properties. *Z. Anorg. Allg. Chem.* **2007**, *633*, 1701-1707.
(139) Hunger, J.: Effects of polar compounds on the dynamics and dielectric properties of room-temperature ionic liquids. Doktorarbeit, Naturwissenschaftlichen Fakultät IV - Chemie und Pharmazie - der Universität Regensburg, **2010**.
(140) Stoppa, A.: Chemical Speciation in Mixtures of Ionic Liquids and Polar Compounds. Doktorarbeit, Naturwissenschaftlichen Fakultät IV - Chemie und Pharmazie - der Universität Regensburg, **2010**.
(141) Burrell, G. L.; Burgar, I. M.; Separovic, F.; Dunlop, N. F.: Preparation of protic ionic liquids with minimal water content and 15N NMR study of proton transfer. *Phys. Chem. Chem. Phys.* **2010**, *12*, 1571-1577.
(142) Nazet, A.: Cooperative dynamics of protic ionic liquids and the influence of polar compounds. Doktorarbeit, Naturwissenschaftlichen Fakultät IV - Chemie und Pharmazie -der Universität Regensburg, **2018**.
(143) Fukaya, Y.; Iizuka, Y.; Sekikawa, K.; Ohno, H.: Bio ionic liquids: room temperature ionic liquids composed wholly of biomaterials. *Green Chem.* **2007**, *9*, 1155-1157.
(144) Hoess, T.: Extraction of Iris pallida Lam. with choline-based ionic liquids. Masterarbeit, Naturwissenschaftlichen Fakultät IV - Chemie und Pharmazie - der Universität Regensburg, **2014**.
(145) Vijayaraghavan, R.; Thompson, B. C.; MacFarlane, D. R.; Kumar, R.; Surianarayanan, M.; Aishwarya, S.; Sehgal, P. K.: Biocompatibility of choline salts as crosslinking agents for collagen based biomaterials. *Chem. Commun. (Cambridge, U. K.)* **2010**, *46*, 294-296.
(146) Muehlbauer, A.: Synthesis and physicochemical characterization of novel biocompatible ionic liquids for the solubilization of biopolymers. Dissertation as co-tutelle, University Lille 1, University Regensburg, **2014**.
(147) Haeckl, K.; Muehlbauer, A.; Ontiveros, J. F.; Marinkovic, S.; Estrine, B.; Kunz, W.; Nardello-Rataj, V.: Carnitine alkyl ester bromides as novel biosourced ionic liquids, cationic hydrotropes and surfactants. *J. Colloid Interface Sci.* **2018**, *511*, 165-173.
(148) King, C.; Shamshina, J. L.; Gurau, G.; Berton, P.; Khan, N. F. A. F.; Rogers, R. D.: A platform for more sustainable chitin films from an ionic liquid process. *Green Chem.* **2017**, *19*, 117-126.
(149) Zhao, Y.; Liu, X.; Wang, J.; Zhang, S.: Effects of anionic structure on the dissolution of cellulose in ionic liquids revealed by molecular simulation. *Carbohydr. Polym.* **2013**, *94*, 723-730.
(150) Greaves, T. L.; Drummond, C. J.: Protic Ionic Liquids: Properties and Applications. *Chem. Rev. (Washington, DC, U. S.)* **2008**, *108*, 206-237.
(151) Hayes, R.; Warr, G. G.; Atkin, R.: Structure and Nanostructure in Ionic Liquids. *Chem. Rev. (Washington, DC, U. S.)* **2015**, *115*, 6357-6426.

(152) Nazet, A.; Buchner, R.: Dielectric Response and Transport Properties of Alkylammonium Formate Ionic Liquids. *submitted to J. Chem. Phys.*
(153) Vaz, F. M.; Wanders, R. J. A.: Carnitine biosynthesis in mammals. *Biochem. J.* **2002**, *361*, 417-429.
(154) Zeisel, S. H.; da, C. K.-A.: Choline: an essential nutrient for public health. *Nutr Rev* **2009**, *67*, 615-23.
(155) Romero, A.; Santos, A.; Tojo, J.; Rodriguez, A.: Toxicity and biodegradability of imidazolium ionic liquids. *J. Hazard. Mater.* **2008**, *151*, 268-273.
(156) Pinkert, A.; Marsh, K. N.; Pang, S.: Alkanolamine Ionic Liquids and Their Inability To Dissolve Crystalline Cellulose. *Ind. Eng. Chem. Res.* **2010**, *49*, 11809-11813.
(157) Zhao, H.; Baker, G. A.; Song, Z.; Olubajo, O.; Crittle, T.; Peters, D.: Designing enzyme-compatible ionic liquids that can dissolve carbohydrates. *Green Chem.* **2008**, *10*, 696-705.
(158) Vuoti, S.: Deep eutectic solvents for biomass fraction. In *An Oral communication at the 3rd International Symposium on Green Chemistry*: La Rochelle France, **2015**.
(159) Ashworth, C. R.; Matthews, R. P.; Welton, T.; Hunt, P. A.: Doubly ionic hydrogen bond interactions within the choline chloride-urea deep eutectic solvent. *Phys. Chem. Chem. Phys.* **2016**, *18*, 18145-18160.
(160) Fischer, V.: Properties and Applications of Deep Eutectic Solvents and Low-Melting Mixtures. Doktorarbeit, Naturwissenschaftlichen Fakultät IV - Chemie und Pharmazie - der Universität Regensburg, **2015**.
(161) Percot, A.; Viton, C.; Domard, A.: Optimization of chitin extraction from shrimp shells. *Biomacromolecules* **2003**, *4*, 12-18.
(162) Franks, N. E.; Varga, J. K.: Process for making precipitated cellulose, patent US4145532 A **1979**.
(163) Abe, M.; Fukaya, Y.; Ohno, H.: Fast and facile dissolution of cellulose with tetrabutylphosphonium hydroxide containing 40 wt% water. *Chem. Commun. (Cambridge, U. K.)* **2012**, *48*, 1808-1810.
(164) Lue, A.; Zhang, L.; Ruan, D.: Inclusion complex formation of cellulose in NaOH-thiourea aqueous system at low temperature. *Macromol. Chem. Phys.* **2007**, *208*, 2359-2366.
(165) Zhang, S.; Sun, N.; He, X.; Lu, X.; Zhang, X.: Physical properties of ionic liquids: database and evaluation. *J. Phys. Chem. Ref. Data* **2006**, *35*, 1475-1517.
(166) Gericke, M.; Schlufter, K.; Liebert, T.; Heinze, T.; Budtova, T.: Rheological Properties of Cellulose/Ionic Liquid Solutions: From Dilute to Concentrated States. *Biomacromolecules* **2009**, *10*, 1188-1194.
(167) Liebner, F.; Patel, I.; Ebner, G.; Becker, E.; Horix, M.; Potthast, A.; Rosenau, T.: Thermal aging of 1-alkyl-3-methylimidazolium ionic liquids and its effect on dissolved cellulose. *Holzforschung* **2010**, *64*, 161-166.
(168) Li, X.; Zhang, Y.; Tang, J.; Lan, A.; Yang, Y.; Gibril, M.; Yu, M.: Efficient preparation of high concentration cellulose solution with complex DMSO/ILs solvent. *J. Polym. Res.* **2016**, *23*, 1-8.
(169) Andanson, J.-M.; Bordes, E.; Devemy, J.; Leroux, F.; Padua, A. A. H.; Gomes, M. F. C.: Understanding the role of co-solvents in the dissolution of cellulose in ionic liquids. *Green Chem.* **2014**, *16*, 2528-2538.
(170) Le, K. A.; Rudaz, C.; Budtova, T.: Phase diagram, solubility limit and hydrodynamic properties of cellulose in binary solvents with ionic liquid. *Carbohydr. Polym.* **2014**, *105*, 237-243.
(171) Olsson, C.; Hedlund, A.; Idstroem, A.; Westman, G.: Effect of methylimidazole on cellulose/ionic liquid solutions and regenerated material therefrom. *J. Mater. Sci.* **2014**, *49*, 3423-3433.
(172) Mohan, M.; Banerjee, T.; Goud, V. V.: Effect of Protic and Aprotic Solvents on the Mechanism of Cellulose Dissolution in Ionic Liquids: A Combined Molecular Dynamics and Experimental Insight. *ChemistrySelect* **2016**, *1*, 4823-4832.

(173) Smith, S. B.; Atureliya, S. K.: Process and solvents for shaping cellulose, patent GB2337990 A. **1999**.
(174) Rinaldi, R.: Instantaneous dissolution of cellulose in organic electrolyte solutions. *Chem. Commun. (Cambridge, U. K.)* **2011**, *47*, 511-513.
(175) Boissou, F.; Muehlbauer, A.; De Oliveira Vigier, K.; Leclercq, L.; Kunz, W.; Marinkovic, S.; Estrine, B.; Nardello-Rataj, V.; Jerome, F.: Transition of cellulose crystalline structure in biodegradable mixtures of renewably-sourced levulinate alkyl ammonium ionic liquids, γ-valerolactone and water. *Green Chem.* **2014**, *16*, 2463-2471.
(176) Gale, E.; Wirawan, R. H.; Silveira, R. L.; Pereira, C. S.; Johns, M. A.; Skaf, M. S.; Scott, J. L.: Directed Discovery of Greener Cosolvents: New Cosolvents for Use in Ionic Liquid Based Organic Electrolyte Solutions for Cellulose Dissolution. *ACS Sustainable Chem. Eng.* **2016**, *4*, 6200-6207.
(177) Zhao, Y.; Liu, X.; Wang, J.; Zhang, S.: Insight into the cosolvent effect of cellulose dissolution in imidazolium-based ionic liquid systems. *J Phys Chem B* **2013**, *117*, 9042-9.
(178) Lv, Y.; Wu, J.; Zhang, J.; Niu, Y.; Liu, C.-Y.; He, J.; Zhang, J.: Rheological properties of cellulose/ionic liquid/dimethylsulfoxide (DMSO) solutions. *Polymer* **2012**, *53*, 2524-2531.
(179) Pratt, K. W.; Koch, W. F.; Wu, Y. C.; Eerezansky, P. A.: Molality-based primary standards of electrolytic conductivity (IUPAC technical report). *Pure Appl. Chem.* **2001**, *73*, 1783-1793.
(180) Ripin, D. H. B.; Vetelino, M.: 2-Methyltetrahydrofuran as an alternative to dichloromethane in 2-phase reactions. *Synlett* **2003**, 2353.
(181) Horvath, I. T.; Mehdi, H.; Fabos, V.; Boda, L.; Mika, L. T.: γ-Valerolactone - a sustainable liquid for energy and carbon-based chemicals. *Green Chem.* **2008**, *10*, 238-242.
(182) Canongia Lopes, J. N.; Costa Gomes, M. F.; Husson, P.; Padua, A. A. H.; Rebelo, L. P. N.; Sarraute, S.; Tariq, M.: Polarity, Viscosity, and Ionic Conductivity of Liquid Mixtures Containing [C4C1im][Ntf2] and a Molecular Component. *J. Phys. Chem. B* **2011**, *115*, 6088-6099.
(183) Schreiner, C.; Zugmann, S.; Hartl, R.; Gores, H. J.: Fractional Walden Rule for Ionic Liquids: Examples from Recent Measurements and a Critique of the So-Called Ideal KCl Line for the Walden Plot. *J. Chem. Eng. Data* **2010**, *55*, 1784-1788.
(184) Harris, K. R.; Woolf, L. A.; Kanakubo, M.: Temperature and Pressure Dependence of the Viscosity of the Ionic Liquid 1-Butyl-3-methylimidazolium Hexafluorophosphate. *J. Chem. Eng. Data* **2005**, *50*, 1777-1782.
(185) Walden, P.: Organic solvents and ionization media. III. Interior friction and its relation to conductivity. *Z. Phys. Chem., Stoechiom. Verwandtschaftsl.* **1906**, *55*, 207-249.
(186) Evans, D. F.; Wennerström, H.: 7. Polymers in colloidal systems. In *The Colloidal Domain: Where Physics, Chemistry, Biology, and Technology Meet*; Wiley, **1999**; pp 379-382.
(187) Mezger, T. G.: 8. Oscillatory tests. In *The rheology handbook: for users of rotational and oscillatory rheometers*; Vincentz Network GmbH & Co KG, **2006**; pp 114-138.
(188) Marinetti, L. J.; Leavell, B. J.; Jones, C. M.; Hepler, B. R.; Isenschmid, D. S.; Commissaris, R. L.: Gamma butyrolactone (GBL) and gamma valerolactone (GVL): Similarities and differences in their effects on the acoustic startle reflex and the conditioned enhancement of startle in the rat. *Pharmacology Biochemistry and Behavior* **2012**, *101*, 602-608.
(189) Alonso, D. M.; Wettstein, S. G.; Dumesic, J. A.: Gamma-valerolactone, a sustainable platform molecule derived from lignocellulosic biomass. *Green Chem.* **2013**, *15*, 584-595.
(190) Zaitseva, A.; Pokki, J.-P.; Le, H. Q.; Alopaeus, V.; Sixta, H.: Vapor-Liquid Equilibria, Excess Enthalpy, and Density of Aqueous γ-Valerolactone Solutions. *J. Chem. Eng. Data* **2016**, *61*, 881-890.
(191) Chanzy, H.; Nawrot, S.; Peguy, A.; Smith, P.; Chevalier, J.: Phase behavior of the quasiternary system N-methylmorpholine N-oxide, water and cellulose. *J. Polym. Sci., Polym. Phys. Ed.* **1982**, *20*, 1909-24.

(192) Biganska, O.; Navard, P.: Phase diagram of a cellulose solvent: N-methylmorpholine-N-oxide-water mixtures. *Polymer* **2003**, *44*, 1035-1039.
(193) Hauru, L. K. J.; Hummel, M.; Michud, A.; Sixta, H.: Dry jet-wet spinning of strong cellulose filaments from ionic liquid solution. *Cellulose (Dordrecht, Neth.)* **2014**, *21*, 4471-4481.
(194) Biganska, O.; Navard, P.; Bedue, O.: Crystallization of cellulose/N-methylmorpholine-N-oxide hydrate solutions. *Polymer* **2002**, *43*, 6139-6145.
(195) Kim, D. B.; Lee, W. S.; Jo, S. M.; Lee, Y. M.; Kim, B. C.: Effect of thermal history on the phase behavior of N-methyl morpholine N-oxide hydrates and their solutions of cellulose. *Polym. J. (Tokyo, Jpn.)* **2001**, *33*, 139-146.
(196) Crosthwaite, J. M.; Muldoon, M. J.; Dixon, J. K.; Anderson, J. L.; Brennecke, J. F.: Phase transition and decomposition temperatures, heat capacities and viscosities of pyridinium ionic liquids. *J. Chem. Thermodyn.* **2005**, *37*, 559-568.
(197) Chanzy, H.; Dube, M.; Marchessault, R. H.: Crystallization of cellulose with N-methylmorpholine N-oxide: a new method of texturing cellulose. *J. Polym. Sci., Polym. Lett. Ed.* **1979**, *17*, 219-26.
(198) Duan, Y.; Freyburger, A.; Kunz, W.; Zollfrank, C.: Cellulose and chitin composite materials from an ionic liquid and a green co-solvent. *Submitted to Carbohydr. Polym.*
(199) Wollinger, A.: Entwicklung einer Messapparatur zur Bestimmung der Elementarprozesse bei der Viskoseherstellung. Masterarbeit, Naturwissenschaftlichen Fakultät IV - Chemie und Pharmazie - der Universität Regensburg, **2012**.
(200) Dandia, A.; Jain, A. K.; Laxkar, A. K.: Ethyl lactate as a promising bio based green solvent for the synthesis of spiro-oxindole derivatives via 1,3-dipolar cycloaddition reaction. *Tetrahedron Lett.* **2013**, *54*, 3929-3932.
(201) Kim, D. B.; Pak, J. J.; Jo, S. M.; Lee, W. S.: Dry jet-wet spinning of cellulose/N-methylmorpholine N-oxide hydrate solutions and physical properties of Lyocell fibers. *Text. Res. J.* **2005**, *75*, 331-341.
(202) Credou, J.; Berthelot, T.: Cellulose: from biocompatible to bioactive material. *J. Mater. Chem. B* **2014**, *2*, 4767-4788.
(203) Pearson, F. G.; Marchessault, R. H.; Liang, C. Y.: Infrared spectra of crystalline polysaccharides. V. Chitin. *J. Polym. Sci.* **1960**, *43*, 101-16.
(204) Muzzarelli, R. A. A.; Morganti, P.; Morganti, G.; Palombo, P.; Palombo, M.; Biagini, G.; Mattioli Belmonte, M.; Giantomassi, F.; Orlandi, F.; Muzzarelli, C.: Chitin nanofibrils/chitosan glycolate composites as wound medicaments. *Carbohydr. Polym.* **2007**, *70*, 274-284.
(205) Nelson, M. L.; O'Connor, R. T.: Relation of certain infrared bands to cellulose crystallinity and crystal latticed type. Part I. Spectra of lattice types I, II, III and of amorphous cellulose. *Journal of Applied Polymer Science* **1964**, *8*, 1311-1324.
(206) Yuan, Y.; Lee, T. R.: Contact Angle and Wetting Properties. In *Surface Science Techniques*; Springer Berlin Heidelberg, **2013**; pp 3-34.

Appendices

Appendix 2.1. Synthesis of 1-allyl-3-methylimidazolium bromide for the dissolution tests

1-Allyl-3-methylimidazolium bromide (AmimBr) was analyzed by ^{1}H- and ^{13}C-NMR measurements in dimethyl sulfoxide-d6. The structure of AmimBr is shown in Figure A.1. The following abbreviations are used to explain the multiplicities: s = singlet, d = doublet, t = triplet, m = multiplet.

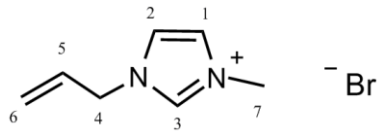

Figure A.1: *Structure of AmimBr.*

AmimBr:

^{1}H-NMR (300 MHz, DMSO-d6): δ (ppm) = 3.90 (s, 3H, C_7), 4.95 (d, J=6.14 Hz, 2H, C_4), 5.19-5.27 (m, 2H, C_6), 5.89-6.03 (m, 1H, C_5), 7.91 (t, J=1.53 Hz, 1H, C_1), 7.93 (t, J=1.47 Hz, 1H, C_2), 9.52 (s, 1H, C_3)

^{13}C-NMR (300 MHz, DMSO-d6): δ (ppm) = 36.00 (C_7), 50.38 (C_4), 120.06 (C_6), 122.00 (C_2), 123.44 (C_1), 131.65 (C_5), 136.31 (C_3)

Appendix 3.1. Impact of GVL on BmimOAc physicochemical properties

Temperature-dependent density, dynamic viscosity, and electrical conductivity data for BmimOAc/GVL mixtures are listed in Table A.1, A.2 and A.3, respectively.

Table A.1: *Density values (expressed in g/cm^3) as function of temperature and of GVL composition for different BmimOAc/GVL mixtures.*

Temperature (°C)	GVL = 0 wt%	GVL = 20.3 wt%	GVL = 50.0 wt%	GVL = 68.4 wt%	GVL = 100 wt%
25.00	1.051	1.053	1.054	1.054	1.049
40.00	1.042	1.043	1.043	1.041	1.035
60.00	1.030	1.030	1.028	1.025	1.016
80.00	1.018	1.017	1.013	1.009	0.997
100.00	1.006	0.999	1.002	0.994	0.983
110.00	1.000	0.992	0.995	0.986	0.974

Table A.2: *Dynamic viscosity values (expressed in mPa.s) as function of temperature and of GVL composition for different BmimOAc/GVL mixtures.*

Temperature (°C)	GVL = 0 wt%	GVL = 20.3 wt%	GVL = 50.0 wt%	GVL = 68.4 wt%	GVL = 100 wt%
25.00	333.695	73.089	13.954	5.576	1.825
40.00	123.295	35.393	8.689	3.872	1.422
60.00	44.675	16.658	5.221	2.594	1.072
80.00	20.848	9.343	3.463	1.874	0.847
100.00	12.111	5.890	2.469	1.420	0.684
110.00	9.433	4.880	2.144	1.261	0.625

Table A.3: *Electrical conductivity values (expressed in mS/cm) as function of temperature and of GVL composition for different BmimOAc/GVL mixtures.*

Temperature (°C)	GVL = 0 wt%	GVL = 20.3 wt%	GVL = 50.0 wt%	GVL = 68.4 wt%
25.00	0.629	1.687	3.120	3.047
40.00	1.608	3.317	4.942	4.477
60.00	4.158	6.678	8.097	6.817
80.00	8.440	11.449	12.027	9.599
100.00	1.454	17.542	16.617	12.773

Appendix 4.1. Recycling of 1-butyl-3-methylimidazolium acetate during the coating procedure of chitin on textiles

Pure γ-valerolactone (GVL), pure 1-butyl-3-methylimidazolium acetate (BmimOAc), recycled BmimOAc a first time (named recycled BmimOAc 1), and recycled BmimOAc a second time (recycled BmimOAc 2) were analyzed by ^{1}H- and ^{13}C-NMR measurements in dimethyl sulfoxide-d6. The structure of BmimOAc and GVL is shown in Figure A.2. The following abbreviations are used to explain the multiplicities: s = singlet, d = doublet, t = triplet, m = multiplet.

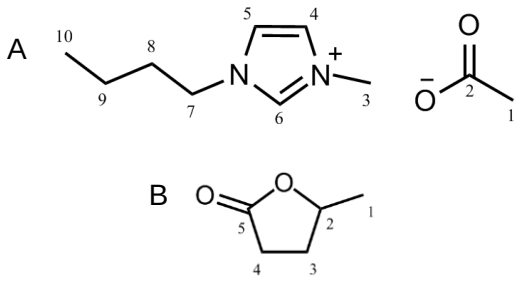

Figure A.22: *Structure of (A) BmimOAc and (B) GVL.*

Pure GVL:

^{1}H-NMR (300 MHz, DMSO-d6): δ (ppm) = 1.30 (d, J=6.31 Hz, 3H, C_1), 1.68-1.81 (m, 1H, C_3), 2.23-2.34 (m, 1H, C_3), 2.46 (t, J=2.27 Hz, 1H, C_4), 2.50 (t, J=2.46 Hz, 1H, C_4), 4.65-4.54 (m, 1H, C_2**)**

^{13}C-NMR (300 MHz, DMSO-d6): δ (ppm) = 20.48 (C_1), 28.44 (C_3), 28.96 (C_4), 76.57 (C_2), 176.92 (C_5)

Pure BmimOAc:

^{1}H-NMR (300 MHz, DMSO-d6): δ (ppm) = 0.85 (t, J= 7.40 Hz, 3H, C_{10}), 1.15-1.27 (m, 2H, C_9), 1.60 (s, 3H, C_1), 1.69-1.79 (m, 2H, C_8), 3.88 (s, 3H, C_3**),** 4.20 (t, J=7.20 Hz, 2H, C_7), 7.88 (t, J=1.62 Hz, 1H, C_4), 7.96 (t, J=1.73 Hz, 1H, C_5), 10.29 (s, 1H, C_6)

^{13}C-NMR (300 MHz, DMSO-d6): δ (ppm) =13.10 (C_{10}), 18.64 (C_9), 25.69 (C_1), 31.33 (C_8), 35.27 (C_3), 48.05 (C_7), 122.16 (C_5), 123.43 (C_4), 137.95 (C_6), 173.15 (C_2)

Recycled BmimOAc 1:

^{1}H-NMR (300 MHz, DMSO-d6): δ (ppm) = 0.86 (t, J=7.44 Hz, 3H, C_{10}), 1.15-1.27 (m, 2H, C_9), 1.57 (s, 3H, C_1), 1.69-1.79 (m, 2H, C_8), 3.88 (s, 3H, C_3**),** 4.20 (t, J=7.19 Hz, 2H, C_7), 7.87 (t, J=1.63 Hz, 1H, C_4), 7.95 (t, J=1.63 Hz, 1H, C_5), 10.29 (s, 1H, C_6)

^{13}C-NMR (300 MHz, DMSO-d6): δ (ppm) =13.11 (C_{10}), 18.64 (C_9), 25.06 (C_1), 31.33 (C_8), 35.27 (C_3), 48.05 (C_7), 122.15 (C_5), 123.43 (C_4), 137.99 (C_6), 173.06 (C_2)

Recycled BmimOAc 2:

^{1}H-NMR (300 MHz, DMSO-d6): δ (ppm) = 0.87 (t, J=7.41 Hz, 3H, C_{10}), 1.16-1.28 (m, 2H, C_9), 1.56 (s, 3H, C_1), 1.70-1.80 (m, 2H, C_8), 3.88 (s, 3H, C_3H3**),** 4.19 (t, J=7.21 Hz, 2H, C_7), 7.83 (t, J=1.64 Hz, 1H, C_4), 7.91 (t, J=1.59 Hz, 1H, C_5), 10.20 (s, 1H, C_6)

^{13}C-NMR (300 MHz, DMSO-d6): δ (ppm) =13.13 (C_{10}), 18.64 (C_9), 26.12 (C_1), 31.32 (C_8), 35.32 (C_3), 48.09 (C_7), 122.11 (C_5), 123.41 (C_4), 137.86 (C_6), 172.95 (C_2)

List of Figures

Figure I.1: Overview of the uses of synthetic polymers in 2012. 1
Figure I.2: Bibliometric analysis from Scifinder® database about the number of publications (including scientific journals, patents, conferences) dealing with biodegradable materials. 3
Figure 1.1: Bibliometric analysis from Scifinder® database about the number of publications (including scientific journals, patents, and conferences) dealing with biopolymers. 6
Figure 1.2: Overview of the main platform molecules produced from lignocellulosic biomass.[18-20] ... 8
Figure 1.3: Molecular structure of cellulose. AGU stands for an anhydroglucose unit and n for the degree of polymerization. 10
Figure 1.4: Intermolecular (blue dotted line) and intramolecular hydrogen bonds (red dotted line) between two parallel cellulose chains.[28] 11
Figure 1.5: (A) Idealized representation of the molecular structure of chitin and (B) real representation of commercial chitin. n stands for the degree of polymerization and DA for the degree of acetylation. 14
Figure 1.6: Relevant examples of non-derivatizing cellulose solvents. 19
Figure 1.7: Proposed interaction between LiCl/DMAc and cellulose acting as the dissolution mechanism by (A) McCormick *et al.* (B) Morgenstern *et al.* 20
Figure 1.8: Hypothetical ability of the three non-derivatizing solvents to arrange in a cyclic formation: (A) DMAc/LiCl (5-ring geometry), (B) DMSO/TBAF (6-ring geometry), (C) NMMO (6-ring geometry).[58] 21
Figure 1.9: Main classical solvents used for chitin dissolution. 22
Figure 1.10: Bibliometric analysis from Scifinder® database dealing with the dissolution of cellulose and of chitin in ILs. 26
Figure 1.11: Relevant cations and anions present in ILs having the capacity to dissolve cellulose. .. 27
Figure 1.12: Dissolution mechanism of cellulose in the IL 1-allyl-3-methylimidazolium chloride (AmimCl) proposed by Zhang *et al.* 31
Figure 1.13: Hypothetical ability of a 1-3-dialkylimidazolium chloride IL to arrange in a 6-ring geometry.[58] 32
Figure 1.14: Bibliometric analysis from Scifinder® database about the number of publications (including scientific journals, patents, and conferences) dealing with the dissolution of cellulose and chitin in DES. 34
Figure 1.15: Schematic of the production process for the materials composed of cellulose and chitin. 38
Figure 1.16: Detailed diagram of the viscose and Lyocell process.[128] 41
Figure 1.17: Schema of the dry-jet wet fiber spinning process used in Lyocell process.[126] 42
Figure 2.1: Overview of the ionic liquids used in the dissolution tests: 1-allyl-3-methylimidazolium bromide (**AmimBr**), 1-ethyl-3-methylimidazolium acetate (**EmimOAc**), 1-butyl-3-methylimidazolium acetate (**BmimOAc**), 1-butyl-3-methylimidazolium hexafluorophosphate (**BmimPF$_6$**), 1-butyl-3-methylimidazolium tetrafluoroborate (**BmimBF$_4$**), 1-hexyl-3-

methylimidazolium bis(trifluoromethyl sulfonyl)imide (**HmimNTf2**), 1-octyl-3-methylimidazolium tetrafluoroborate (**OmimBF$_4$**), choline butanoate (**ChC$_4$**), choline lactate (**ChLac**), butylcarnitine bromide (**C$_4$CarBr**), imidazolium formate up to nonanoate (**MimC$_1$-C$_9$**), ethylammonium formate (**EAF**), butylammonium formate (**BuAF**), pyrrolidinium formate up to propionate (**PyrC$_1$-C$_3$**), pyrrolidinium hydrogen sulfate (**PyrHSO$_4$**), tetraalkyl ammonium sulfate Ammoeng 102 (**A102**), and N-methyl-N-butyl-pyrrolidinium dicyanoamide (**P$_{14}$DCA**). Tallow is a C_{18} acyl group. 55
Figure 2.2: (A) Mixture containing 3 wt% of α-chitin dissolved in BmimOAc, (B) its image obtained by polarized light microscope, (C) mixture containing 10 wt% of microcrystalline cellulose dissolved in BmimOAc, and (D) its image obtained by polarized light microscope. The white object in solution is a magnetic stirrer. 57
Figure 2.3: Chitin in EmimOAc after different dissolution methods: (A) magnetic stirring and heating at 90 °C, (B) Ultra-Turrax and heating at 90 °C, (C) microwave irradiation and heating at 55 °C, and (D) ultrasonication and heating at 80 °C. Objects in solutions are magnetic stirrers in (A)/(C) and Ultra-Turrax disperser in (B). 58
Figure 2.4: Structure of (A) Ammoeng 102 and (B) Ammoeng 110 chloride. 60
Figure 2.5: Overview of the hydrogen bond acceptors (**HBA**) and the hydrogen bond donors (**HBD**) for the formation of deep eutectic solvents used in the dissolution tests. **CCU** corresponds to the DES choline chloride/urea, **CCT** to choline chloride/thiourea, **ECU** to ethylammonium chloride/urea, and **BU** to betaine/urea. 61
Figure 2.6: Appearance of the mixtures containing (A) 1 wt% of chitin, (C) 1 wt% of MCC, in choline chloride/urea (1:2) after dissolution test by mechanical stirring at 80 °C. (B) is the corresponding micrograph to the chitin solution and (D) to the MCC solution obtained by polarized light microscope. The white object in solutions is a magnetic stirrer. 62
Figure 2.7: Appearance of the solutions containing (A) 1 wt% of chitin, (B) 1 wt% of MCC, in choline chloride/thiourea (1:2) after dissolution test by ultrasonication at 80 °C. 63
Figure 2.8: Appearance of the mixtures containing (A) 1 wt% of purified chitin, (C) 1 wt% of unpurified chitin, in choline chloride/urea (1:2) after dissolution test by mechanical stirring at 100 °C. (B) is the related micrograph to the purified chitin solution and (D) to the unpurified solution obtained by polarized light microscope. The white object in solutions is a magnetic stirrer. 65
Figure 2.9: Overview of the organic solvents used in the dissolution experiments: 2-methyltetrahydrofuran (**MTHF**), 2-methylfuran (**MF**), 2,5-dimethylfuran (**DMF**), γ-valerolactone (**GVL**), choline hydroxide (**ChOH**), ethyl lactate (**EL**), ethyl acetate (**EA**), γ-butyrolactone (**GBL**), γ-hexalactone (**GHL**), propylene carbonate (**PC**), N-methylmorpholine N-oxide monohydrate (**NMMO mono.**), dimethyl sulfoxide (**DMSO**), and tetrabutylphosphonium hydroxide (**TBPOH**). 67
Figure 3.1: Appearance of the mixtures containing either microcrystalline cellulose (MCC) or chitin, BmimOAc, and 20 wt% of co-solvent (2-methylfuran, 2,5-dimethylfuran, 2-methyltetrahydrofuran, or GVL) after the dissolution test. The white rods in the solutions are magnetic stirrers. 79
Figure 3.2: GVL-tolerance in mixtures to dissolve 1-10 wt% of MCC in BmimOAc and 1-2 wt% chitin in BmimOAc at 110 °C. The proportion of BmimOAc in each solution can be calculated according to the following equation: 100 - wt%(MCC or chitin) - wt%(GVL). 81
Figure 3.3: Dynamic viscosity of pure GVL, mixtures composed of BmimOAc and GVL, and pure BmimOAc as a function of temperature. Lines correspond to the best fits using the Vogel-Fulcher-Tammann equation. 83

Figure 3.4: Effect of GVL on the viscosity of BmimOAc/GVL mixtures at 25 °C. The line corresponds to the best fit using an exponential equation. The inset represents the linear change of $\ln(\eta/\eta_{IL})$ as a function of GVL mole fraction using Equation 3.6. 85
Figure 3.5: Walden plot of pure BmimOAc and mixtures composed of BmimOAc/GVL. The solid line corresponds to the "ideal" behavior of an 1 M aqueous KCl solution and the dashed line to the best linear fits.[183] 86
Figure 3.6: Autocorrelation functions obtained by DLS for BmimOAc/GVL mixtures at 25 °C. 87
Figure 3.7: Loss modulus (G'', solid symbol) and storage modulus (G', open symbol) as a function of angular frequency for the solutions composed of 5 wt% MCC dissolved in BmimOAc with different amount of GVL: (A) 0 and 20 wt%, (B) 40 and 65 wt% at 25 °C. 89
Figure 3.8: Complex viscosity as a function of angular velocity for the solutions composed of 5 wt% MCC dissolved in BmimOAc with different amounts of GVL at 25 °C. 89
Figure 3.9: Effect of GVL on the complex viscosity for cellulose solutions composed of 5 wt% MCC dissolved in BmimOAc and in BmimOAC/GVL (75/20 wt%). The viscosity values were measured at an angular velocity of 1.18 rad/s at different temperatures. The lines correspond to the best exponential fits. 90
Figure 3.10: Loss modulus (G'', solid symbol) and storage modulus (G', open symbol) as a function of angular frequency for the solutions composed of 1 wt% chitin dissolved in only BmimOAc and of 1 wt% chitin dissolved in BmimOAc and in presence of 20 wt% GVL at 25 °C. 91
Figure 3.11: Complex viscosity as a function of angular velocity for the solutions composed of 1 wt% chitin dissolved in BmimOAc with 0 and 20 wt% GVL at 25 °C. 92
Figure 3.12: Effect of GVL on the complex viscosity for chitin solutions: 1 wt% chitin dissolved in BmimOAc and in BmimOAC/GVL (79/20 wt%). The viscosity values were measured at an angular velocity of 1.18 rad/s at different temperatures. The lines correspond to the best exponential fits. 92
Figure 3.13: Tolerance of co-solvents in mixtures to dissolve MCC at concentrations ranging from 1 to 10 wt% in NMMO mono. at 80 °C. The proportion of NMMO mono. in each solution can be calculated according to the following equation: 100 - wt%(MCC) - wt%(co-solvent). 94
Figure 3.14: Tolerance of GVL in mixtures to dissolve cellulose pulp in concentration ranging from 1 to 3 wt% in NMMO mono. at 80 °C. The proportion of NMMO mono. in each solution can be calculated according to the following equation: 100 - wt%(cellulose pulp) - wt%(co-solvent). 95
Figure 3.15: Pictures of samples after dissolution at 80 °C. (A) 8 wt% MCC dissolved in NMMO mono. (B) 8 wt% MCC dissolved in NMMO mono./GVL (64/28 wt%). (C) 5 wt% MCC dissolved in NMMO mono. (D) 5 wt% MCC dissolved in NMMO mono./GVL (58/37 wt%). The white rod in the solutions is a magnetic stirrer. 97
Figure 3.16: DSC heating curves of NMMO mono./GVL mixtures recorded at a scan speed of 20 °C/min, showing the effect of GVL concentration. The second heating cycle is represented as well as the method to obtain the melting temperature T_m defined as the onset of the endothermic peak. 98
Figure 3.17: Evolution of the melting temperature of NMMO mono./GVL mixtures as a function of GVL concentration. 98
Figure 3.18: Autocorrelation functions obtained by DLS for mixtures composed of NMMO mono. And GVL at 40 °C. 99

Figure 3.19: Loss modulus (G‘‘, solid symbol) and storage modulus (G‘, open symbol) as a function of angular frequency for the cellulose dopes composed of 3 wt% cellulose pulp dissolved in NMMO mono./GVL at 25 °C. 101
Figure 3.20: Complex viscosity as a function of angular velocity for the cellulose dopes composed of 3 wt% cellulose pulp dissolved in NMMO mono./GVL at 25 °C. 101
Figure 3.21: DSC thermograms of the second heating and cooling cycle measured at a heating scan rate of 5 °C/min and a cooling scan rate of 2 °C/min for various cellulose dopes: (A) 1 wt% MCC dissolved in NMMO mono. depicting the DSC behavior of the Group I, (B) 8 wt% MCC dissolved in NMMO mono. (Group II), (C) 8 wt% MCC dissolved in NMMO mono./GVL (64/28 wt%, Group III), and (D) 10 wt% MCC dissolved in NMMO mono. (Group IV). 105
Figure 4.1: Schematic of the first self-developed fiber spinning apparatus. 114
Figure 4.2: Schematic of the (A) 200 µm-/(B) 80 µm-monofilament spinneret.[199] 115
Figure 4.3: Schematic of the second self-developed fiber spinning apparatus..... 116
Figure 4.4: Schematic of the third self-developed fiber spinning apparatus. 117
Figure 4.5: Schematic of the chitin coating method on cellulose material..... 118
Figure 4.6: Contact angle (Θ) of a water drop on a silicon wafer surface (Θ < 90°). 121
Figure 4.7: Experimental setup for the water permeability test. 121
Figure 4.8: Measurement setup for the O_2 permeability experiment..... 123
Figure 4.9: Measurement cell for the O_2 permeability measurement. (A) View of the Plexiglas measurement window where the sensor spot will be stuck. (B) View of the counterplate containing the film sample. 123
Figure 4.10: Surface structure of cellulose fibers spun with an 80 µm spinneret from a solution of 5 wt% cellulose, 58 wt% NMMO mono., and 37 wt% GVL at different temperatures: (A) 25 °C (B) 30 °C (C) 40 °C. 126
Figure 4.11: Cross section view of generated cellulose fibers from a solution of 5 wt% cellulose, 58 wt% NMMO mono., and 37 wt% GVL and with an 80 µm spinneret at (A) 25 °C, (B) 30 °C, and (C) 40 °C. 127
Figure 4.12: Surface structure of cellulose/chitin fibers spun from a solution of 0.5 wt% chitin, 1 wt% cellulose, 20 wt% GVL, and 78.5 wt% BmimOAc at 70 °C with a 200 µm spinneret. (A) Regular and (B) irregular fiber segments. 130
Figure 4.13: (A, B, C) Pictures and (B’) SEM images of chitin coated cellulose filters exposed for (A) 1 min, (B) 3 min, and (C) 5 min on the chitin solution during the coating process. (1) represents the chitin side and (2) the untreated filter paper side of each coated materials. 131
Figure 4.14: Dissolution time of 1 wt% of the textiles (Tencel, cotton, Viscose, and Modal) and 1 wt% of filter paper in BmimOAc at 100 °C. 132
Figure 4.15: Appearance of the untreated and chitin coated textiles..... 133
Figure 4.16: SEM images of the coated textiles obtained from (A) the untreated side of the coated Viscose, (B) the chitin side of the coated Viscose, (C) the cross section of the coated Viscose, (D) the cross section of the coated Tencel, (E) the cross section of a coated cotton, and (F) the cross section of the coated Modal. 134
Figure 4.17: FTIR-ATR spectra of the chitin coated side for the prepared textiles. 135
Figure 4.18: Comparative FTIR-ATR spectra of each reference textile, (A) Tencel, (B) cotton, (C) Viscose, and (D) Modal with its corresponding untreated side on the coated materials. 136

Figure 4.19: (A) Contact angle and (B) absorption time of a 2 µL water drop on the surface of the textile materials non-coated and coated with chitin (CS stands for Chitin Side and TS for Textile Side). 139
Figure 4.20: Comparative evolution of the water concentration in the ethyl lactate cell over time between each uncoated and coated textile. (A) Tencel, (B) cotton, (C) Viscose, and (D) Modal. 140
Figure 4.21: Oxygen partial pressure over time measured in the O_2 permeation chamber for (A) all the non-coated and coated textiles and (B) specific for the coated materials with chitin. 142
Figure C.1: Overview of the chapters in this work. 1487
Figure C.2: Overview of the solvents efficient for cellulose and chitin dissolution: 1-butyl-3-methyl-imidazolium acetate (BmimOAc), 1-allyl-3-methylimidazolium bromide (AmimBr), tetrabutylphosphonium hydroxide (TBPOH), N-methylmorpholine-N-oxide monohydrate (NMMO mono.), 1-ethyl-3-methyl-imidazolium acetate (EmimOAc)..... 148
Figure C.3: Overview of the produced biodegradable materials. 148
Figure A.1: Structure of AmimBr. 163
Figure A.2: Structure of (A) BmimOAc and (B) GVL. 165

List of Tables

Table 1.1: Percentage of cellulose present in some plants.[24] 9
Table 1.2: Percentage of chitin present in some of its main sources. 13
Table 1.3: Examples of some ILs able to dissolve cellulose, their cellulose dissolving capacities according to the DP of cellulose and the solubility conditions. 28
Table 1.4: Examples of ILs able to dissolve chitin, their chitin dissolving capacities according to the information given by the authors about the chitin used. 29
Table 1.5: Examples of DESs able to dissolve cellulose and/or chitin, their dissolving capacities according to the information given by the authors on the polymer used and the solubility conditions. The data written in brackets are extracted from the work of Sharma et al. 36
Table 1.6: Applications of cellulose and chitin materials according to their form. 39
Table 2.1: Water content in mass fraction of the ILs used in the dissolution tests after drying. 52
Table 2.2: Dissolution experiments of microcrystalline cellulose (MCC) and α-chitin in different ionic liquids (ILs). 56
Table 2.3: Dissolution experiments of microcrystalline cellulose (MCC) and α-chitin in various deep eutectic solvents (DESs). 62
Table 2.4: Dissolution experiments of microcrystalline cellulose and α-chitin in organic solvents, which do not belong to the category DES or IL. 68
Table 3.1: Water content in mass fraction of the co-solvents used in the tolerance tests with NMMO mono. after drying with 3 Å molecular sieves 74
Table 3.2: Effect of GVL on the dissolution duration of MCC in BmimOAc at 110 °C. 82
Table 3.3: Values of the constant α from Equation 3.6 as a function of temperature. 85
Table 3.4: Dipole moment of diluents estimated in the gas phase with MOPAC (PM6). 94
Table 3.5: Effect of GVL on the dissolution duration of MCC in NMMO mono. at 80 °C. 96
Table 3.6: Variation of the thermal properties obtained by DSC for cellulose dopes composed of MCC, NMMO mono. and GVL. T_c stands for crystallization temperature, T_m for melting temperature, and T_g for glass transition temperature. 104
Table 4.1: Spinning conditions and their effects on the spinnability of cellulose dope and on the fiber structure. 125
Table 4.2: Properties of cellulose fibers spun with an 80 µm spinneret and from a solution of 5 wt% cellulose, 58 wt% NMMO mono., and 37 wt% GVL and properties of commercial TENCEL® fibers. 127
Table 4.3: Spinning conditions and their effects on the spinnability of cellulose dopes and on the fiber structure. 128
Table 4.4: Fiber properties of regenerated cellulose fibers spun from NMMO/GVL solution by Lenzing AG and commercial TENCEL® fibers. 129
Table 4.5: Main absorption bands and their assignment for the different cellulosic textiles. 137
Table 4.6: Water permeability coefficient, P_{H_2O}, , with corresponding standard deviations. 141
Table 4.7: Oxygen permeability coefficients, P_{O_2}, , with corresponding standard deviations. 143

Table A.1: Density values (expressed in g/cm^3) as function of temperature and of GVL composition for different BmimOAc/GVL mixtures. 164
Table A.2: Dynamic viscosity values (expressed in mPa.s) as function of temperature and of GVL composition for different BmimOAc/GVL mixtures..... 164
Table A.3: Electrical conductivity values (expressed in mS/cm) as function of temperature and of GVL composition for different BmimOAc/GVL mixtures. 164

List of Publications

Papers

(1) Auriane Freyburger, Yaqing Duan, Cordt Zollfrank, Thomas Röder, Werner Kunz
Chitin coated cellulosic textiles as natural barrier materials
Accepted in Lenziger Berichte

(2) Yaqing Duan, Auriane Freyburger, Werner Kunz, Cordt Zollfrank
Cellulose and chitin composite materials from an ionic liquid and a green co-solvent
Carbohydrate Polymers, **2018**, *192*, 159-165

(3) Yaqing Duan, Auriane Freyburger, Werner Kunz, Cordt Zollfrank
Lignin/Chitin Films and Their Adsorption Characteristics for Heavy Metal Ions
Accepted in ACS Sustainable Chemistry & Engineering

Inventor's notification and patent application

(1) Auriane Freyburger, Yaqing Duan, Cordt Zollfrank, Werner Kunz
Modifiziertes Niedertemperatur-Lyocell Verfahren

(2) Auriane Freyburger, Yaqing Duan, Cordt Zollfrank, Werner Kunz
Process for the preparation of a cellulose product
Publication number: WO2017211798
Publication date: 14.12.2017

Oral communication

(1) Auriane Freyburger
Recycling and high value production of novel bio-hybrid polymers from cellulose and chitin
3rd International Symposium on Green Chemistry, **Mai 2015**, La Rochelle – France

Posters

(1) Auriane Freyburger, Yaqing Duan, Cordt Zollfrank, Werner Kunz
Neuartige biogene Hybridpolymere aus Cellulose und Chitin
Auftaktveranstaltung und Fachtagung - Projektverbund ForCYCLE, **Januar 2014**, München - Deutschland

(2) Auriane Freyburger, Yaqing Duan, Cordt Zollfrank, Werner Kunz
Recycling and high value production of novel bio-hybrid polymers from cellulose and chitin
16th Day of formulation - „Formulation and sustainable development", **December 2014**, Villeneuve d'Ascq – France

(3) Auriane Freyburger, Yaqing Duan, Cordt Zollfrank, Werner Kunz
Recycling and high value production of novel bio-hybrid polymers from cellulose and chitin
3rd International Symposium on Green Chemistry, **Mai 2015**, La Rochelle – France

(4) Auriane Freyburger, Yaqing Duan, Cordt Zollfrank, Werner Kunz
Neuartige biogene Hybridpolymere aus Cellulose und Chitin
Zwischensymposium Projektverbund ForCYCLE und Leitfaden Abfallvermeidung in der Bayerischen Akademie der Wissenschaften, **November 2015**, München – Deutschland

(5) Auriane Freyburger, Yaqing Duan, Cordt Zollfrank, Werner Kunz
Neuartige biogene Hybridpolymere aus Cellulose und Chitin
Abschlusssymposium des Projektverbund ForCYCLE, **Februar 2017**, Augsburg - Deutschland

Declaration

Hiermit erkläre ich, dass ich die vorliegende Dissertation ohne unzulässige Hilfe Dritter und ohne Benutzung anderer als der angegebenen Hilfsmittel angefertigt habe.

Die aus anderen Quellen direkt oder indirekt übernommenen Daten und Konzepte sind unter Angabe des Literaturzitats gekennzeichnet.

Die Arbeit wurde bisher weder im In- noch Ausland in gleicher oder ähnlicher Form einer anderen Prüfungsbehörde vorgelegt.

_____ Regensburg,

_____
(Auriane Freyburger)